

(NASA-TM-X-62360) LOW SPEED AERODYNAMIC  
CHARACTERISTICS OF AN 0.075-SCALE F-15  
AIRPLANE MODEL AT HIGH ANGLES OF ATTACK AND  
SIDESLIP (NASA) 118 p HC A06/MF A01

N78-10019

Unclassified  
CSCL 01A G3/02 50800

NASA TECHNICAL  
MEMORANDUM

NASA TM X-62,360

NASA TM X-62,360

LOW SPEED AERODYNAMIC CHARACTERISTICS OF AN 0.075-SCALE  
F-15 AIRPLANE MODEL AT HIGH ANGLES OF ATTACK AND SIDESLIP

Daniel N. Petroff, Stanley H. Scher and Lee E. Cohen

Ames Research Center  
Moffett Field, California 94035

REPRODUCED BY  
**NATIONAL TECHNICAL  
INFORMATION SERVICE**  
U. S. DEPARTMENT OF COMMERCE  
SPRINGFIELD, VA. 22161

July 1974

NOTICE

THIS DOCUMENT HAS BEEN REPRODUCED  
FROM THE BEST COPY FURNISHED US BY  
THE SPONSORING AGENCY. ALTHOUGH IT  
IS RECOGNIZED THAT CERTAIN PORTIONS  
ARE ILLEGIBLE, IT IS BEING RELEASED  
IN THE INTEREST OF MAKING AVAILABLE  
AS MUCH INFORMATION AS POSSIBLE.

1 Report No. NASA TM X-62,360	2. Government Accession No.	3. Recipient's Catalog No.
4. Title and Subtitle <b>LOW SPEED AERODYNAMIC CHARACTERISTICS OF AN 0.075-SCALE F-15 AIRPLANE MODEL AT HIGH ANGLES OF ATTACK AND SIDESLIP</b>		5. Report Date July 1974
7 Author(s) Daniel N. Petroff, Stanley H. Scher** and Lee E. Cohen*		6 Performing Organization Code
9. Performing Organization Name and Address NASA Ames Research Center, Moffett Field, Calif. and ARO, Inc., Moffett Field, Calif. 94035		8. Performing Organization Report No.
		10. Work Unit No. 760-17-01
		11 Contract or Grant No.
		13. Type of Report and Period Covered Technical Memorandum
12 Sponsoring Agency Name and Address National Aeronautics and Space Administration Washington, D. C. 20546		14. Sponsoring Agency Code
15 Supplementary Notes * ARO, Inc., Moffett Field, Calif. 94035 ** Project Engineer, NASA LaRC		
16 Abstract <p>An 0.075-scale model representative of the F-15 airplane was tested in the Ames 12-Foot Pressure Wind Tunnel at a Mach number of 0.16 to determine static longitudinal and lateral-directional characteristics at spin attitudes for Reynolds numbers from 1.48 to 16.4 million per meter (0.45 to 5.0 million per foot). Angles of attack ranged from 0 to +90° and from -40° to -80° while angles of sideslip were varied from -20° to +30°. Data were obtained for nacelle inlet ramp angles of 0 and 11° with the left and right stabilators deflected 0, -25°, and differentially 5° and -5°. The normal pointed nose and two alternate nose shapes were also tested along with several configurations of external stores.</p> <p>Analysis of the results indicate that at higher Reynolds numbers there is a slightly greater tendency to spin inverted than at lower Reynolds numbers. Use of a hemispherical nose in place of the normal pointed nose provided an over-correction in simulating yawing-moment effects at high Reynolds numbers; use of an asymmetrical beveled nose provided an even larger over-correction at positive sideslip angles and an effect in the wrong direction at negative sideslip angles.</p>		
17. Key Words (Suggested by Author(s)) F-15 airplane      Wind Tunnel test Hi alpha            Spin Hi Reynolds Static aerodynamics		18. Distribution Statement
19 Security Classif. (of this report) Unclassified		20 Security Classif. (of this page) Unclassified
		21. Rep. No. 118
		22. Incl. 94.7%

## CONTENTS

	Page
SUMMARY .....	1
INTRODUCTION .....	1
NOMENCLATURE .....	2
TEST FACILITY .....	5
MODEL DESCRIPTION .....	6
TESTING AND PROCEDURE .....	6
DATA REDUCTION .....	7
RESULTS AND DISCUSSION .....	8
REFERENCES .....	10
TABLES	
1. MODEL GEOMETRY .....	11
2. INDEX OF DATA FIGURES .....	13
FIGURES	
1. AXIS SYSTEMS .....	14
2. MODEL DRAWINGS .....	15
3. MODEL INSTALLATION PHOTOGRAPHS .....	29
4. DATA .....	31

(THIS PAGE INTENTIONALLY LEFT BLANK)

LOW SPEED AERODYNAMIC CHARACTERISTICS OF AN 0.075-SCALE  
F-15 AIRPLANE MODEL AT HIGH ANGLES OF ATTACK AND SIDESLIP

By Daniel N. Petroff, Stanley H. Scher\* and Lee E. Cohen\*\*

Ames Research Center

SUMMARY

An 0.075-scale model representative of the F-15 airplane was tested in the Ames 12-Foot Pressure Wind Tunnel at a Mach number of 0.16 to determine static longitudinal and lateral-directional characteristics at spin attitudes for Reynolds numbers from 1.48 to 16.4 million per meter (0.45 to 5.0 million per foot). Angles of attack ranged from 0 to +90° and from -40° to -80° while angles of sideslip were varied from -20° to +30°. Data were obtained for nacelle inlet ramp angles of 0 and 11° with the left and right stabilators deflected 0, -25°, and differentially 5° and -5°. The normal pointed nose and two alternate nose shapes were also tested along with several configurations of external stores.

Analysis of the results indicate that at higher Reynolds numbers there is a slightly greater tendency to spin inverted than at lower Reynolds numbers. Use of a hemispherical nose in place of the normal pointed nose provided an over-correction in simulating yawing-moment effects at high Reynolds numbers; use of an asymmetrical beveled nose provided an even larger over-correction at positive sideslip angles and an effect in the wrong direction at negative sideslip angles.

There were found to be no significant effects of changing inlet ramp angle and adding external stores on the aerodynamic characteristics. At angles of attack between 30° and 60° deflection of the stabilators provided an increase in directional stability.

INTRODUCTION

With the advent of highly maneuverable military aircraft, it was found that a large proportion of aircraft losses were caused by the aircraft entering out-of-control and spinning motions. The Department of the Air Force has required the evaluation of these motions on aircraft such as the McDonnell Douglas F-15. The tests being reported in this paper were made to support theoretical analysis of F-15 upright stall/spin motions, and

\* Project engineer, NASA LaRC

\*\* Project engineer, ARO, Inc.

to support inverted spin-model tests in the spin tunnel. The model is representative of the F-15.

Upright-attitude force tests were made to provide static aerodynamic data at high angles of attack and sideslip with various control deflections and stores to support theoretical analysis of F-15 upright stall/spin motions. Inverted-attitude force tests were made to evaluate the effects of Reynolds number on the crossflow characteristics on the fuselage ahead of the wing. In some cases, these crossflow effects can cause appreciably different side forces and yawing moments on a small-scale model from those obtained at the same attitudes on the full-scale configuration (references 1 and 2). When these effects do occur, they are usually in the angle-of-attack range between 40° and 90° for upright spins and between -40° and -90° for inverted spins. In the course of conducting investigations of aircraft spin and recovery characteristics in the spin tunnel, small-scale models must necessarily be used. It has been found that for some configurations, the Reynolds number effects are so marked that model spin and recovery characteristics do not represent the spin and recovery characteristics of the full-scale airplane.

In general, a wind tunnel Reynolds number force test program is conducted on a given design to determine if spin tunnel results could be appreciably altered by Reynolds number effects. When such effects are found, various "fixes" are investigated on the wind tunnel model in an attempt to minimize these effects. Then, a similar "fix" is placed on the spin tunnel model so that its side force and yawing moment characteristics in the spin are more representative of the larger scale model.

#### NOMENCLATURE

The axis systems and sign conventions are shown in figure 1. Data are presented in the body-axis coordinate system. Because the data were computer plotted the corresponding plot symbol, where used, is given together with the conventional symbol.

<u>Symbol</u>	<u>Plot Symbol</u>	<u>Definition</u>
$A_c$		cavity area
b	BREF	wing span
$\bar{c}$		wing mean aerodynamic chord, M.A.C.
$C_A$	CA	axial-force coefficient, axial force/qS

$C_D$	CD	drag coefficient, drag/qS
$C_L$	CL	lift coefficient, lift/qS
$C_\lambda$	CBL	rolling-moment coefficient, rolling moment/qSb
$C_m$	CLM	pitching-moment coefficient, pitching moment/qSc
$C_N$	CN	normal-force coefficient, normal force/qS
$C_n$	CYN	yawing-moment coefficient, yawing moment/qSb
$C_Y$	CY	side-force coefficient, side force/qS
L	LREF	reference length
M	MACH	freestream Mach number
p		freestream static pressure
$p_c$		cavity pressure
q		freestream dynamic pressure
Re/L	RN/L	unit Reynolds number, million per meter
S	SREF	wing area
$\alpha$	ALPHA	angle of attack
$\beta$	BETA	angle of sideslip
$\delta_{a_L}$	AIL-L	left aileron deflection angle, positive trailing edge down
$\delta_{a_R}$	AIL-R	right aileron deflection angle, positive trailing edge down
$\delta_r$	RUDDER	rudder deflection angle, positive trailing edge to the left looking forward
$\delta_{st_L}$	STB-L	left stabilator deflection angle, positive trailing edge down

$\delta_{stR}$	STB-R	right stabilator deflection angle, positive trailing edge down
$\rho$	RHO	duct inlet ramp angle
Configuration Code		
$a_{15}$	A15	gun bump fairing, right-hand
$a_{16}$	A16	wing root fairing, left-hand
$B_{156}$	B156	fuselage
$d_{22f}$	D22F	shroud/exit choke, normal flow
$d_{22g}$	D22G	shroud/exit choke, blocked flow
$D_{41}$	D41	inlet
$Fa_{17}$	F17	flaps
$Fa_{18}$	A18	ailerons
$H_{36}$	H36	horizontal stabilators
$J_8$	J8	MER 200
$M_{12}$	M12	radome
$Mx$	MX	alternate nose shape, 45° left-hand bevel
$My$	MY	alternate nose shape, hemispherical
$T_{23}$	T23	600 gallon fuel tank
$T_{25}$	T25	sparrows (two forward and two aft)
$T_{57}$	T57	QRC-249 ECM pod
$T_{64}$	T64	SUU-13/A

$T_{66}$	T66	BLU-32/B
$V_{172}$	V172	vertical tails
$W_{118}$	W118	wing
$Y_{22}$	Y22	inboard wing pylons
$Y_{24}$	Y24	centerline pylon
$Y_x$	YX	outboard wing pylons
BASIC	$B_{156} \ W_{118} \ D_{41} \ H_{36} \ V_{172} \ T_{25}$	
A	$J_8(3) \ T_{66} \ Y_{24}$	
B	$J_8(6) \ T_{64}(2) \ Y_{22}$	
C	$T_{57}(2) \ Y_x$	
D	$J_8(3) \ T_{64} \ Y_{22}$	
E	$T_{23} \ Y_{24}$	
F	$T_{25}$	
G	$-M_{12} + M_x$	
H	$-M_{12} + M_y$	

#### TEST FACILITY

The Ames 12-Foot Pressure Wind Tunnel is a variable density, low turbulence wind tunnel which operates in the Mach number range of 0.1 to 0.94. The wind tunnel is powered by a two-stage, axial flow fan driven by electric motors totaling 12,000 horsepower. Airspeed in the test section is controlled by variation of the fan's rotative speed. Eight fine-mesh screens in the settling chamber together with a contraction ratio of 25 to 1, provide an airstream of exceptionally low turbulence.

## MODEL DESCRIPTION

The model was an 0.075-scale F-15 airplane. The geometry of the model is given in table 1, drawings of the model are presented as figure 2, and photographs of the model installation are included as figure 3.

The model is a twin engine, mid-wing, supersonic fighter aircraft configuration with a 45° wing leading edge sweep and a compound trailing edge sweep. At the wing root the wing section is a NACA 64A(.55)0(5.9), $a=0.8$  mod. airfoil. Advancing further outboard the wing section changes to a NACA 64A(.55)0(4.6), $a=0.8$  mod. airfoil, and then to a NACA 64A-20(3.5), $a=0.8$  mod. airfoil. At the wing tip it is a NACA 64A-20(3.0), $a=0.8$  mod. airfoil. The twin vertical tails are NACA 000(5.0)-64 airfoils at the root and blend into a NACA 000(3.5)-64 airfoil at the tip. The horizontal stabilators have a NACA 000(5.5)-64 airfoil at the root and blend into a NACA 000(2.5)-64 airfoil at the tip.

Various combinations of stores and their supporting pylons were mounted on the underside of the model and are presented in figures 2 (2) to 2 (n).

The model was tested with two alternate nose configurations: a hemispherical nose having a radius of curvature of 1.11cm which shortened the normal nose length by 1.824cm; and a 45° left-hand beveled nose which shortened the normal nose by .318cm.

The control surfaces utilized during the test were the ailerons and horizontal stabilators. The ailerons were 13.283cm in span with a 23.8 per cent wing chord. The horizontal stabilator was a pivoting horizontal tail in which the entire tail rotates.

The aft end of the model, between the vertical tails, was modified to accept the sting support.

## TESTING AND PROCEDURE

The investigation was conducted at a Mach number of 0.16 and at Reynolds numbers of 1.48 to 16.4 million per meter (0.45 to 5.0 million per foot). Data were obtained at angles of attack from -80° to 90° and at sideslip angles from -20° to 30°.

The left and right horizontal stabilator deflections were set at 0 and 0, -25° and -25°, and 5° and -5°, respectively. The ailerons and rudder remained at zero deflection throughout the test.

The basic configuration was B<sub>156</sub> W<sub>118</sub> D<sub>41</sub> H<sub>36</sub> V<sub>172</sub> T<sub>25</sub>. Model configuration changes consisted of the addition of various combinations of stores including MER200, BLU-32/B, SUU-13/A, QRC-249 ECM POD and a 600-gallon fuel tank with their associated pylons. Two alternate nose configurations were also tested.

The model was provided with boundary layer transition strips. These strips were of No. 120 carborundum grit with a width of .127cm. Grit density was approximately 59/cm. The strips were located 3.81cm aft of the tip of the airplane nose and at 5 percent chord of the wings, horizontal and vertical tails, and 1.9cm from the leading edge around the engine inlet ducts. When the model was tested for the effect of the nose configurations, no transition grit was used on the model and all stores were removed.

At angles of attack from 40° to 90° and -40° to -80° the engine nacelle ducts were plugged to simulate stalled engines. At other angles of attack the ducts were flow-through simulating normal engine operation. The inlet ramp angle of the ducts was set at either 0 or 11°.

The model was sting mounted on a turntable which permitted the variation of either angle of attack or sideslip. Aerodynamic forces and moments on the model were measured using a Task internal six-component strain gage balance. The balance cavity pressure was measured using a pressure transducer. An angle of attack transducer at the base of the support system was used to measure the angle of attack and a Selsyn was used to measure the turntable rotation.

Tunnel static pressure was measured in the plenum surrounding the test section and no blockage corrections were applied. Prior calibration of the wind tunnel with large blockage models showed plenum pressure to be essentially identical to free-stream static pressure and this pressure is currently being used for all high attitude tests.

#### DATA REDUCTION

The six-component force and moment data were reduced about the model moment reference center in the body axis system. The axis systems are defined in figure 1 and the moment center was assumed to be at fuselage station 106.142cm and waterline 22.131cm. The angle of attack and angle of sideslip were corrected for deflection of the sting and balance under aerodynamic load. Angle of attack and appropriate aerodynamic coefficients were corrected for model weight tares and tunnel wall interference effects (reference 3). The wall correction values are as follows:

$$\Delta\alpha = 0.2568 C_L \quad \Delta C_m(\text{tail on}) = 0.001343 C_L$$

$$\Delta C_D = 0.004020 C_L \quad \Delta C_m(\text{tail off}) = 0.0008763 C_L$$

A stream angle of up to  $2^\circ$  at zero angle of attack is known to exist in the vicinity of the model due to the influence of the support system fairing on the tunnel floor (see figure 3). No stream angle corrections were applied to the data.

Three samples of all balance and tunnel static pressure data were averaged for each data point and then reduced to coefficient form.

The balance cavity pressure was measured and the body axial force coefficient was corrected as follows:

$$C_A = C_{A_{\text{uncorrected}}} + \frac{(p_c - p) A_c}{qS}$$

Data repeatability was estimated by reviewing repeat points and is as follows:

$$C_N = \pm 0.025$$

$$C_\alpha = \pm 0.003$$

$$C_A = \pm 0.002$$

$$\alpha = \pm 0.04^\circ$$

$$C_Y = \pm 0.014$$

$$\beta = \pm 0.04^\circ$$

$$C_m = \pm 0.010$$

$$Re/L = \pm 0.07 \times 10^6 \text{ per m}$$

$$C_n = \pm 0.003$$

$$M = \pm 0.001$$

## RESULTS AND DISCUSSION

Computer plotted data are presented in figures 4 through 9. An index to the plotted data is given in table 2.

The effects of Reynolds number on the aerodynamic coefficients of the model for a given angle of attack and angle of sideslip are presented in figure 4. The effects of angle of attack and angle of sideslip on the aerodynamic characteristics at a Reynolds number of 13.1 million per meter (4 million per foot) for two values of nacelle inlet ramp angle are presented in figures 5 and 6, respectively. The effects of sideslip angle on the aerodynamic characteristics at a Reynolds number of 13.1 million per meter (4 million per foot) are presented in figure 7 for several stabilator angles and in figure 8 for several configurations of external stores. The

effects of sideslip angle on the aerodynamic characteristics at Reynolds numbers of 1.48 and 16.4 million per meter (0.45 and 5.0 million per foot) for three fuselage nose shapes are presented in figure 9.

Analysis of the results presented in figure 4 indicate that at angles of attack of  $-80^\circ$ ,  $-70^\circ$ ,  $-60^\circ$  the model adequately simulates full scale when comparing the lateral-directional coefficients, especially  $C_n$  which is an important parameter in its effects on spin characteristics (reference 1 and 2). At an angle of attack of  $-50^\circ$ , there was a Reynolds number effect in that a positive value of  $C_n$  at  $10^\circ$  of sideslip at high Reynolds number became a negative value of  $C_n$  at low Reynolds number (see page 39, and see similar effects on pages 24, 29, and 34). At an angle of attack of  $-40^\circ$ , some Reynolds number effects were also evident, but the effects were not consistent and in some cases were opposite to the effect already discussed for an angle of attack of  $-50^\circ$  (for example of an opposite effect, see page 40).

In general, the results presented in figure 4 indicate that the airplane may have a slightly greater tendency to spin inverted than would the small-scale spin model.

At an angle of attack of  $-50^\circ$  use of the hemispherical nose shape as a "fix" on the model at low Reynolds number changed the  $C_n$  data to be more like the  $C_n$  data at high Reynolds number when the basic tip was on; however, an over-correction is indicated. The data showed that use of the asymmetrical beveled nose is not promising because it provided an even larger over-correction at  $+10^\circ$  of sideslip and also because it provided an increment in the wrong direction at negative sideslips (see figure 9, page 86). The use of the hemispherical nose as a "limited fix" for full scale simulation will require further analysis.

At an angle of attack of  $-40^\circ$  neither the hemispherical nose nor the asymmetrical beveled nose appeared useful as a Reynolds number "fix". The hemispherical nose caused little or no change and the beveled nose provided an increment in the wrong direction at positive sideslips (see figure 9, page 87).

From the data presented in figures 5 and 6 it is seen that there was little effect of changing the inlet ramp angle on the variation of the aerodynamic coefficients with angle of attack and sideslip. The only coefficient to be appreciably affected by changing the ramp angle from 0 to  $11^\circ$  was the axial-force coefficient.

The data presented in figure 7 show that at angles of attack between  $30^\circ$  and  $60^\circ$  deflection of the stabilators can be used to increase the directional stability. Differential deflection of the stabilators is more effective in increasing directional stability at the higher angles of attack.

The data presented in figure 8 show no significant effects of adding external stores on the aerodynamic characteristics.

Ames Research Center  
National Aeronautics and Space Administration  
Moffett Field, California 94035

July 3, 1974

#### REFERENCES

1. Neilhouse, Anshal I.; Klinar, Walter J.; and Scher, Stanley H.: Status of Spin Research for Recent Airplane Designs. NASA TR R-57, 1960. (Supersedes NACA RML 57F12).
2. Polhaums, Edward C.: Effect of Flow Incidence and Reynolds Number on Low-Speed Aerodynamic Characteristics of Several Noncircular Cylinders With Applications to Directional Stability and Spinning. NASA TR R-29, 1959.
3. Sivells, James; and Salmi, Rachel: Jet-Boundary Corrections for Complete and Semispan Swept Wings in Closed Circular Wind Tunnels. NACA TN2454, 1951.

TABLE 1. - MODEL GEOMETRY

(Dimensions Cm or Cm<sup>2</sup>)Fuselage (B<sub>156</sub>)

Length	134.247
Cavity pressure	51.936

Wing (W<sub>118</sub>)

Span (reference)	97.63
Area (reference)	3177.3
Root chord (theoretical)	52.070
Root chord (actual)	57.432
Tip chord	13.018
Mean aerodynamic chord (reference)	36.439
Aspect ratio	3.01
Maximum t/c	0.059
Taper ratio	0.250
Dihedral	-1.0°
Incidence	0°
Leading-edge sweep	45.0°
0.25c sweep	38.63°
Trailing-edge sweep	0.0° up to BL. 29.530cm 11.42° from BL. 29.530cm to wing tip.
Section:	at BL. 15.216 NACA 64A(.55)0(5.9), $a=0.8$ mod. airfoil at BL. 29.530 NACA 64A(.55)0(4.6), $a=0.8$ mod. airfoil at BL. 42.812 NACA 64A-20(3.5), $a=0.8$ mod. airfoil at BL. 48.920 NACA 64A-20(3.0), $a=0.8$ mod. airfoil

Horizontal Stabilator (H<sub>36</sub>)

Semi span	17.916
Area	313.548/side
Exposed area	643.818
Root chord	26.137
Tip chord	8.891
Exposed M.A.C.	18.922
Exposed aspect ratio	2.05
Maximum t/c	0.055
Exposed taper ratio	0.34
Dihedral	0°
Leading-edge sweep	50.0°
0.25c sweep	43.34°
Trailing-edge sweep	12.5°

Section: at BL.: 13.335: NACA 000(5.5)-64 airfoil  
at BL. 31.251: NACA 000(2.5)-64 airfoil

Vertical tail (V<sub>172</sub>)

Exposed area	327.019/side
Root chord (2.634cm above FRP)	21.920
Tip chord	5.834
Exposed M.A.C.	15.423
Height from FRP	26.219
Exposed aspect ratio	1.7
Maximum t/c	0.050
Exposed taper ratio	0.226
Leading-edge sweep	36.57°
0.25c sweep	29.74°
Trailing-edge sweep	3.41°
Toe out	2.00°
Section: at root: NACA 000(5.0)-64	
at tip: NACA 000(3.5)-64	

TABLE 2. - INDEX OF DATA FIGURES

Figure	Title	Page
4	Variation of aerodynamic characteristics with Reynolds number at various angles of attack.	1
5	Effect of ramp angle on aerodynamic characteristics, Reynolds number equals 13.1 million per meter.	41
6	Effect of ramp angle on aerodynamic characteristics, Reynolds number equals 13.1 million per meter.	51
7	Effect of stabilators on aerodynamic characteristics, Reynolds number equals 13.1 million per meter.	59
8	Effect of stores on aerodynamic characteristics, Reynolds number equals 13.1 million per meter.	71
9	Effect of nose shape for two Reynolds numbers at various angles of attack, zero control surface deflections.	83

**Notes:**

- Positive directions of force coefficients, moment coefficients, and angles are indicated by arrows
- For clarity, origins of wind and stability axes have been displaced from the center of gravity

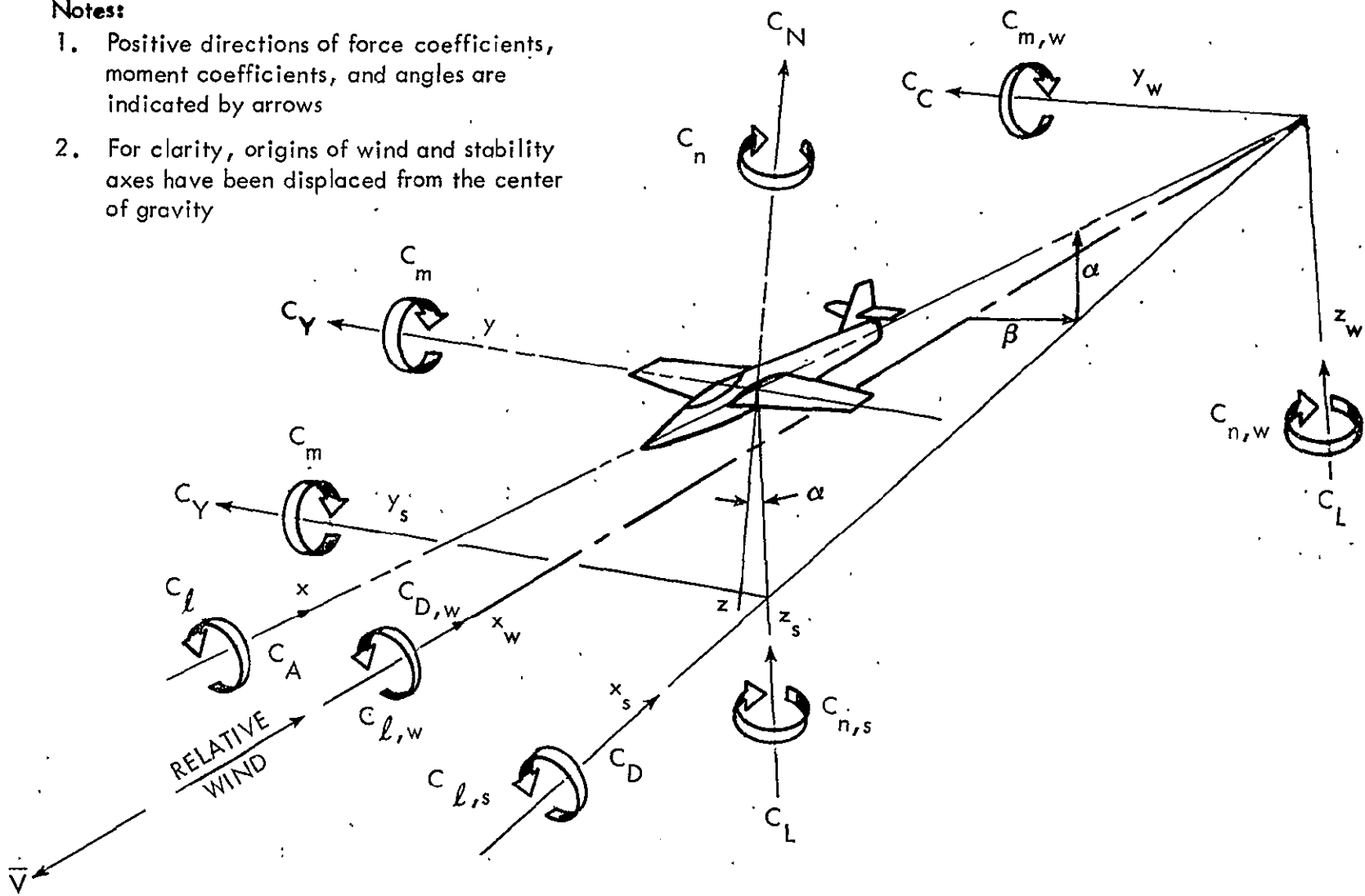
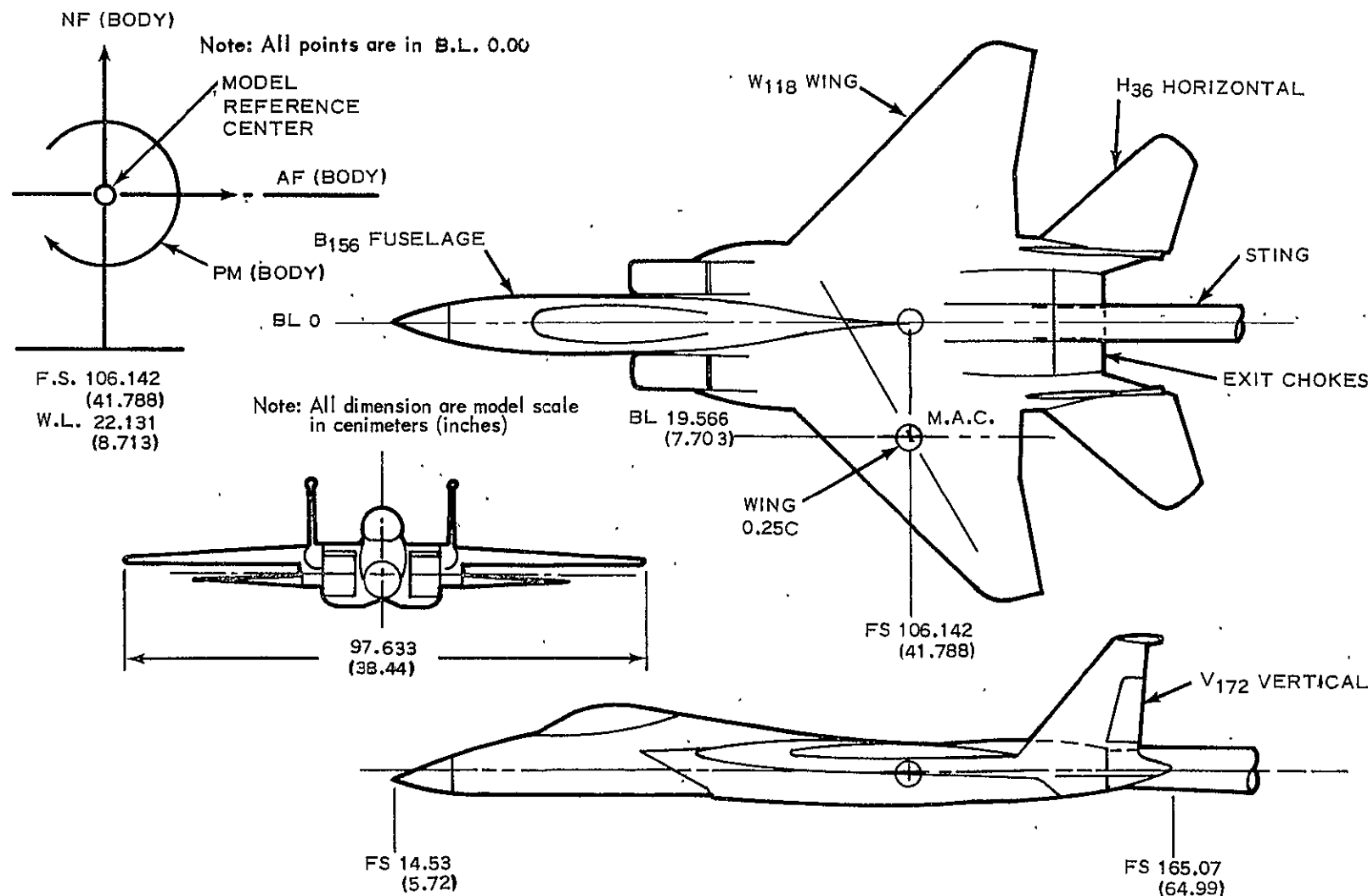
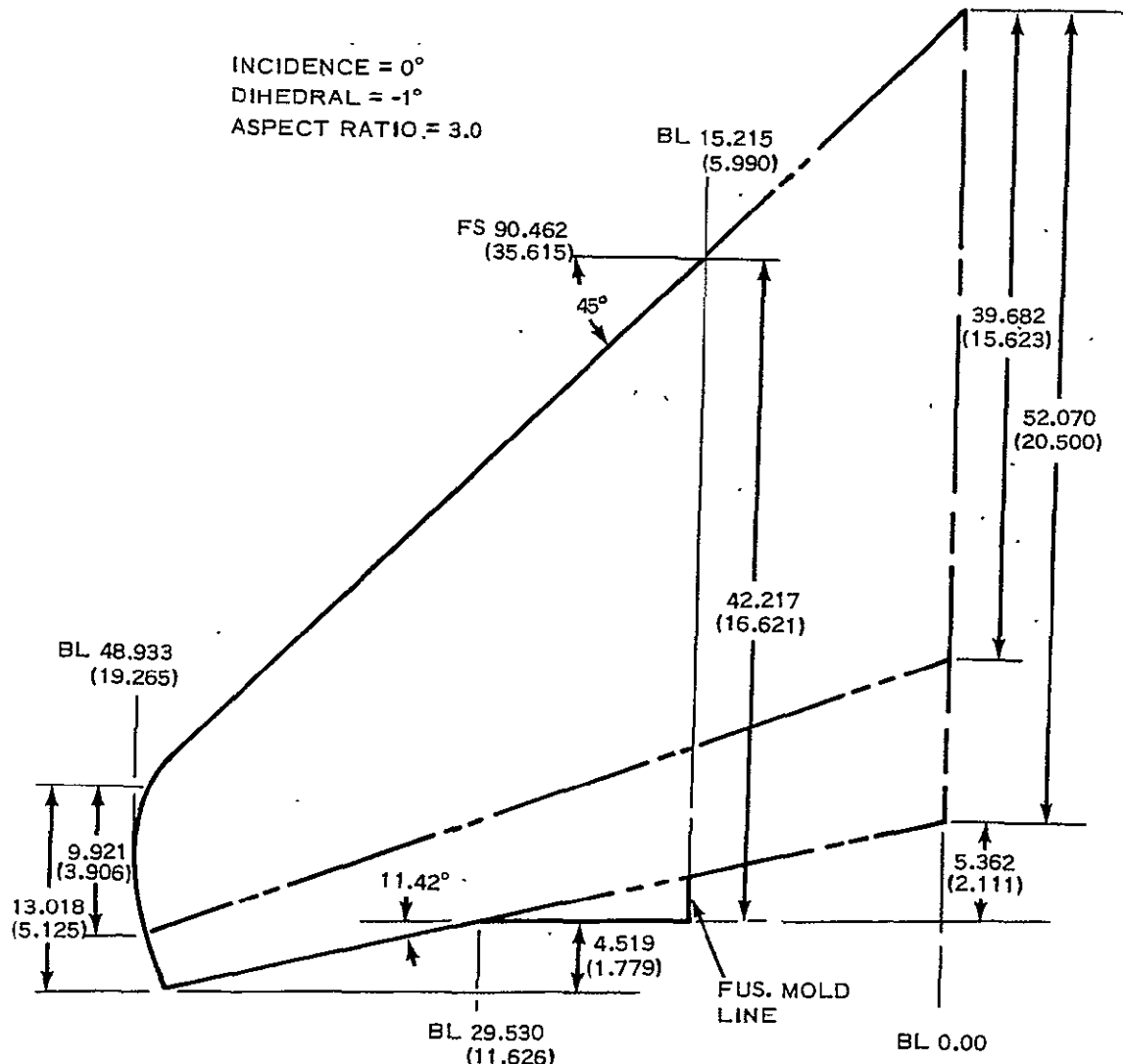


Figure 1. - Axis systems.



(a) General arrangement of the F-15 model

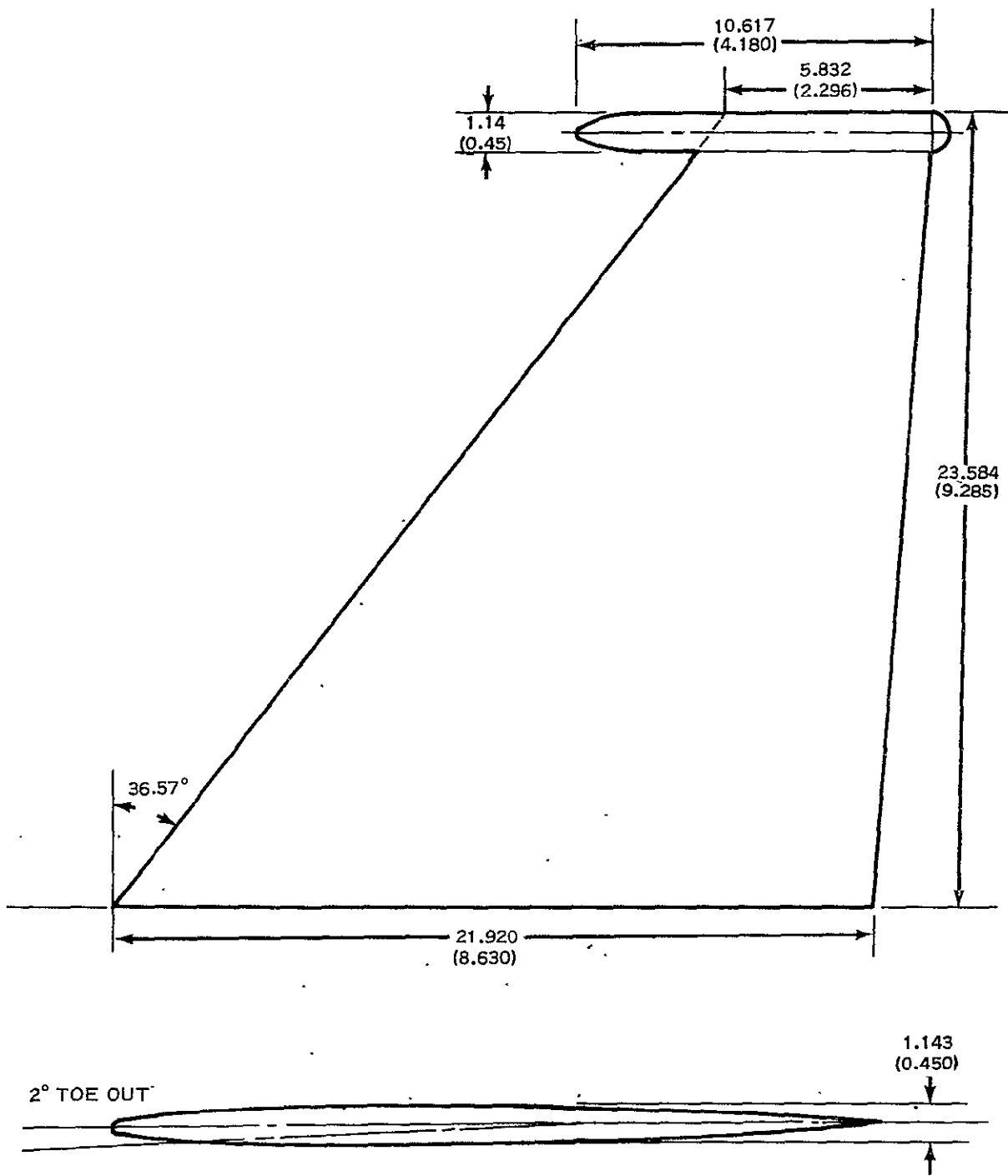
Figure 2.—Model drawings.



(b) Wing ( $W_{118}$ )

Figure 2.—Continued.

ORIGINAL PAGE IS  
OF POOR QUALITY

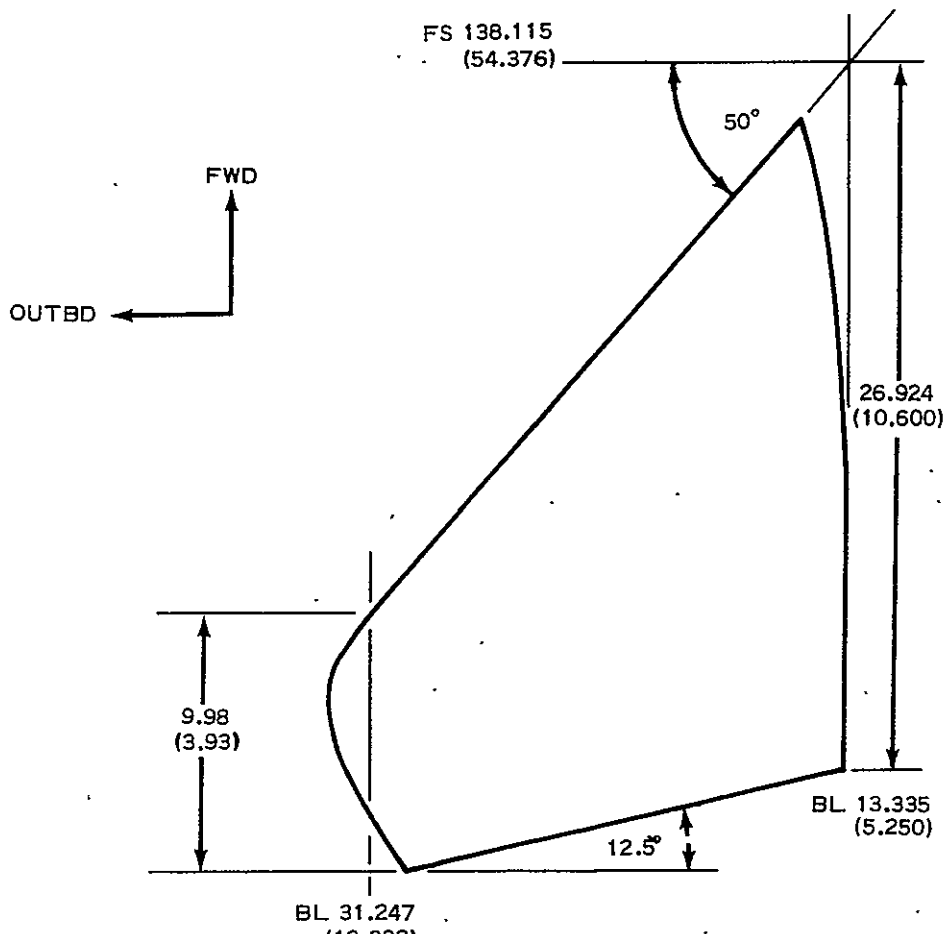


Note: All dimensions are model scale  
in centimeters (inches)

(c) Vertical stabilizer (V<sub>172</sub>)

Figure 2.--Continued.

DIHEDRAL =  $0^\circ$   
INCIDENCE =  $0^\circ$  IN WL 21.3 (8.4) PLANE  
ASPECT RATIO = 2.05

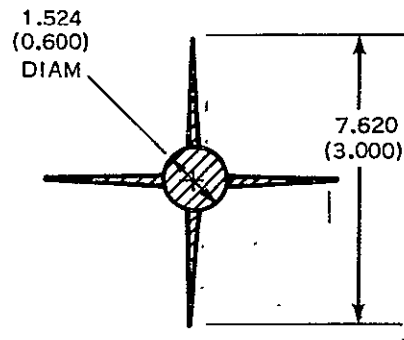
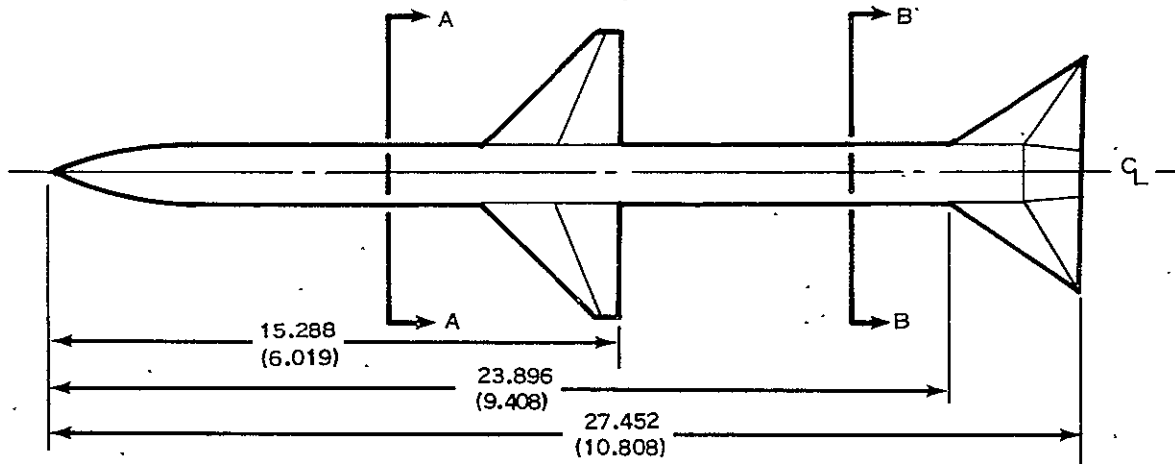


Note: All dimensions are model scale.  
in centimeters (inches)

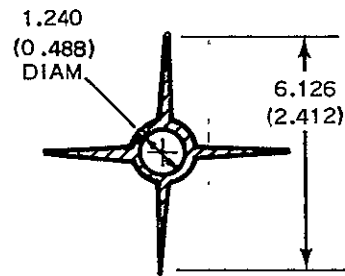
(d) Horizontal stabilator (H<sub>36</sub>)

Figure 2.—Continued.

ORIGINAL PAGE IS  
OF POOR QUALITY.



VIEW LOOKING AFT

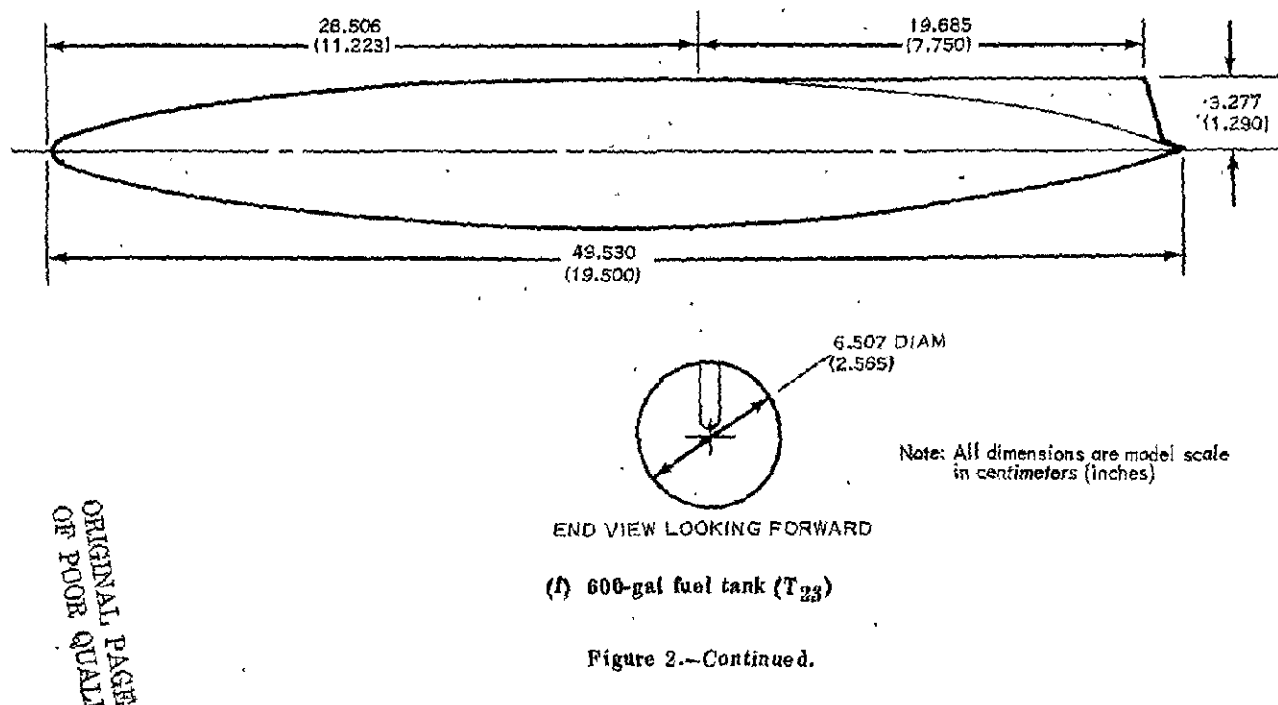


VIEW LOOKING FORWARD

Note: All dimensions are model scale  
in centimeters (inches)

(e) Sparrows (T<sub>25</sub>)

Figure 2.-Continued.



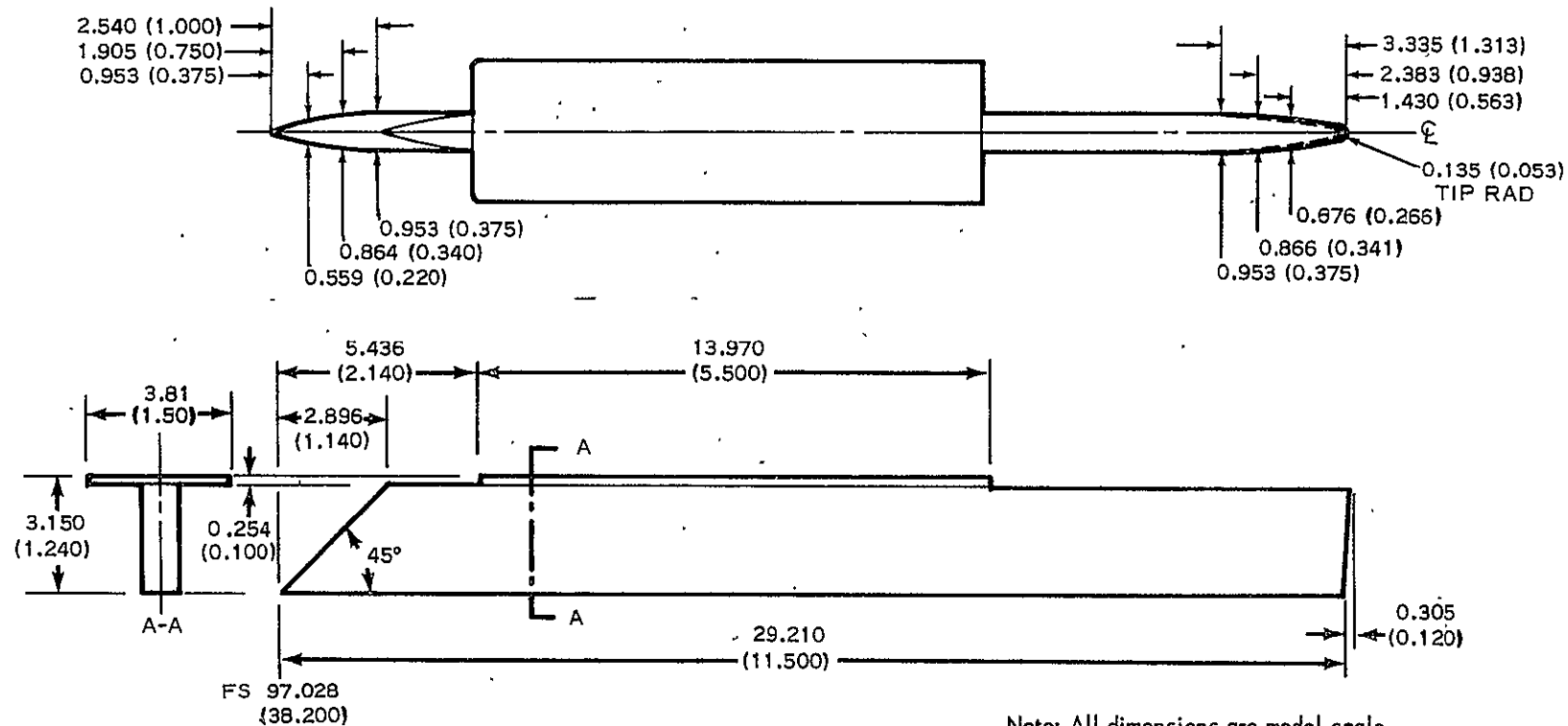
(g) Inboard wing pylon (Y<sub>22</sub>)

Figure 2--Continued.

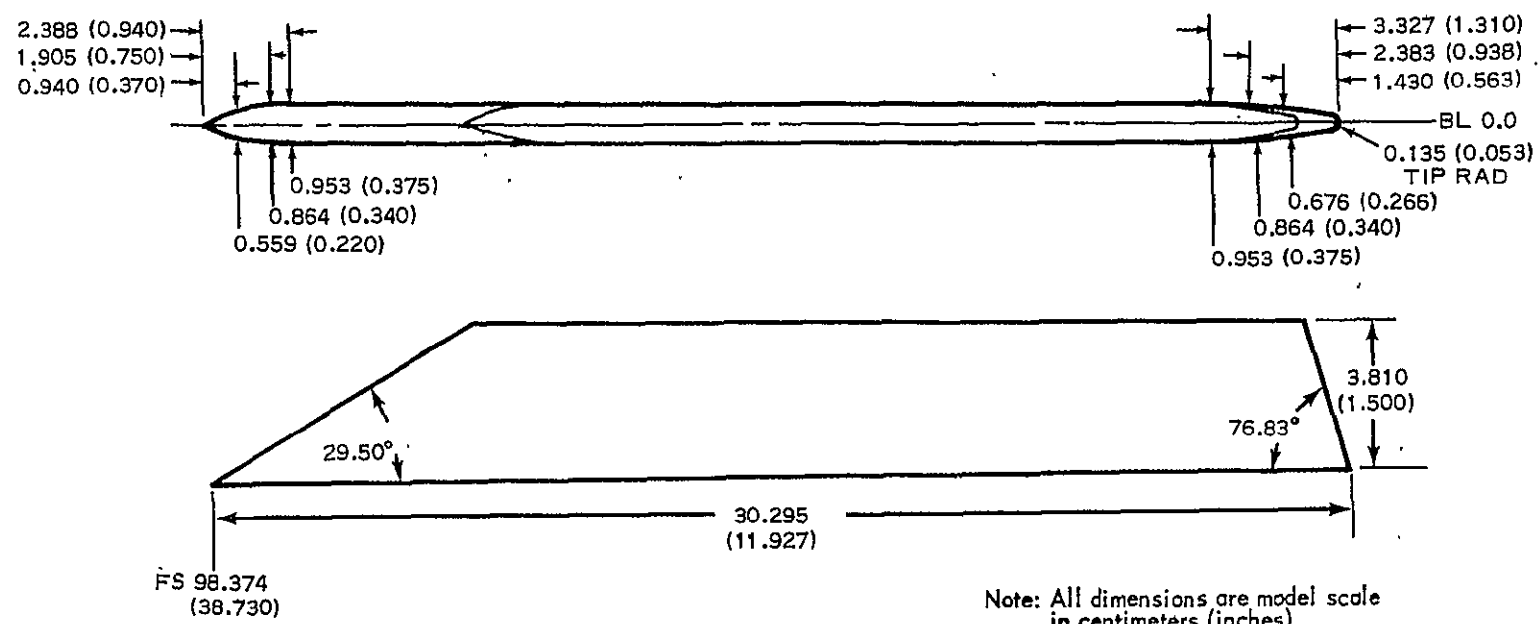
(h) Center pylon (Y<sub>24</sub>)

Figure 2.--Continued.

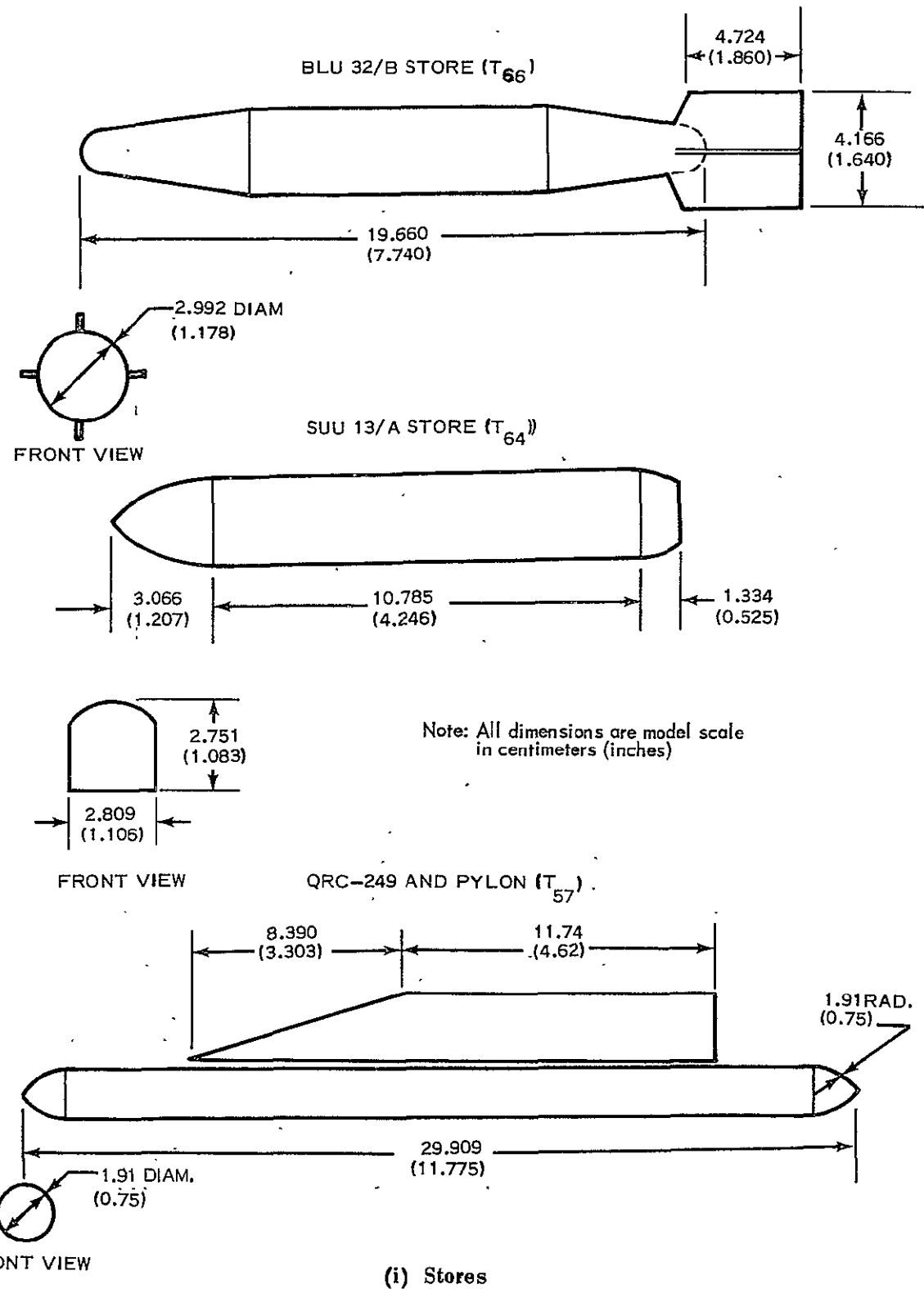
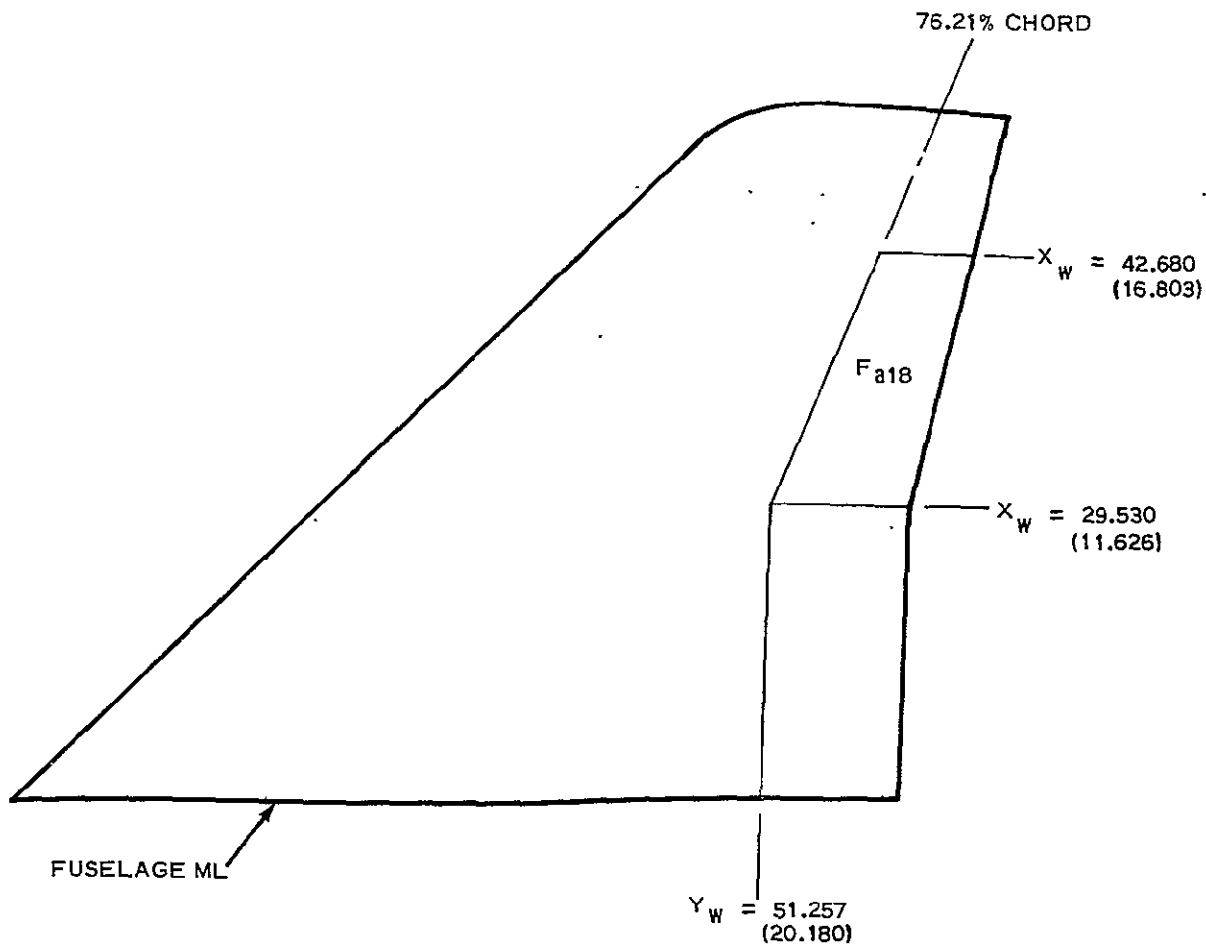


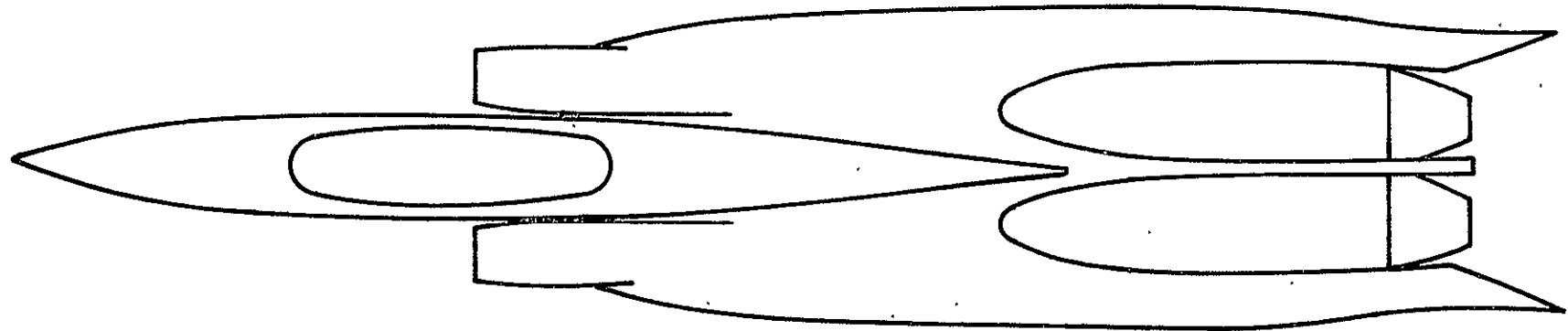
Figure 2.--Continued.



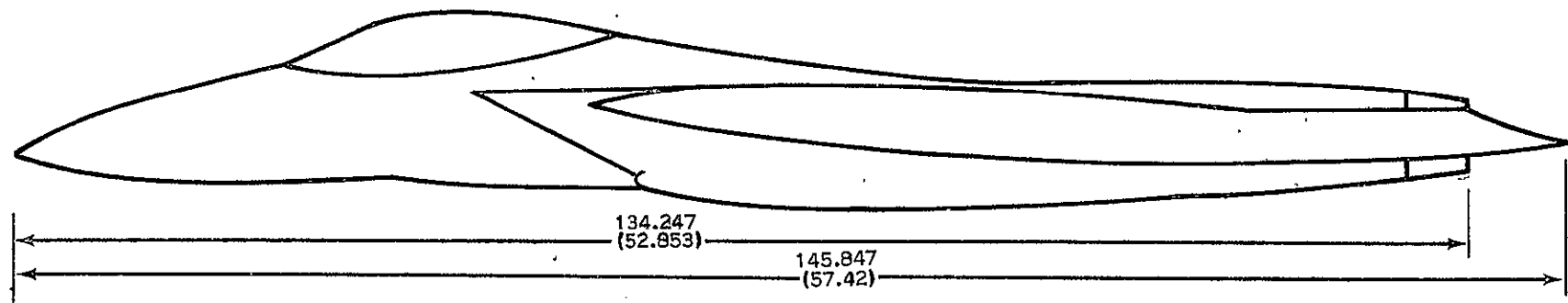
Note: All dimensions are model scale  
in centimeters (inches)

(j) Aileron (F<sub>a18</sub>)

Figure 2.—Continued.



PLAN VIEW

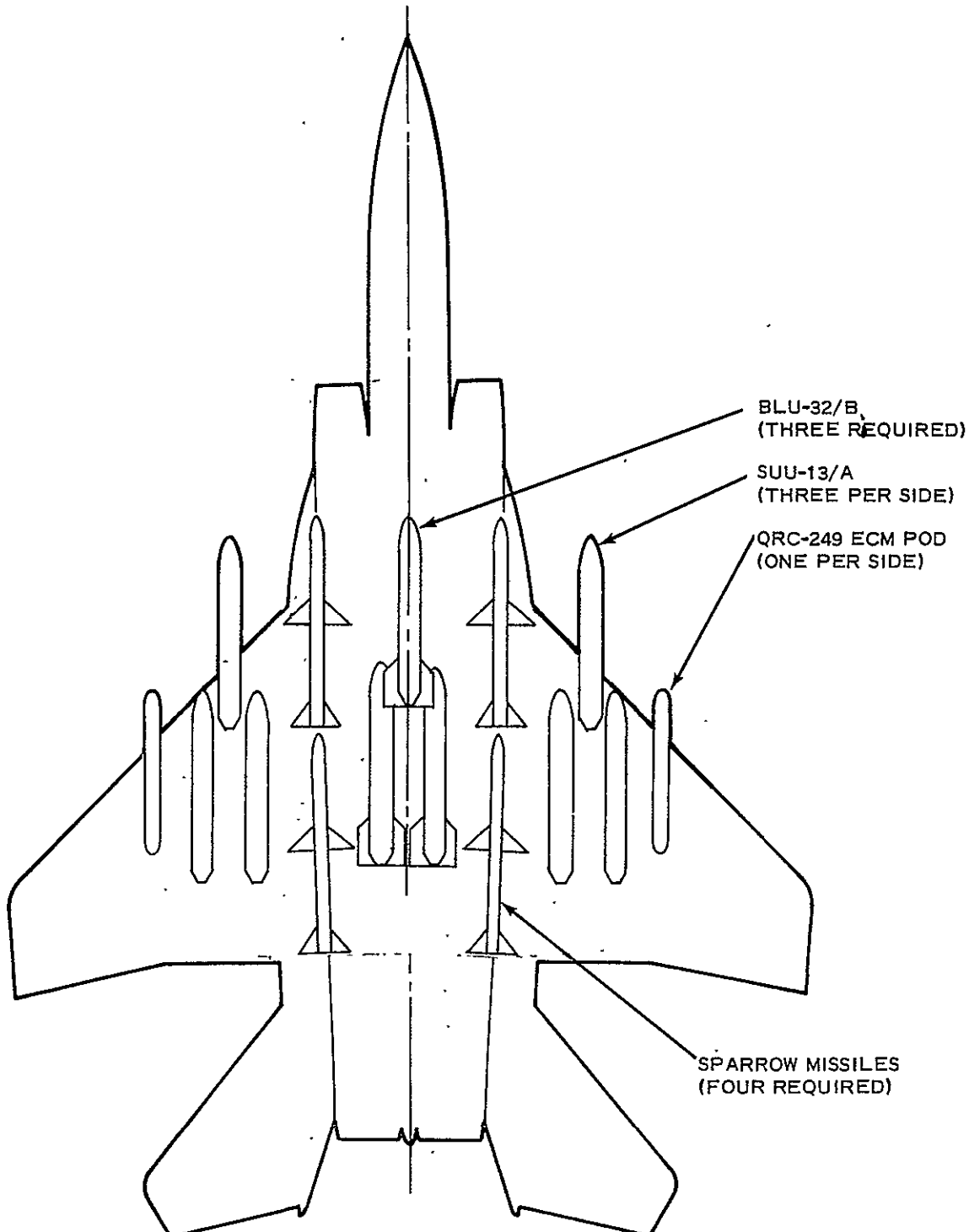


SIDE VIEW

(k) B<sub>156</sub> fuselage with M<sub>12</sub> radome

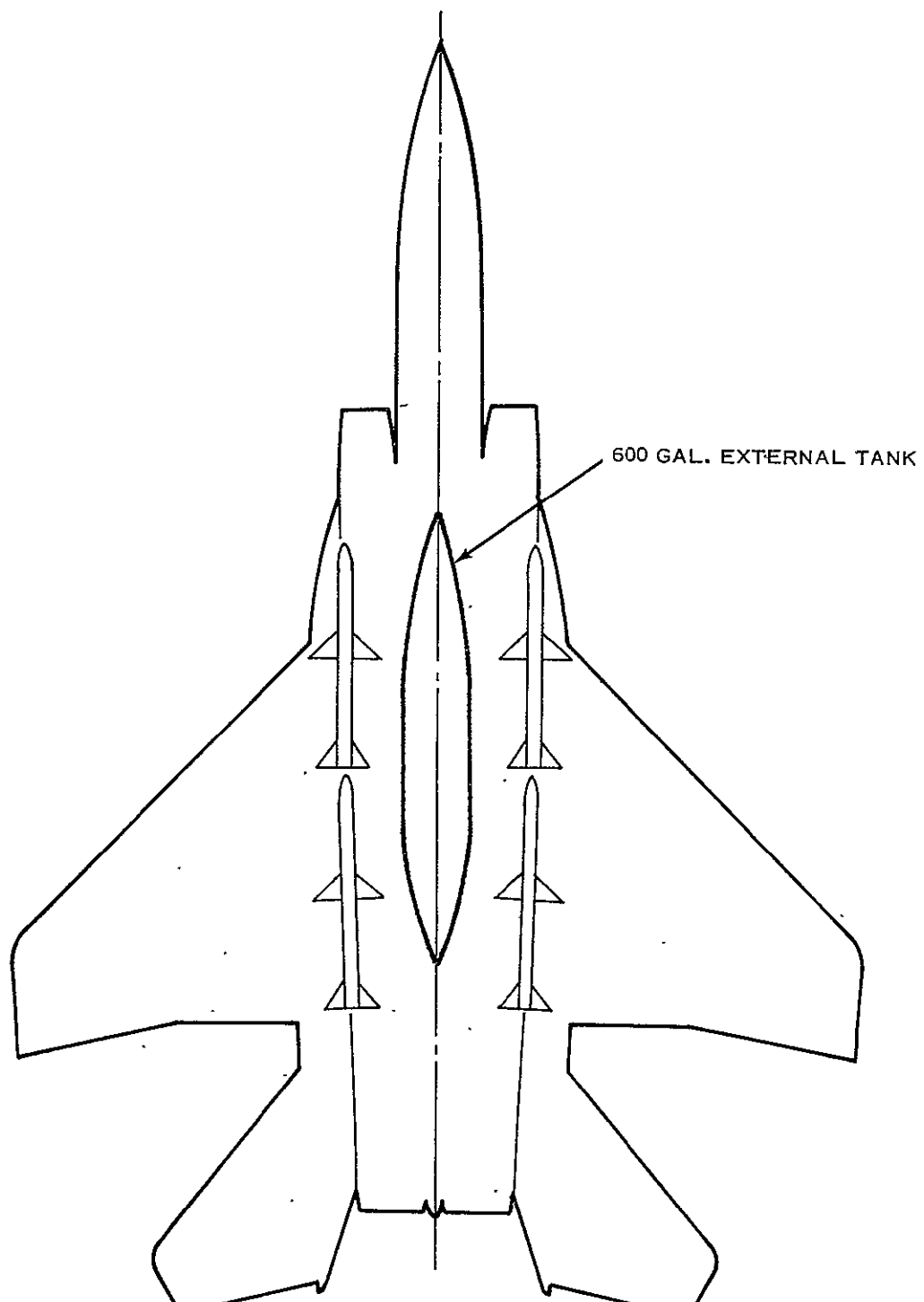
Note: All dimensions are model scale  
in centimeters (inches)

Figure 2.—Continued.



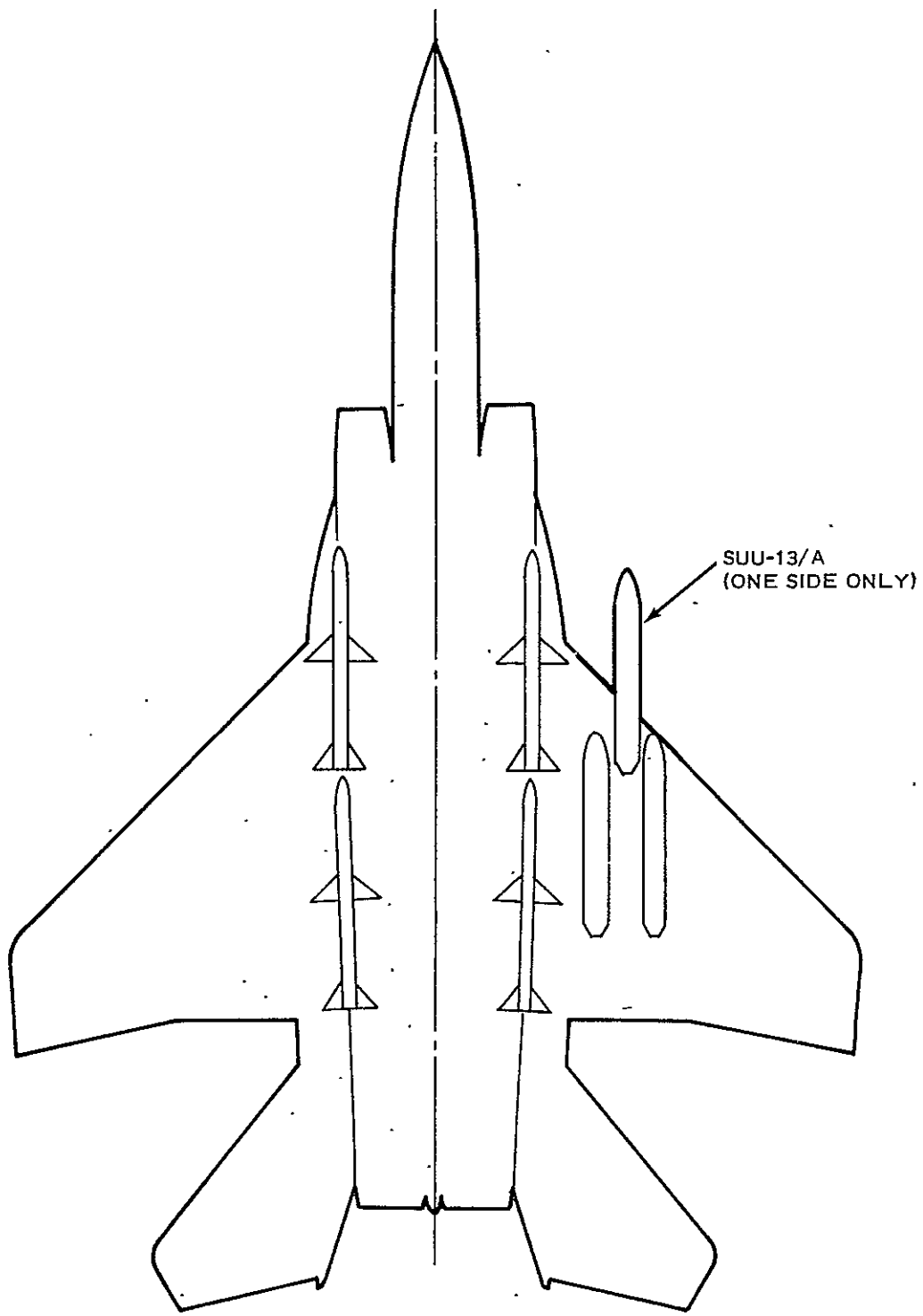
(l) External store loadings

Figure 2.--Continued.



(m) External store loadings

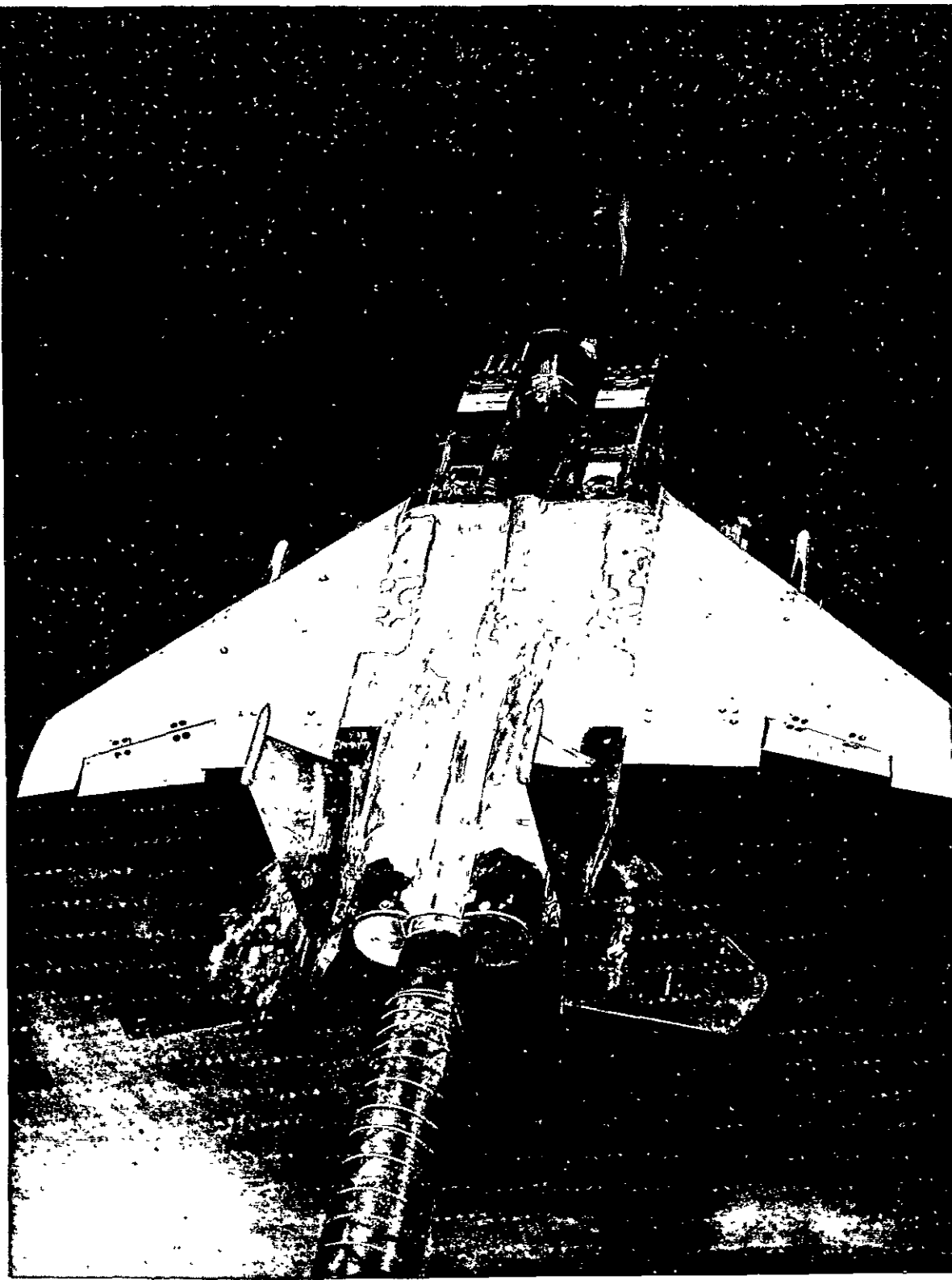
Figure 2.--Continued.



(n) External store loadings

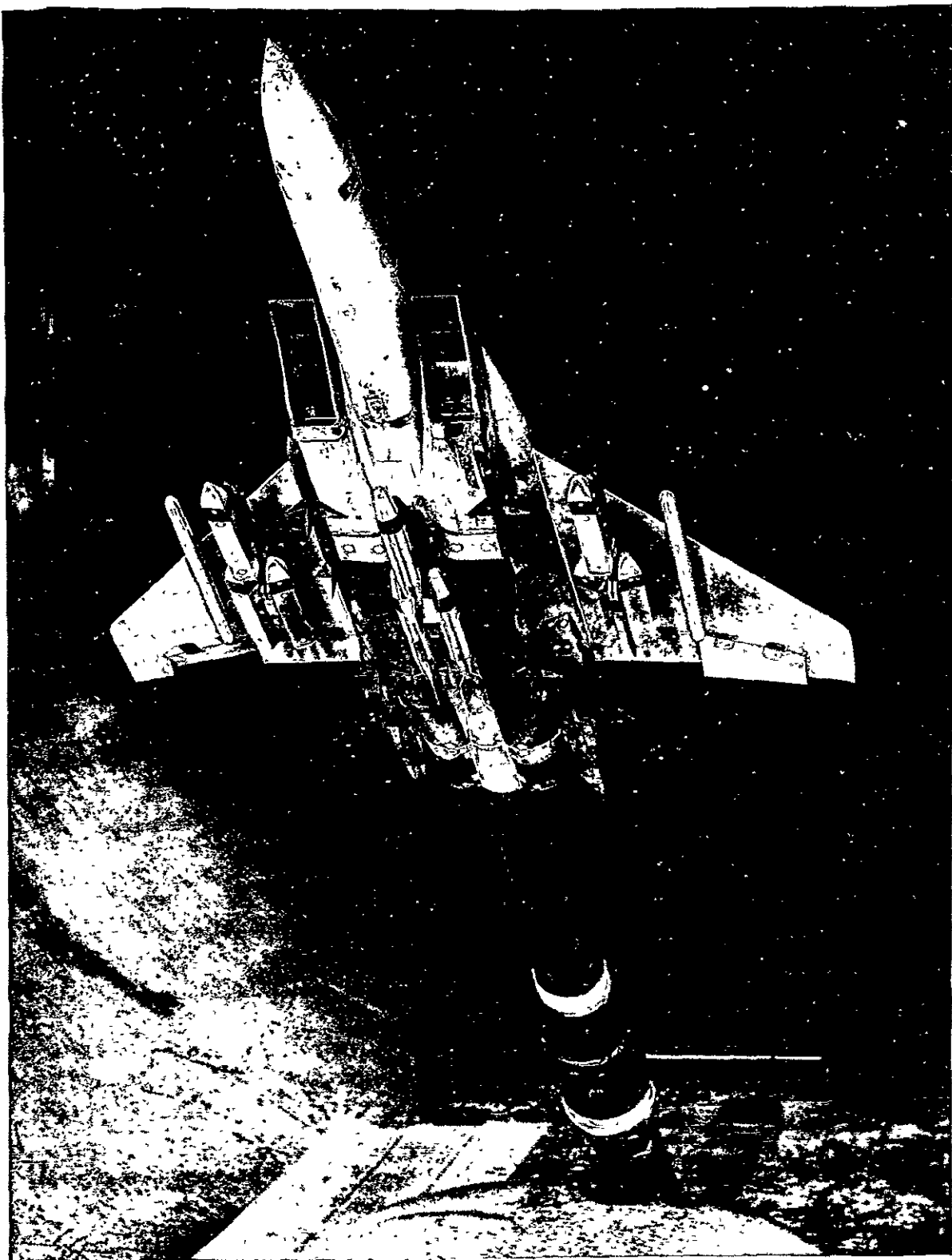
Figure 2.— Concluded.

ORIGINAL PAGE IS  
OF POOR QUALITY



(a) Top view

Figure 3. - Model installation photographs.



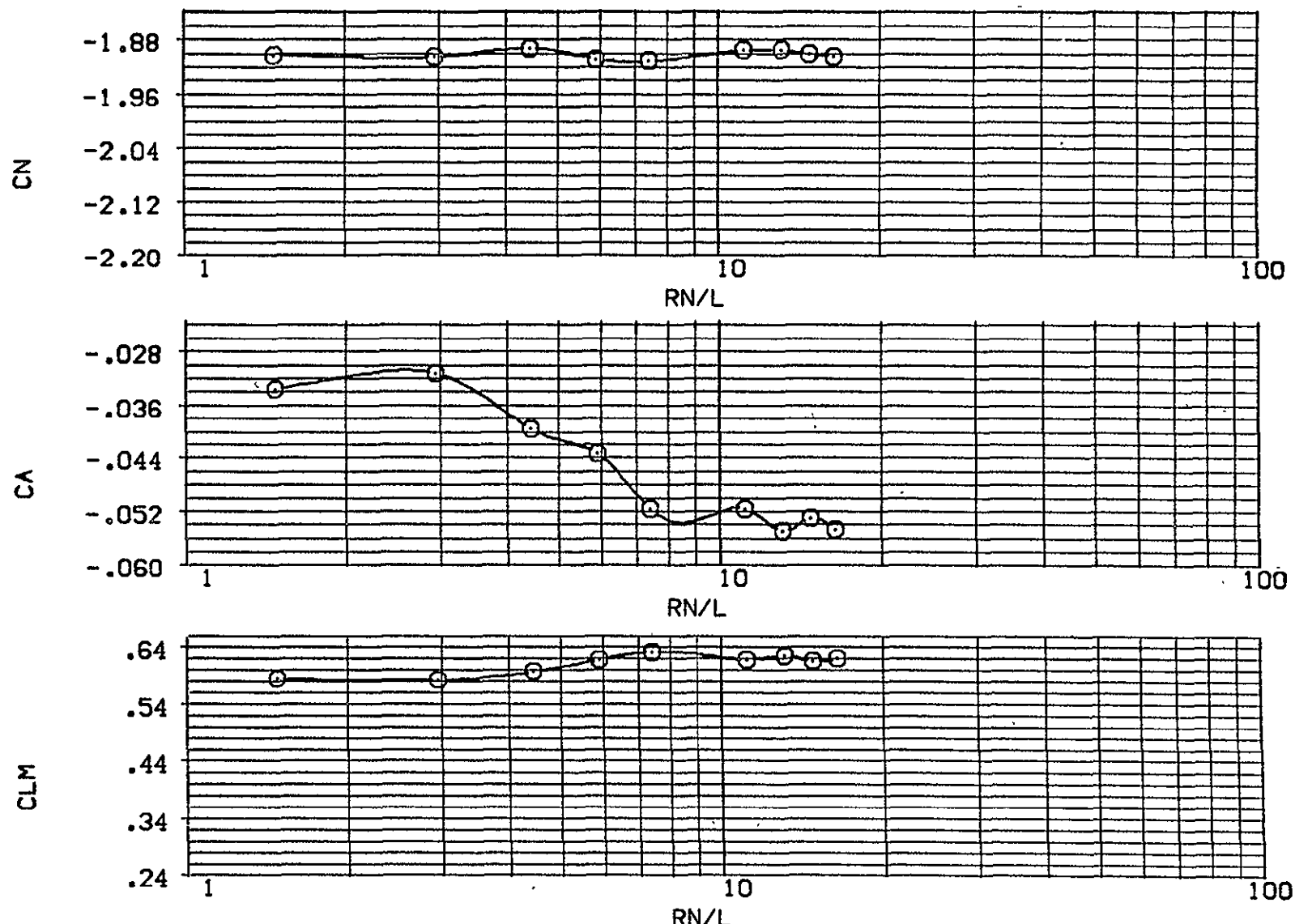
(b) Bottom view

Figure 3. - Concluded.

BASIC, RH<sub>0</sub>=11 - F

(DDW020)

SYMBOL	ALPHA	PARAMETRIC VALUES			DATASET	RN/L	DATA SOURCE	
		BETA	AIL-L	STB-L			DATASET	RN/L
O	-80.000	-20.000	.000	.000	DDW020	1.476	DDW021	2.952
		AIL-R	.000	STB-L	DDW022	4.428	DDW023	5.904
		STB-R	.000		DDW024	7.413	DDW025	11.152
					DDW026	13.120	DDW027	14.760
					DDW028	16.400		



ORIGINAL PAGE IS  
OF POOR QUALITY

FIG. 4 VARIATION OF AERO. CHAR. WITH REYNOLDS NO. AT VARIOUS ANGLES OF ATTACK.

SYMBOL	ALPHA	PARAMETRIC VALUES			.000	DATASET	DATA SOURCE		
		BETA	AIL-L	STB-L			RN/L	DATASET	RN/L
O	-70.000	-20.000	.000	.000	DDW020	1.476	DDW021	2.952	
		AIL-R	.000	STB-L	DDW022	4.428	DDW023	5.904	
		STB-R	.000		DDW024	7.413	DDW025	11.152	
					DDW026	13.120	DDW027	14.760	
					DDW028	16.400			

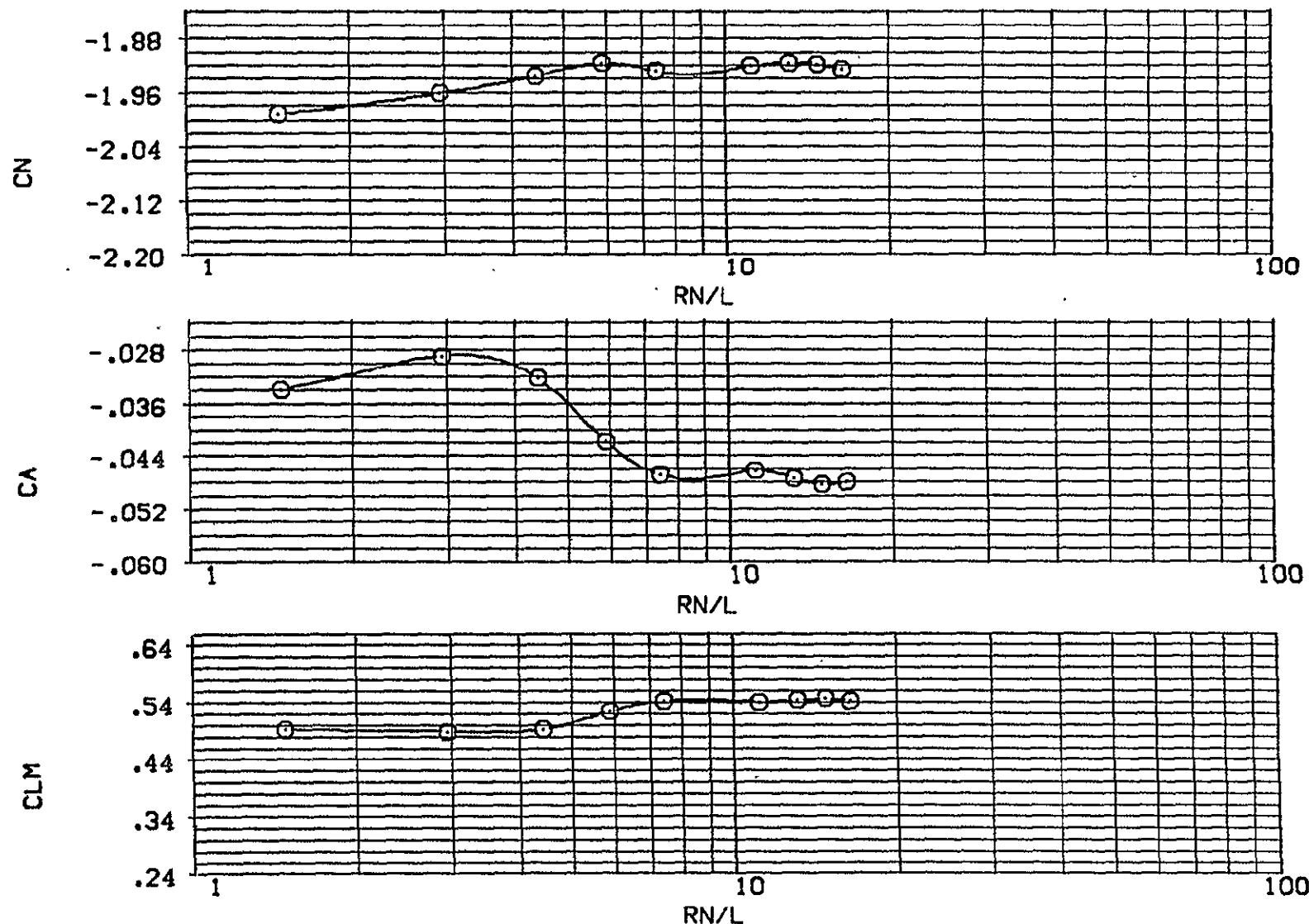


FIG. 4 VARIATION OF AERO. CHAR. WITH REYNOLDS NO. AT VARIOUS ANGLES OF ATTACK.

BASIC, RHO=11 - F

(DDW020)

SYMBOL	ALPHA	BETA	PARAMETRIC VALUES	.000	DATASET	RN/L	DATA SOURCE	DATASET	RN/L
O	-60.000	BET <sub>A</sub>	-20.000	AIL-L	.000	DDW020	1.476	DDW021	2.952
		AIL-R	.000	STB-L	.000	DDW022	4.428	DDW023	5.904
		STB-R	.000			DDW024	7.413	DDW025	11.152
						DDW026	13.120	DDW027	14.760
						DDW028	16.400		

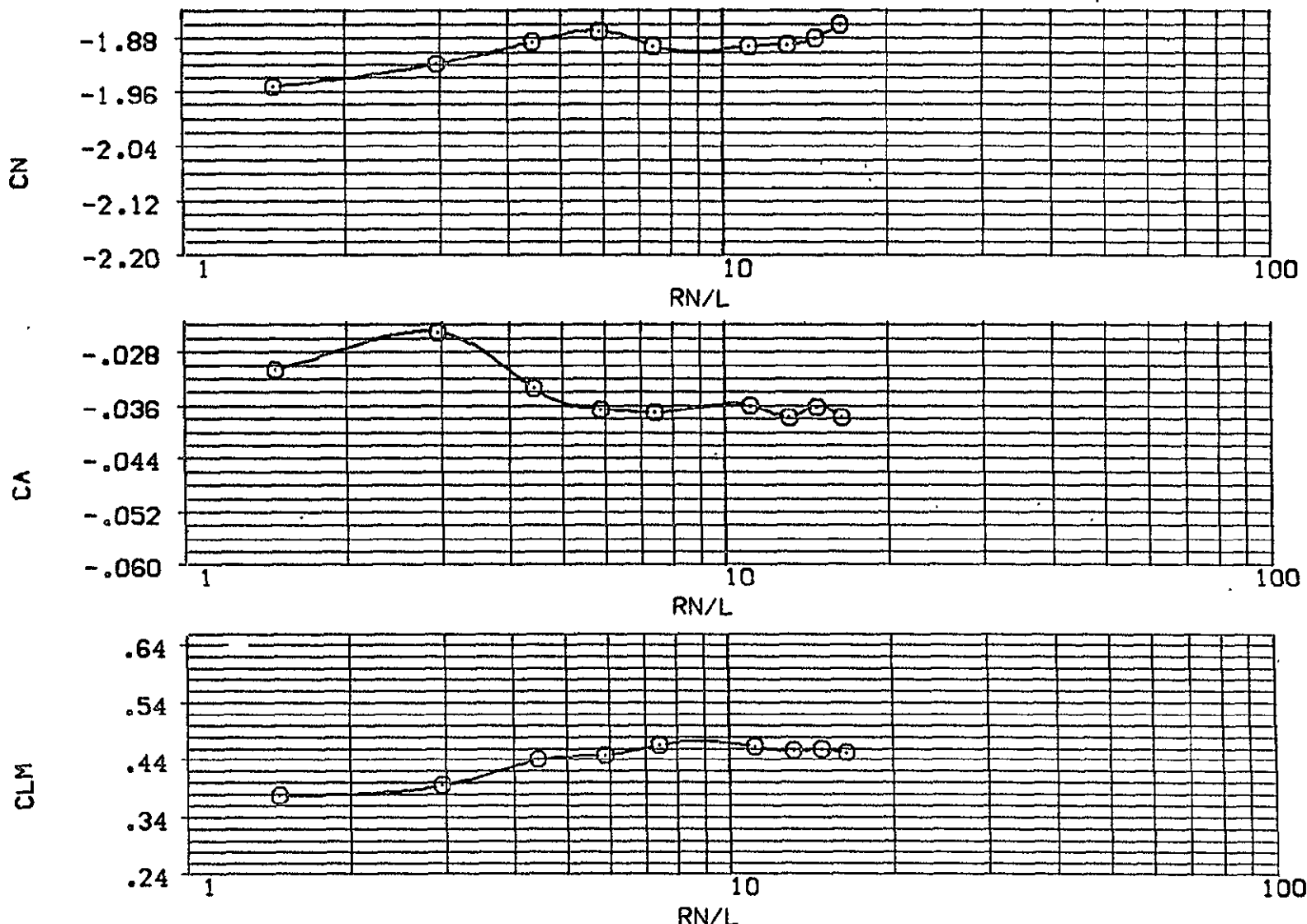


FIG. 4 VARIATION OF AERO. CHAR. WITH REYNOLDS NO. AT VARIOUS ANGLES OF ATTACK.

ORIGINAL PAGE IS  
OF POOR  
QUALITY

SYMBOL	ALPHA	BETA	PARAMETRIC VALUES	.000	DATASET	RN/L	DATA SOURCE
O	-50.000	BETA	-20.000	AIL-L	,000	DDW020	1.476
		AIL-R	,000	STB-L		DDW022	4.428
		STB-R	,000			DDW024	7.413
						DDW026	13.120
						DDW028	16.400

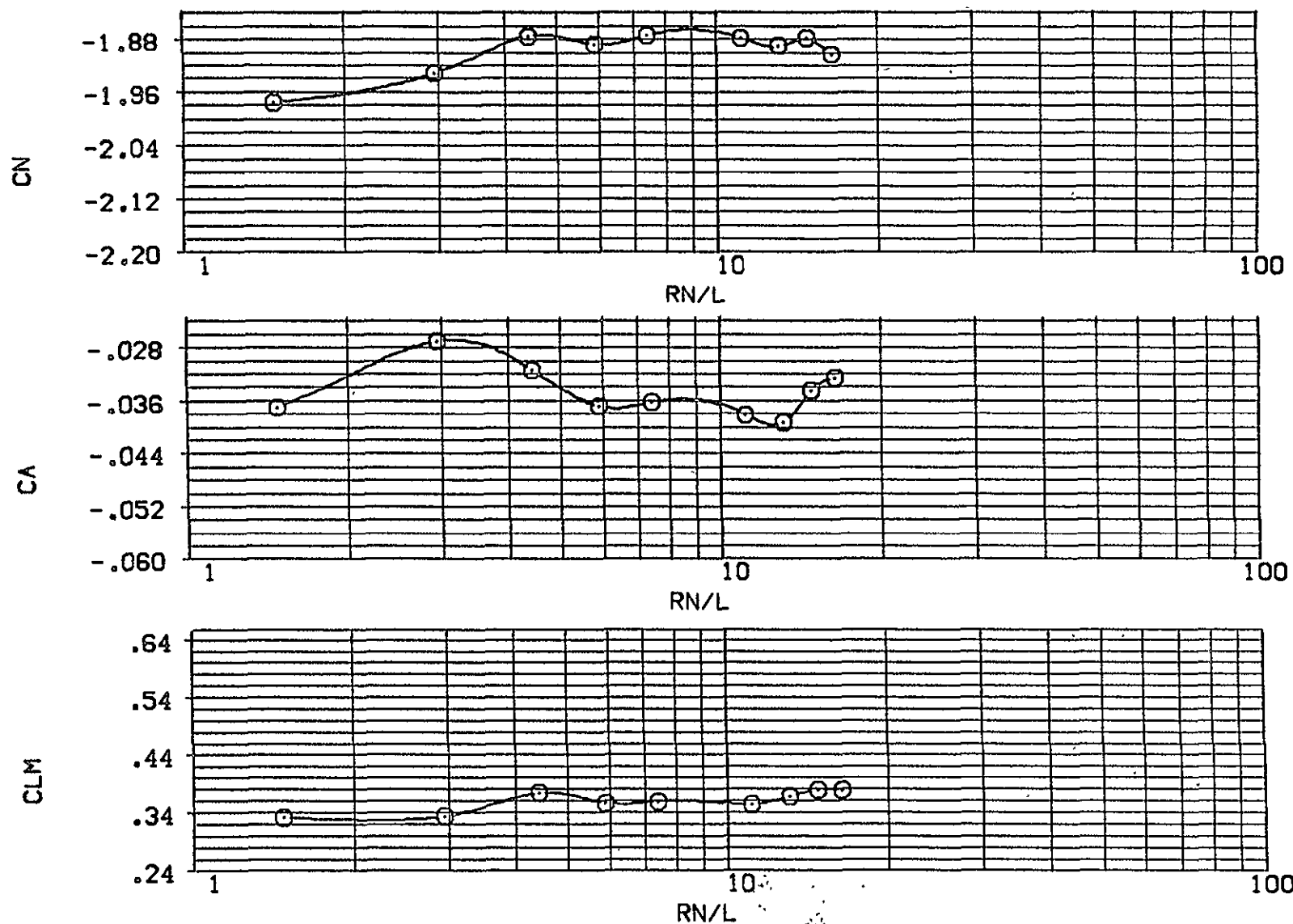


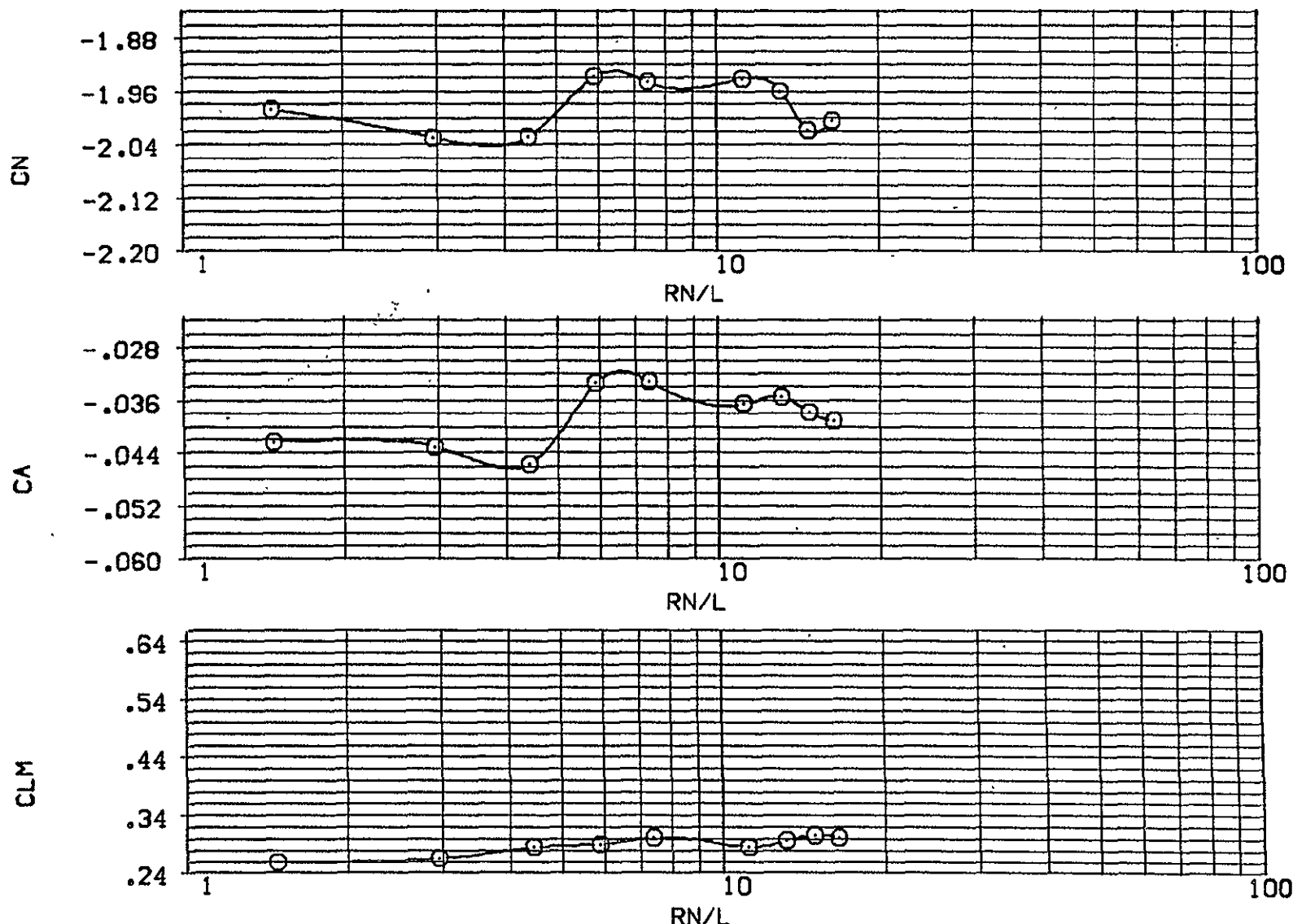
FIG. 4 VARIATION OF AERO. CHAR. WITH REYNOLDS NO. AT VARIOUS ANGLES OF ATTACK.

BASIC, RHO=11 - F

(DDW020)

SYMBOL    ALPHA    BETA    PARAMETRIC VALUES  
 O    -40.000    -20.000    AIL-L  
       AIL-R    .000    STB-L  
       STB-R    .000

.000	DATASET	RN/L	DATA SOURCE	DATASET	RN/L
.000	DDW020	1.476	DDW020	DDW021	2.952
	DDW022	4.428		DDW023	5.904
	DDW024	7.413		DDW025	11.152
	DDW026	13.120		DDW027	14.760
	DDW028	16.400			



36  
ORIGINAL PAGE IS  
OF POOR QUALITY

FIG. 4 VARIATION OF AERO. CHAR. WITH REYNOLDS NO. AT VARIOUS ANGLES OF ATTACK.

SYMBOL	ALPHA	PARAMETRIC VALUES			DATASET	DATA SOURCE		
		BETA	AIL-L	STB-L		RN/L	DATASET	RN/L
O	-80.000	.000	.000	.000	DDW020	1.476	DDW021	2.952
					DDW022	4.428	DDW023	5.904
					DDW024	7.413	DDW025	11.152
					DDW026	13.120	DDW027	14.760
					DDW028	16.400		

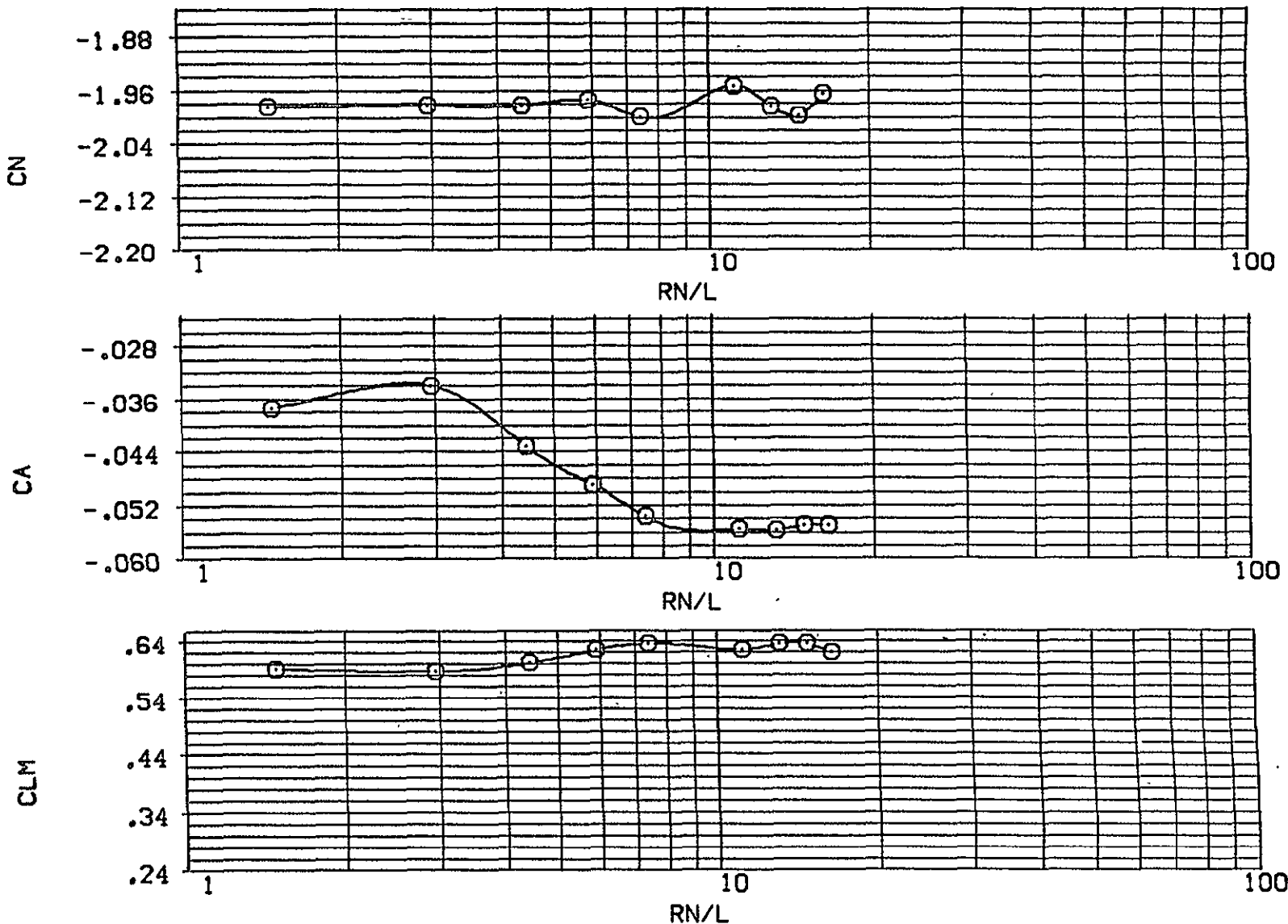


FIG. 4 VARIATION OF AERO. CHAR. WITH REYNOLDS NO. AT VARIOUS ANGLES OF ATTACK.

BASIC, RH0=11 - F

(DDW020)

SYMBOL O ALPHA -70.000 BETA -10.000 AIL-L .000  
 AIL-R .000 STB-L .000  
 STB-R .000

PARAMETRIC VALUES  
 .000 DATASET RN/L DATASET RN/L  
 DDW020 1.476 DDW021 2.952  
 DDW022 4.428 DDW023 5.904  
 DDW024 7.413 DDW025 11.152  
 DDW026 13.120 DDW027 14.760  
 DDW028 16.400

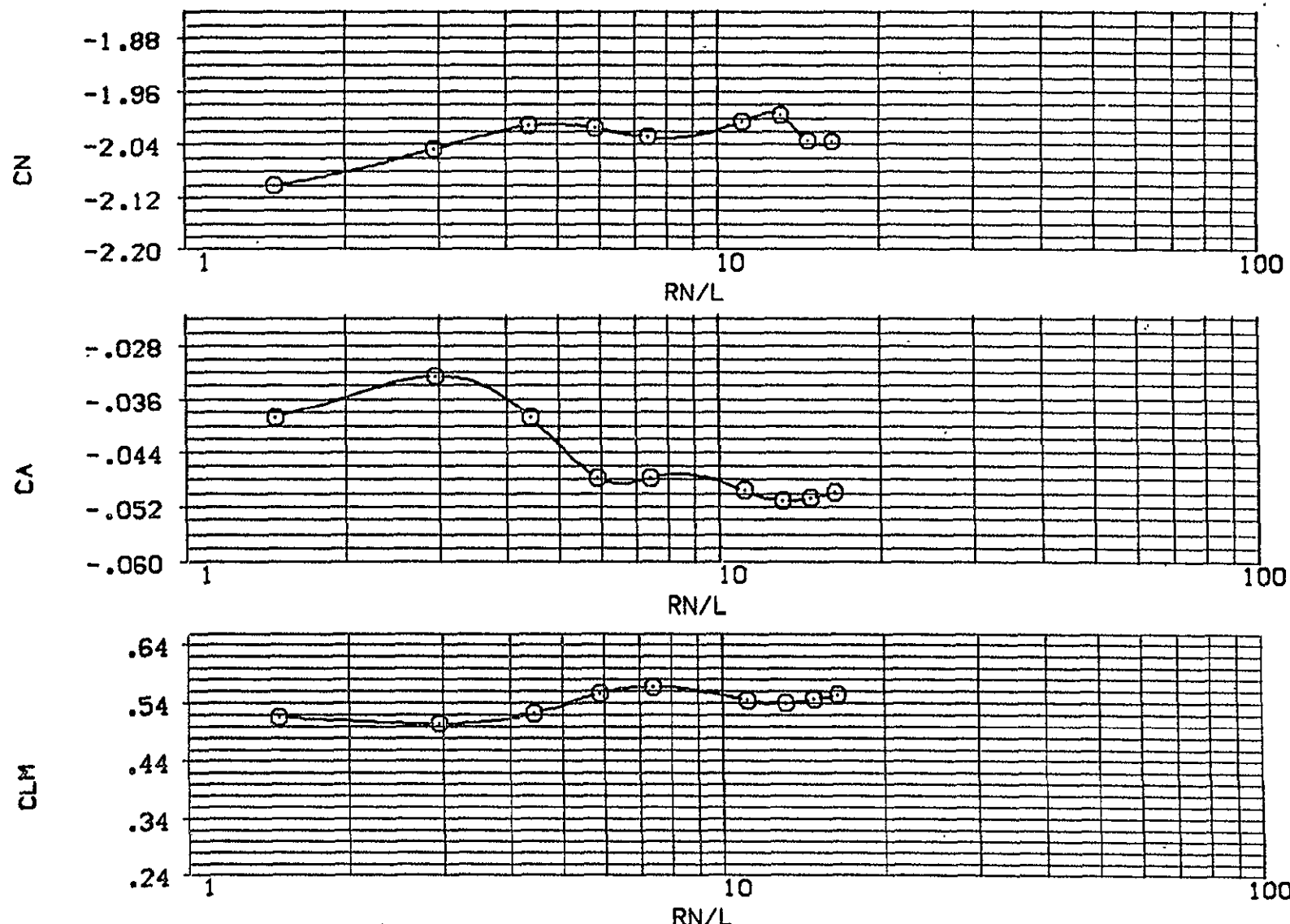
ORIGINAL PAGE IS  
OF POOR QUALITY

FIG. 4 VARIATION OF AERO. CHAR. WITH REYNOLDS NO. AT VARIOUS ANGLES OF ATTACK.

SYMBOL	ALPHA	PARAMETRIC VALUES			,000	DATASET	RN/L	DATA SOURCE	
		BETA	A1L-L	STB-L				DATASET	RN/L
O	-60.000	.000	.000	.000	DDW020	1.476	DDW021	2.952	
					DDW022	4.428	DDW023	5.904	
					DDW024	7.413	DDW025	11.152	
					DDW026	13.120	DDW027	14.760	
					DDW028	16.400			

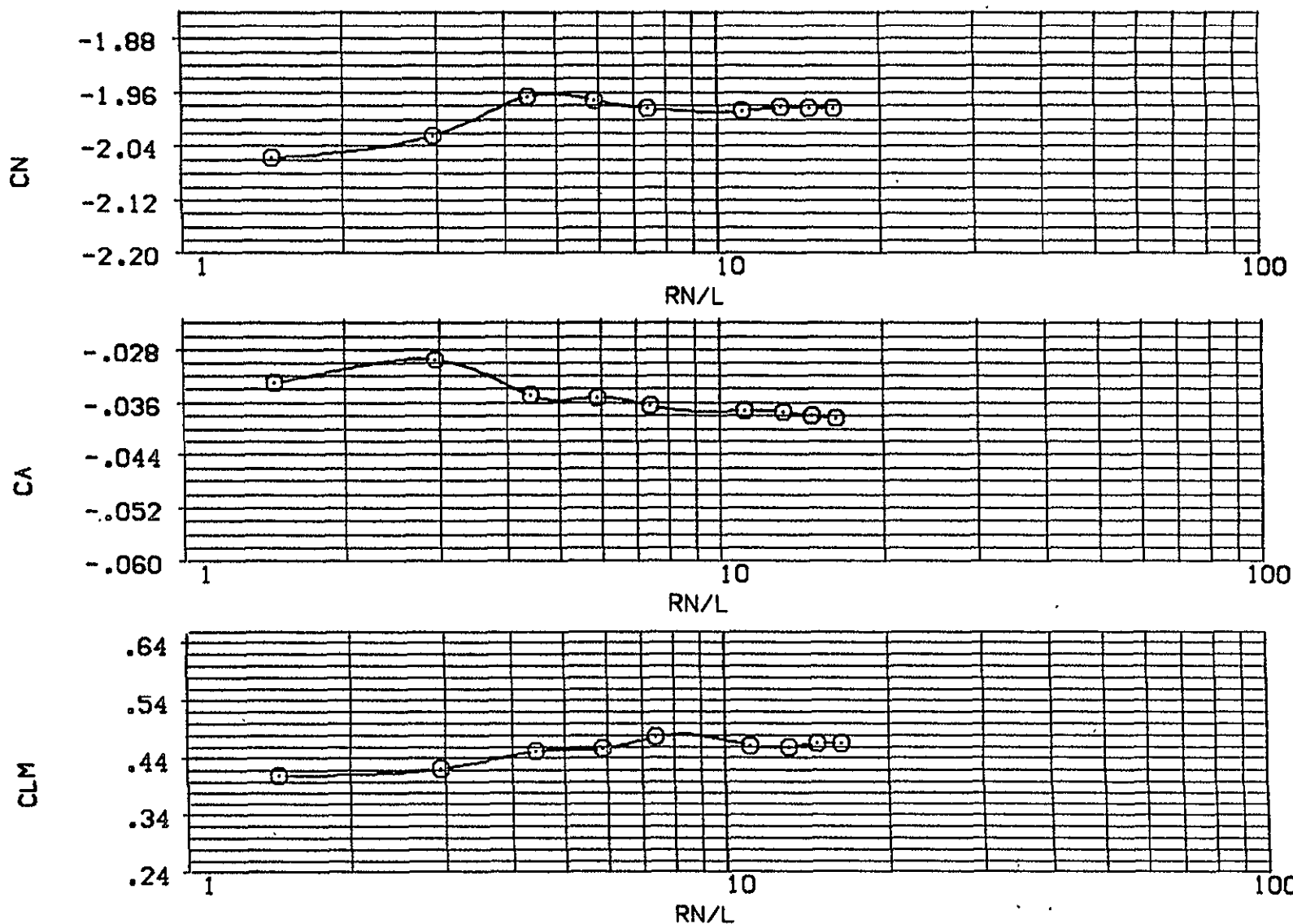


FIG. 4 VARIATION OF AERO. CHAR. WITH REYNOLDS NO. AT VARIOUS ANGLES OF ATTACK.

BASIC, RHO=11 - F

(DDW020)

SYMBOL	ALPHA	BETA	PARAMETRIC VALUES	.000	DATASET	RN/L	DATA SOURCE	DATASET	RN/L
O	-50.000	-10.000	AIL-L	.000	DDW020	1.476	DDW021	2.952	
		AIL-R	.000	DDW022	4.428	DDW023	5.904		
		STB-R	.000	DDW024	7.413	DDW025	11.152		
				DDW026	13.120	DDW027	14.760		
				DDW028	16.400				

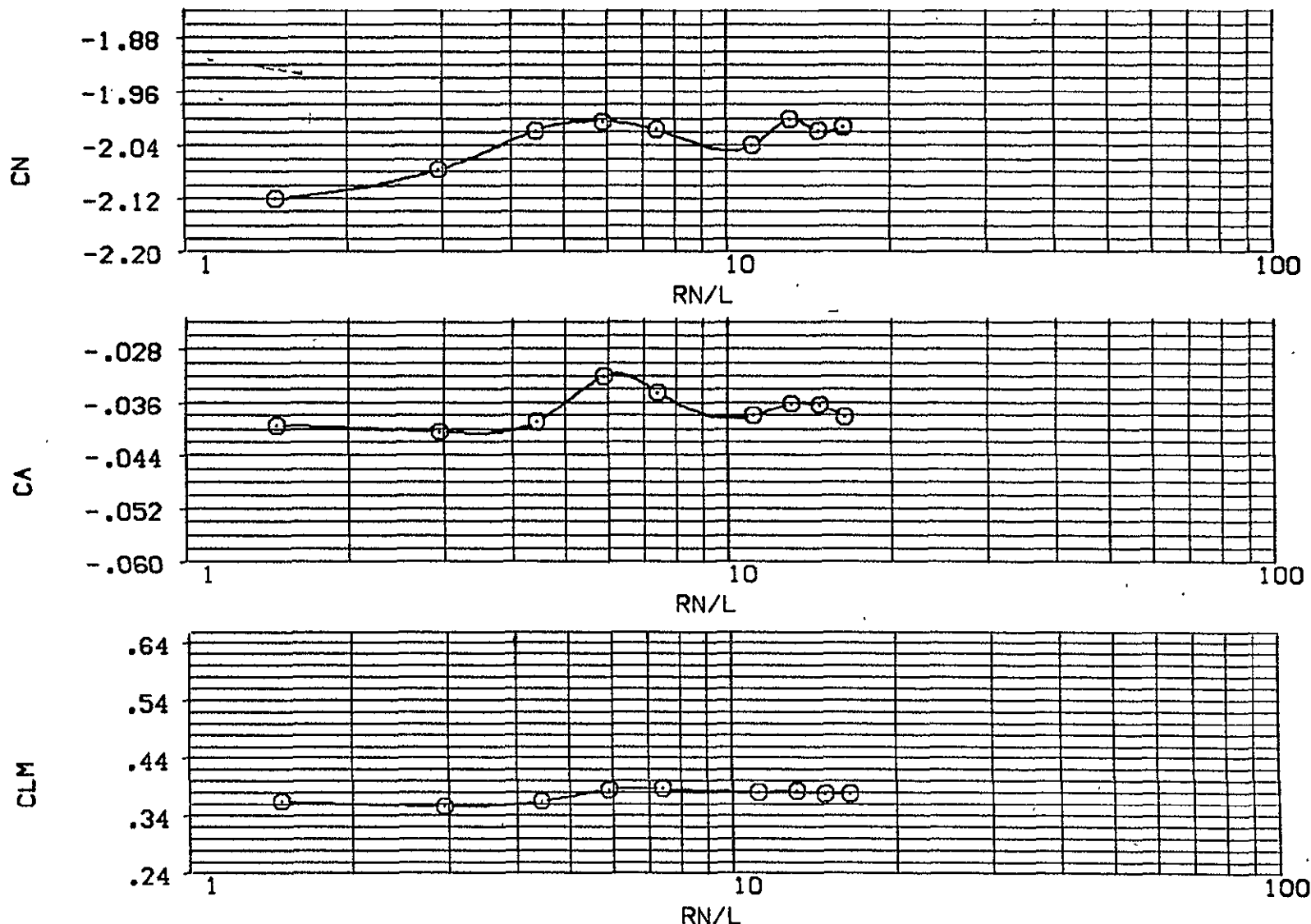
ORIGINAL PAGE IS  
OF POOR QUALITY

FIG. 4 VARIATION OF AERO. CHAR. WITH REYNOLDS NO. AT VARIOUS ANGLES OF ATTACK.

SYMBOL	ALPHA	PARAMETRIC VALUES			.000	DATASET	DATA SOURCE		
		BETA	AIL-L	STB-L			RN/L	DATASET	RN/L
O	-40.000	.000	.000	.000	DDW020	1.476	DDW021	2.952	
					DDW022	4.428	DDW023	5.904	
					DDW024	7.413	DDW025	11.152	
					DDW026	13.120	DDW027	14.760	
					DDW028	16.400			

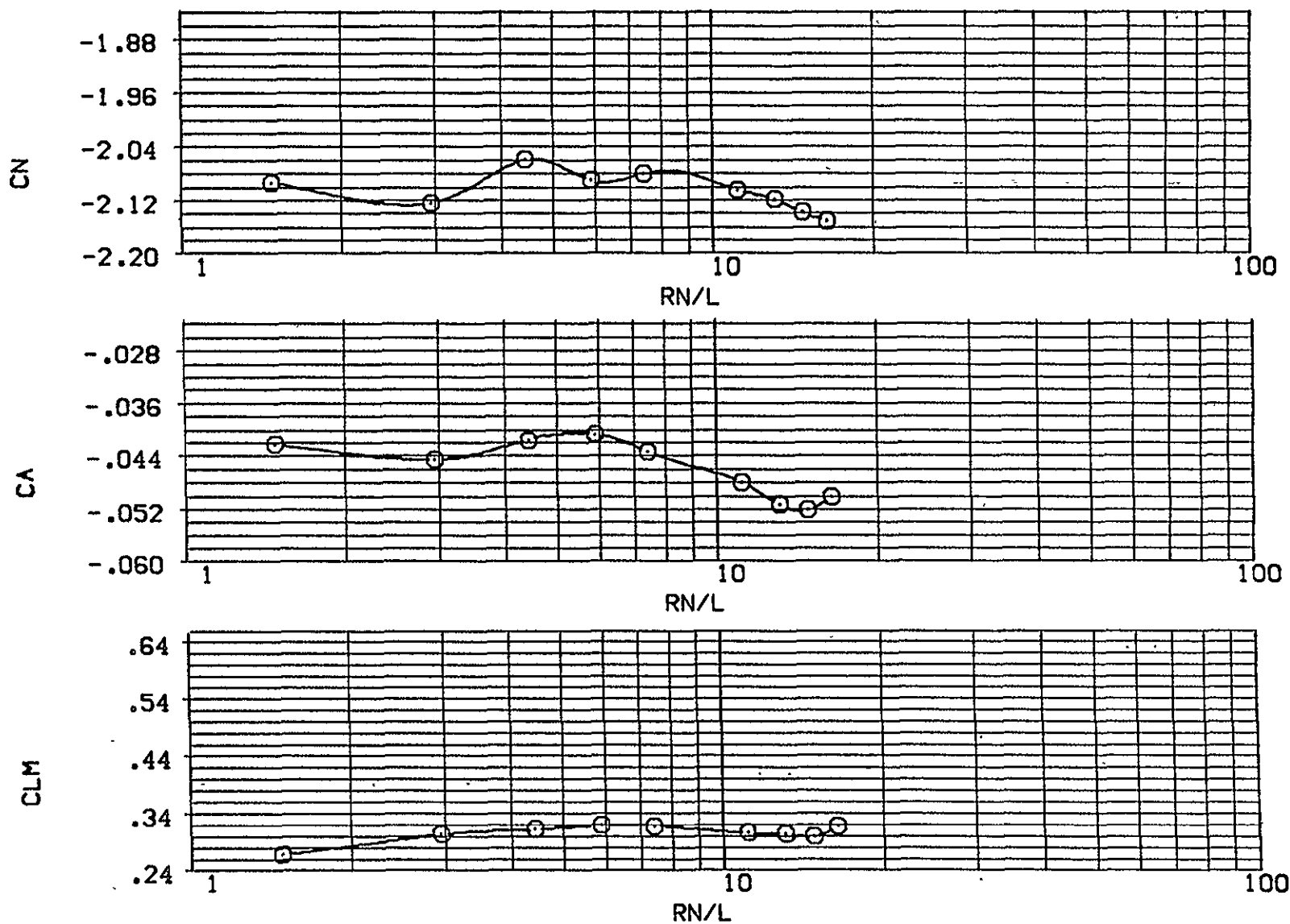


FIG. 4 VARIATION OF AERO. CHAR. WITH REYNOLDS NO. AT VARIOUS ANGLES OF ATTACK.

BASIC, RH<sub>0</sub>=11 - F

(DDW020)

SYMBOL	ALPHA	PARAMETRIC VALUES			DATASET	RN/L	DATA SOURCE	
		BETA	.000	AIL-L			.000	DATASET
O	-80.000	AIL-R	.000	STB-L	DDW020	1.476	DDW021	2.952
		STB-R	.000		DDW022	4.428	DDW023	5.904
					DDW024	7.413	DDW025	11.152
					DDW026	13.120	DDW027	14.760
					DDW028	16.400		

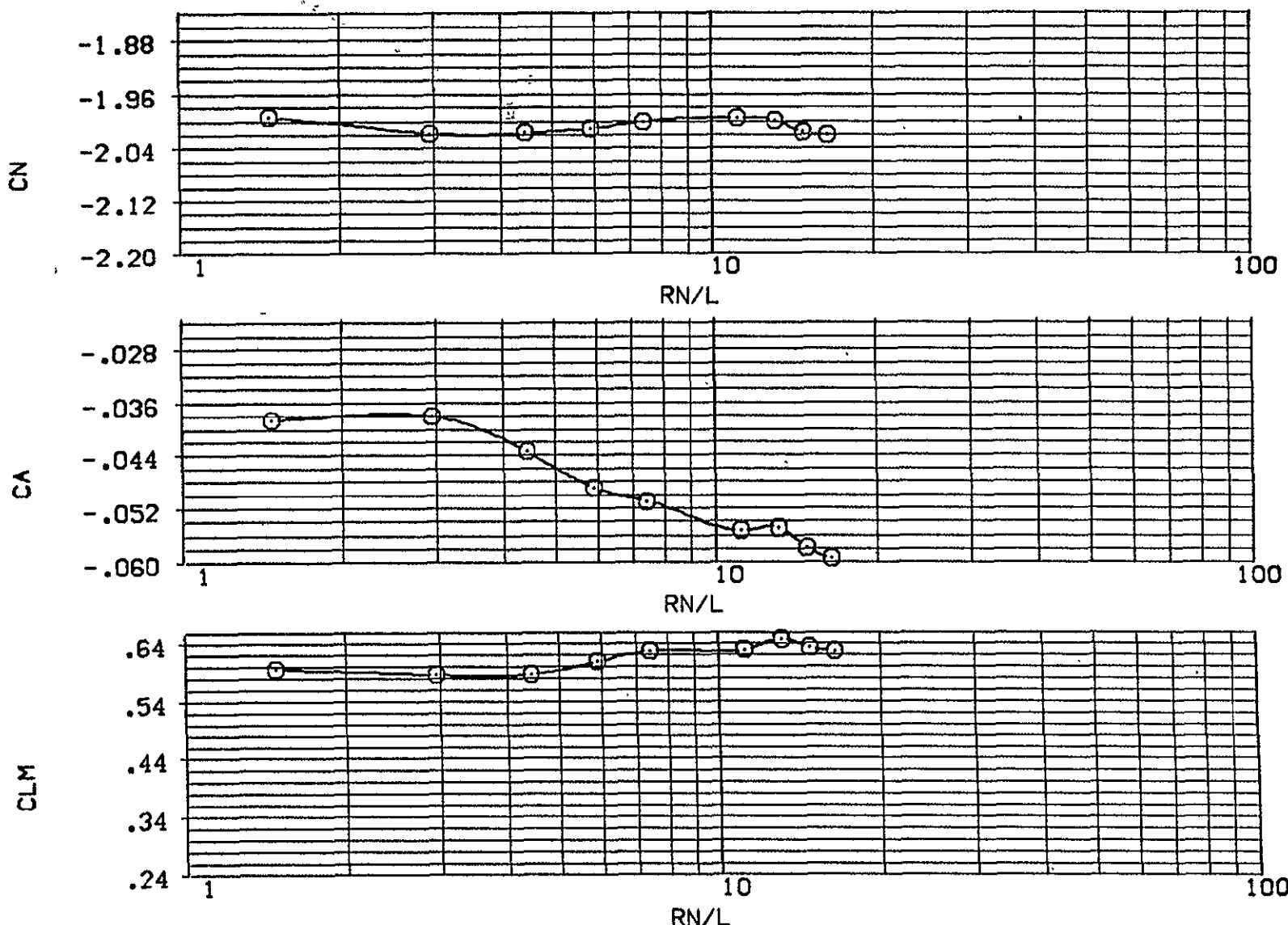
ORIGINAL PAGE IS  
OF POOR QUALITY

FIG. 4 VARIATION OF AERO. CHAR. WITH REYNOLDS NO. AT VARIOUS ANGLES OF ATTACK.

SYMBOL	ALPHA	BETA	PARAMETRIC VALUES	.000	AIL-L	STB-L	.000	DATASET	DATA SOURCE	RN/L	DATASET	RN/L
O	-70.000							DDW020	DDW021	1.476	DDW021	2.952
		AIR-R	.000		STB-L		.000	DDW022	DDW023	4.428	DDW023	5.904
		STB-R	.000					DDW024	DDW025	7.413	DDW025	11.152
								DDW026	DDW027	13.120	DDW027	14.760
								DDW028		16.400		

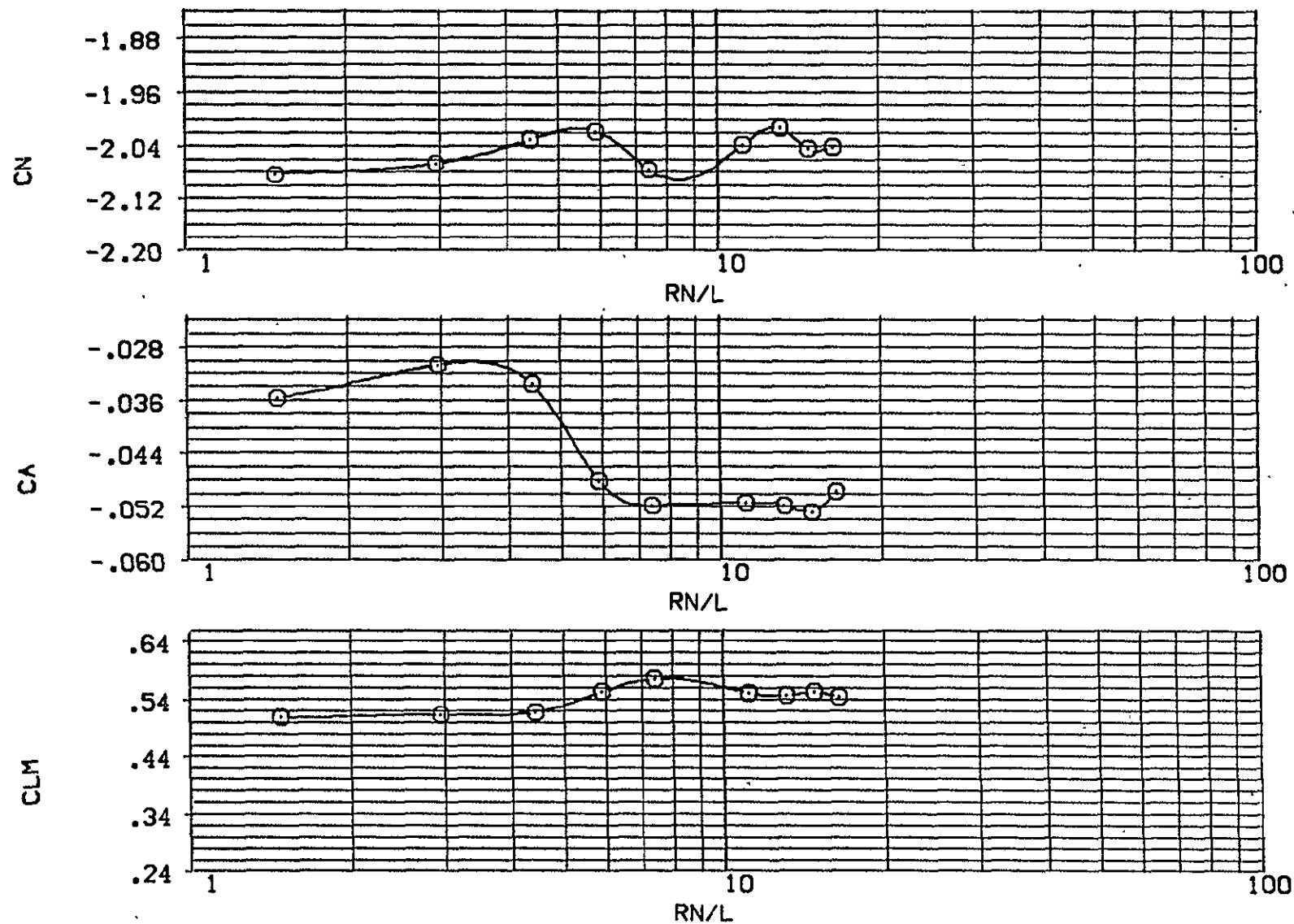
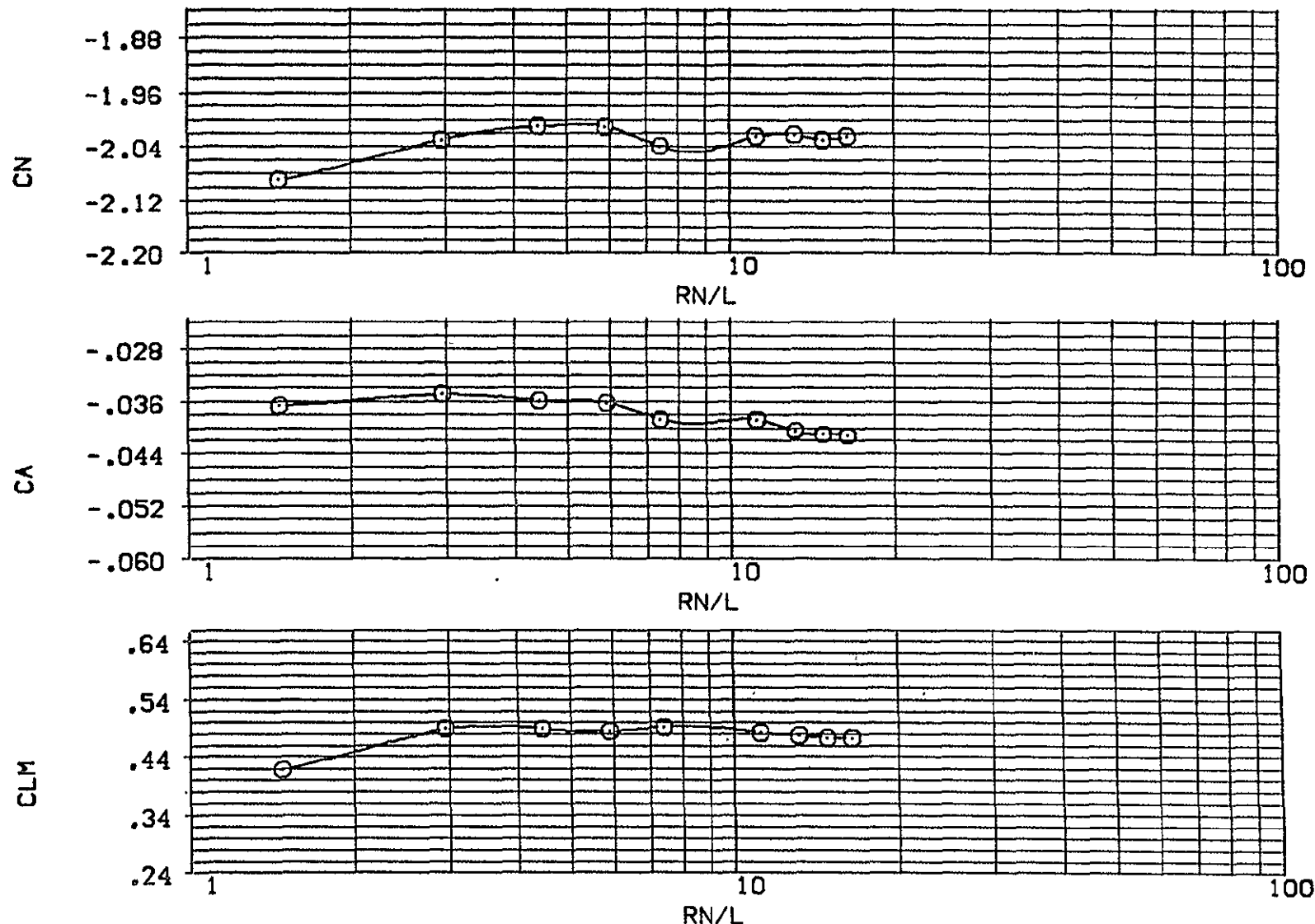


FIG. 4 VARIATION OF AERO. CHAR. WITH REYNOLDS NO. AT VARIOUS ANGLES OF ATTACK.

BASIC, RHO=11 - F

(DDW020)

SYMBOL	ALPHA	PARAMETRIC VALUES			DATASET	RN/L	DATA SOURCE	
		BETA	AIL-L	STB-L			DATASET	RN/L
O	-60.000	.000	AIL-R	.000	DDW020	1.476	DDW021	2.952
			STB-R	.000	DDW022	4.428	DDW023	5.904
					DDW024	7.413	DDW025	11.152
					DDW026	13.120	DDW027	14.760
					DDW028	16.400		



ORIGINAL PAGE IS  
OF POOR QUALITY

FIG. 4 VARIATION OF AERO. CHAR. WITH REYNOLDS NO. AT VARIOUS ANGLES OF ATTACK.

SYMBOL	ALPHA	PARAMETRIC VALUES			DATASET	RN/L	DATA SOURCE	
		BETA	AIL-L	STB-L			DATASET	RN/L
O	-50.000	.000	AIL-R	.000	DDW020	1.476	DDW021	2.952
			AIL-R	.000	DDW022	4.428	DDW023	5.904
			STB-R	.000	DDW024	7.413	DDW025	11.152
					DDW026	13.120	DDW027	14.760
					DDW028	16.400		

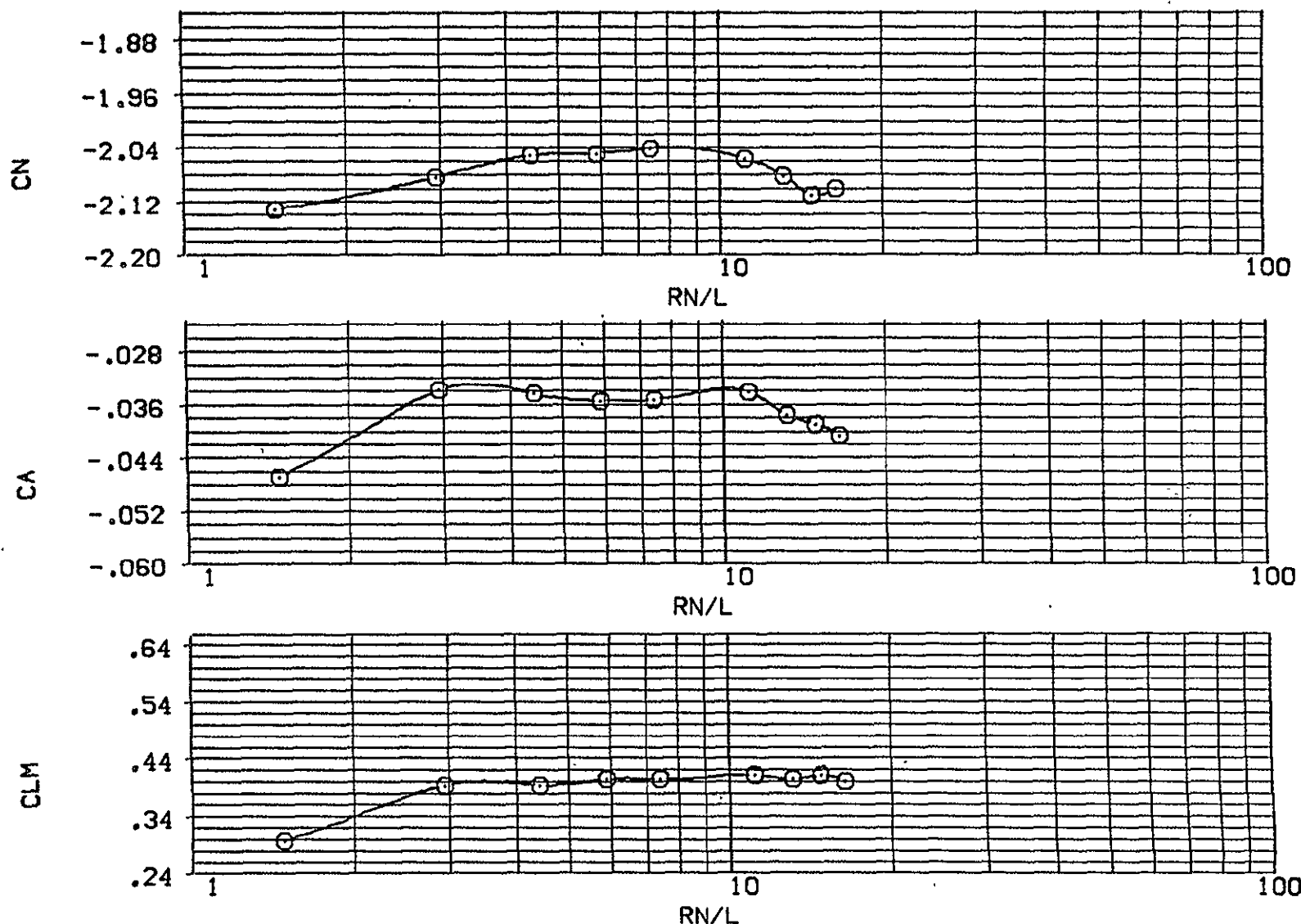
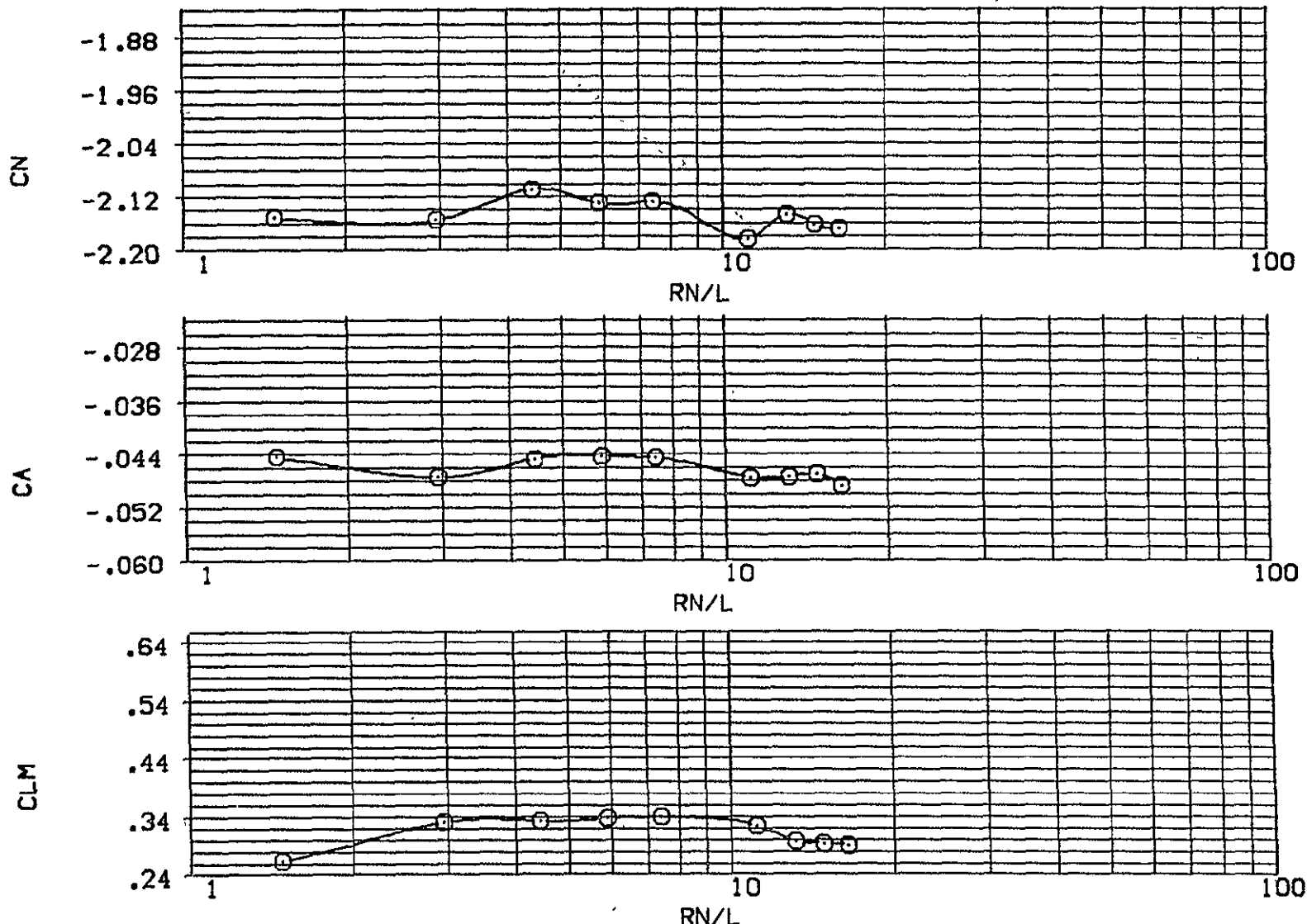


FIG. 4 VARIATION OF AERO. CHAR. WITH REYNOLDS NO. AT VARIOUS ANGLES OF ATTACK.

BASIC, RH<sub>0</sub>=11 - F

(DDW020)

SYMBOL	ALPHA	PARAMETRIC VALUES			DATASET	RN/L	DATA SOURCE		
		BETA	.000	AIL-L			.000	DDW020	1.476
O	-40.000	AIL-R	.000	STB-L	.000	DDW022	4.428	DDW023	5.904
		STB-R	.000			DDW024	7.413	DDW025	11.152
						DDW026	13.120	DDW027	14.760
						DDW028	16.400		



ORIGINAL PAGE IS  
ORIGINALLY POOR  
QUALITY

46

FIG. 4 VARIATION OF AERO. CHAR. WITH REYNOLDS NO. AT VARIOUS ANGLES OF ATTACK.

BASIC, RH0=11 - F

(DDW020)

SYMBOL	ALPHA	PARAMETRIC VALUES			DATASET	DATA SOURCE		
		BETA	AIL-L	STB-L		RN/L	DATASET	RN/L
O	-80.000	.000	.000	.000	DDW020	1.476	DDW021	2.952
					DDW022	4.428	DDW023	5.904
					DDW024	7.413	DDW025	11.152
					DDW026	13.120	DDW027 <sup>1</sup>	14.760
					DDW028	16.400		

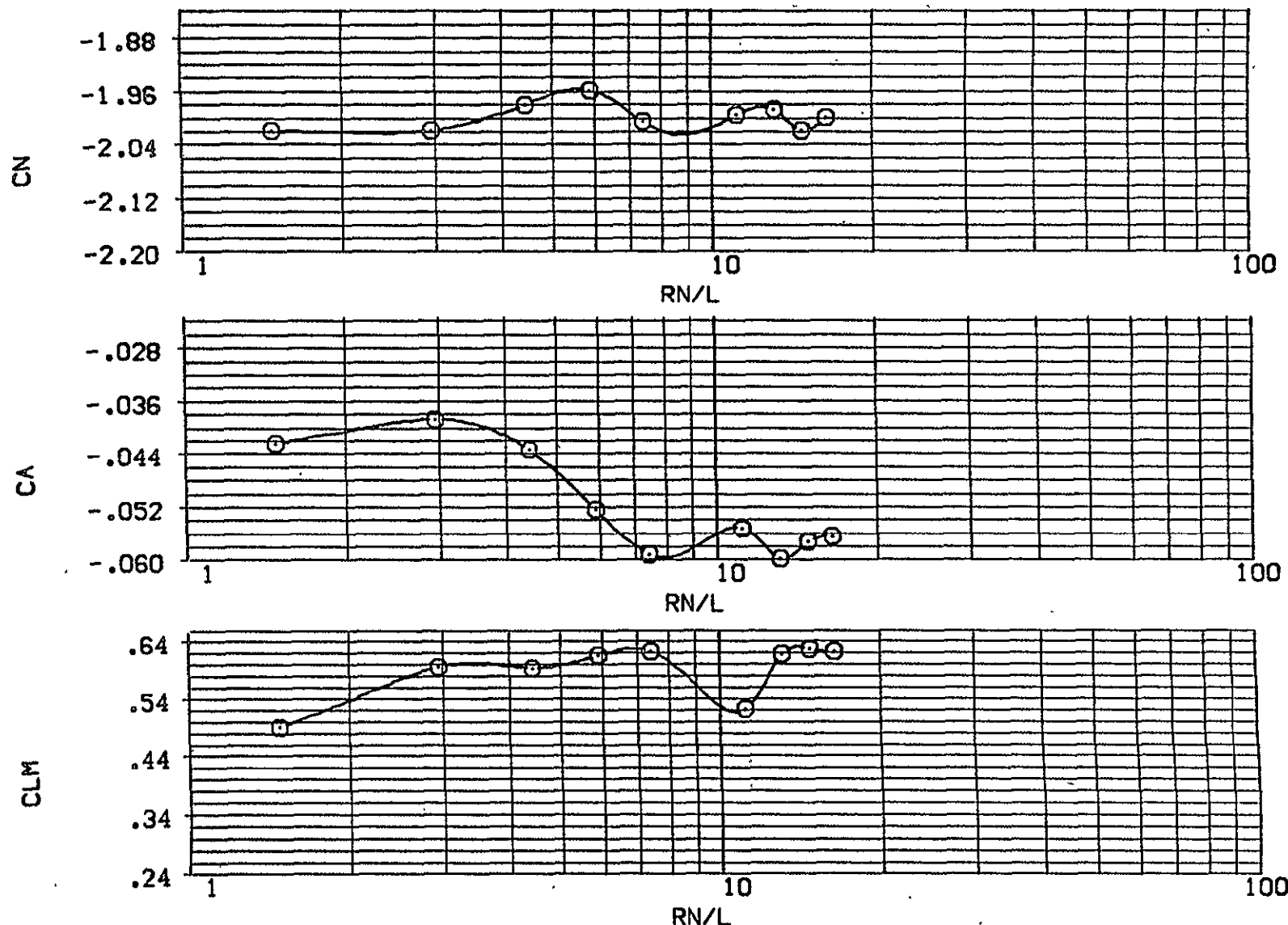
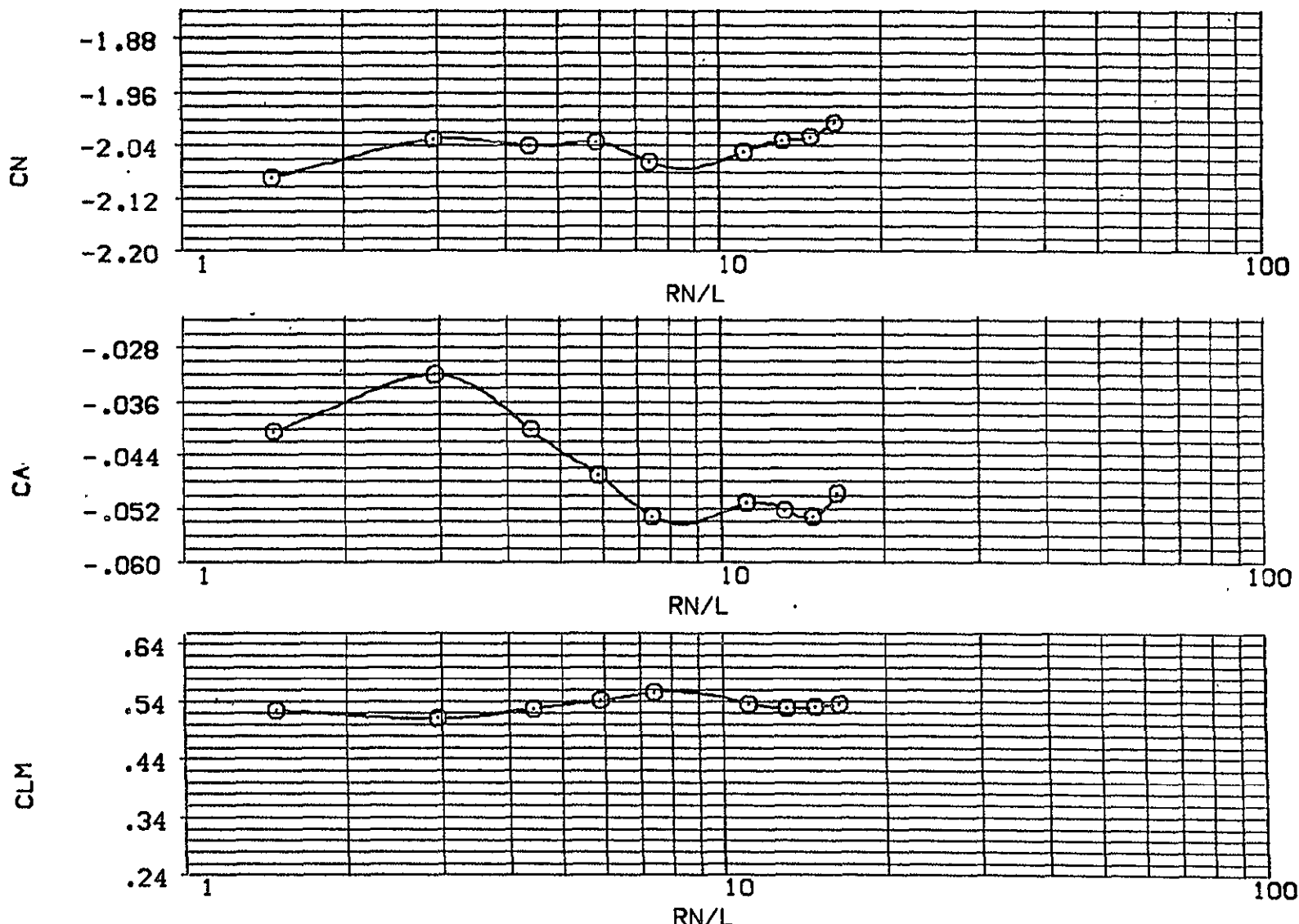


FIG. 4 VARIATION OF AERO. CHAR. WITH REYNOLDS NO. AT VARIOUS ANGLES OF ATTACK.

BASIC, RH0=11 - F

(DDW020)

SYMBOL	ALPHA	BETA	PARAMETRIC VALUES	.000	DATA SOURCE	RN/L	DATASET	RN/L
O	-70.000	10.000	AIL-L		DDW020	1.476	DDW021	2.952
		AIL-R	.000	.000	DDW022	4.428	DDW023	5.904
		STB-R	.000		DDW024	7.413	DDW025	11.152
					DDW026	13.120	DDW027	14.760
					DDW028	16.400		



ORIGINAL PAGE IS  
OF POOR  
QUALITY

FIG. 4 VARIATION OF AERO. CHAR. WITH REYNOLDS NO. AT VARIOUS ANGLES OF ATTACK.

SYMBOL	ALPHA	PARAMETRIC VALUES			DATASET	DATA SOURCE			
		BETA	10.000	AIL-L		RN/L	DATASET	RN/L	
O	-60.000	AIL-R	.000	STB-L	.000	DDW020	1.476	DDW021	2.952
		STB-R	.000			DDW022	4.428	DDW023	5.904
						DDW024	7.413	DDW025	11.152
						DDW026	13.120	DDW027	14.760
						DDW028	16.400		

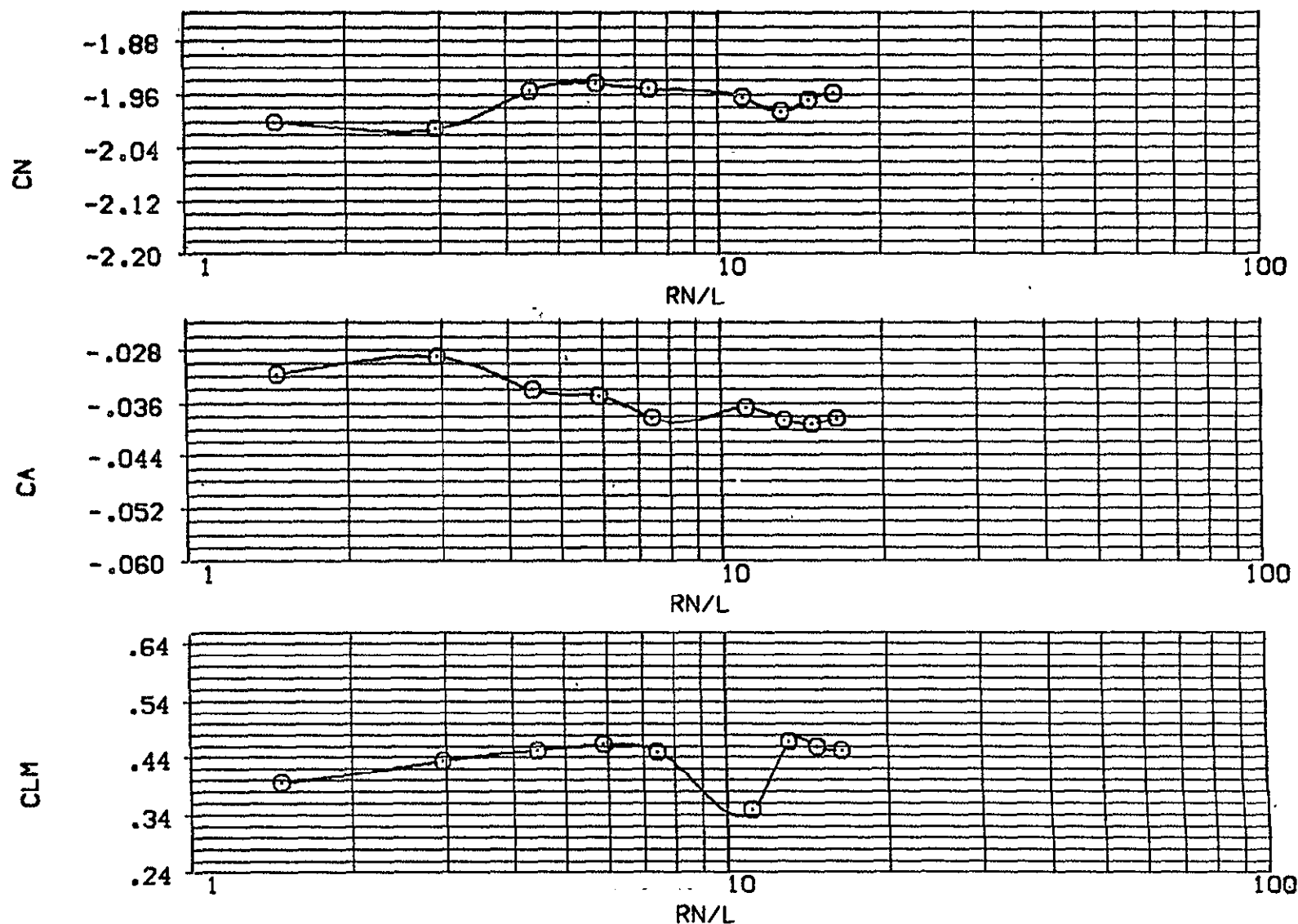


FIG. 4 VARIATION OF AERO. CHAR. WITH REYNOLDS NO. AT VARIOUS ANGLES OF ATTACK.

BASIC, RH<sub>0</sub>=11 - F

(DDW020)

SYMBOL	ALPHA	BETA	PARAMETRIC VALUES	.000	DATASET	DATA SOURCE	RN/L	DATASET	RN/L
O	-50.000	10.000	AIL-L	.000	DDW020	DDW020	1.476	DDW021	2.952
			AIL-R	.000	DDW022	DDW023	4.428	DDW024	5.904
			STB-R	.000	DDW024	DDW025	7.413	DDW026	11.152
					DDW026	DDW027	13.120	DDW028	14.760
							16.400		

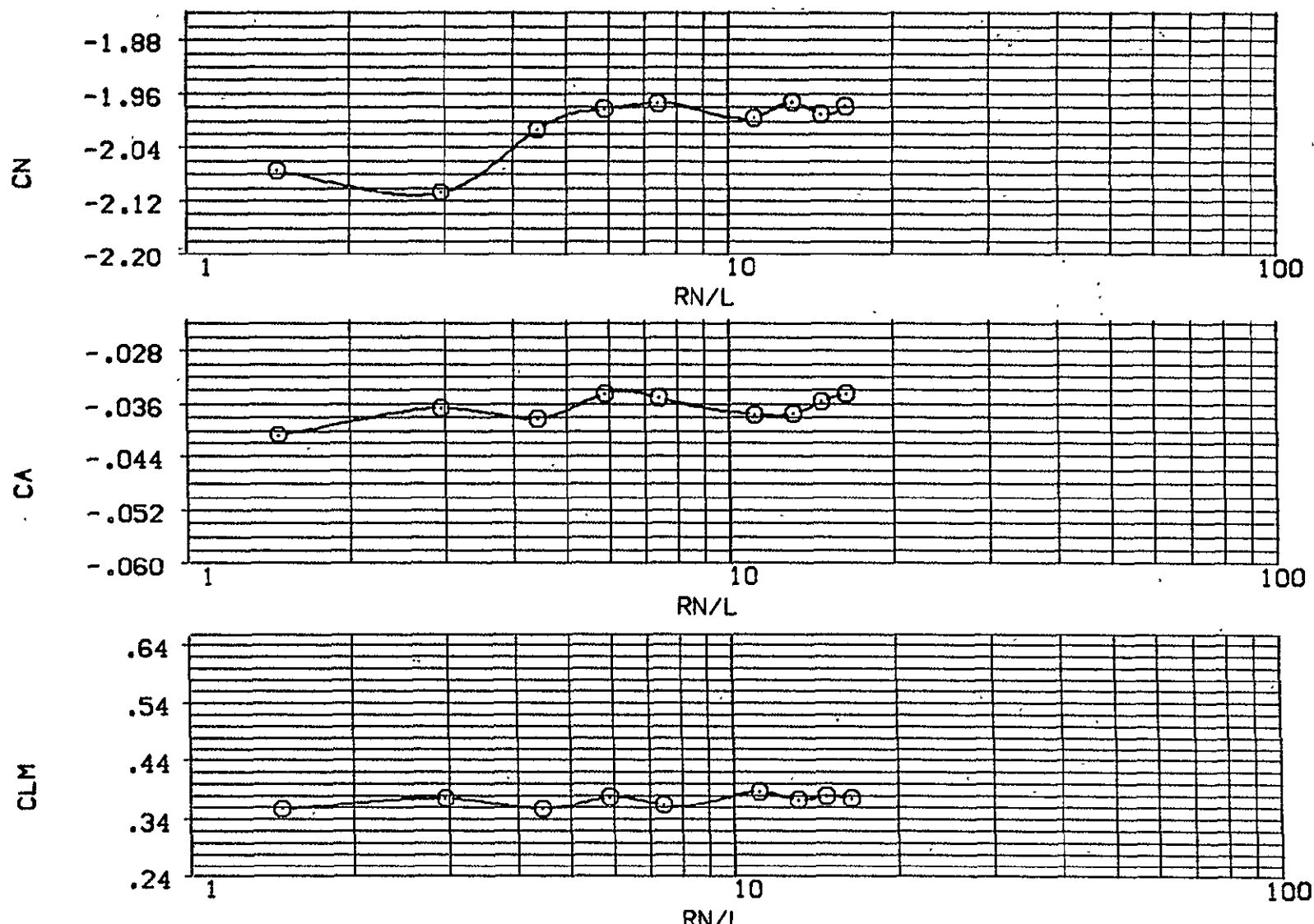


FIG. 4 VARIATION OF AERO. CHAR. WITH REYNOLDS NO. AT VARIOUS ANGLES OF ATTACK.

SYMBOL	ALPHA	PARAMETRIC VALUES			,000	DATASET	DATA SOURCE		
		BETA	10.000	AIL-L			RN/L	DATASET	RN/L
O	-40.000	AIL-R	.000	STB-L	,000	DDW020	1.476	DDW021	2.952
		STB-R	.000			DDW022	4.428	DDW023	5.904
						DDW024	7.413	DDW025	11.152
						DDW026	13.120	DDW027	14.760
						DDW028	16.400		

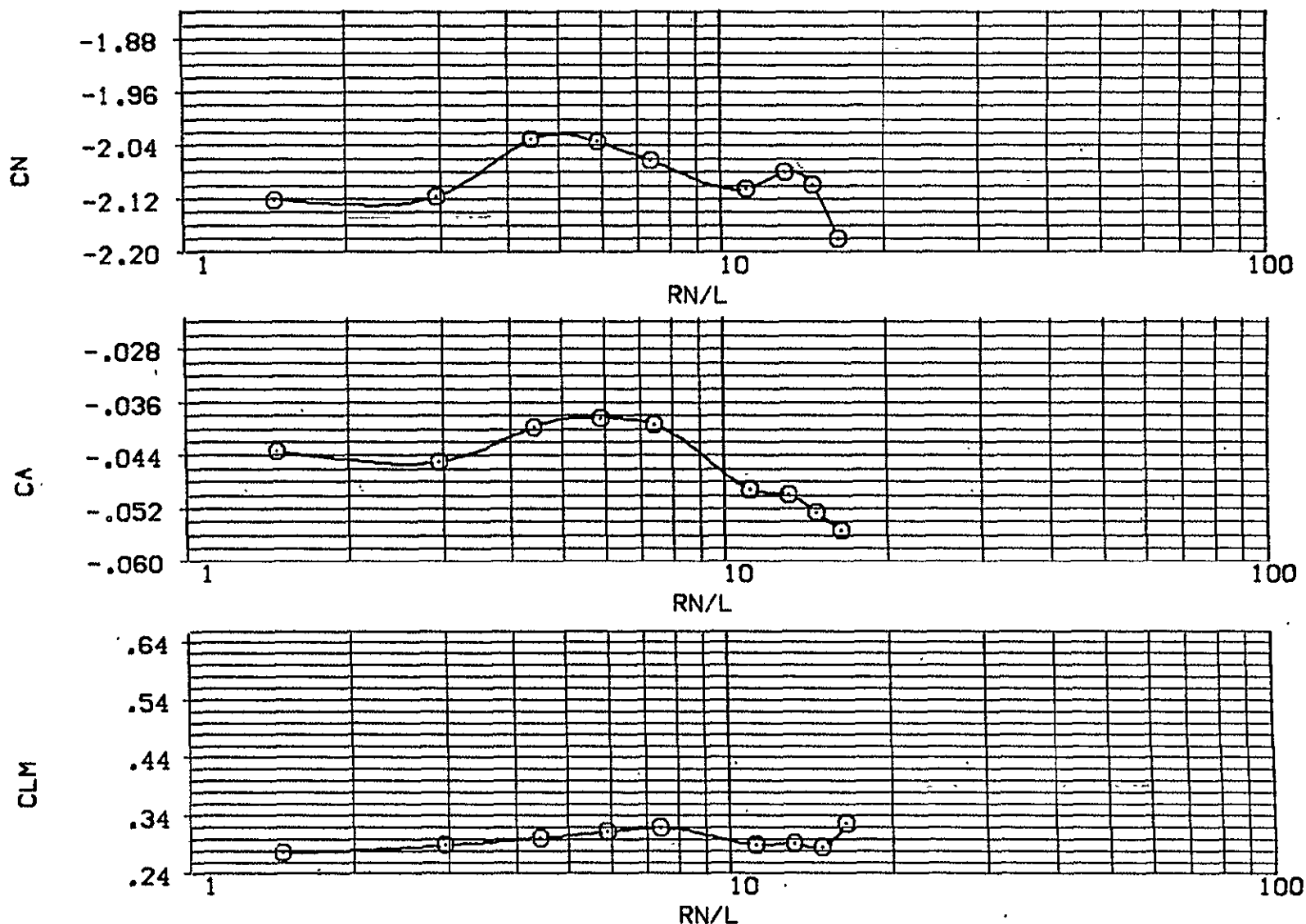
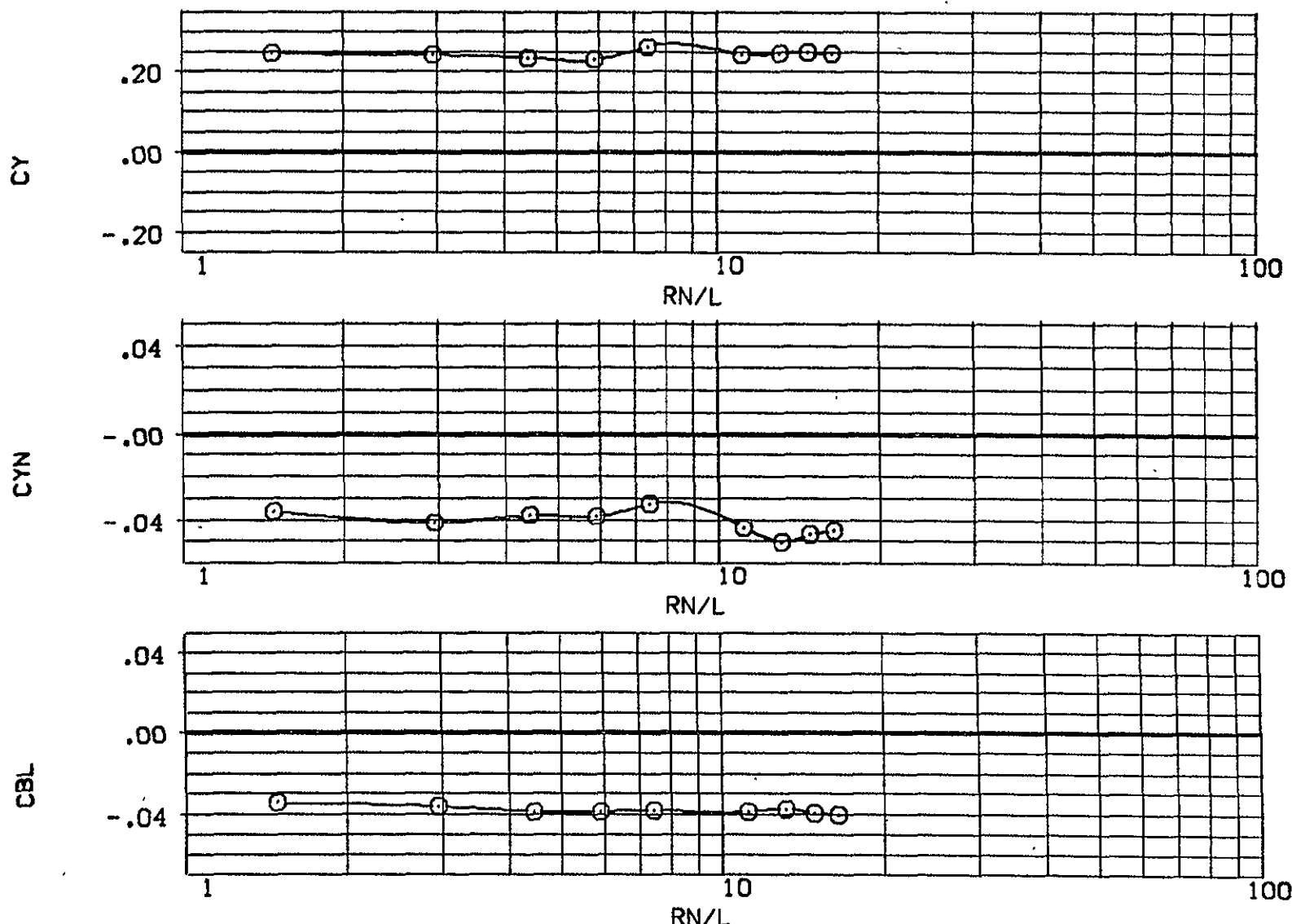


FIG. 4 VARIATION OF AERO. CHAR. WITH REYNOLDS NO. AT VARIOUS ANGLES OF ATTACK.

BASIC, RHO=11 - F

(DDW020)

SYMBOL	ALPHA	PARAMETRIC VALUES			DATASET	DATA SOURCE	DATASET	RN/L	
		BETA	AIL-R	STB-L					
O	-80.000	-20.000	.000	.000	DDW020	DDW020	1.476	DDW021	2.952
					DDW022	DDW022	4.428	DDW023	5.904
					DDW024	DDW024	7.413	DDW025	11.152
					DDW026	DDW026	13.120	DDW027	14.760
					DDW028	DDW028	16.400		



ORIGINAL PAGE IS  
OF POOR QUALITY.

FIG. 4 VARIATION OF AERO. CHAR. WITH REYNOLDS NO. AT VARIOUS ANGLES OF ATTACK.

SYMBOL	ALPHA	BETA	PARAMETRIC VALUES	.000	DATASET	RN/L	DATA SOURCE
O	-70.000		-20.000 AIL-L		DDW020	1.476	DDW021 - 2.952
		AIL-R	.000 STB-L		DDW022	4.428	DDW023 5.904
		STB-R	.000		DDW024	7.413	DDW025 11.152
					DDW026	13.120	DDW027 14.760
					DDW028	16.400	

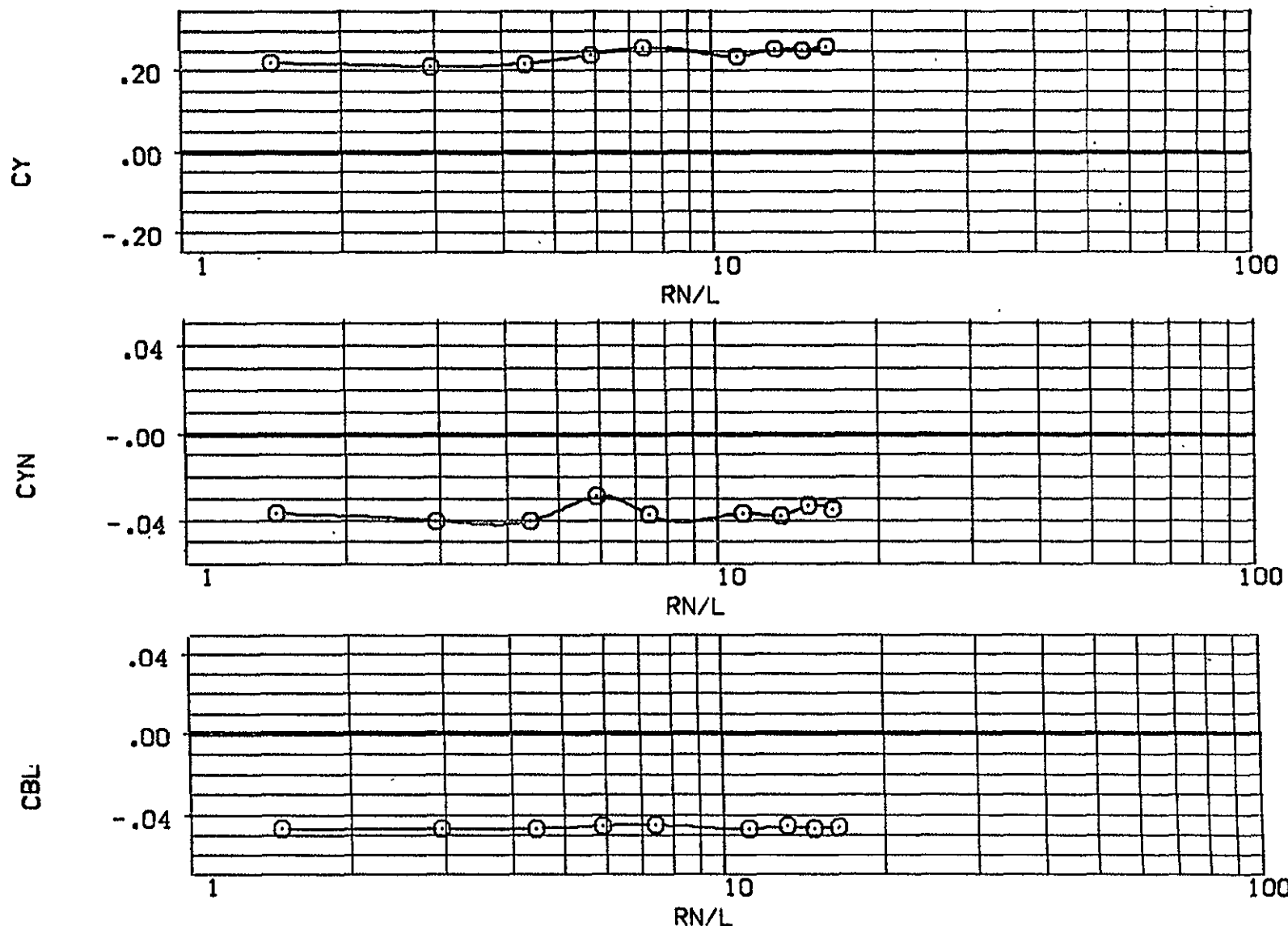


FIG. 4 VARIATION OF AERO. CHAR. WITH REYNOLDS NO. AT VARIOUS ANGLES OF ATTACK.

BASIC. RHO=11 ~ F

(DDW020)

SYMBOL	ALPHA	PARAMETRIC VALUES			DATASET	DATA SOURCE
		BETA	AIL-L	STB-L		
O	-60.000	-20.000	.000	.000	DDW020	RN/L
		AIL-R	.000	STB-L	DDW022	DDW021 2.952
		STB-R	.000		DDW024	DDW023 5.904
					DDW026	DDW025 11.152
					DDW028	DDW027 14.760

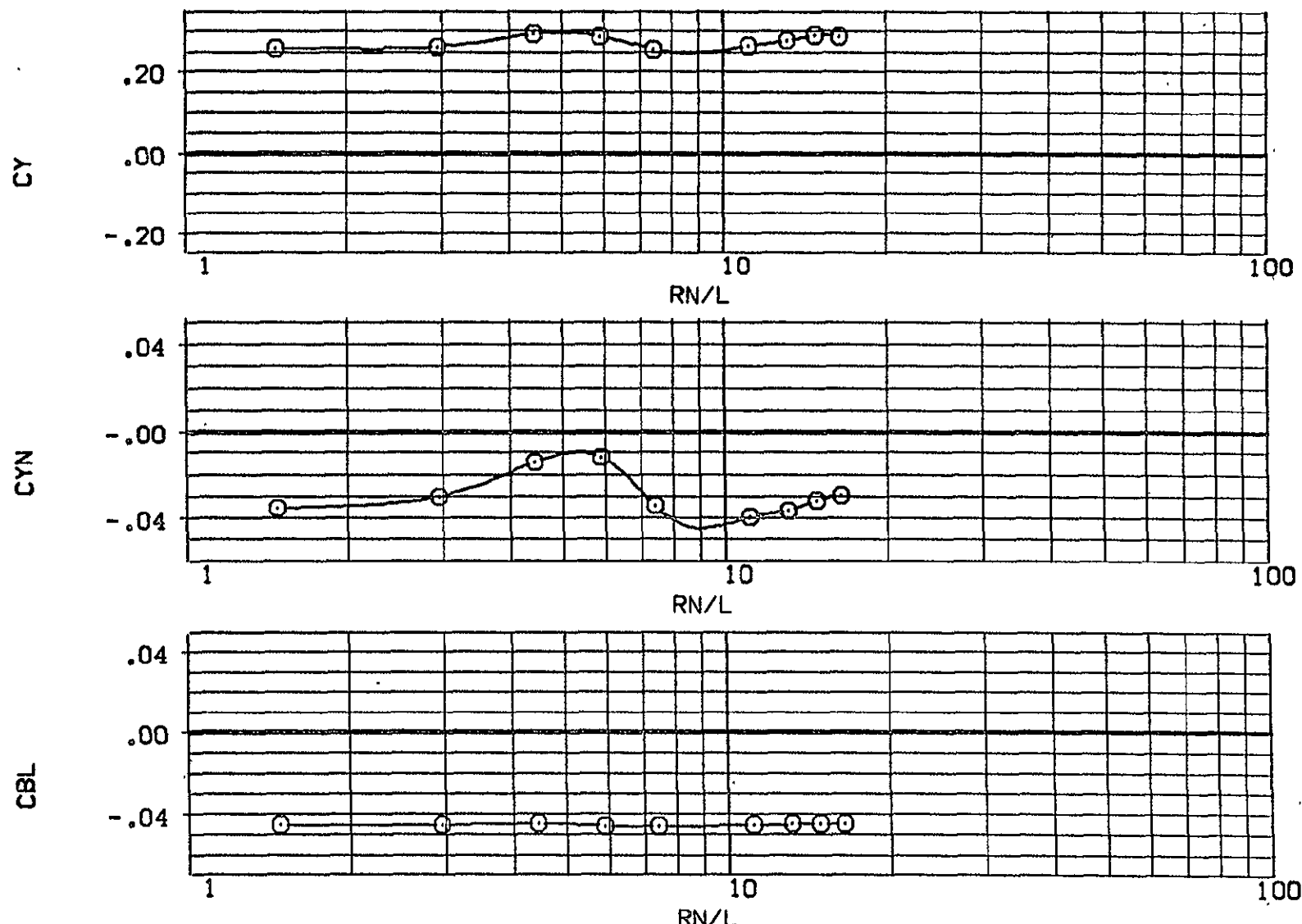
ORIGINAL PAGE IS  
OF POOR QUALITY

FIG. 4 VARIATION OF AERO. CHAR. WITH REYNOLDS NO. AT VARIOUS ANGLES OF ATTACK.

SYMBOL	ALPHA	PARAMETRIC VALUES			DATASET	RN/L	DATA SOURCE		
		BETA	AIL-L	STB-L			AIL-R	STB-R	DDW020
O	-50.000	-20.000	.000	.000	.000	DDW020	1.476	DDW021	2.952
						DDW022	4.428	DDW023	5.904
						DDW024	7.413	DDW025	11.152
						DDW026	13.120	DDW027	14.760
						DDW028	16.400		

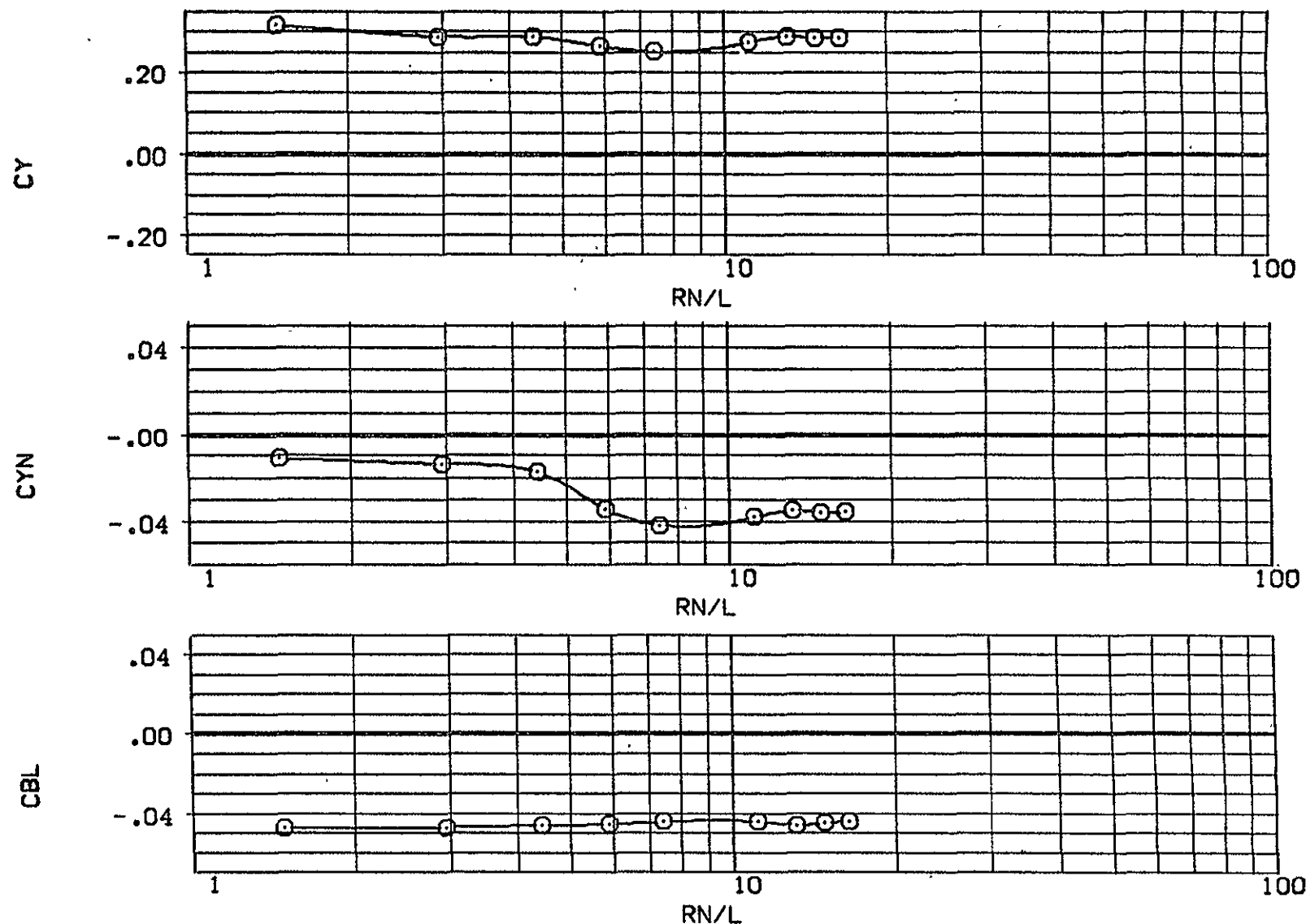


FIG. 4 VARIATION OF AERO. CHAR. WITH REYNOLDS NO. AT VARIOUS ANGLES OF ATTACK.

56

BASIC.  $RHO=11 - F$

(DDW020)

SYMBOL	ALPHA	PARAMETRIC VALUES			DATASET	DATA SOURCE		
		BETA	AIL-R	STB-L		RN/L	DATASET	RN/L
O	-40.000	-20.000	AIL-L	.000	DDW020	1.476	DDW021	2.952
			STB-L	.000	DDW022	4.428	DDW023	5.904
					DDW024	7.413	DDW025	11.152
					DDW026	13.120	DDW027	14.760
					DDW028	16.400		

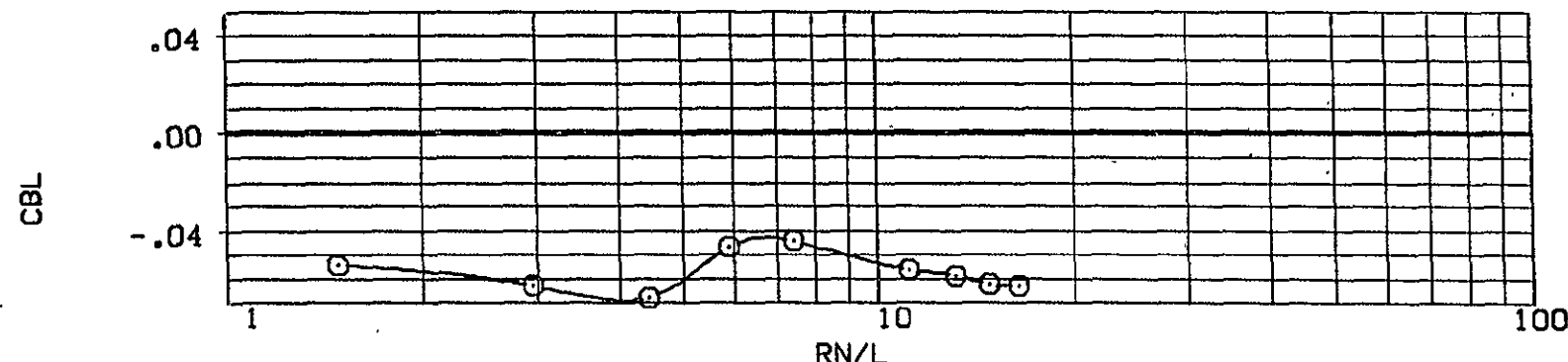
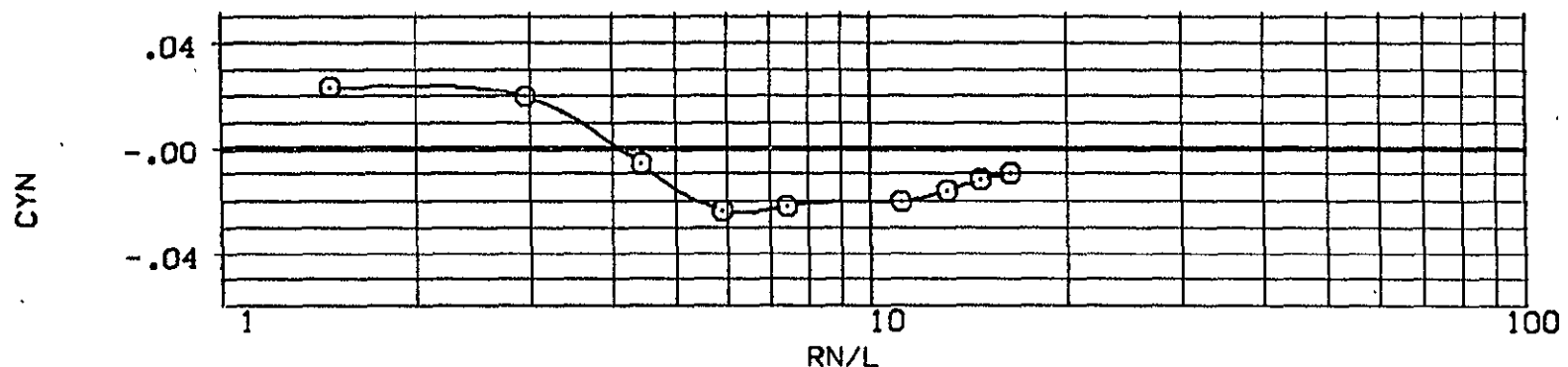
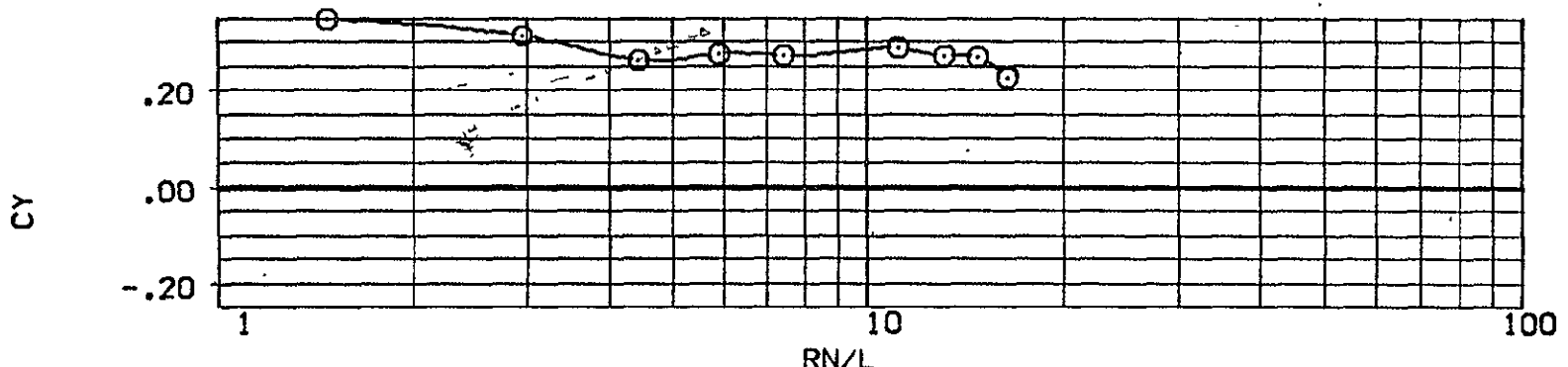


FIG. 4 VARIATION OF AERO. CHAR. WITH REYNOLDS NO. AT VARIOUS ANGLES OF ATTACK.

SYMBOL	ALPHA	PARAMETRIC VALUES			DATA SOURCE
O	-80.000	BETA	-10.000	AIL-L	RN/L
		AIL-R	.000	STB-L	Dataset
		STB-R	.000		RN/L
				.000 DDW020	1.476 DDW021 2.952
				DDW022 4.428 DDW023 5.904	
				DDW024 7.413 DDW025 11.152	
				DDW026 13.120 DDW027 14.760	
				DDW028 16.400	

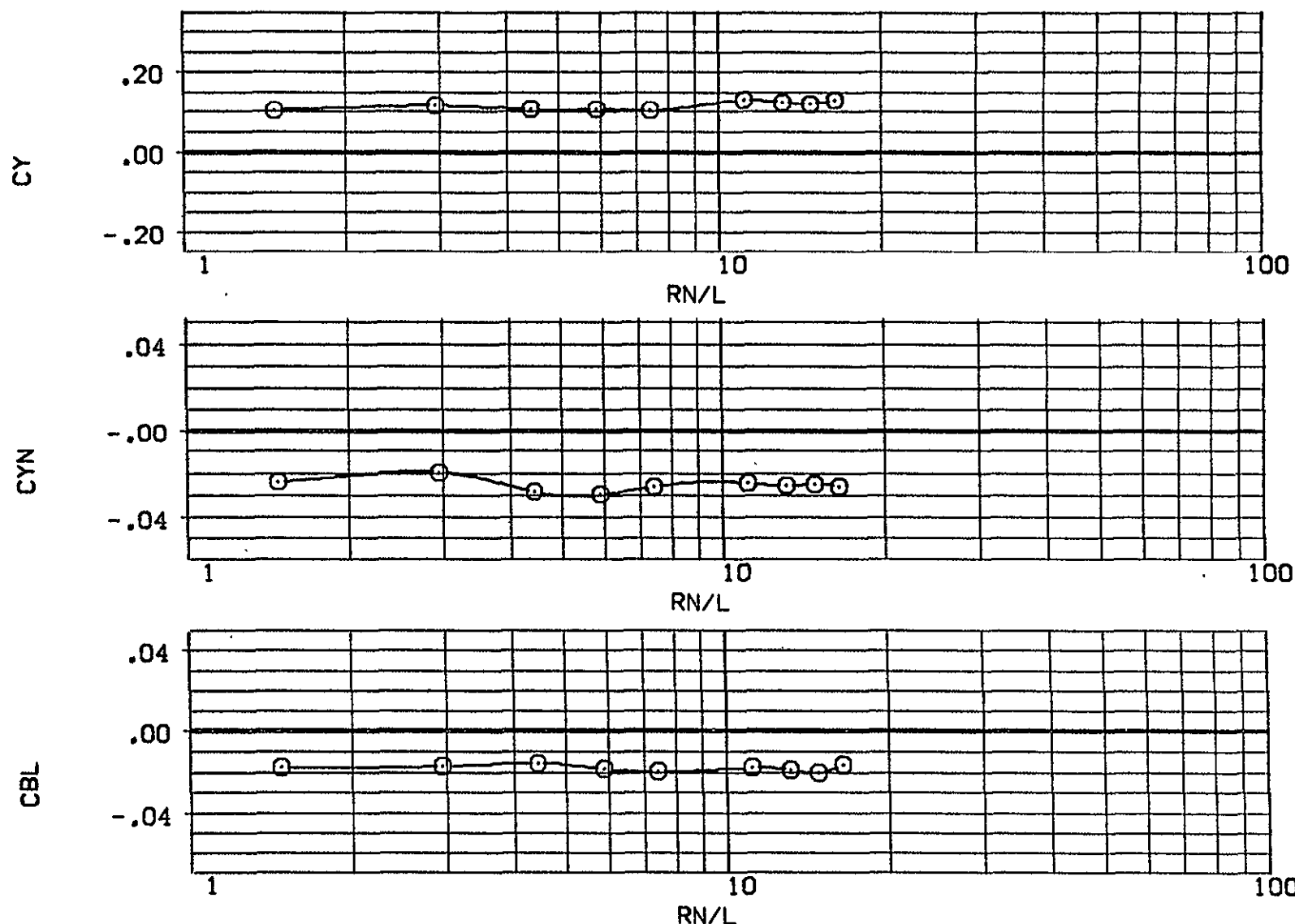


FIG. 4 VARIATION OF AERO. CHAR. WITH REYNOLDS NO. AT VARIOUS ANGLES OF ATTACK,

BASIC, RH0=11 - F

(DDW020)

SYMBOL	ALPHA	PARAMETRIC VALUES			DATASET	RN/L	DATA SOURCE	
		BETA	AIL-L	STB-L			DATASET	RN/L
O	-70.000	-10.000	.000	.000	DDW020	1.476	DDW021	2.952
		AIL-R	.000	STB-L	DDW022	4.428	DDW023	5.904
		STB-R	.000		DDW024	7.413	DDW025	11.152
					DDW026	13.120	DDW027	14.760
					DDW028	16.400		

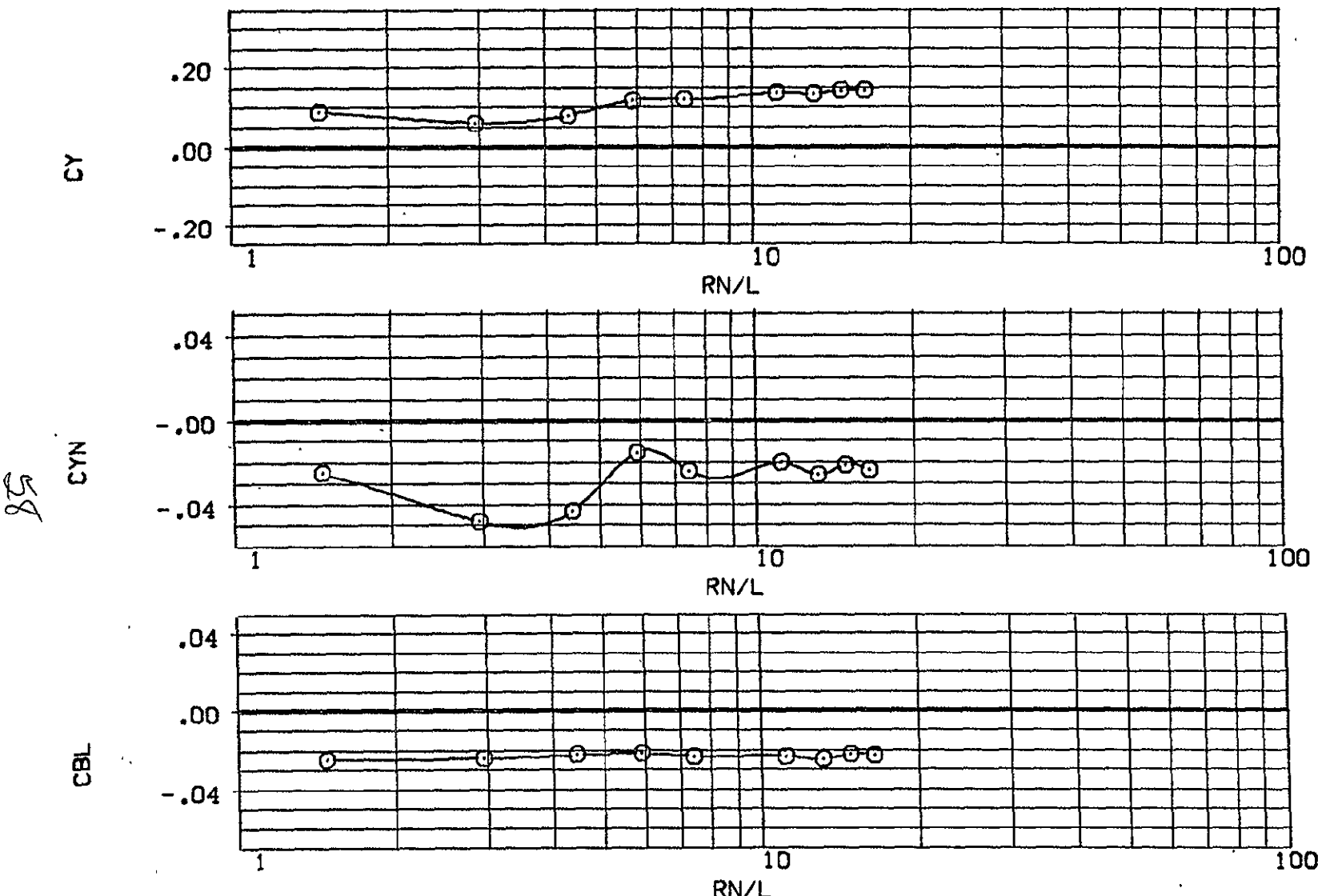


FIG. 4 VARIATION OF AERO. CHAR. WITH REYNOLDS NO. AT VARIOUS ANGLES OF ATTACK.

SYMBOL	ALPHA	PARAMETRIC VALUES			DATASET	RN/L	DATA SOURCE	
		BETA	AIL-L	STB-L			DATASET	RN/L
O	-60.000	-10.000	.000	.000	DDW020	1.476	DDW021	2.952
					DDW022	4.428	DDW023	5.904
					DDW024	7.413	DDW025	11.152
					DDW026	13.120	DDW027	14.760
					DDW028	16.400		

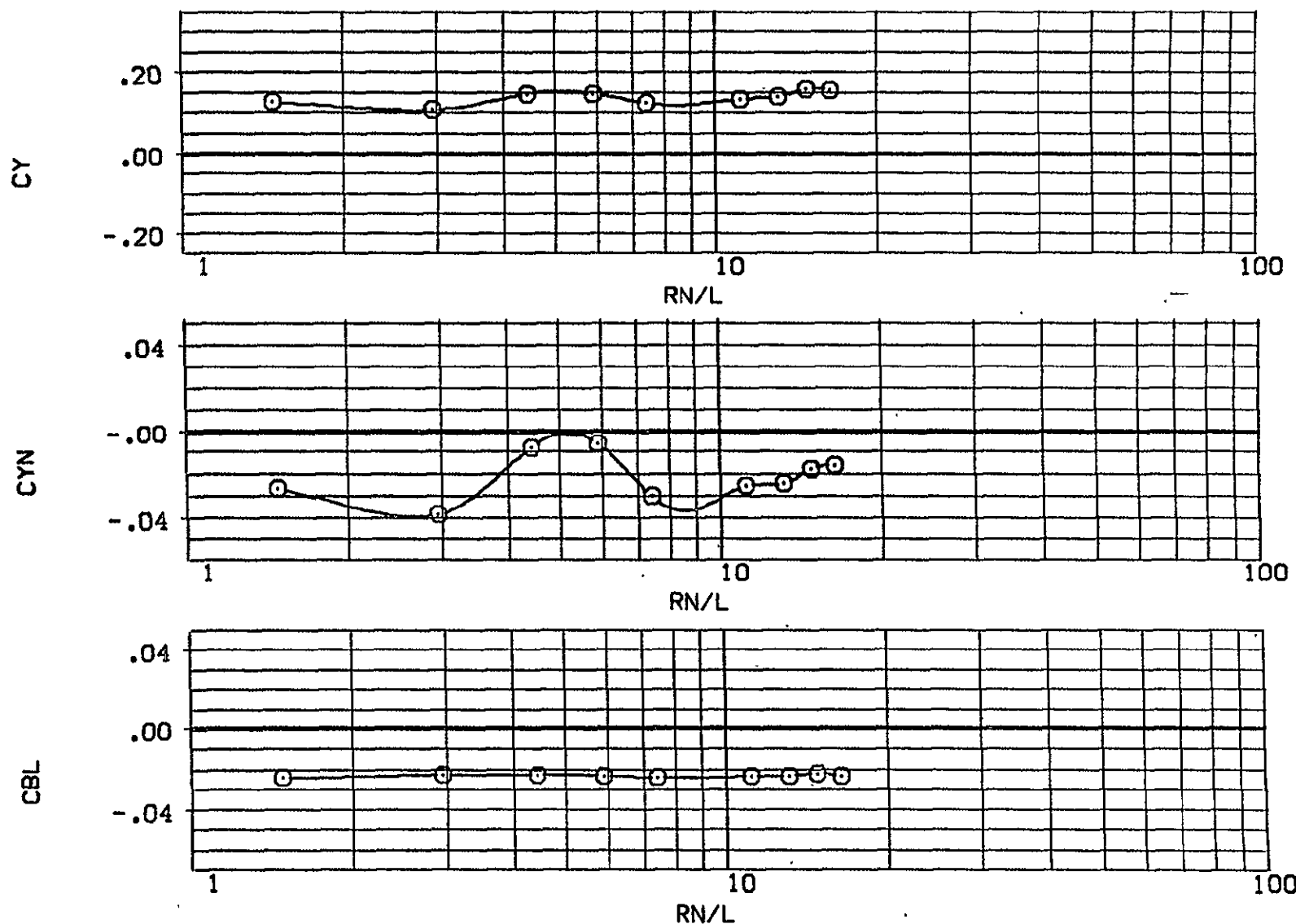
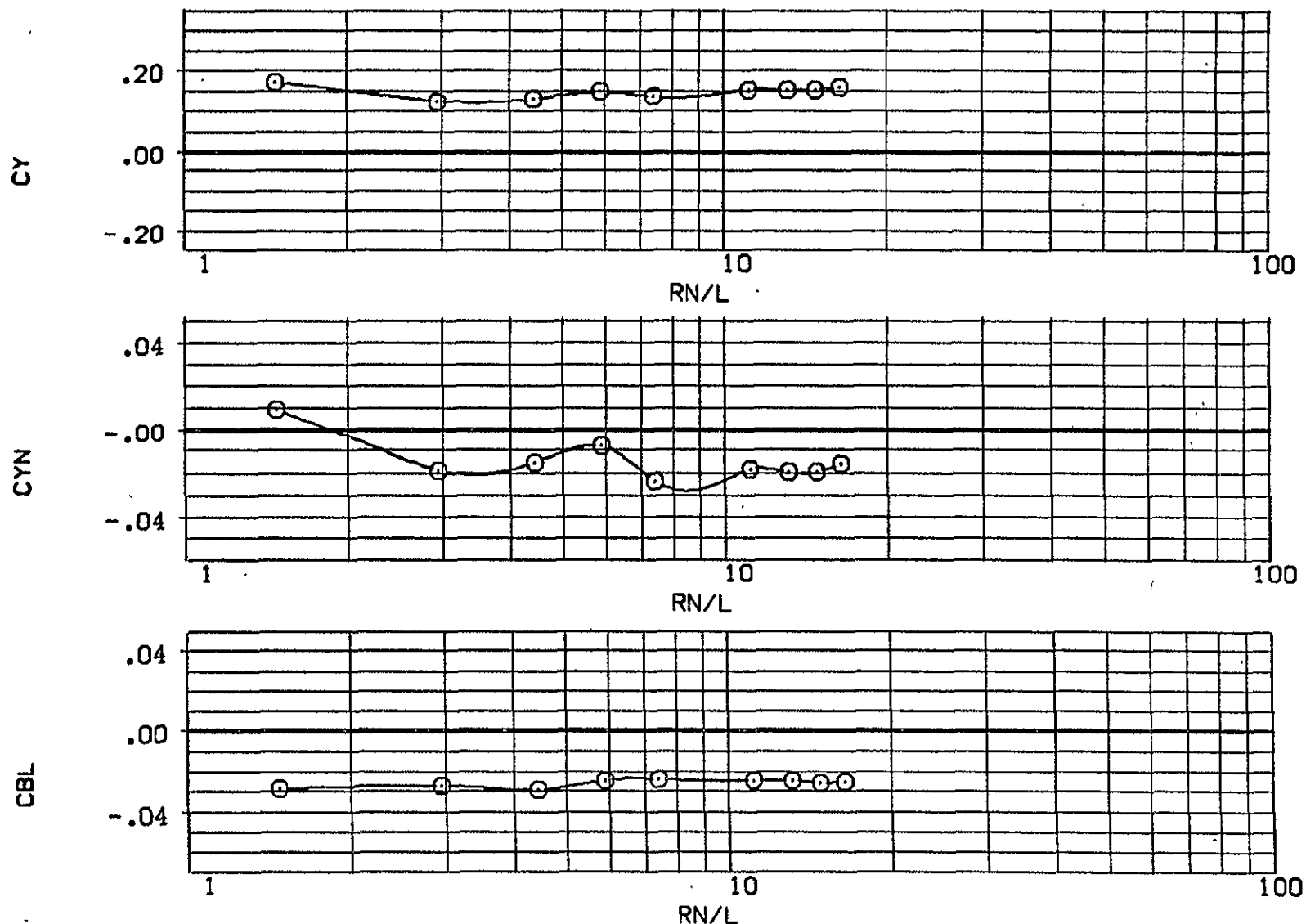


FIG. 4 VARIATION OF AERO. CHAR. WITH REYNOLDS NO. AT VARIOUS ANGLES OF ATTACK.

BASIC, RH<sub>0</sub>=11 - F

(DDW020)

SYMBOL	ALPHA	PARAMETRIC VALUES			.000	DATASET	DATA SOURCE		
		BETA	AIL-R	STB-L			RN/L	DATASET	RN/L
O	-50.000	-10.000	.000	.000	DDW020	1.476	DDW021	2.952	
					DDW022	4.428	DDW023	5.904	
					DDW024	7.413	DDW025	11.152	
					DDW026	13.120	DDW027	14.760	
					DDW028	16.400			



60  
ORIGINAL PAGE IS  
OF POOR QUALITY

FIG. 4 VARIATION OF AERO. CHAR. WITH REYNOLDS NO. AT VARIOUS ANGLES OF ATTACK.

SYMBOL	ALPHA	PARAMETRIC VALUES			.000	DATASET	DATA SOURCE	
		BETA	AIL-R	STB-L			RN/L	DATASET
O	-40.000	.000	.000	.000	DDW020	1.476	DDW021	2.952
					DDW022	4.428	DDW023	5.904
					DDW024	7.413	DDW025	11.152
					DDW026	13.120	DDW027	14.760
					DDW028	16.400		

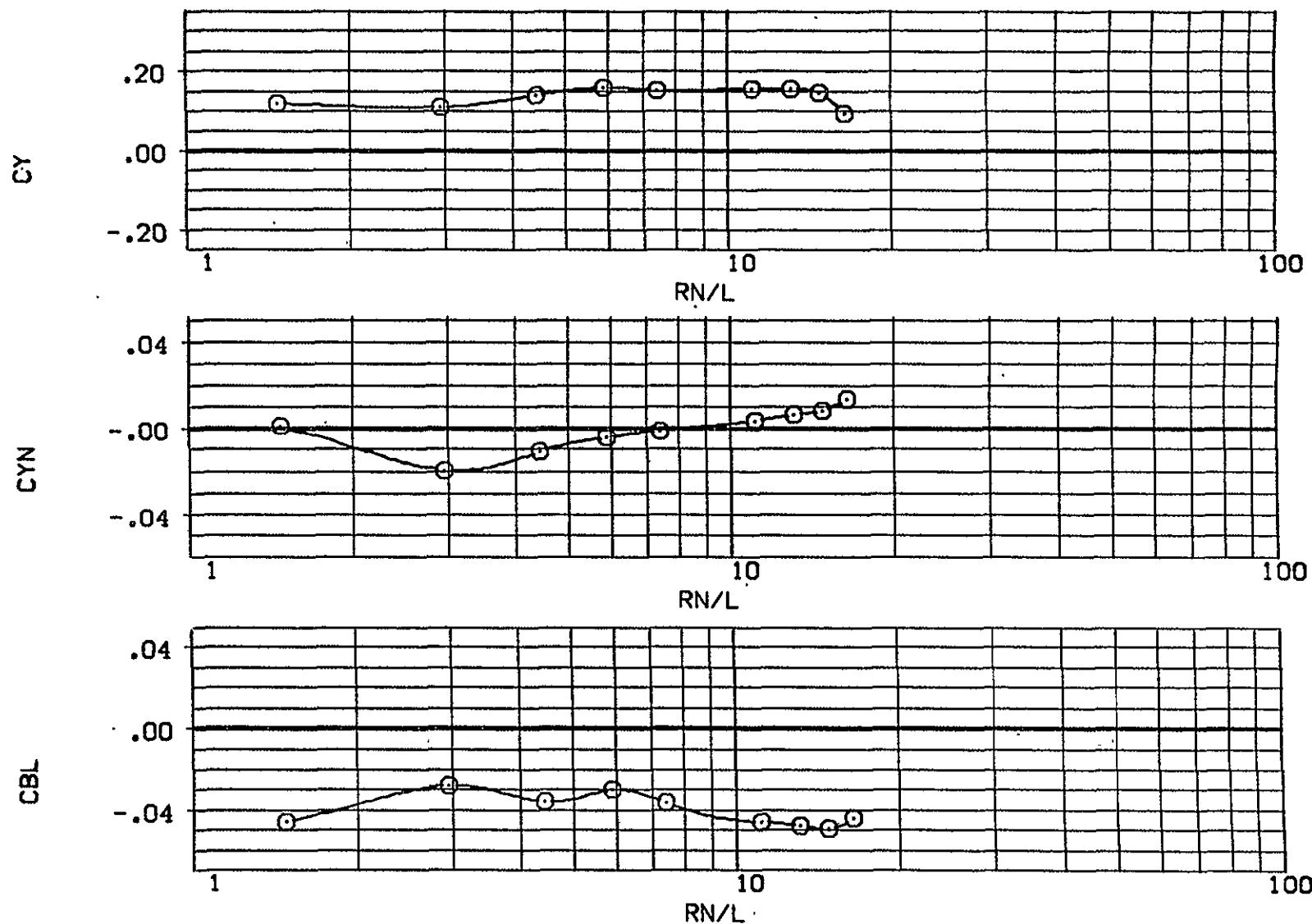


FIG. 4 VARIATION OF AERO. CHAR. WITH REYNOLDS NO. AT VARIOUS ANGLES OF ATTACK.

BASIC, RH<sub>0</sub>=11 - F

(DDW020)

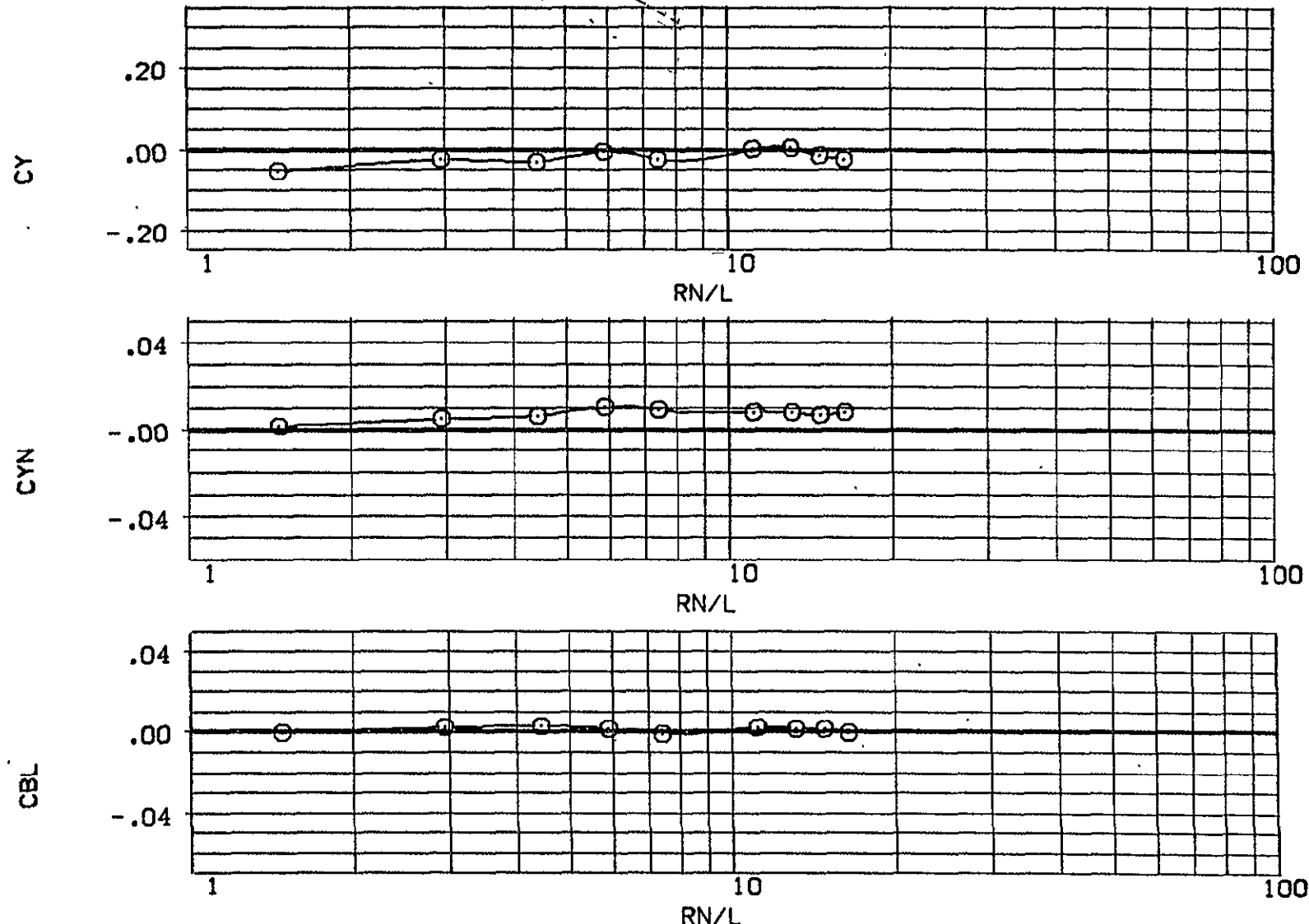
SYMBOL  
O ALPHA  
-90.000PARAMETRIC VALUES  
BETA .000 AIL-L .000  
AIL-R .000 STB-L .000  
STB-R .000.000 DATASET  
DDW020 .000 DDW022 .000 DDW024 .000 DDW026 .000 DDW028 .000DATA SOURCE  
RN/L DATASET RN/L  
DDW021 2.952  
DDW023 5.904  
DDW025 11.152  
DDW027 14.760

FIG. 4 VARIATION OF AERO. CHAR. WITH REYNOLDS NO. AT VARIOUS ANGLES OF ATTACK.

BASIC, RH<sub>0</sub>=11 - F

(DDW020)

SYMBOL	ALPHA	PARAMETRIC VALUES			DATASET	DATA SOURCE		
		BETA	AIL-L	STB-L				
O	-70.000	.000	.000	.000	DDW020	RN/L		
		AIL-R	.000	STB-L	DDW022	DDW021	1.476	2.952
		STB-R	.000		DDW024	DDW023	4.428	5.904
					DDW026	DDW025	7.413	11.152
					DDW028	DDW027	13.120	14.760
							16.400	

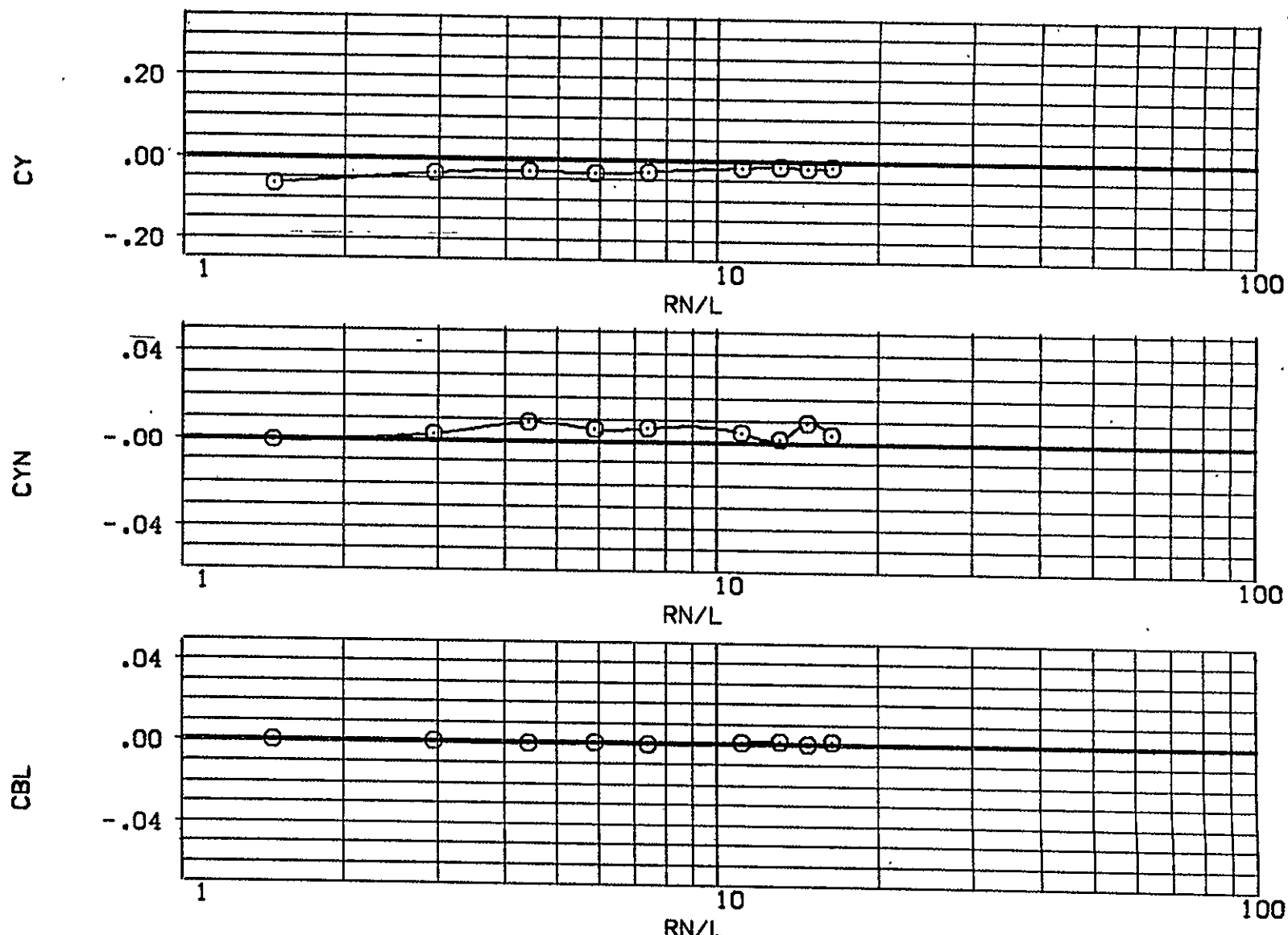
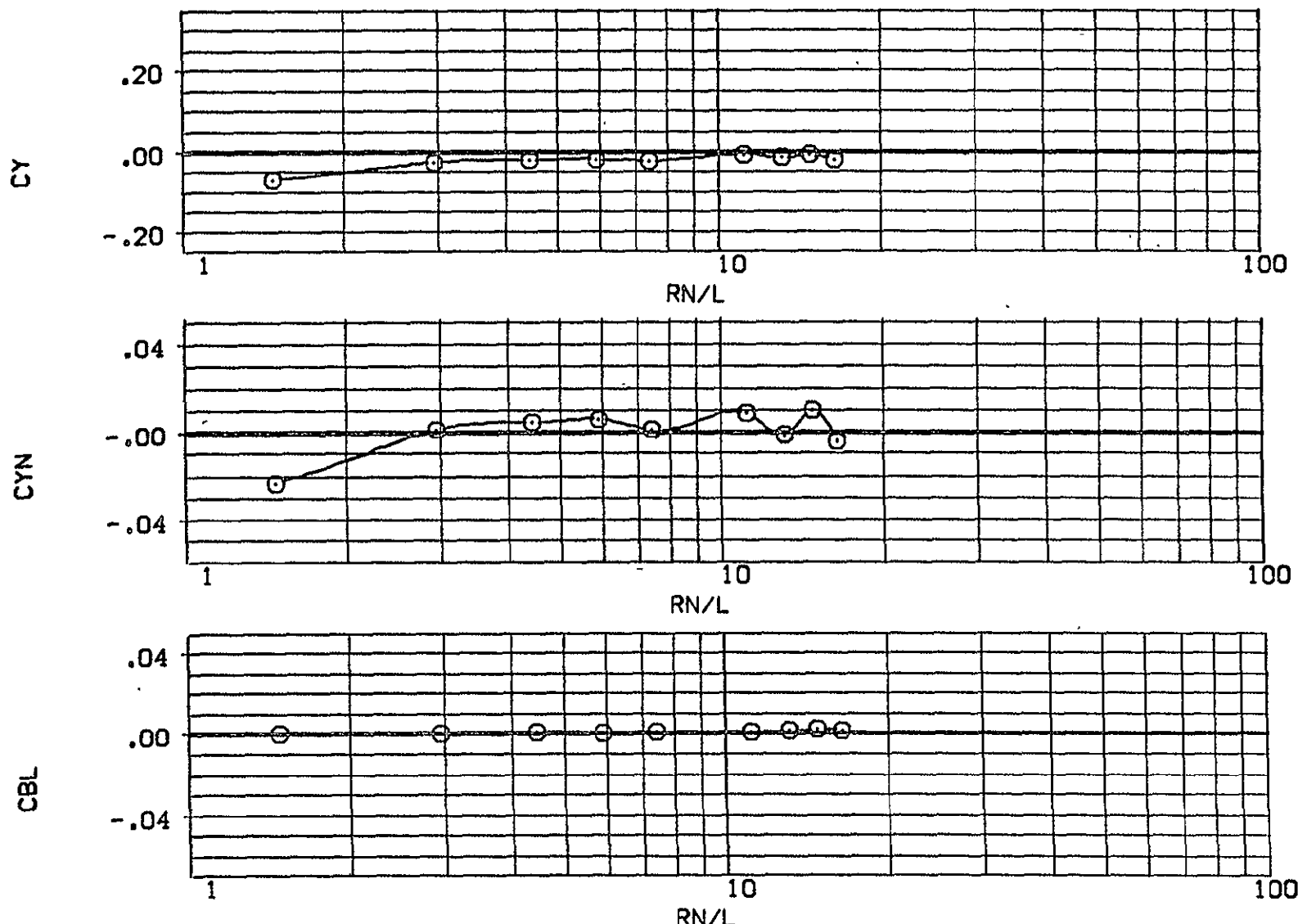


FIG. 4 VARIATION OF AERO. CHAR. WITH REYNOLDS NO. AT VARIOUS ANGLES OF ATTACK.

BASIC, RH<sub>0</sub>=11 - F

(DDW020)

SYMBOL	ALPHA	PARAMETRIC VALUES			DATASET	DATA SOURCE			
		BETA	.000	AIL-L			RN/L	DATASET	RN/L
O	-60.000	AIL-R	.000	STB-L	.000	DDW020	1.476	DDW021	2.952
		AIL-R	.000	STB-L		DDW022	4.128	DDW023	5.904
		STB-R	.000			DDW024	7.413	DDW025	11.152
						DDW026	13.120	DDW027	14.760
						DDW028	16.400		



ORIGINAL PAGE IS  
OF POOR QUALITY

FIG. 4 VARIATION OF AERO. CHAR. WITH REYNOLDS NO. AT VARIOUS ANGLES OF ATTACK.

SYMBOL	ALPHA	PARAMETRIC VALUES			DATASET	RN/L	DATA SOURCE		
		BETA	.000	AIL-L			AIL-R	STB-L	STB-R
O	-50.000	.000	.000	.000	.000	DDW020	1.476	DDW021	2.952
						DDW022	4.428	DDW023	5.904
						DDW024	7.413	DDW025	11.152
						DDW026	13.120	DDW027	14.760
						DDW028	16.400		

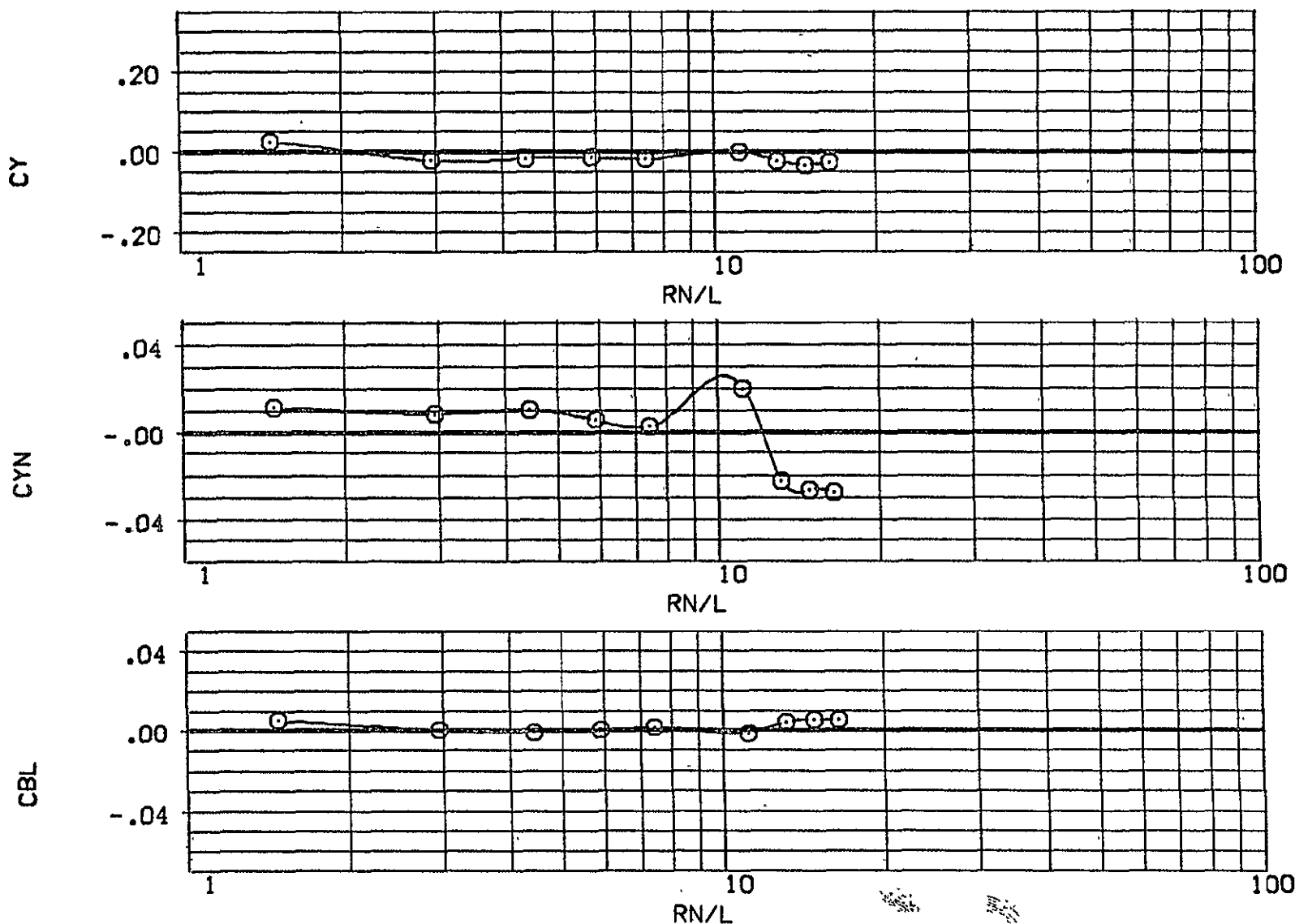
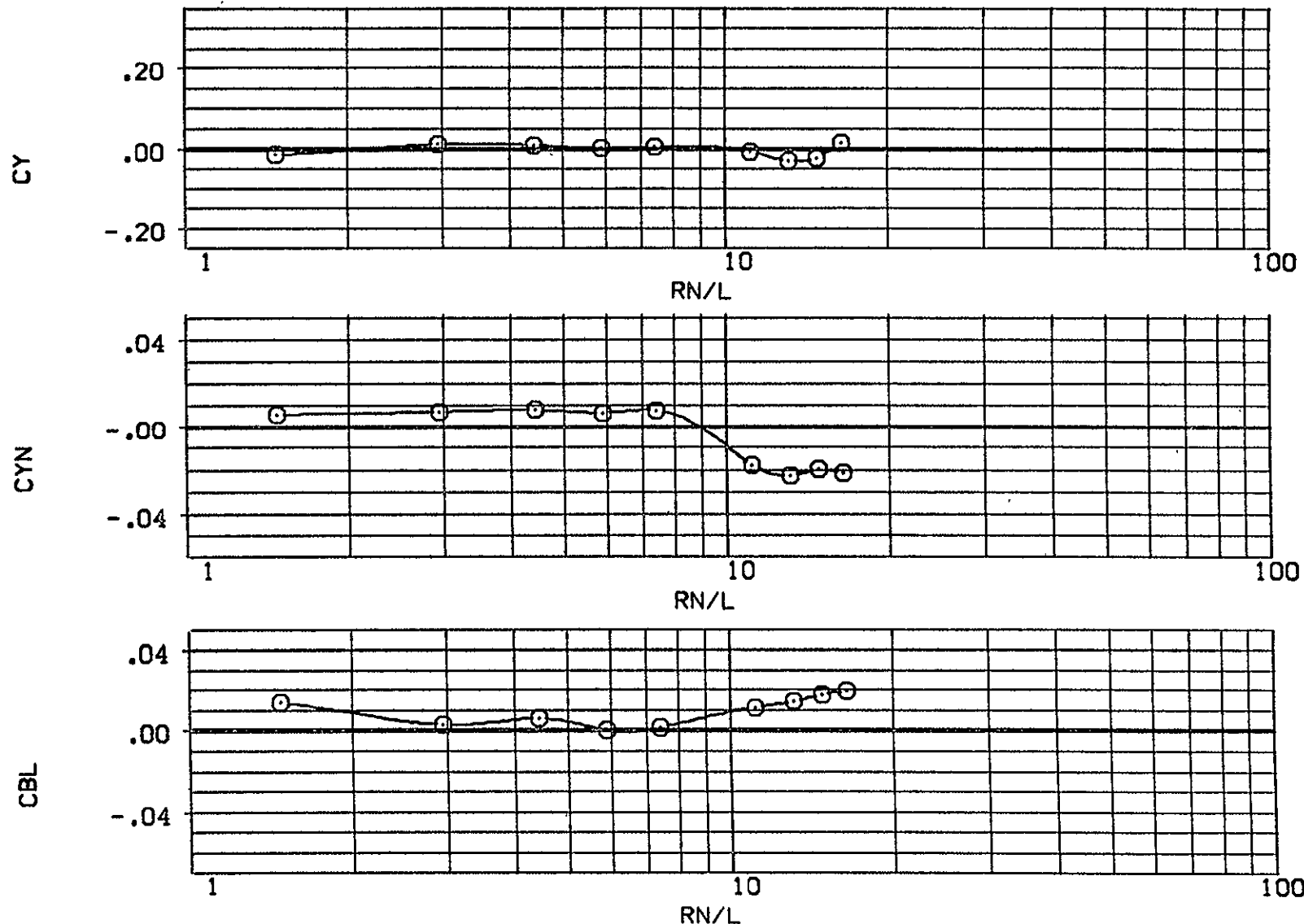


FIG. 4 VARIATION OF AERO. CHAR. WITH REYNOLDS NO. AT VARIOUS ANGLES OF ATTACK.

BASIC, RH<sub>0</sub>=11 - F

(DDW020)

SYMBOL	ALPHA	PARAMETRIC VALUES			DATASET	RN/L	DATA SOURCE	
		BETA	.000	AIL-L			.000	DATASET
O	-40.000	AIL-R	.000	STB-L	DDW020	1.476	DDW021	2.952
		STB-R	.000		DDW022	4.428	DDW023	5.904
					DDW024	7.413	DDW025	11.152
					DDW026	13.120	DDW027	14.760
					DDW028	16.400		



69  
ORIGINAL PAGE IS  
OF POOR  
QUALITY

FIG. 4 VARIATION OF AERO. CHAR. WITH REYNOLDS NO. AT VARIOUS ANGLES OF ATTACK.

SYMBOL	ALPHA	PARAMETRIC VALUES			DATASET	RN/L	DATA SOURCE	
		BETA	AIL-L	STB-L			DATASET	RN/L
O	-80.000	.000	.000	.000	DDW020	1.476	DDW021	2.952
		AIL-R	.000	.000	DDW022	4.428	DDW023	5.904
		STB-R	.000	.000	DDW024	7.413	DDW025	11.152
				DDW026	13.120	DDW027	14.760	
				DDW028	16.400			

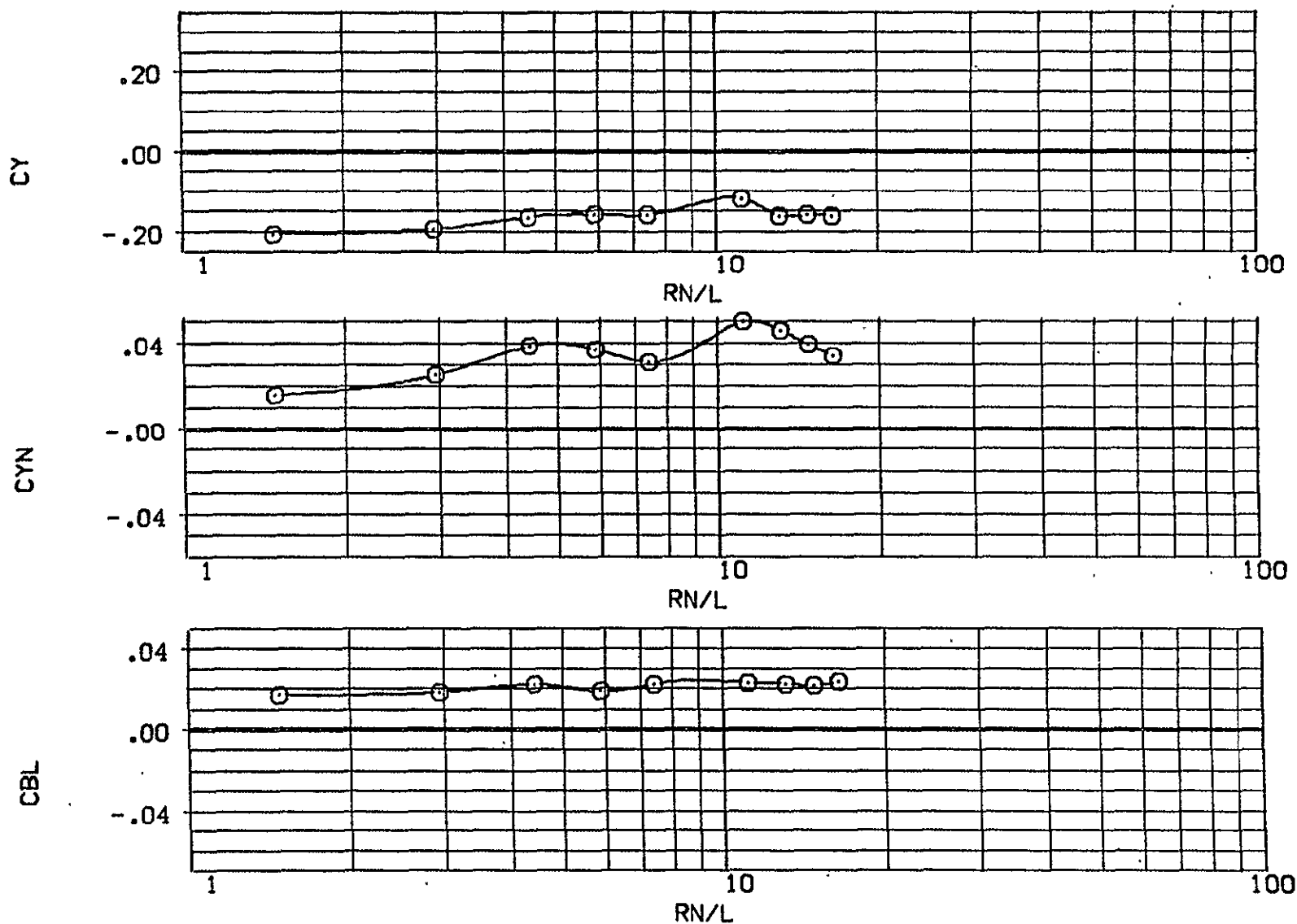


FIG. 4 VARIATION OF AERO. CHAR. WITH REYNOLDS NO. AT VARIOUS ANGLES OF ATTACK.

BASIC.  $RHO=11 - F$

[DDW020]

SYMBOL	ALPHA	PARAMETRIC VALUES			DATASET	DATA SOURCE		
		BETA	AIL-L	STB-L		RN/L	Dataset	RN/L
O	-70.000	.000	.000	.000	DDW020	1.476	DDW021	2.952
					DDW022	4.428	DDW023	5.904
					DDW024	7.413	DDW025	11.152
					DDW026	13.120	DDW027	14.760
					DDW028	16.400		

ORIGINAL PAGE IS  
OF POOR QUALITY

66

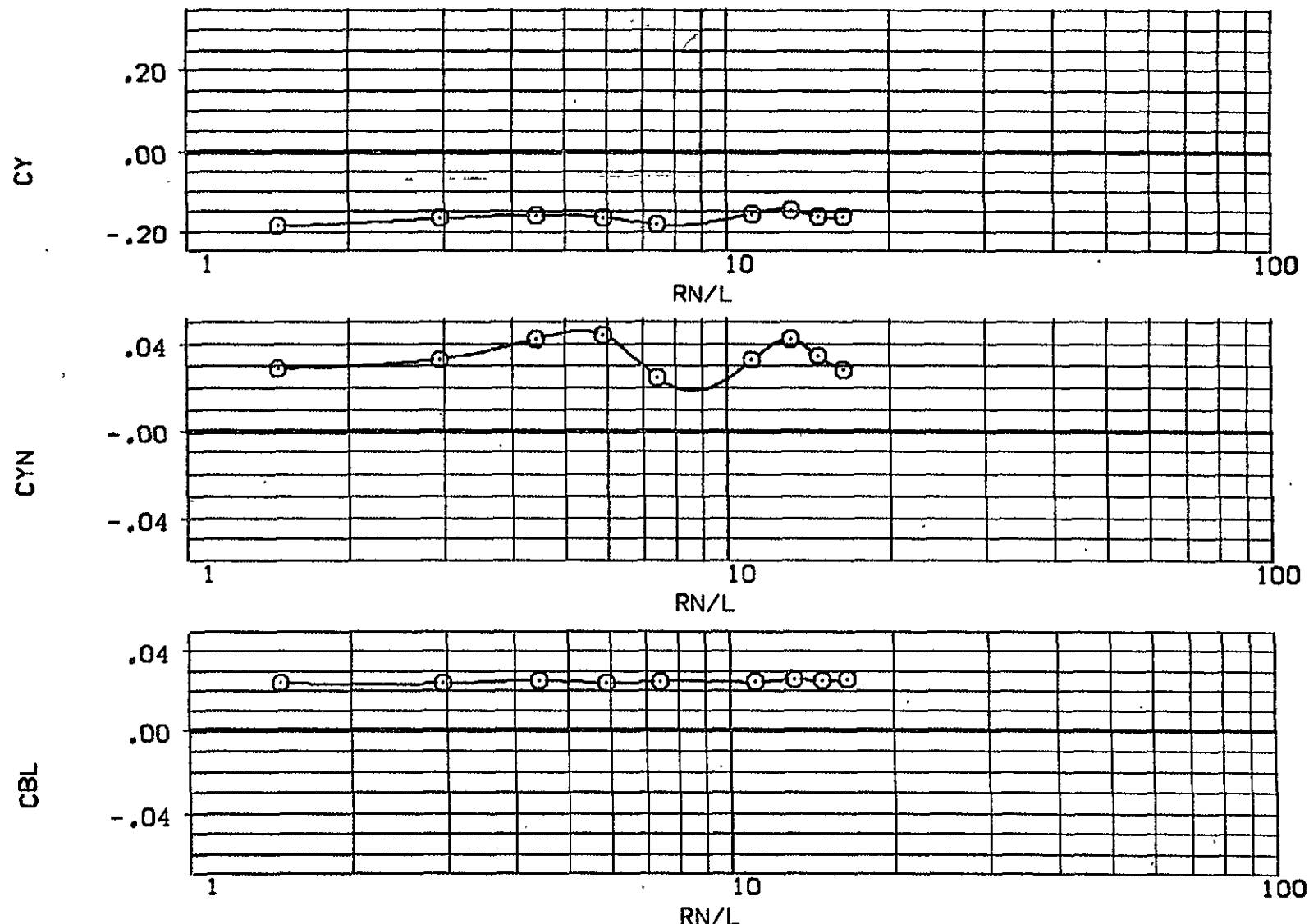


FIG. 4 VARIATION OF AERO. CHAR. WITH REYNOLDS NO. AT VARIOUS ANGLES OF ATTACK.

SYMBOL    ALPHA    BETA    PARAMETRIC VALUES    DATA SOURCE

O	-60.000	BETA	10.000	AIL-L	.000	DATASET	RN/L	DATASET	RN/L
		AIL-R	.000	STB-L	.000	DDW020	1.476	DDW021	2.952
		STB-R	.000			DDW022	4.428	DDW023	5.904
						DDW024	7.413	DDW025	11.152
						DDW026	13.120	DDW027	14.760
						DDW028	16.400		

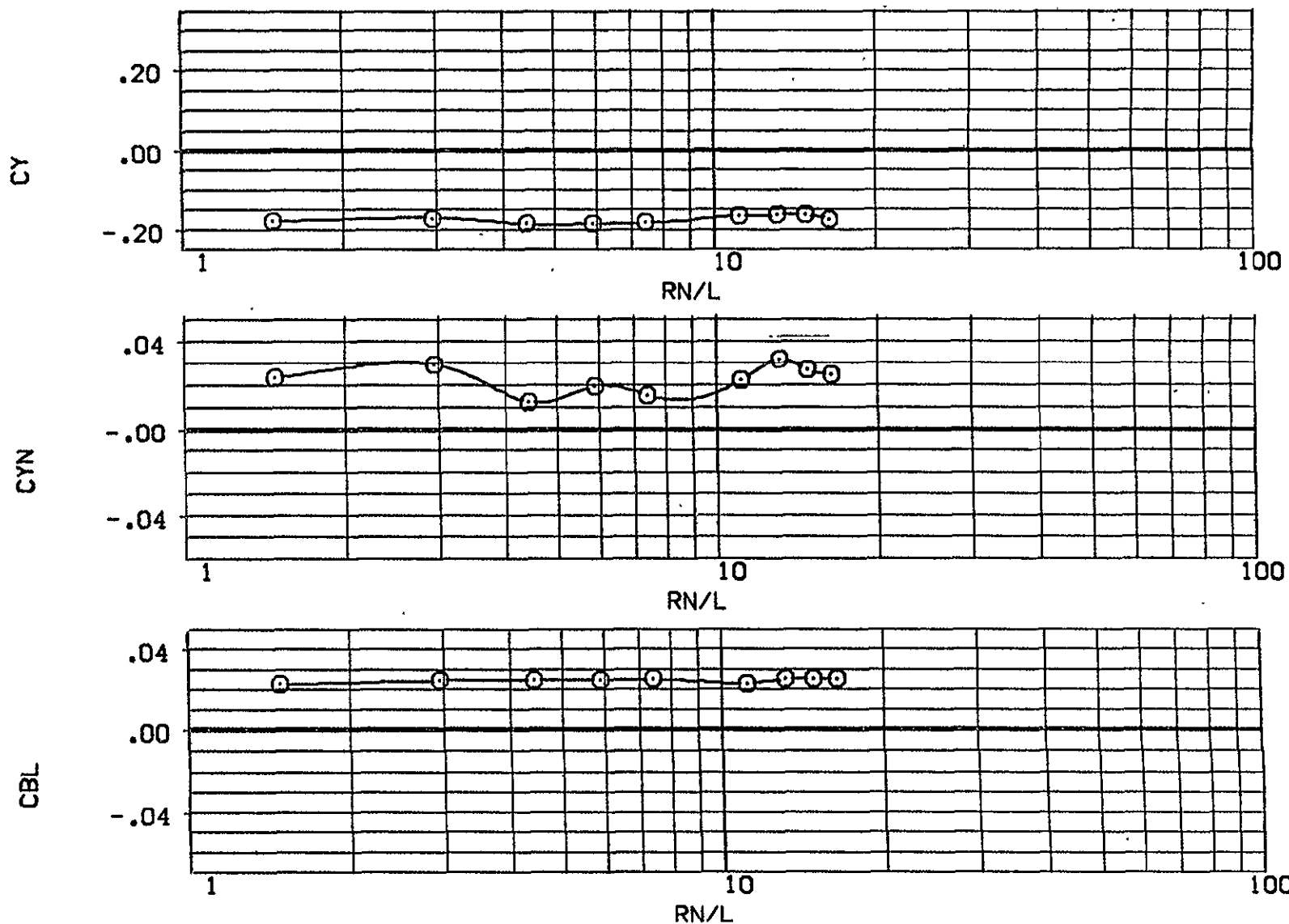


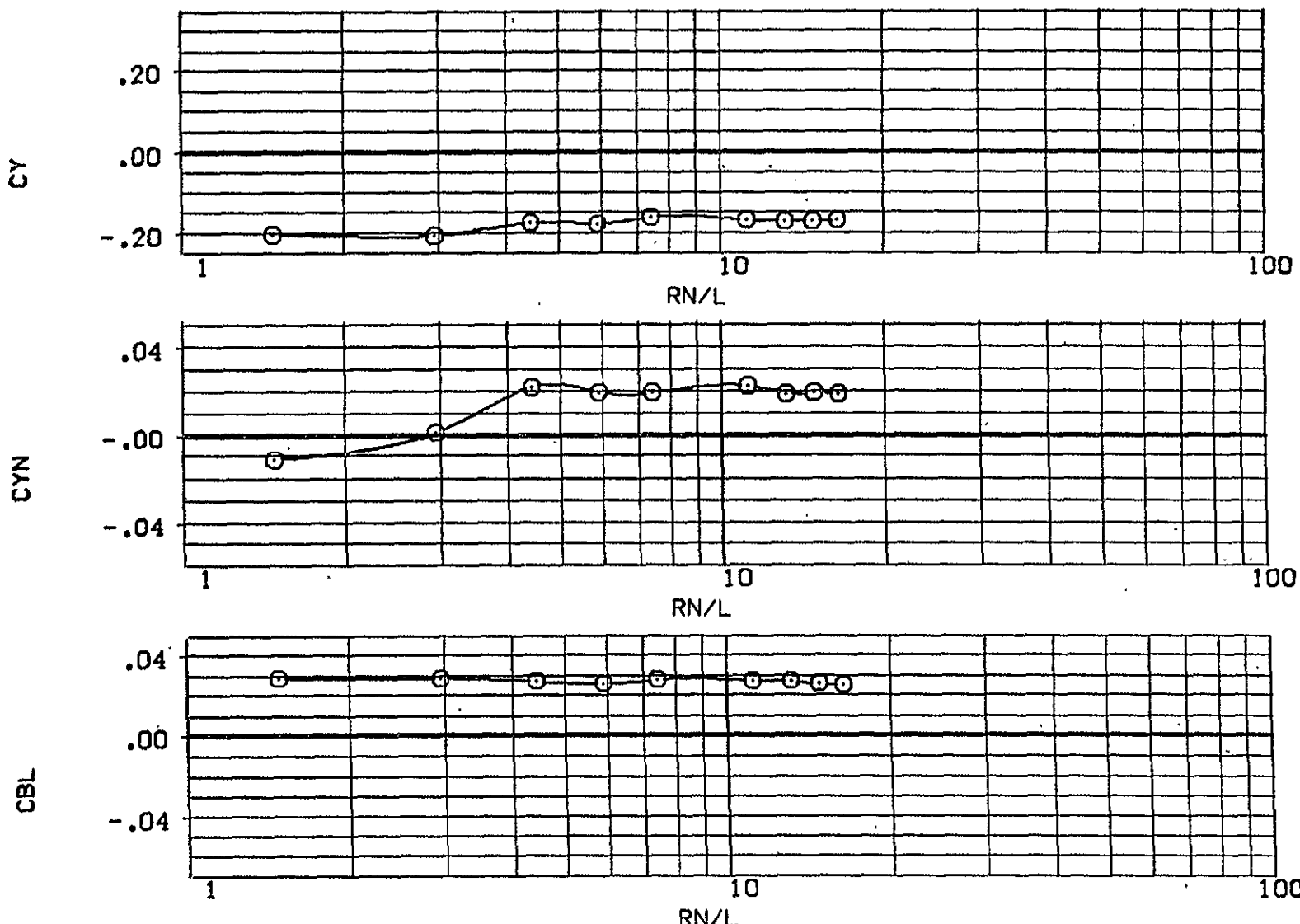
FIG. 4 VARIATION OF AERO. CHAR. WITH REYNOLDS NO. AT VARIOUS ANGLES OF ATTACK.

BASIC, RHO=11 - F

(DDW020)

<b>SYMBOL</b>	<b>ALPHA</b>	<b>PARAMETRIC VALUES</b>		
O	-50.000	<b>BETA</b>	10.000	AIL-L
		AIL-R	.000	STB-L
		STB-R	.000	

DATA SOURCE				
.000	DATASET	RN/L	DATASET	RN/L
.000	DDW020	1.476	DDW021	2.952
	DDW022	4.428	DDW023	5.904
	DDW024	7.413	DDW025	11.152
	DDW026	13.120	DDW027	14.760
	DDW028	16.400		



ORIGINAL PAGE IS  
OF POOR QUALITY

FIG. 4 VARIATION OF AERO. CHAR. WITH REYNOLDS NO. AT VARIOUS ANGLES OF ATTACK.

SYMBOL	ALPHA	PARAMETRIC VALUES			DATASET	DATA SOURCE	
		BETA	AIL-L	.000		RN/L	DATASET
O	-40.000	10.000	.000	DDW020	1.476	DDW021	2.952
	AIL-R	.000	STB-L	DDW022	4.428	DDW023	5.904
	STB-R	.000		DDW024	7.413	DDW025	11.152
				DDW026	13.120	DDW027	14.760
				DDW028	16.400		

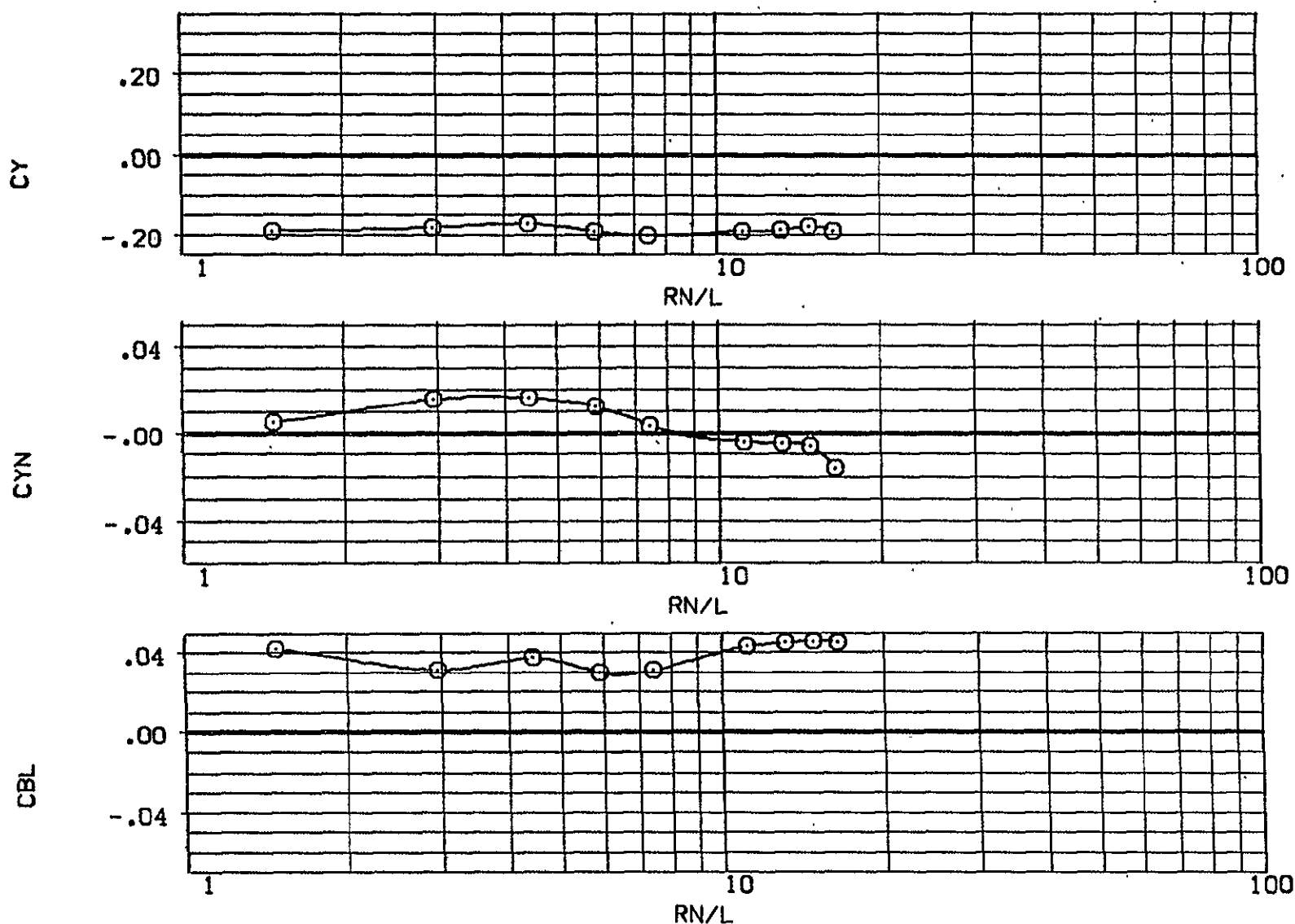


FIG. 4 VARIATION OF AERO. CHAR. WITH REYNOLDS NO. AT VARIOUS ANGLES OF ATTACK.

DATA SET SYMBOL CONFIGURATION DESCRIPTION  
 (BDW001) (100A9) BASIC, RHO=0 + GRIT  
 (600A8) (100A9) BASIC, RHO=11 + GRIT

AIL-L AIL-R STB-L STB-R  
 :000 :000 :000 :000

ORIGINAL PAGE 1  
OF POOR  
QUALITY

72

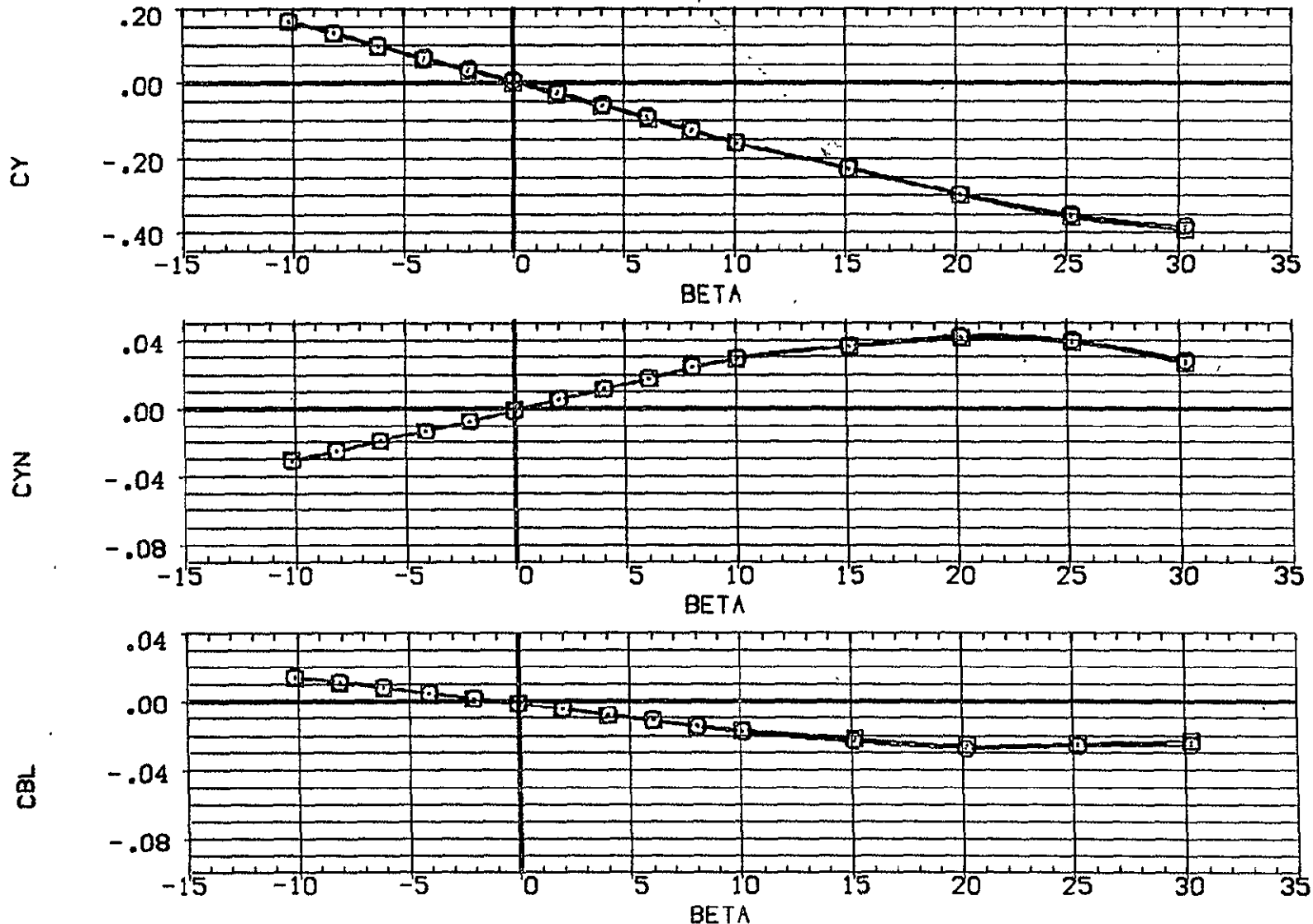


FIG. 5 EFFECT OF RAMP ANGLE ON AERODYNAMIC CHAR., REYNOLDS NO.= 13.12 MIL.

(A) ALPHA = -.11

PAGE 41

DATA SET SYMBOL CONFIGURATION DESCRIPTION  
 {BDW001} O BASIC, RHO=0 + GRIT  
 {BDW009} □ BASIC, RHO=11 + GRIT

	AIL-L	AIL-R	STB-L	STB-R
{BDW001}	:000	:000	:000	:000
{BDW009}	.000	.000	.000	.000

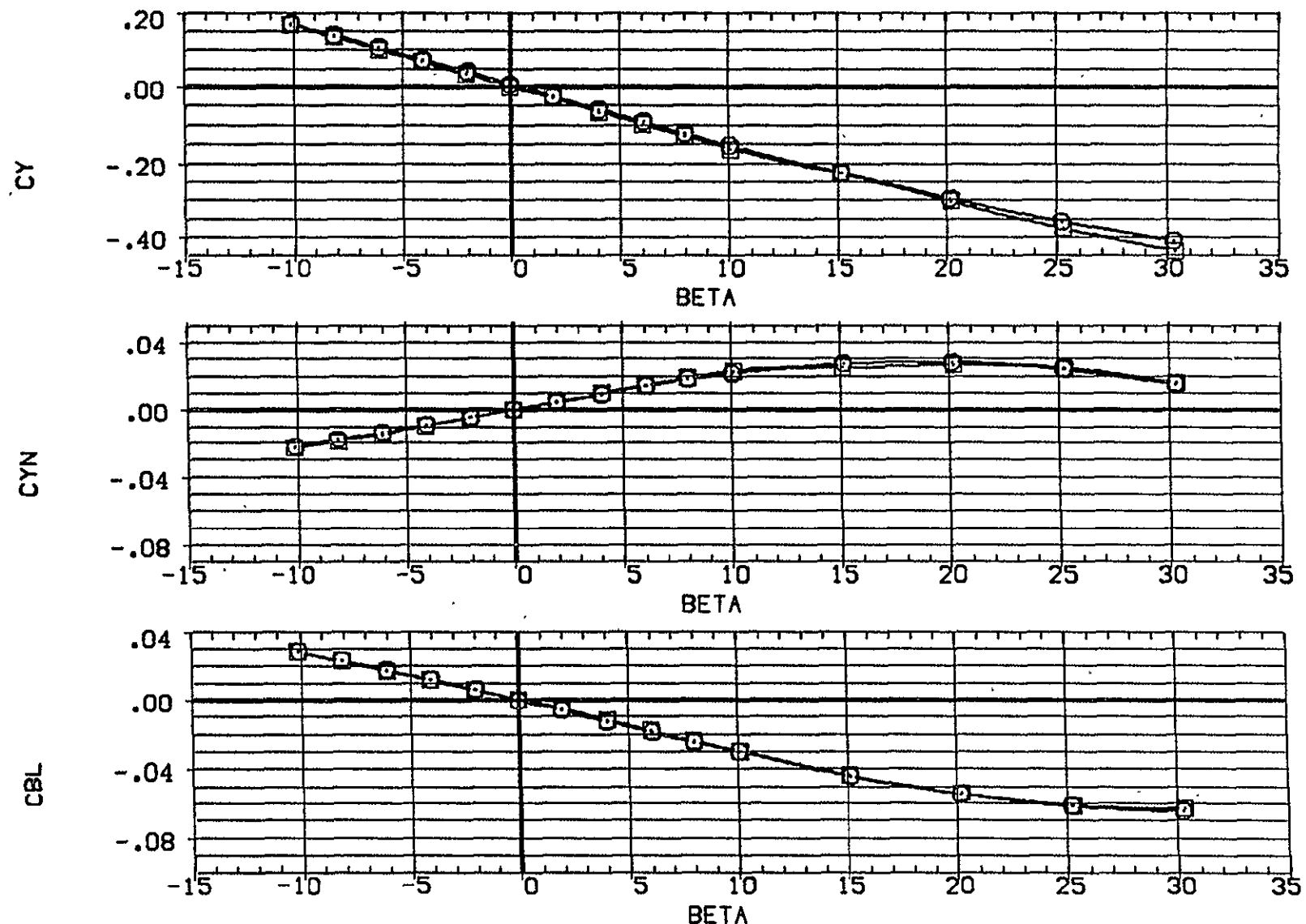


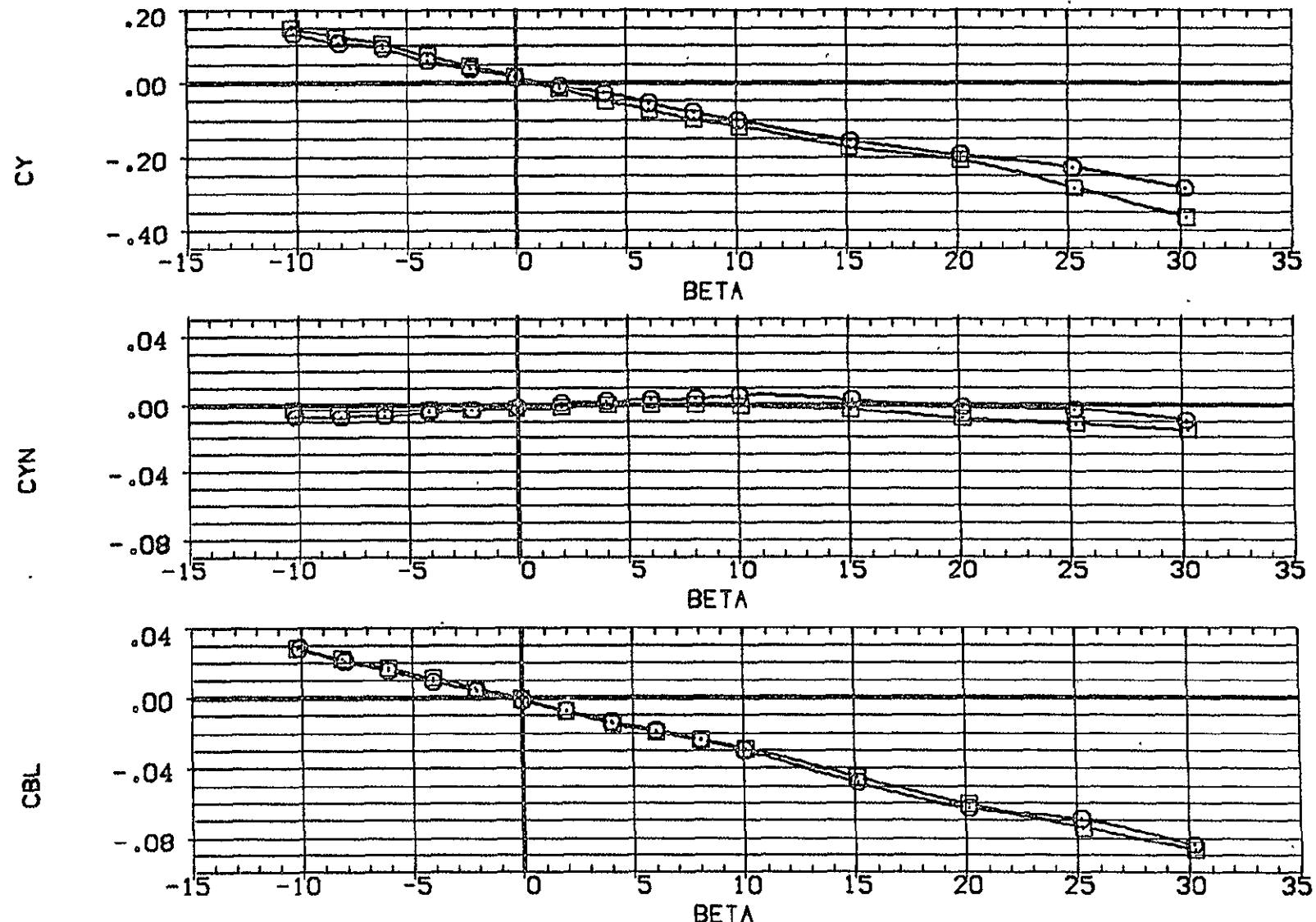
FIG. 5 EFFECT OF RAMP ANGLE ON AERODYNAMIC CHAR., REYNOLDS NO.= 13.12 MIL.

(B) ALPHA = 10.46

PAGE 42

DATA SET SYMBOL CONFIGURATION DESCRIPTION  
 (BDW001) (100AD8)  
 BASIC, RHO=0 + GRIT  
 (600AD8) (600AD8)  
 BASIC, RHO=11 + GRIT

AIL-L AIL-R STB-L STB-R  
 .000 .000 .000 .000  
 .000 .000 .000 .000



ORIGINAL PAGE IS  
OF POOR QUALITY

74

FIG. 5 EFFECT OF RAMP ANGLE ON AERODYNAMIC CHAR., REYNOLDS NO.= 13.12 MIL.  
 (C)ALPHA = 21.00

DATA SET SYMBOL CONFIGURATION DESCRIPTION  
 {BDW001} O BASIC, RHO=0 + GRIT  
 {BDW009} □ BASIC, RHO=11 + GRIT

	AIL-L	AIL-R	STB-L	STB-R
{BDW001}	.000	.000	.000	.000
{BDW009}	.000	.000	.000	.000

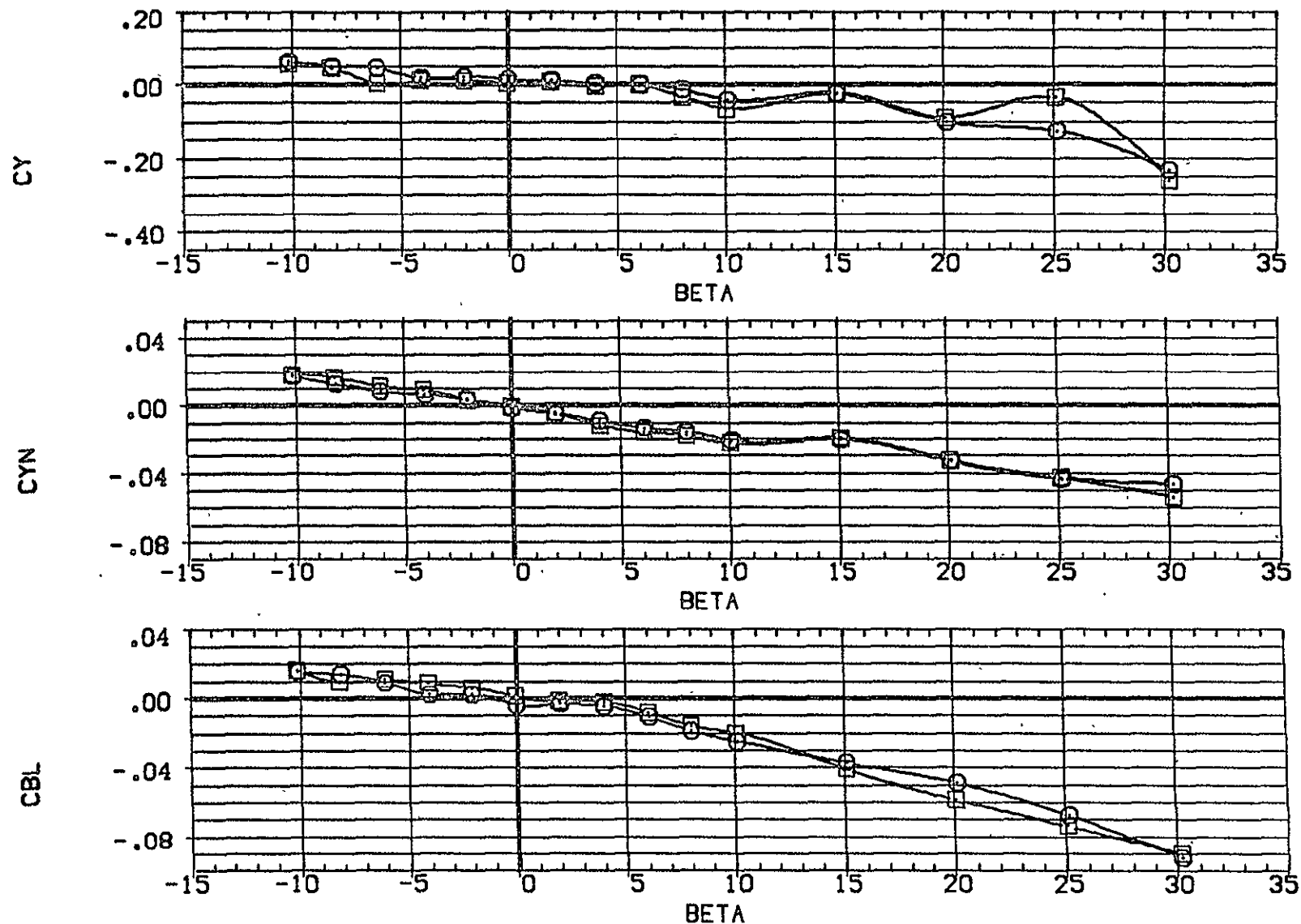


FIG. 5 EFFECT OF RAMP ANGLE ON AERODYNAMIC CHAR., REYNOLDS NO.= 13.12 MIL.

(D)ALPHA = 31.29

PAGE 44

DATA SET SYMBOL CONFIGURATION DESCRIPTION  
(BDWOOD) (1001) DATA NOT AVAILABLE  
(BDWOOD) (6000) BASIC, RHO=1.1 + GRIT

AIL-L AIL-R STB-L STB-R  
.000 .000 .000 .000  
.000 .000 .000 .000

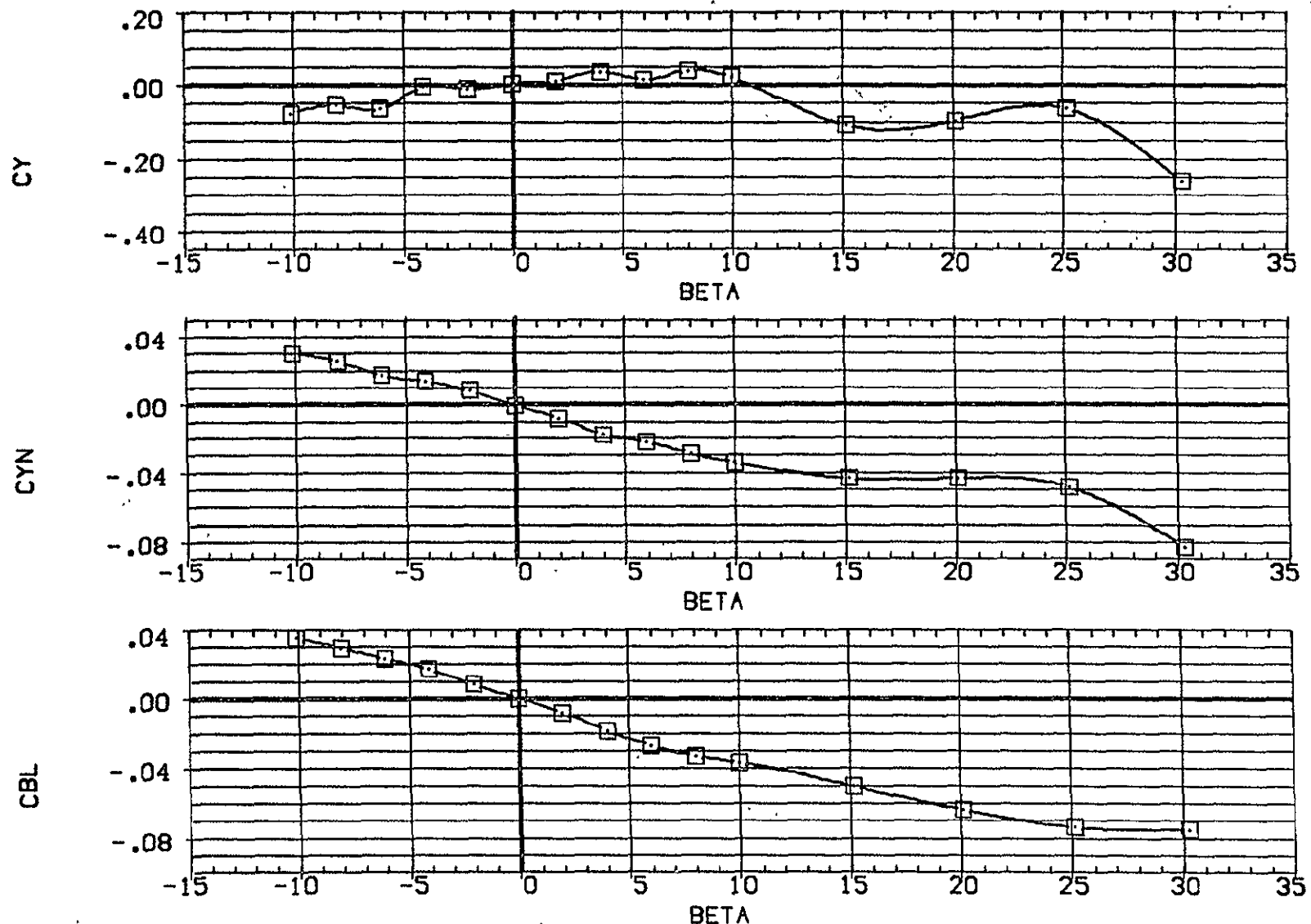


FIG. 5 EFFECT OF RAMP ANGLE ON AERODYNAMIC CHAR., REYNOLDS NO.= 13.12 MIL.

(E) ALPHA = 41.34

PAGE 45

DATA SET SYMBOL CONFIGURATION DESCRIPTION  
 (BDW001)  BASIC, RHO=0 + GRIT  
 (BDW009)  BASIC, RHO=11 + GRIT

AIL-L	AIL-R	STB-L	STB-R
:000	:000	:000	:000
:000	:000	:000	:000

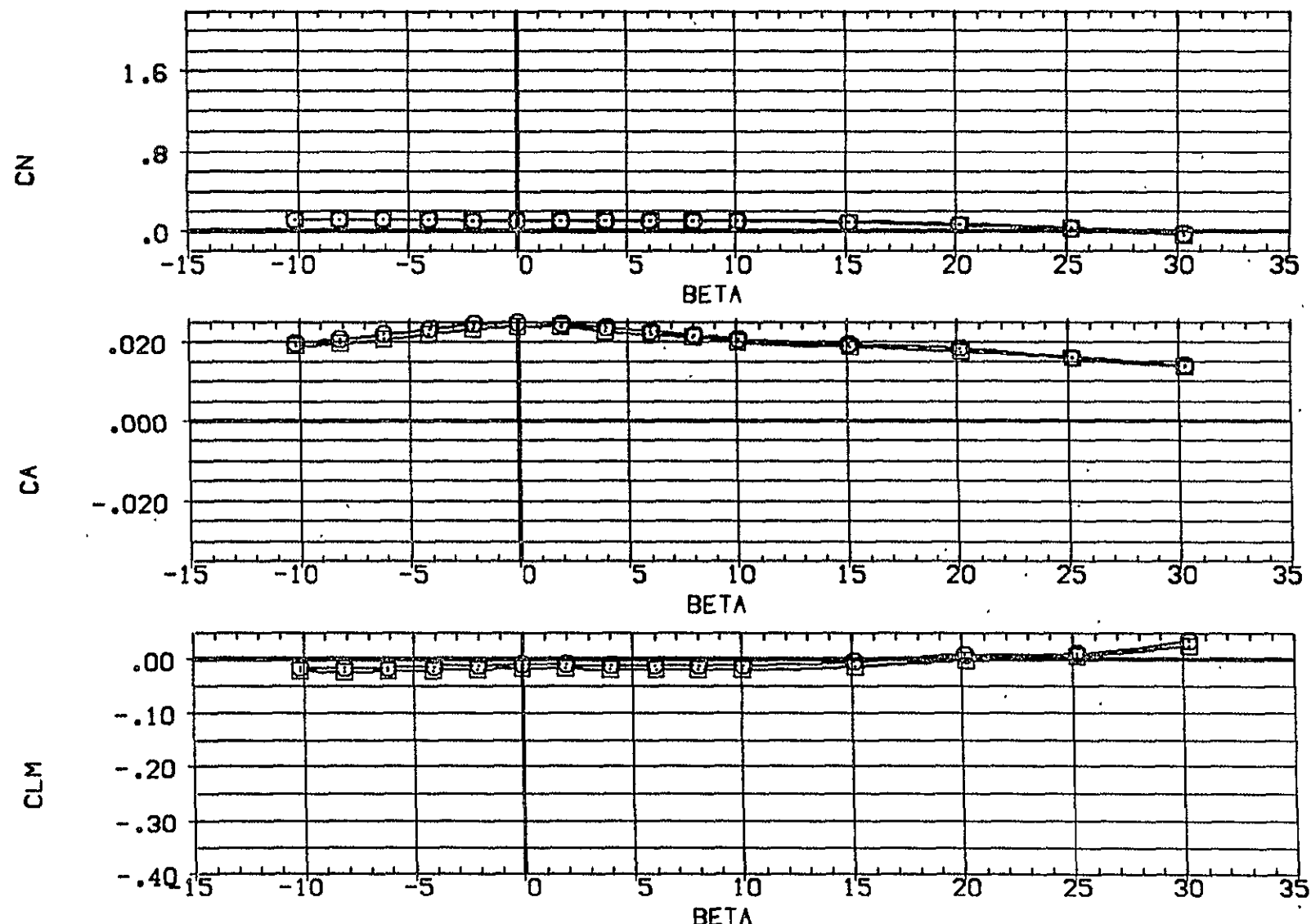


FIG. 5 EFFECT OF RAMP ANGLE ON AERODYNAMIC CHAR., REYNOLDS NO.= 13.12 MIL.

(A) ALPHA = -.11

PAGE 46

ORIGINAL PAGE IS  
OF POOR QUALITY

DATA SET SYMBOL CONFIGURATION DESCRIPTION  
(800001) O BASIC: RHO=0 + GRIT  
(800008) □ BASIC: RHO=11 + GRIT

AIL-L AIL-R STB-L STB-R  
.000 .000 .000 .000  
.000 .000 .000 .000

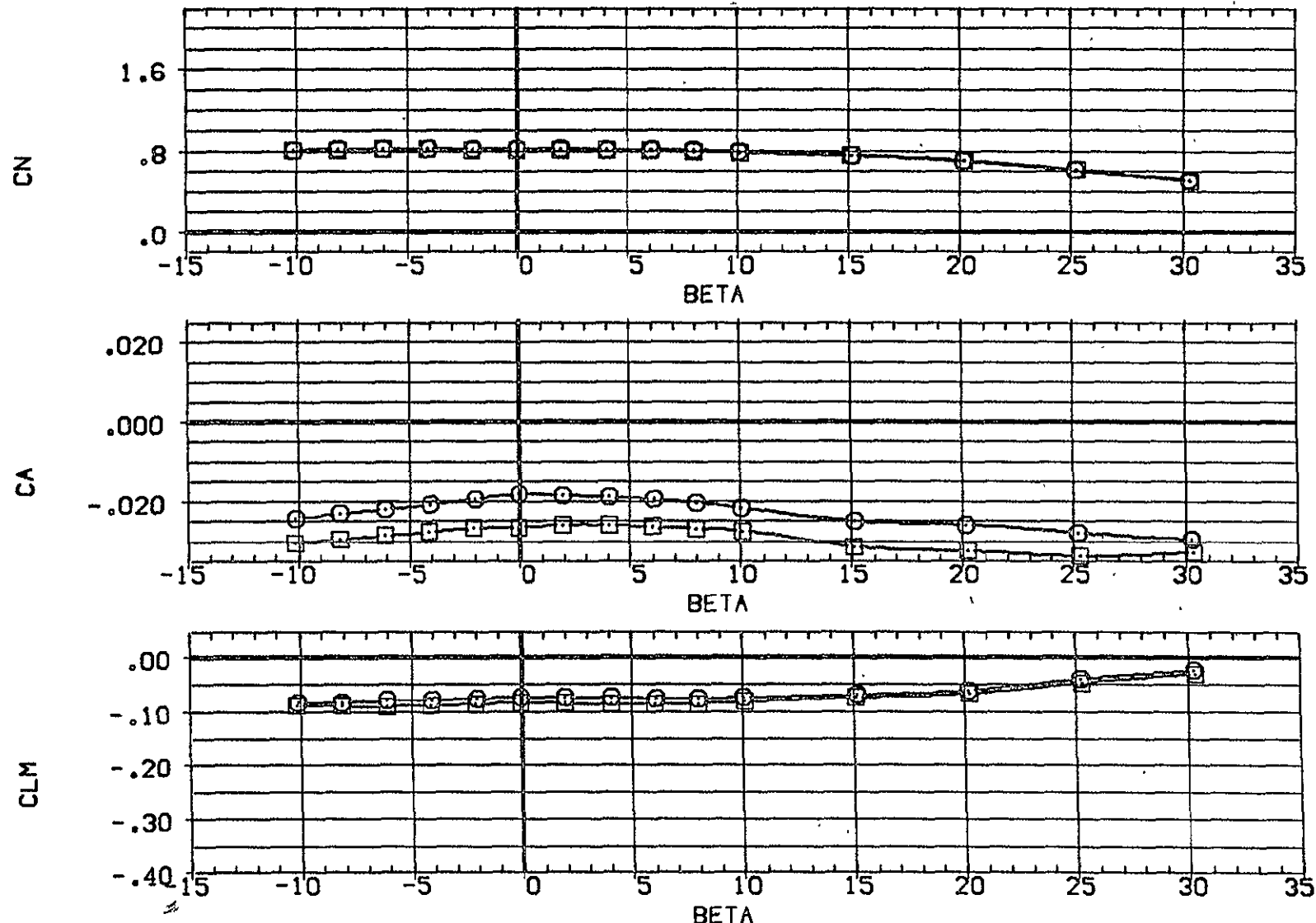


FIG. 5 EFFECT OF RAMP ANGLE ON AERODYNAMIC CHAR., REYNOLDS NO.= 13.12 MIL.  
(B)ALPHA = 10.46

DATA SET SYMBOL CONFIGURATION DESCRIPTION  
 {BDW001} BASIC, RHO=0 + GRIT  
 {BDW009} BASIC, RHO=11 + GRIT

	AIL-L	AIL-R	STB-L	STB-R
{BDW001}	.000	.000	.000	.000
{BDW009}	.000	.000	.000	.000

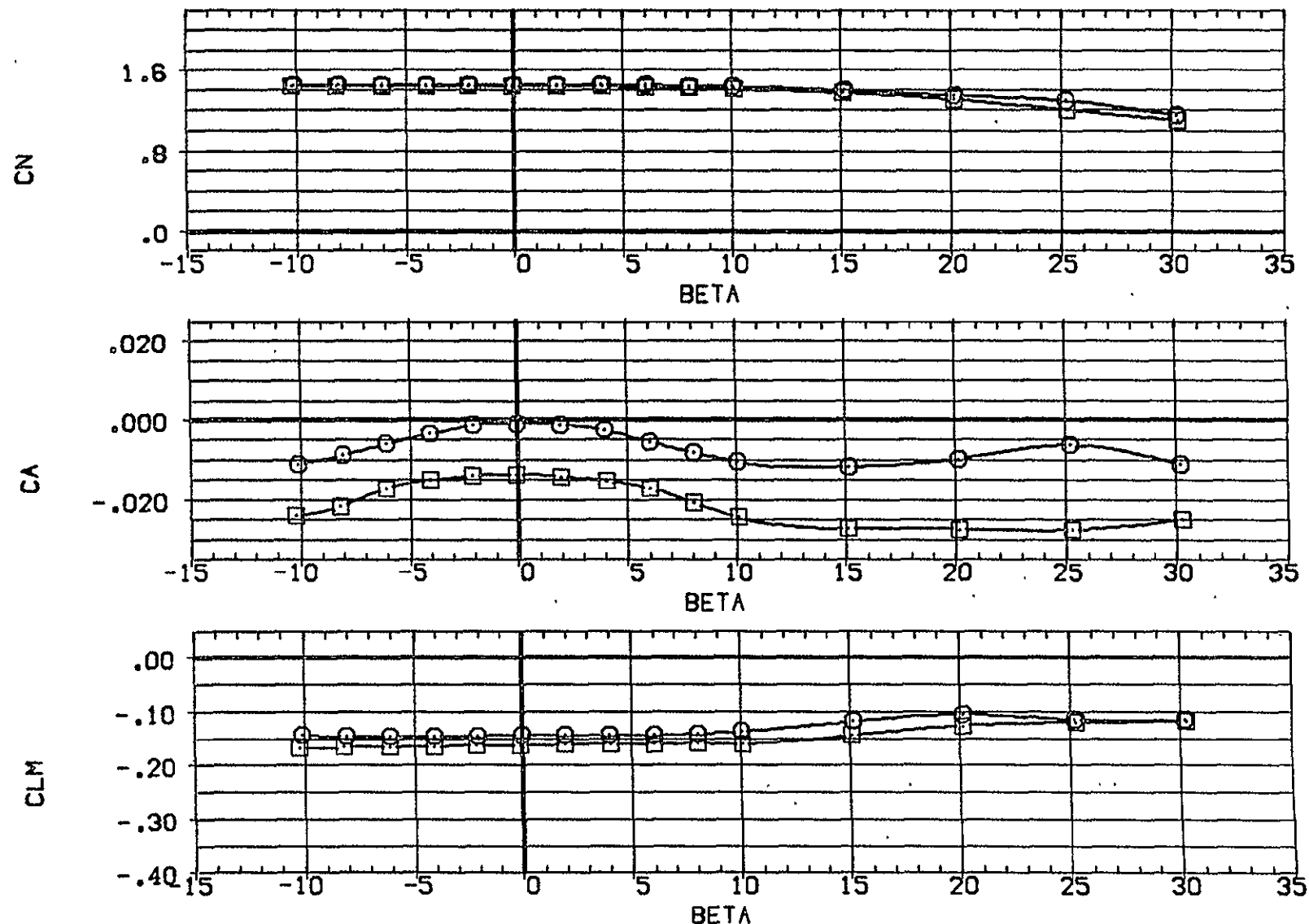


FIG. 5 EFFECT OF RAMP ANGLE ON AERODYNAMIC CHAR., REYNOLDS NO.= 13.12 MIL.

(C)ALPHA = 21.00

PAGE 48

ORIGINAL PAGE IS  
OF POOR QUALITY

DATA SET SYMBOL CONFIGURATION DESCRIPTION  
(BDW001) O BASIC, RHO=0 + GRIT  
(BDW009) □ BASIC, RHO=11 + GRIT

AIL-L AIL-R STB-L STB-R  
.000 .000 .000 .000  
.000 .000 .000 .000

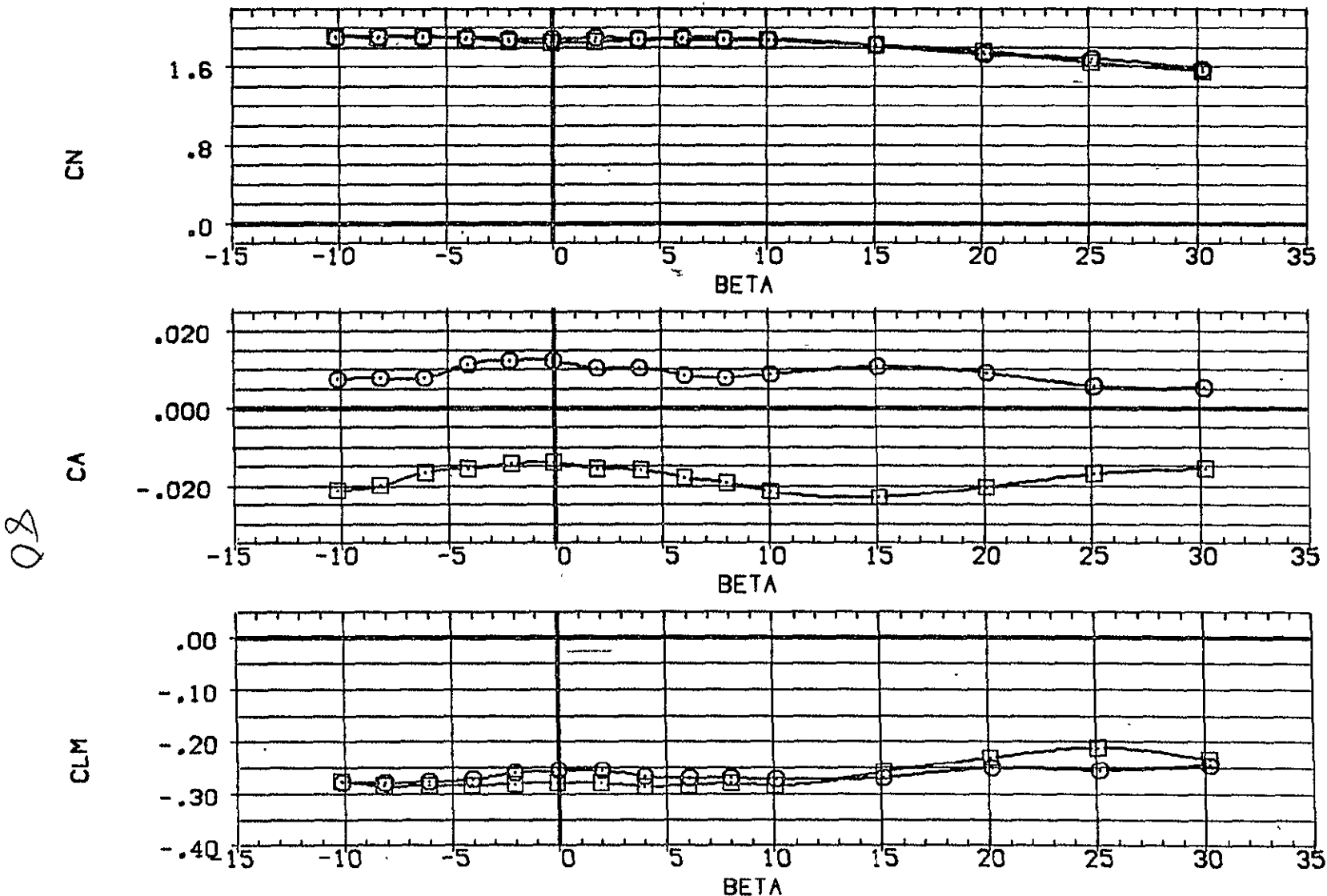


FIG. 5 EFFECT OF RAMP ANGLE ON AERODYNAMIC CHAR., REYNOLDS NO.= 13.12 MIL.

(D)ALPHA = 31.29

PAGE 49

DATA SET SYMBOL CONFIGURATION DESCRIPTION  
 (BDV001) DATA NOT AVAILABLE  
 (BDV009) BASIC, RHO=1.1 + GRIT

	AIL-L	AIL-R	STB-L	STB-R
(BDV001)	.000	.000	.000	.000
(BDV009)	.000	.000	.000	.000

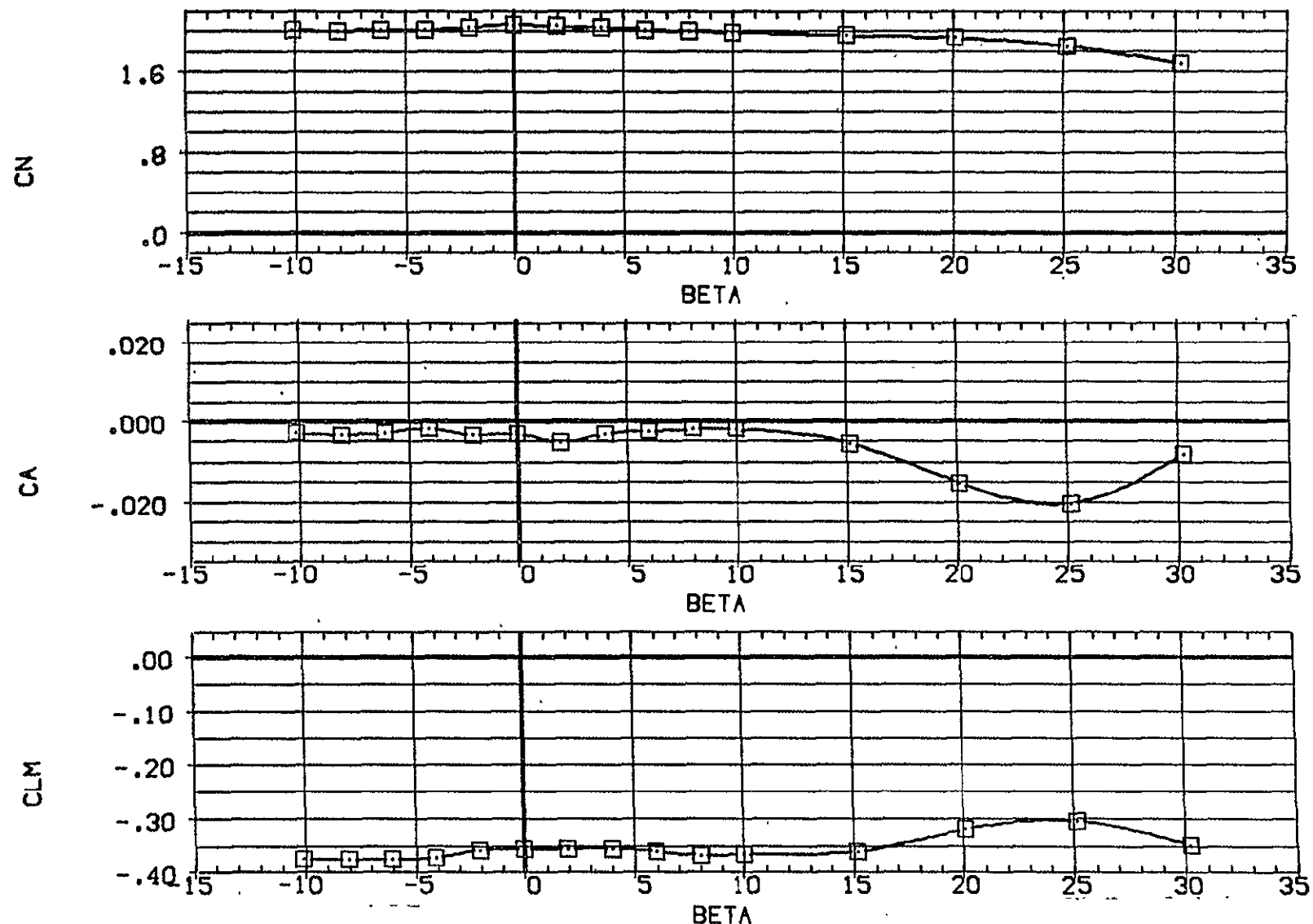


FIG. 5 EFFECT OF RAMP ANGLE ON AERODYNAMIC CHAR., REYNOLDS NO.= 13.12 MIL.

CEDALPHA = 41.34

PAGE 50

DATA SET SYMBOL CONFIGURATION DESCRIPTION  
 (EDW001) O BASIC. RHO=0 + GRIT  
 (EDW009) □ BASIC. RHO=11 + GRIT

AIL-L	AIL-R	STB-L	STB-R
.000	.000	.000	.000
.000	.000	.000	.000

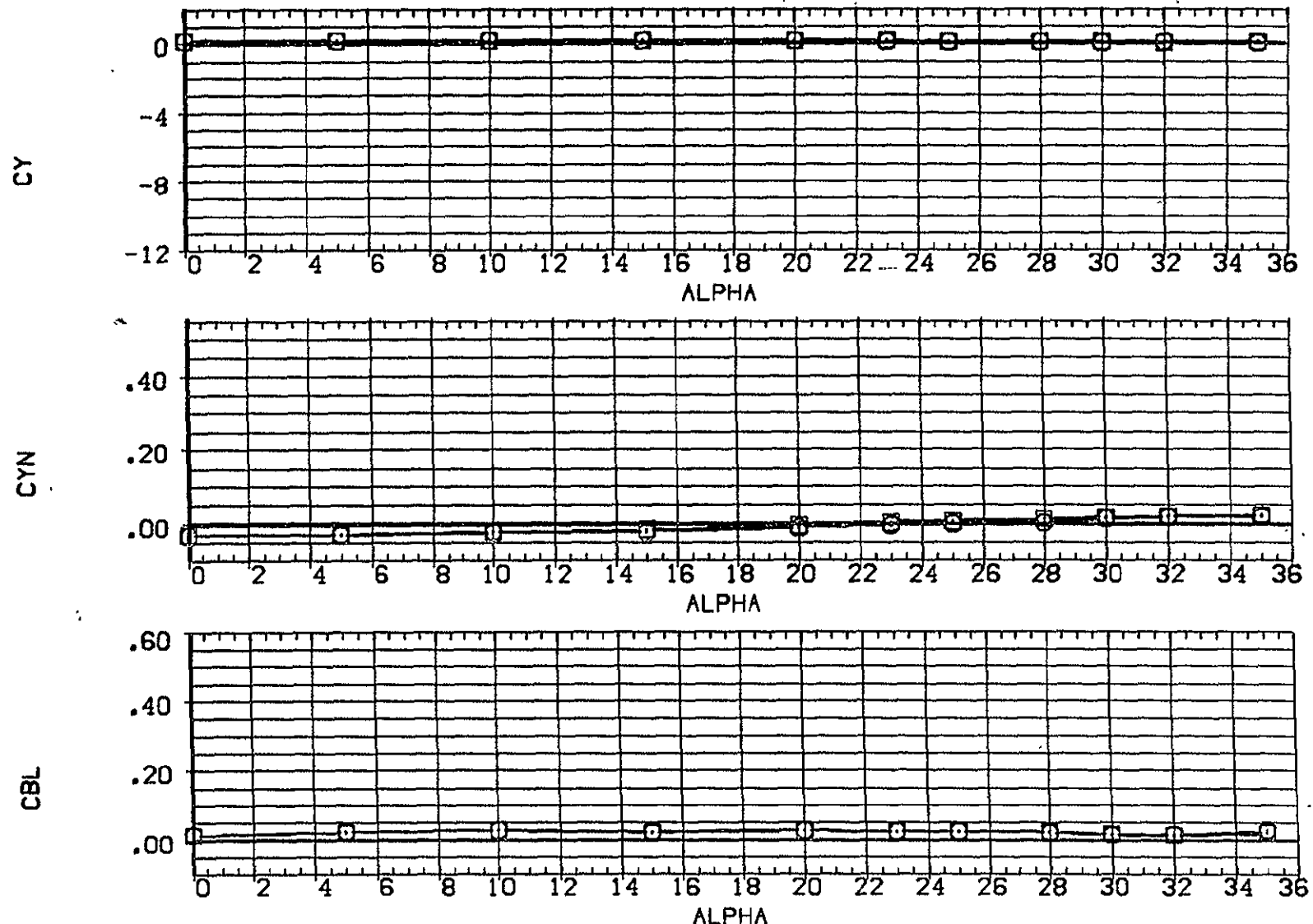


FIG. 6 EFFECT OF RAMP ANGLE ON AERODYNAMIC CHAR., REYNOLDS NO.= 13.12 MIL.

(A) BETA = -10.00

PAGE 51

DATA SET SYMBOL CONFIGURATION DESCRIPTION  
 (EDW001)  BASIC, RHO=0 + GRIT  
 (EDW009)  BASIC, RHO=11 + GRIT

AIL-L	AIL-R	STB-L	STB-R
.000	.000	.000	.000
.000	.000	.000	.000

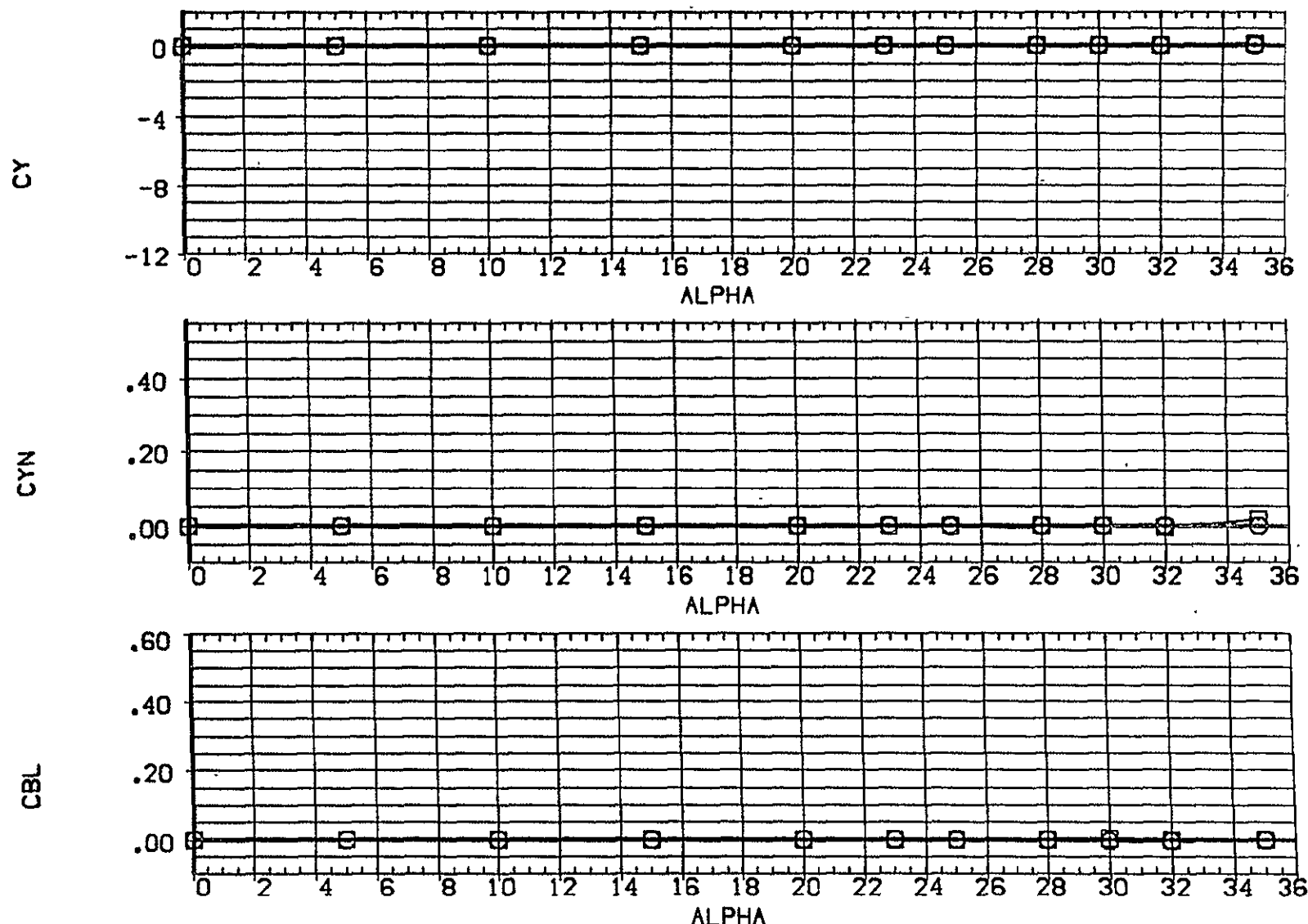


FIG. 6 EFFECT OF RAMP ANGLE ON AERODYNAMIC CHAR., REYNOLDS NO.= 13.12 MIL.

(B)BETA = .00

PAGE 52

ORIGINAL PAGE IS  
OF POOR QUALITY

DATA SET SYMBOL CONFIGURATION DESCRIPTION  
(EDW001) O BASIC, RHO=0 + GRIT  
(EDW009) □ BASIC, RHO=11 + GRIT

AIL-L AIL-R STB-L STB-R  
.000 .000 .000 .000  
.000 .000 .000 .000

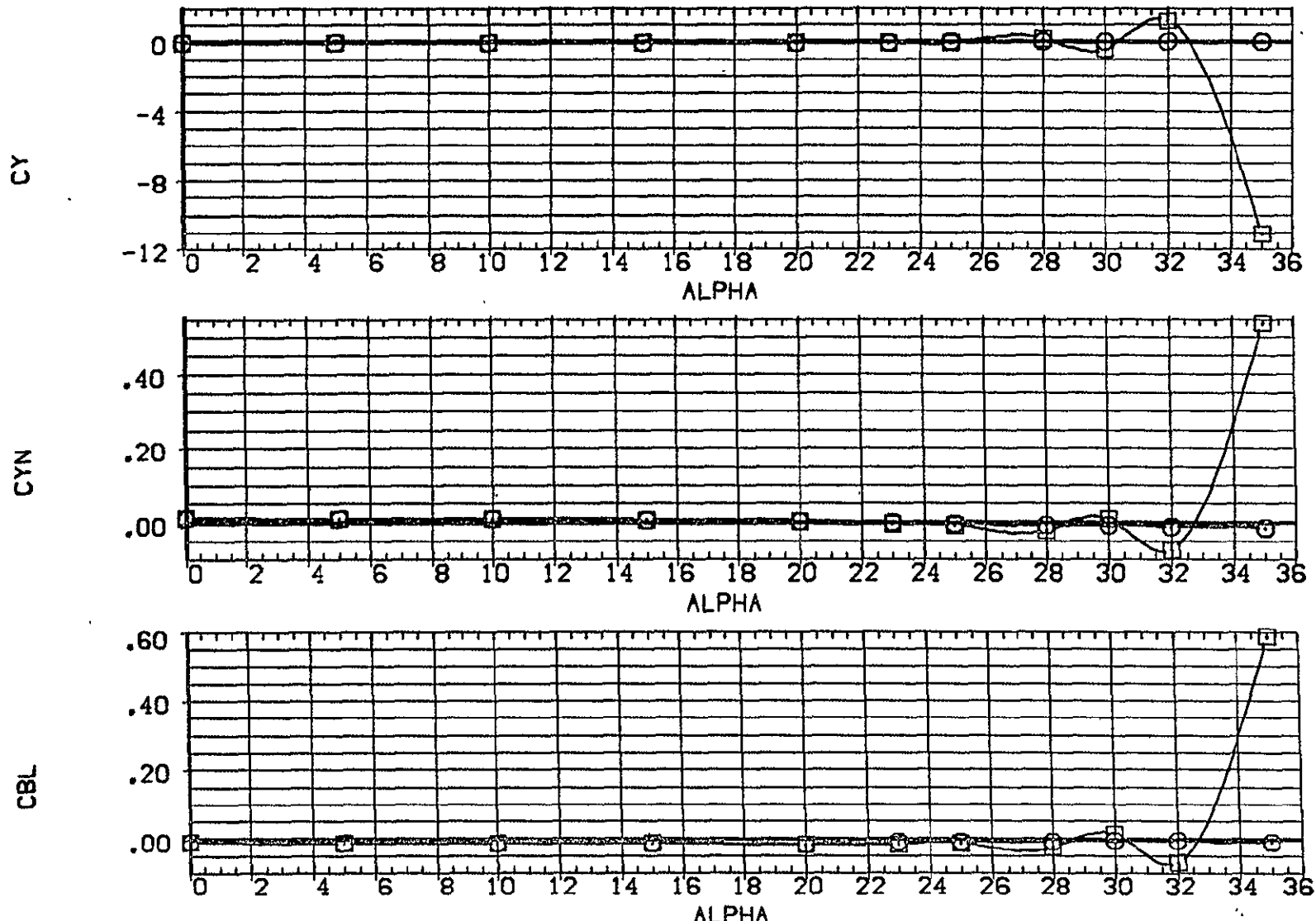


FIG. 6 EFFECT OF RAMP ANGLE ON AERODYNAMIC CHAR., REYNOLDS NO.= 13.12 MIL.

(C)BETA = 4.00

PAGE 53

DATA SET SYMBOL CONFIGURATION DESCRIPTION  
 (EDW001)  BASIC, RHO=0 + GRIT  
 (EDW009)  BASIC, RHO=11 + GRIT

AIL-L	AIL-R	STB-L	STB-R
.000	.000	.000	.000
.000	.000	.000	.000

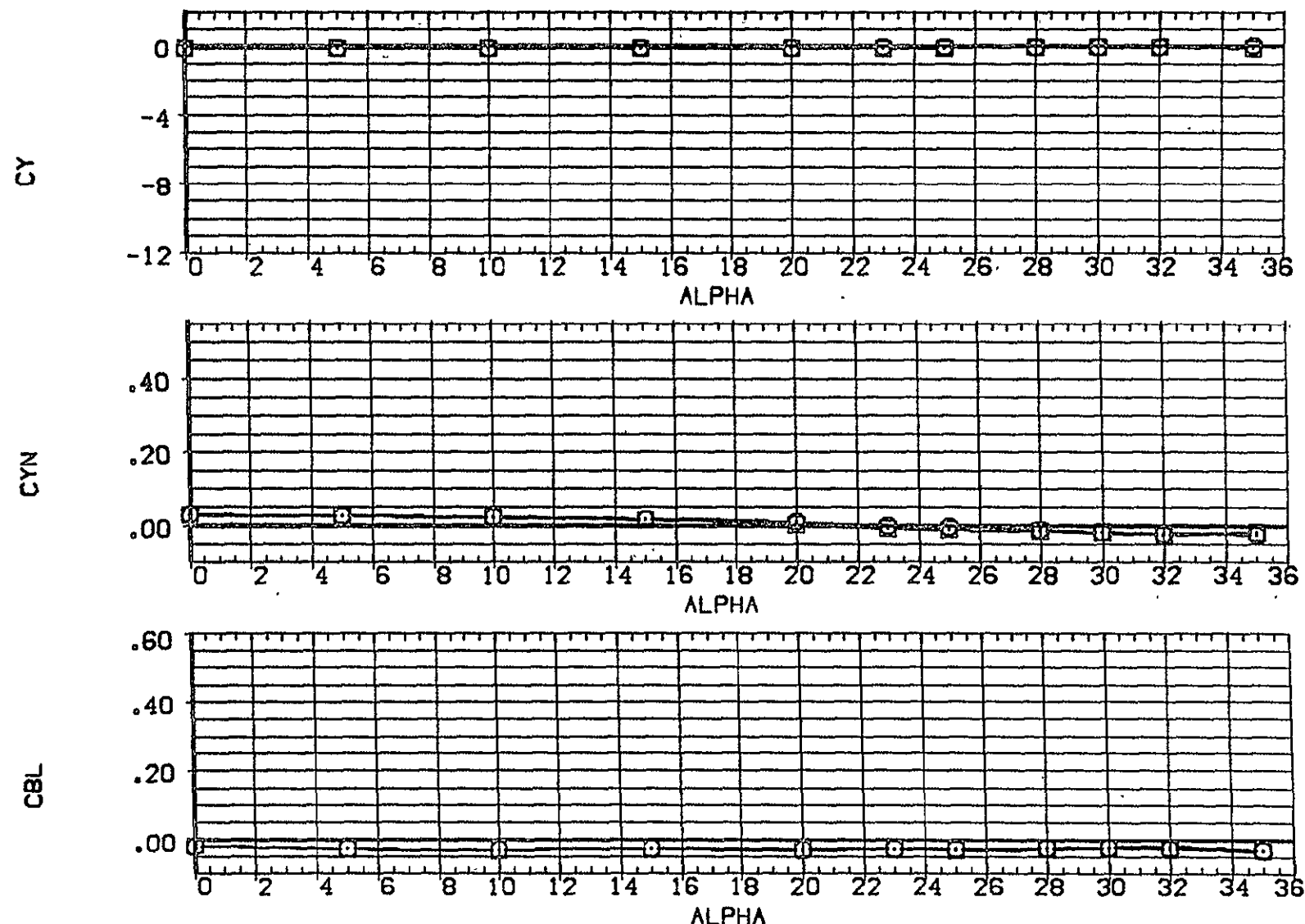


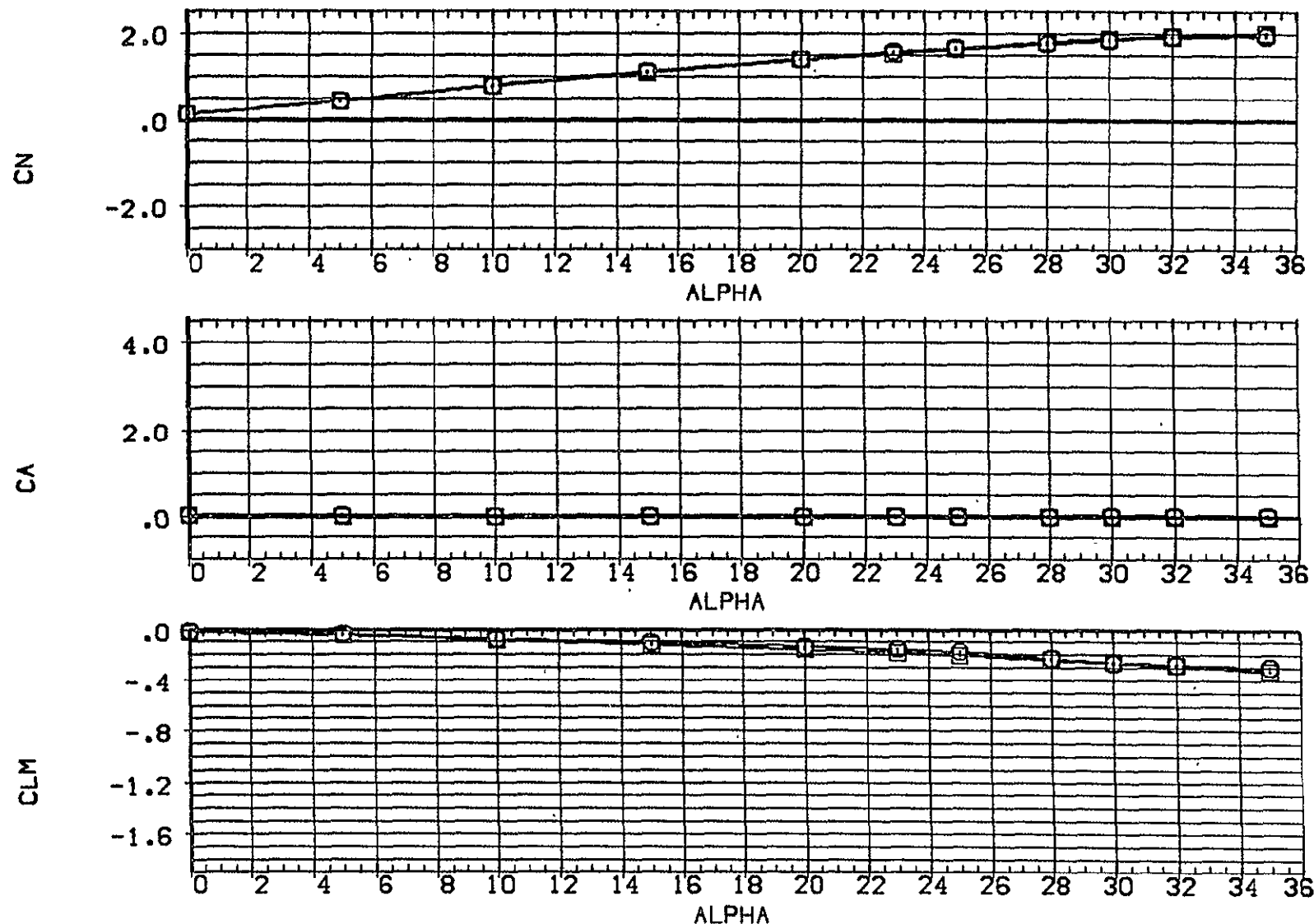
FIG. 6 EFFECT OF RAMP ANGLE ON AERODYNAMIC CHAR., REYNOLDS NO.= 13.12 MIL.

(D)BETA = 10.00

PAGE 54

DATA SET SYMBOL CONFIGURATION DESCRIPTION  
 (EDW001)  $\square$  BASIC: RHO=0 + GRIT  
 (EDW009)  $\square$  BASIC: RHO=11 + GRIT

AIL-L	AIL-R	STB-L	STB-R
.000	.000	.000	.000
.000	.000	.000	.000



96  
ORIGINAL PAGE IS  
POOR QUALITY

FIG. 6 EFFECT OF RAMP ANGLE ON AERODYNAMIC CHAR., REYNOLDS NO.= 13.12 MIL.

CABETA = -10.00

PAGE 55

DATA SET SYMBOL CONFIGURATION DESCRIPTION  
(EDW001) O BASIC, RHO=0 + GRIT  
(EDW009) □ BASIC, RHO=11 + GRIT

AIL-L AIL-R STB-L STB-R  
.000 .000 .000 .000  
.000 .000 .000 .000

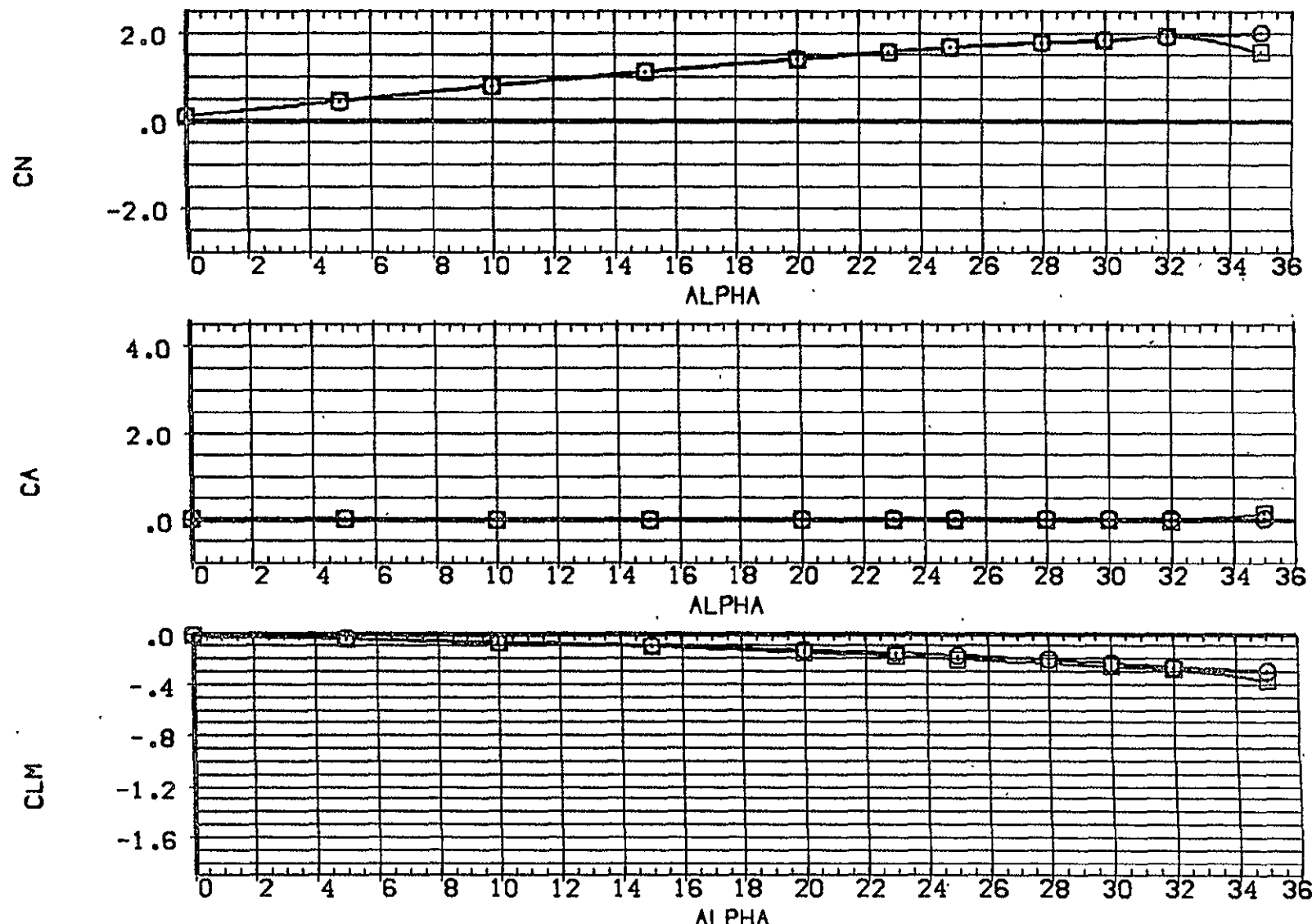


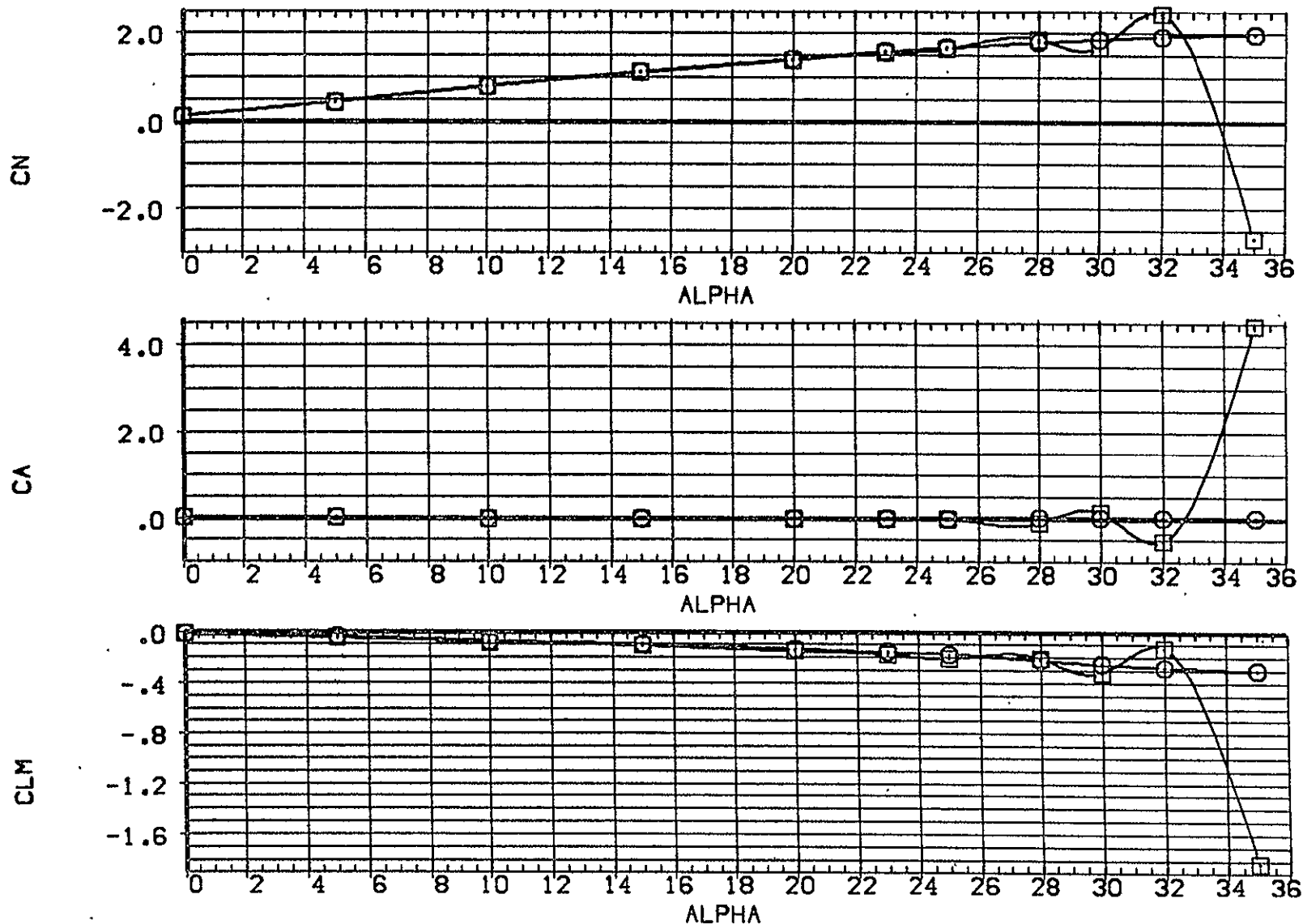
FIG. 6 EFFECT OF RAMP ANGLE ON AERODYNAMIC CHAR., REYNOLDS NO.= 13.12 MIL.

(B)BETA = .00

PAGE 56

DATA SET SYMBOL CONFIGURATION DESCRIPTION  
 (EDW001) O BASIC, RHO=0 + GRIT  
 (EDW009) □ BASIC, RHO=11 + GRIT

	AIL-L	AIL-R	STB-L	STB-R
(EDW001)	.000	.000	.000	.000
(EDW009)	.000	.000	.000	.000



ORIGINAL PAGE IS  
OF POOR QUALITY

88

FIG. 6 EFFECT OF RAMP ANGLE ON AERODYNAMIC CHAR., REYNOLDS NO.= 13.12 MIL.

(C)BETA = 4.00

PAGE 57

DATA SET SYMBOL CONFIGURATION DESCRIPTION  
 {EDW001]  BASIC, RHO-0 + GRIT  
 {EDW009]  BASIC, RHO-11 + GRIT

	AIL-L	AIL-R	STB-L	STB-R
{EDW001]	.000	.000	.000	.000
{EDW009]	.000	.000	.000	.000

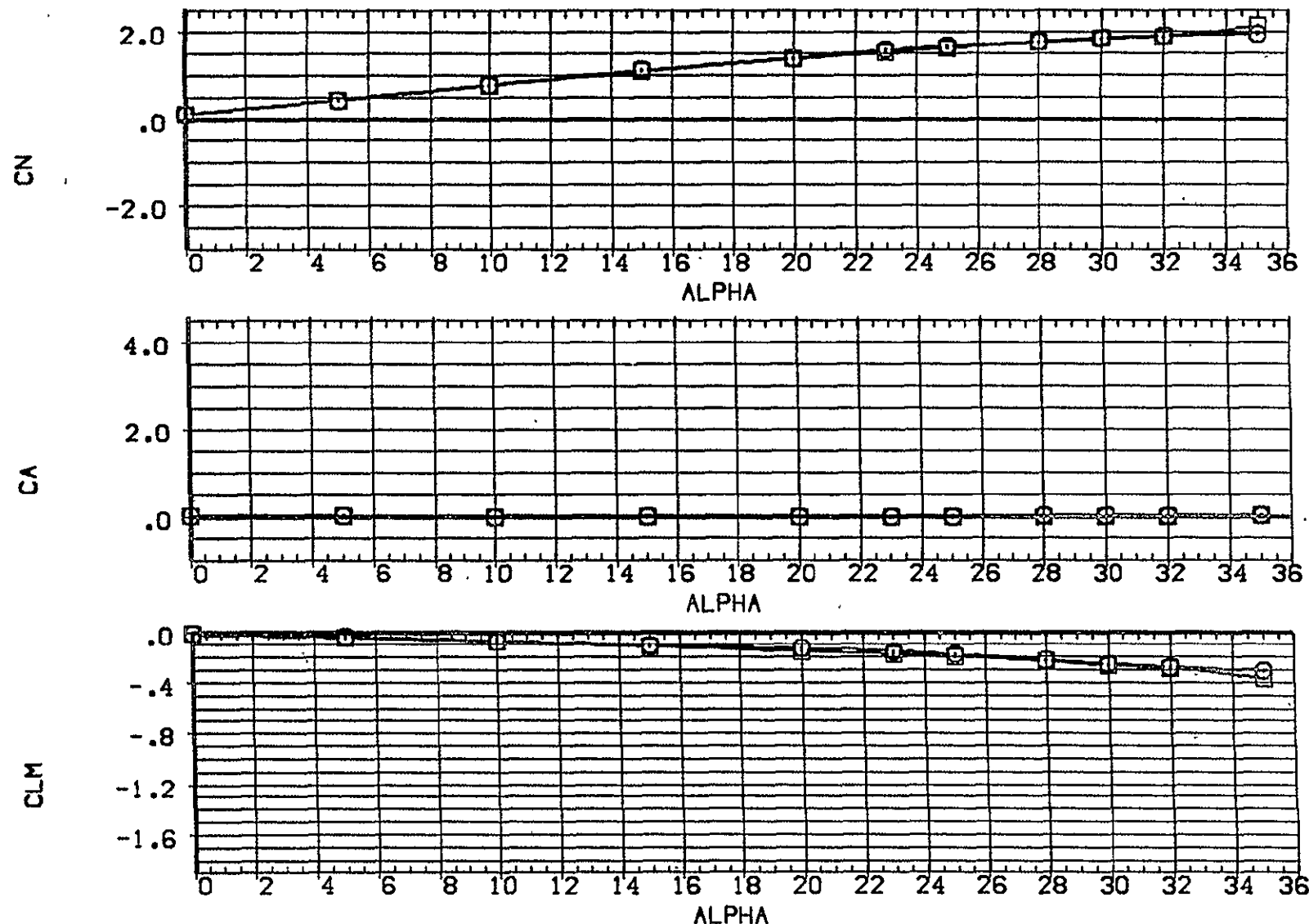


FIG. 6 EFFECT OF RAMP ANGLE ON AERODYNAMIC CHAR., REYNOLDS NO.= 13.12 MIL.

DD(BETA) = 10.00

PAGE 58

DATA SET SYMBOL CONFIGURATION DESCRIPTION  
 (CDW009)  $\square$  BASIC, RHO=11 + GRIT  
 (CDW010)  $\square$  BASIC, RHO=11 + GRIT  
 (CDW011)  $\diamond$  DATA NOT AVAILABLE

	AIL-L	AIL-R	STB-L	STB-R
(CDW009)	.000	.000	.000	.000
(CDW010)	.000	.000	-25.000	-25.000
(CDW011)	.000	.000	5.000	-5.000

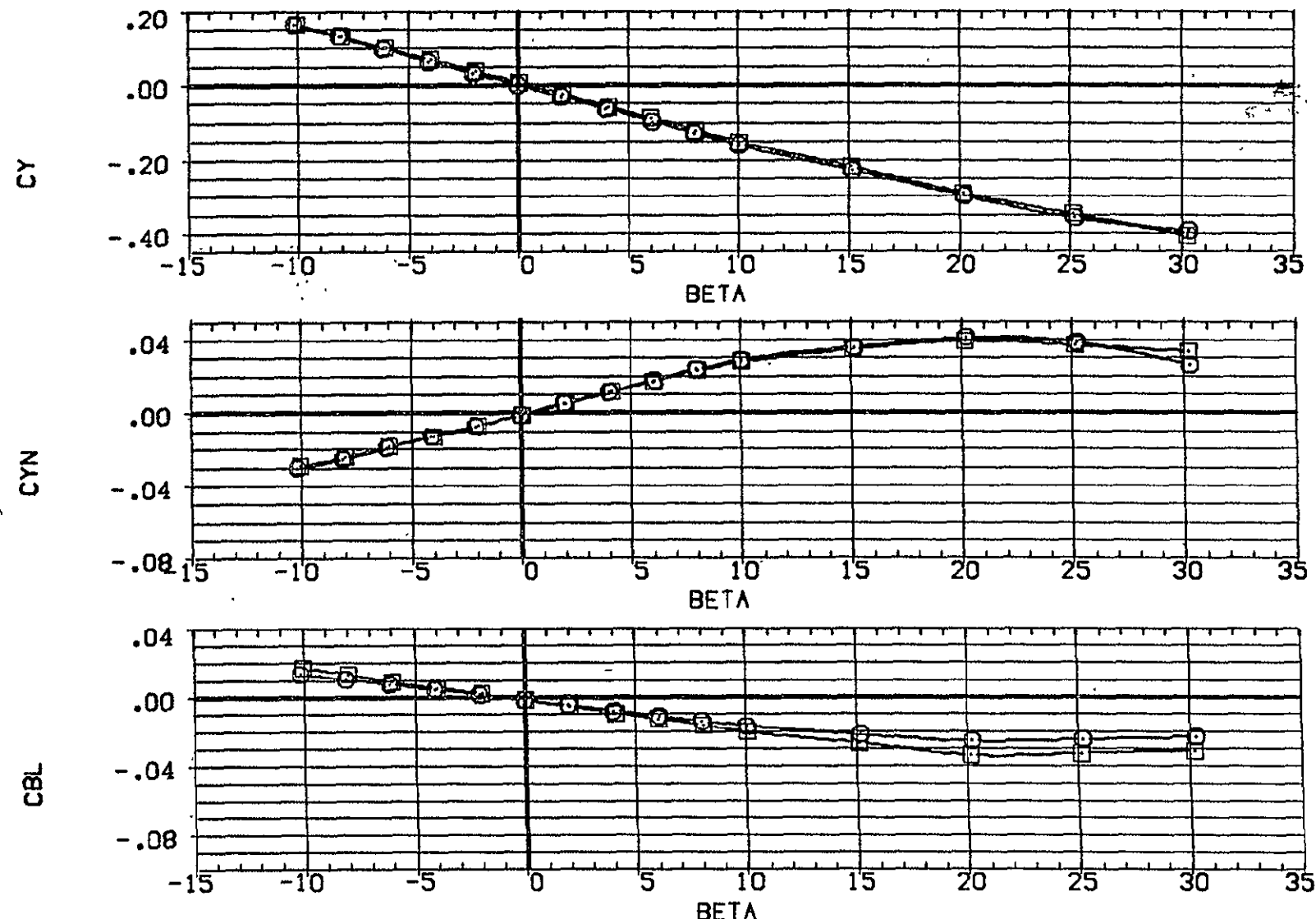


FIG. 7 EFFECT OF STABILATORS ON AERODYNAMIC CHAR., REYNOLDS NO.= 13.12 MIL.

$\Delta\alpha = -.10$

PAGE 59

DATA SET SYMBOL CONFIGURATION DESCRIPTION  
 (CDV009) O BASIC, RHO=11 + GRIT  
 (CDV010) □ BASIC, RHO=11 + GRIT  
 (CDV011) ◊ DATA NOT AVAILABLE

	AIL-L	AIL-R	STB-L	STB-R
(CDV009)	.000	.000	.000	.000
(CDV010)	.000	.000	-25,000	-25,000
(CDV011)	.000	.000	5,000	-5,000

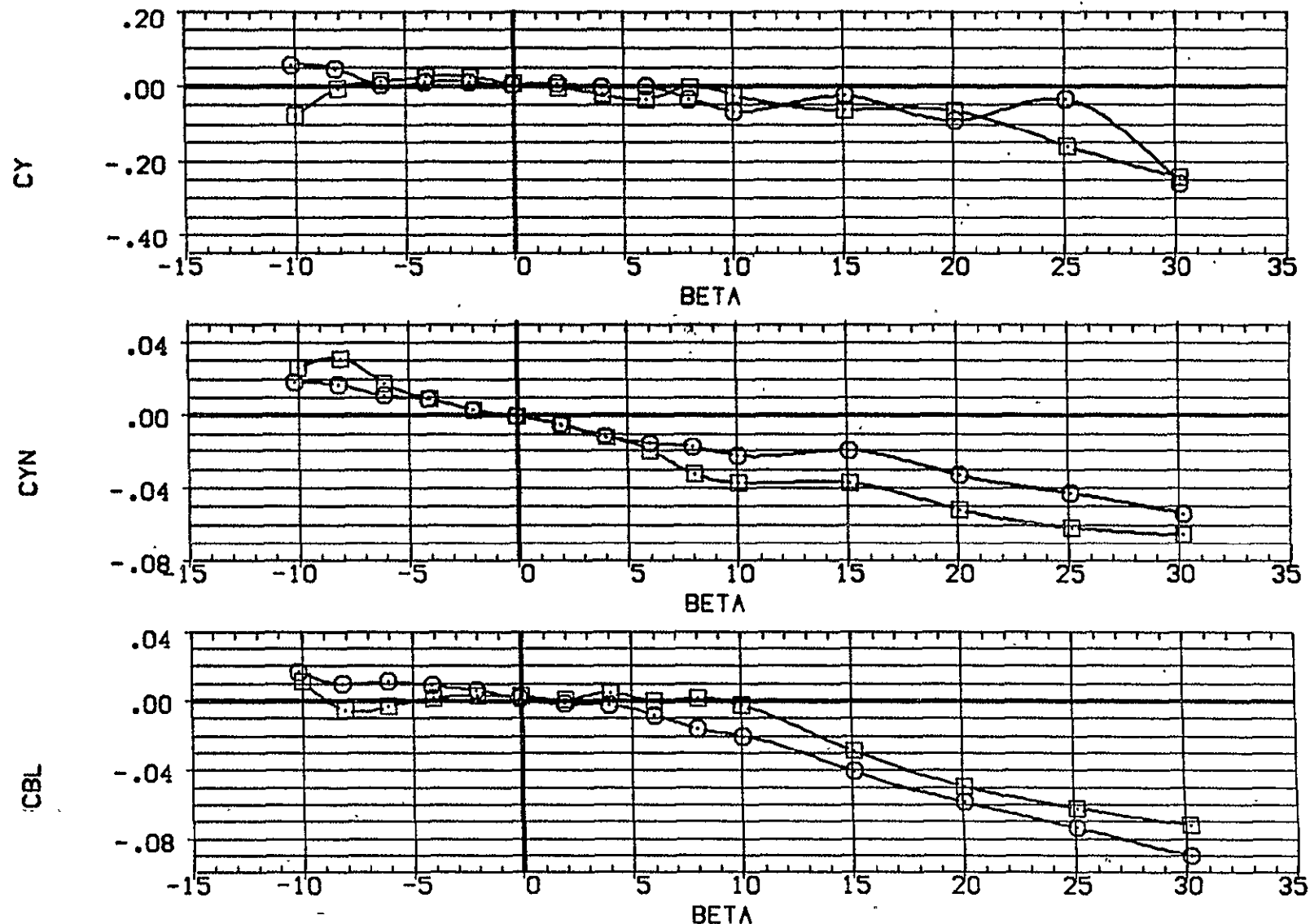


FIG. 7 EFFECT OF STABILATORS ON AERODYNAMIC CHAR., REYNOLDS NO.= 13.12 MIL.

(B)ALPHA = 31.33

PAGE 60

DATA SET SYMBOL CONFIGURATION DESCRIPTION  
 (CDW009)  $\square$  BASIC, RHO=11 + GRIT  
 (CDW010)  $\square$  BASIC, RHO=11 + GRIT  
 (CDW011)  $\diamond$  BASIC, RHO=11 + GRIT

	AIL-L	AIL-R	STB-L	STB-R
(CDW009)	.000	.000	.000	.000
(CDW010)	.000	.000	-25.000	-25.000
(CDW011)	.000	.000	5.000	-5.000

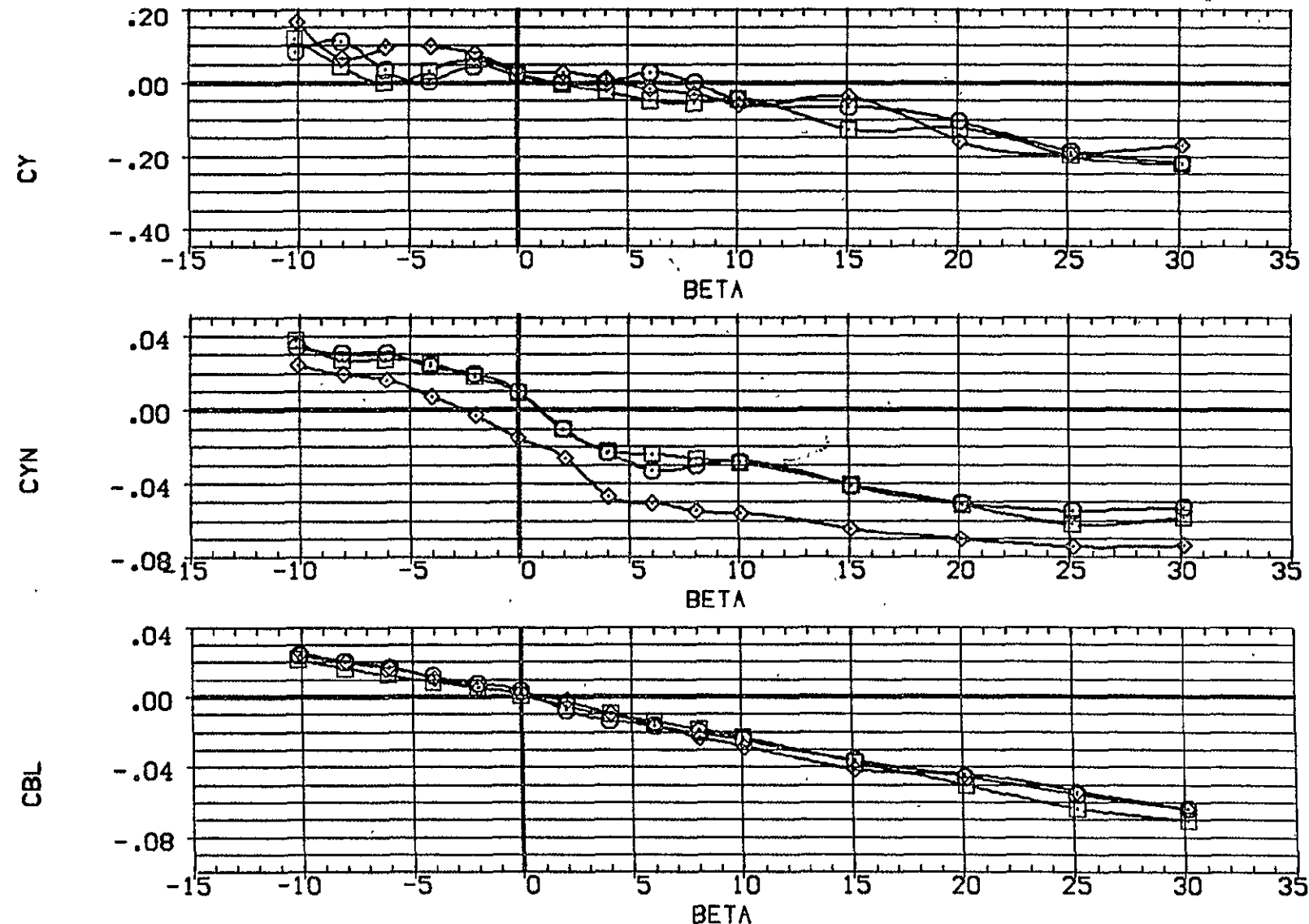


FIG. 7 EFFECT OF STABILATORS ON AERODYNAMIC CHAR., REYNOLDS NO.= 13.12 MIL.

(C)ALPHA = 51.37

PAGE 61

DATA SET SYMBOL CONFIGURATION DESCRIPTION  
 (CDV009) BASIC, RHO=11 + GRIT  
 (CDV010) BASIC, RHO=11 + GRIT  
 (CDV011) BASIC, RHO=11 + GRIT

	AIL-L	AIL-R	STB-L	STB-R
(CDV009)	.000	.000	.000	.000
(CDV010)	.000	.000	-25.000	-25.000
(CDV011)	.000	.000	5.000	-5.000

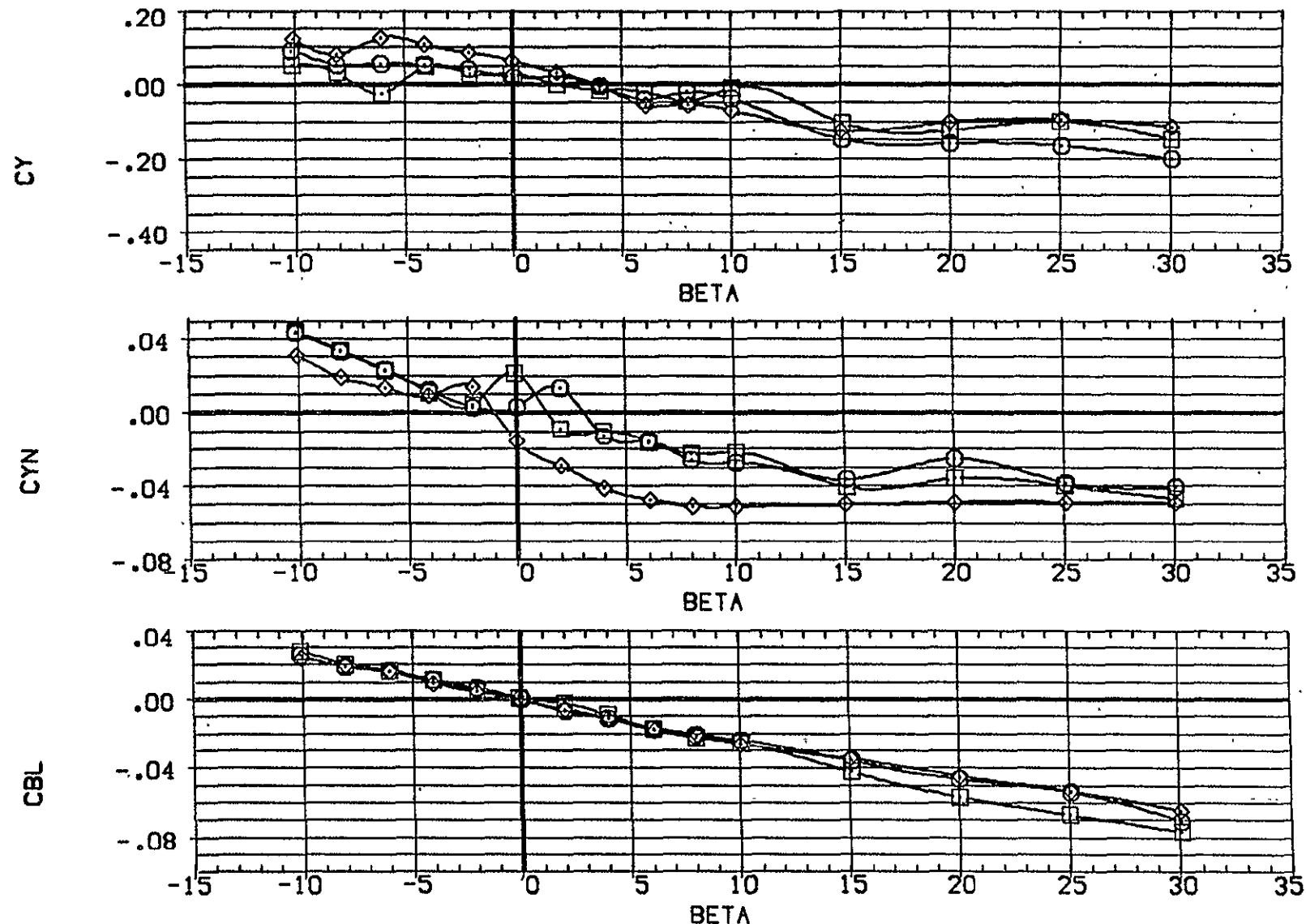


FIG. 7 EFFECT OF STABILATORS ON AERODYNAMIC CHAR., REYNOLDS NO.= 13.12 MIL.

(D)ALPHA = 61.28

PAGE 62

DATA SET SYMBOL CONFIGURATION DESCRIPTION  
 (CDW009) ○ BASIC, RHO=11 + GRIT  
 (CDW010) □ BASIC, RHO=11 + GRIT  
 (CDW011) ◊ BASIC, RHO=11 + GRIT

	AIL-L	AIL-R	STB-L	STB-R
(CDW009)	.000	.000	-25.000	-25.000
(CDW010)	.000	.000	5.000	-5.000
(CDW011)				

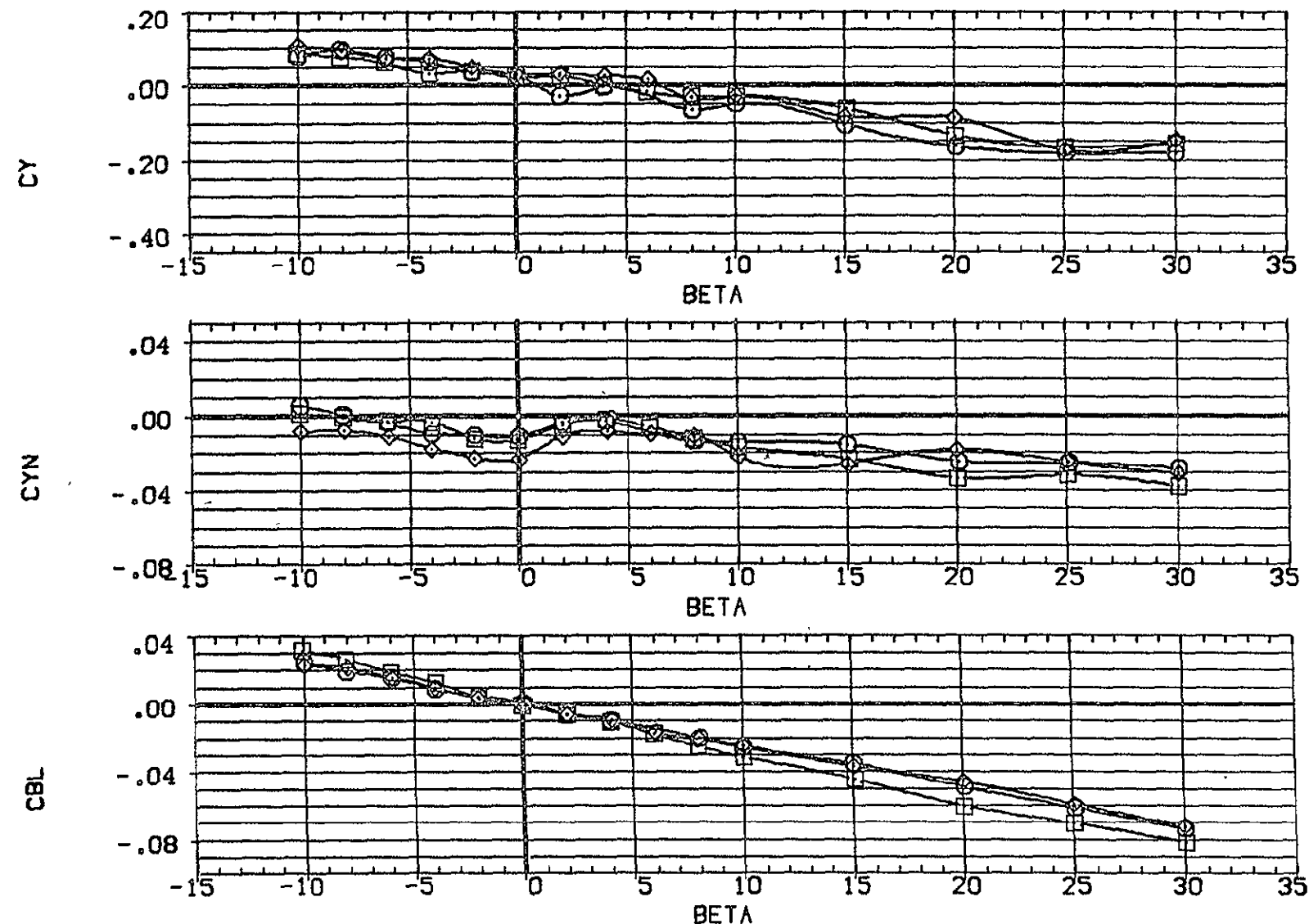


FIG. 7 EFFECT OF STABILATORS ON AERODYNAMIC CHAR., REYNOLDS NO.= 13.12 MIL.  
 (E)ALPHA = 71.30

DATA SET SYMBOL CONFIGURATION DESCRIPTION  
 (CDV009) O BASIC: RHO=11 + GRIT  
 (CDV010) □ BASIC: RHO=11 + GRIT  
 (CDV011) ◊ BASIC: RHO=11 + GRIT

	AIL-L	AIL-R	STB-L	STB-R
(CDV009)	.000	.000	.000	.000
(CDV010)	.000	.000	-25.000	-25.000
(CDV011)	.000	.000	5.000	-5.000

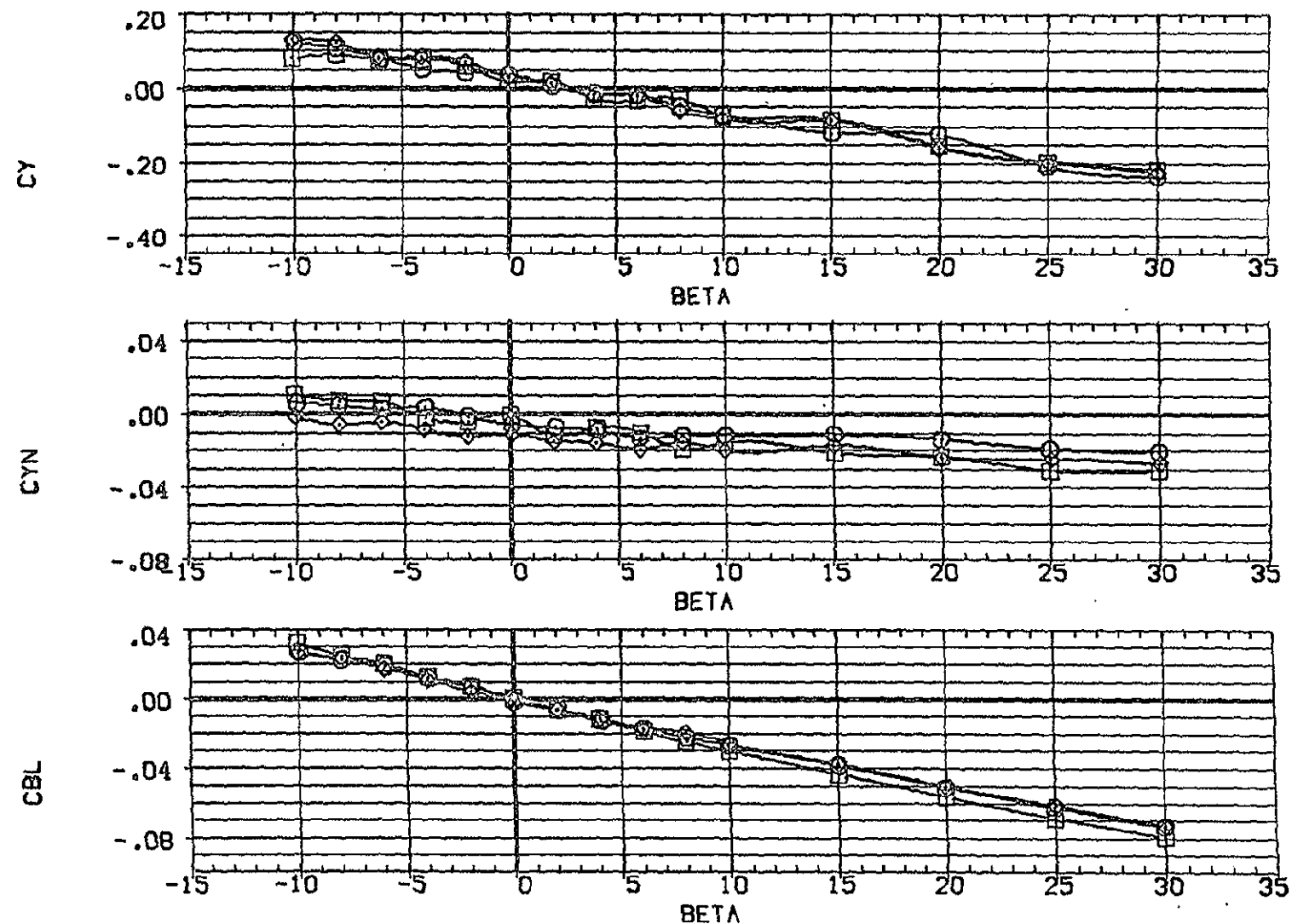


FIG. 7 EFFECT OF STABILATORS ON AERODYNAMIC CHAR., REYNOLDS NO.= 13.12 MIL.

(F)ALPHA = 88.24

PAGE 64

C-2

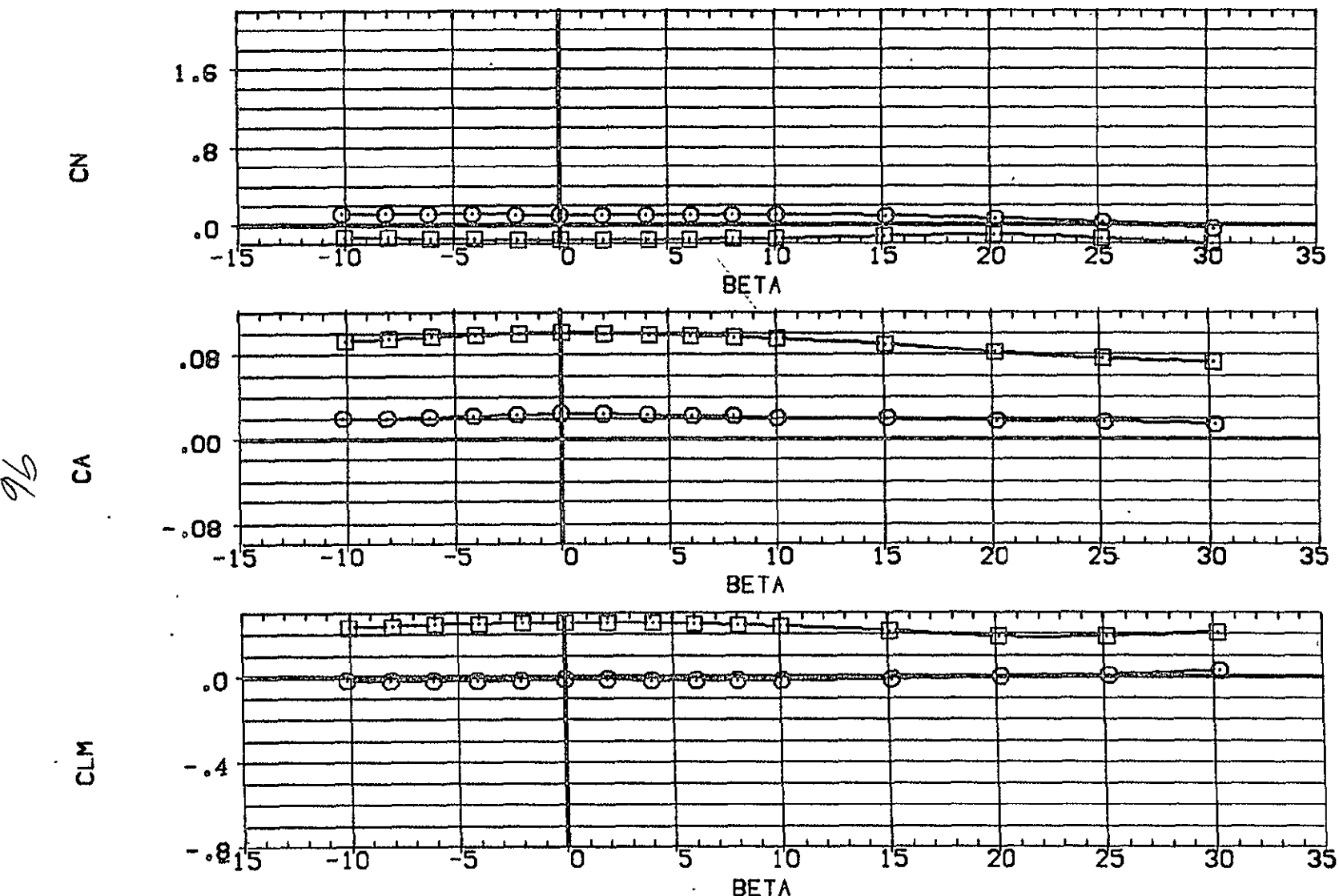
ORIGINAL PAGE IS  
OF POOR QUALITY

FIG. 7 EFFECT OF STABILATORS ON AERODYNAMIC CHAR., REYNOLDS NO.= 13.12 MIL.

(A) ALPHA = -.10

PAGE 65

DATA SET SYMBOL CONFIGURATION DESCRIPTION  
 (CDW009) O BASIC, RHO=11 + GRIT  
 (CDW010) □ BASIC, RHO=11 + GRIT  
 (CDW011) ◊ DATA NOT AVAILABLE

	AIL-L	AIL-R	STB-L	STB-R
(CDW009)	.000	.000	.000	.000
(CDW010)	.000	.000	-25.000	-25.000
(CDW011)	.000	.000	5.000	-5.000

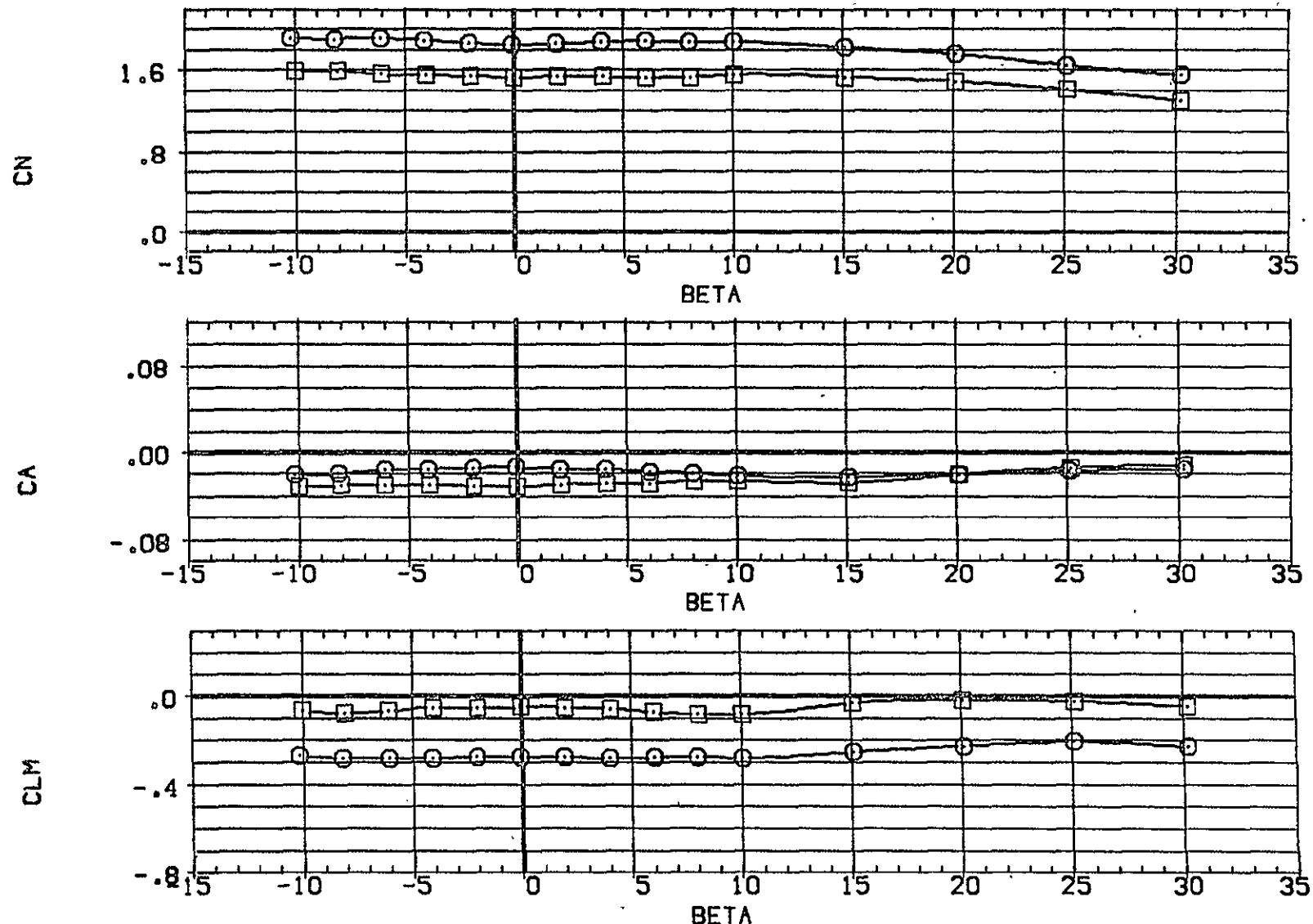


FIG. 7 EFFECT OF STABILATORS ON AERODYNAMIC CHAR., REYNOLDS NO.= 13.12 MIL.

(B) ALPHA = 31.33

PAGE -66

DATA SET SYMBOL CONFIGURATION DESCRIPTION  
 {CDW009}  $\square$  BASIC, RHO=1.1 + GRIT  
 {CDW010}  $\square$  BASIC, RHO=1.1 + GRIT  
 {CDW011}  $\diamond$  BASIC, RHO=1.1 + GRIT

AIL-L	AIL-R	STB-L	STB-R
.000	.000	.000	.000
.000	.000	-25.000	-25.000
.000	.000	5.000	-5.000

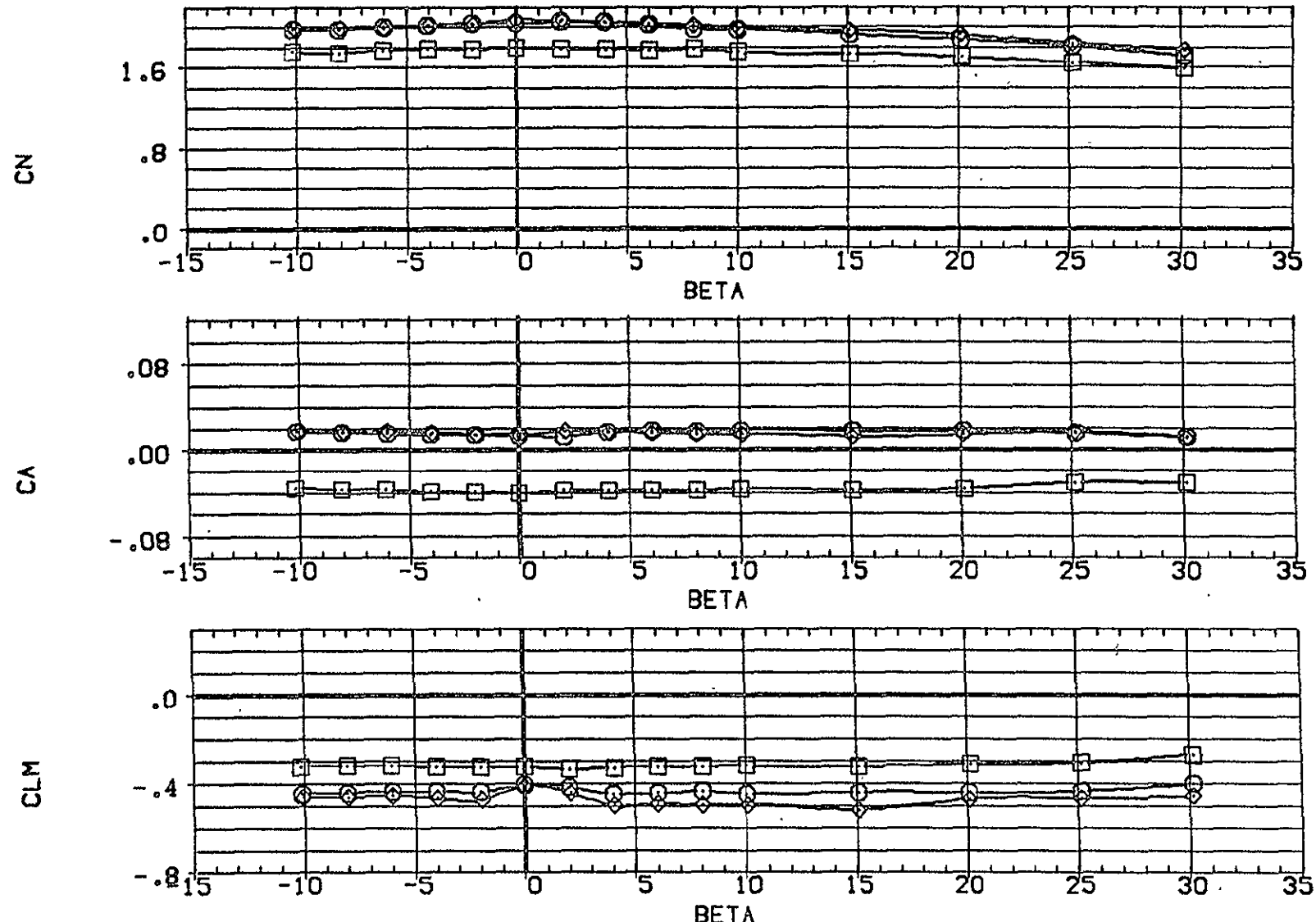


FIG. 7 EFFECT OF STABILATORS ON AERODYNAMIC CHAR., REYNOLDS NO.= 13.12 MIL.

(C)ALPHA = 51.37

PAGE 67

DATA SET SYMBOL CONFIGURATION DESCRIPTION

[CDW009]	$\circ$	BASIC, RH0-11 + GRIT
[CDW010]	$\square$	BASIC, RH0-11 + GRIT
[CDW011]	$\diamond$	BASIC, RH0-11 + GRIT

AIL-L	AIL-R	STB-L	STB-R
.000	.000	.000	.000
.000	.000	-25,000	-25,000
.000	.000	5,000	-5,000

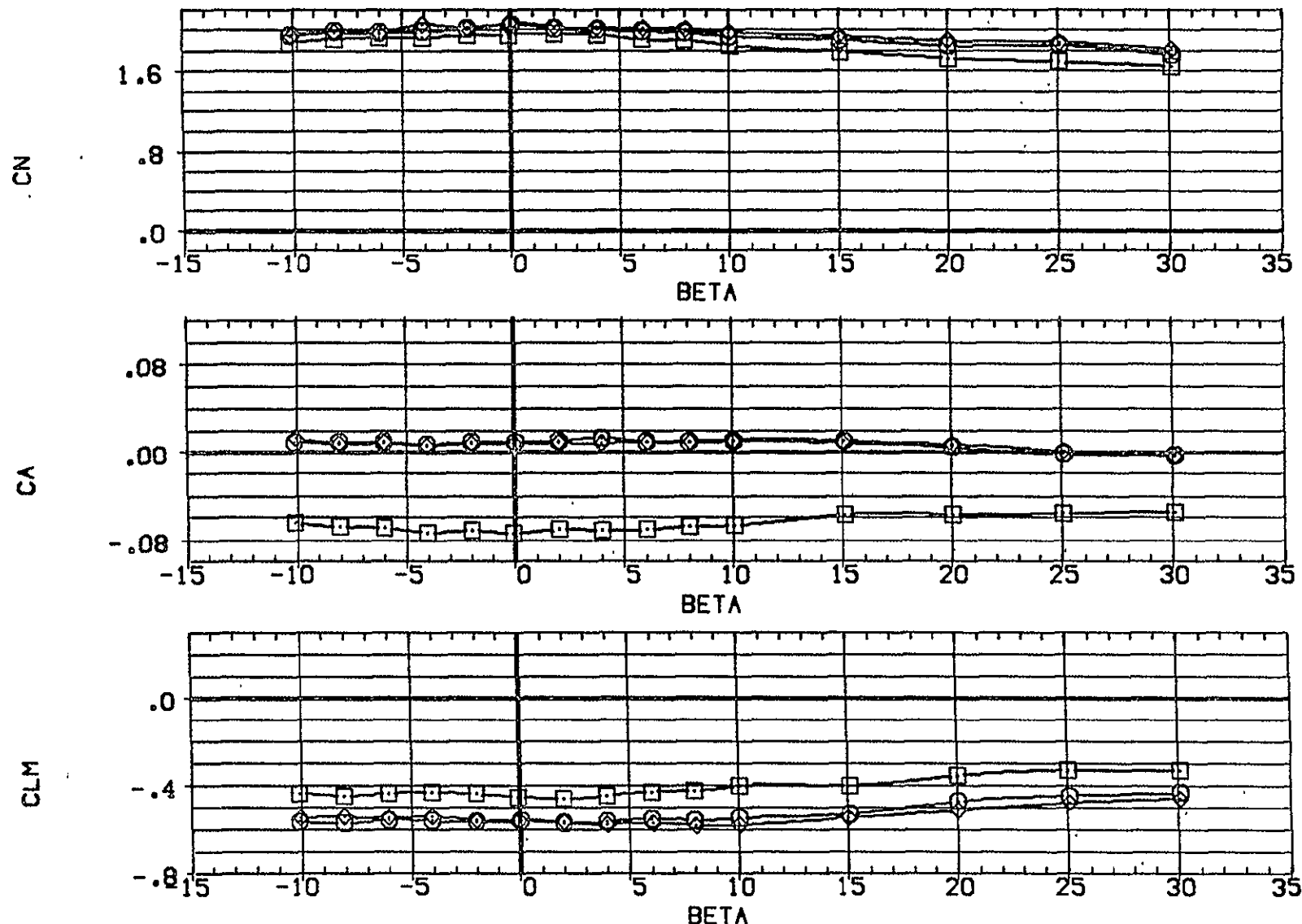


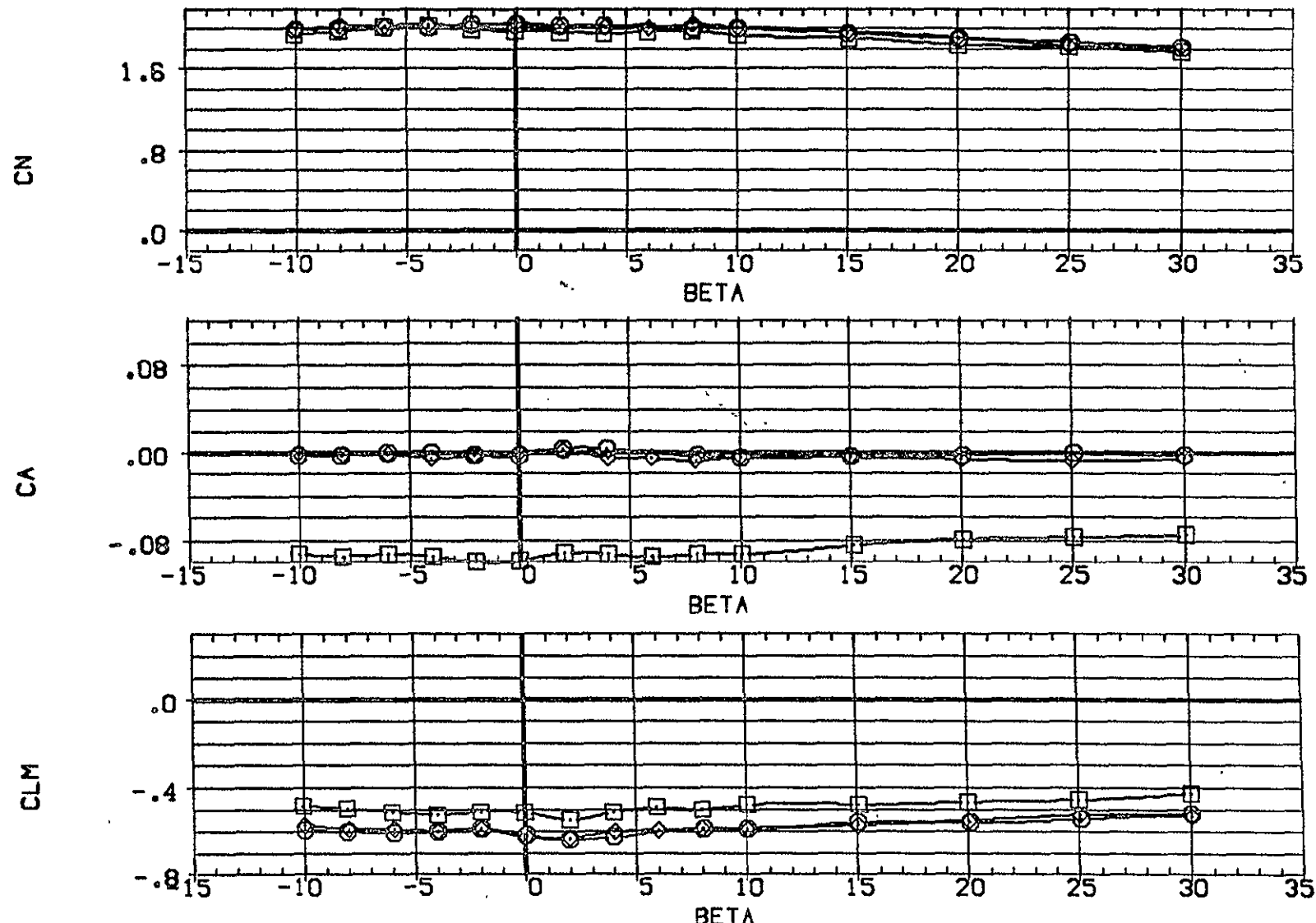
FIG. 7 EFFECT OF STABILATORS ON AERODYNAMIC CHAR., REYNOLDS NO.= 13.12 MIL.

(D)ALPHA = 61.28

PAGE 68

DATA SET SYMBOL CONFIGURATION DESCRIPTION  
 (CDW009) ○ BASIC: RHO-II + GRIT  
 (CDW010) □ BASIC: RHO-II + GRIT  
 (CDW011) ◇ BASIC: RHO-II + GRIT

AIL-L	AIL-R	STB-L	STB-R
.000	.000	.000	.000
.000	.000	-25.000	-25.000
.000	.000	5.000	-5.000



ORIGINAL PAGE IS  
OF POOR  
QUALITY

001

FIG. 7 EFFECT OF STABILATORS ON AERODYNAMIC CHAR., REYNOLDS NO.= 13.12 MIL.

(E)ALPHA = 71.30

PAGE 69

DATA SET SYMBOL CONFIGURATION DESCRIPTION

[COW009]	○	BASIC, RHO=1.1 + GRIT
[COW010]	□	BASIC, RHO=1.1 + GRIT
[COW011]	◇	BASIC, RHO=1.1 + GRIT

AIL-L	AIL-R	STB-L	STB-R
.000	.000	.000	.000
.000	.000	-25.000	-25.000
.000	.000	5.000	-5.000

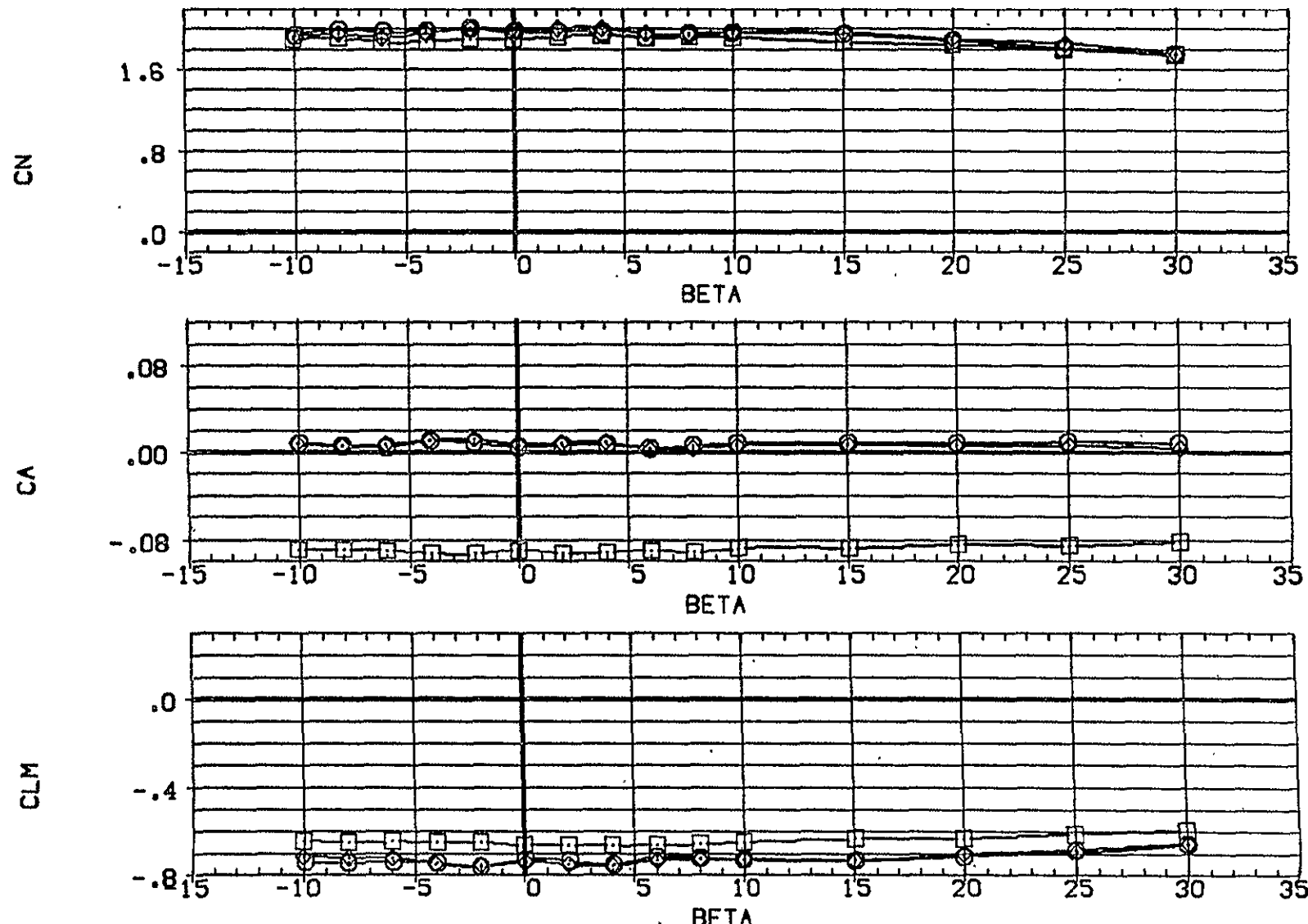


FIG. 7 EFFECT OF STABILATORS ON AERODYNAMIC CHAR., REYNOLDS NO.= 13.12 MIL.

(F) ALPHA = 88.24

PAGE 70

DATA SET SYMBOL CONFIGURATION DESCRIPTION

(CDW010)	$\square$	BASIC, RHO=11 + GRIT
(CDW012)	$\square$	BASIC, RHO=11 + GRIT + A + B + C
(CDW014)	$\diamond$	DATA NOT AVAILABLE
(CDW015)	$\times$	DATA NOT AVAILABLE

AIL-L	AIL-R	STB-L	STB-R
.000	.000	-25.000	-25.000
.000	.000	-25.000	-25.000
.000	.000	-25.000	-25.000
.000	.000	-25.000	-25.000

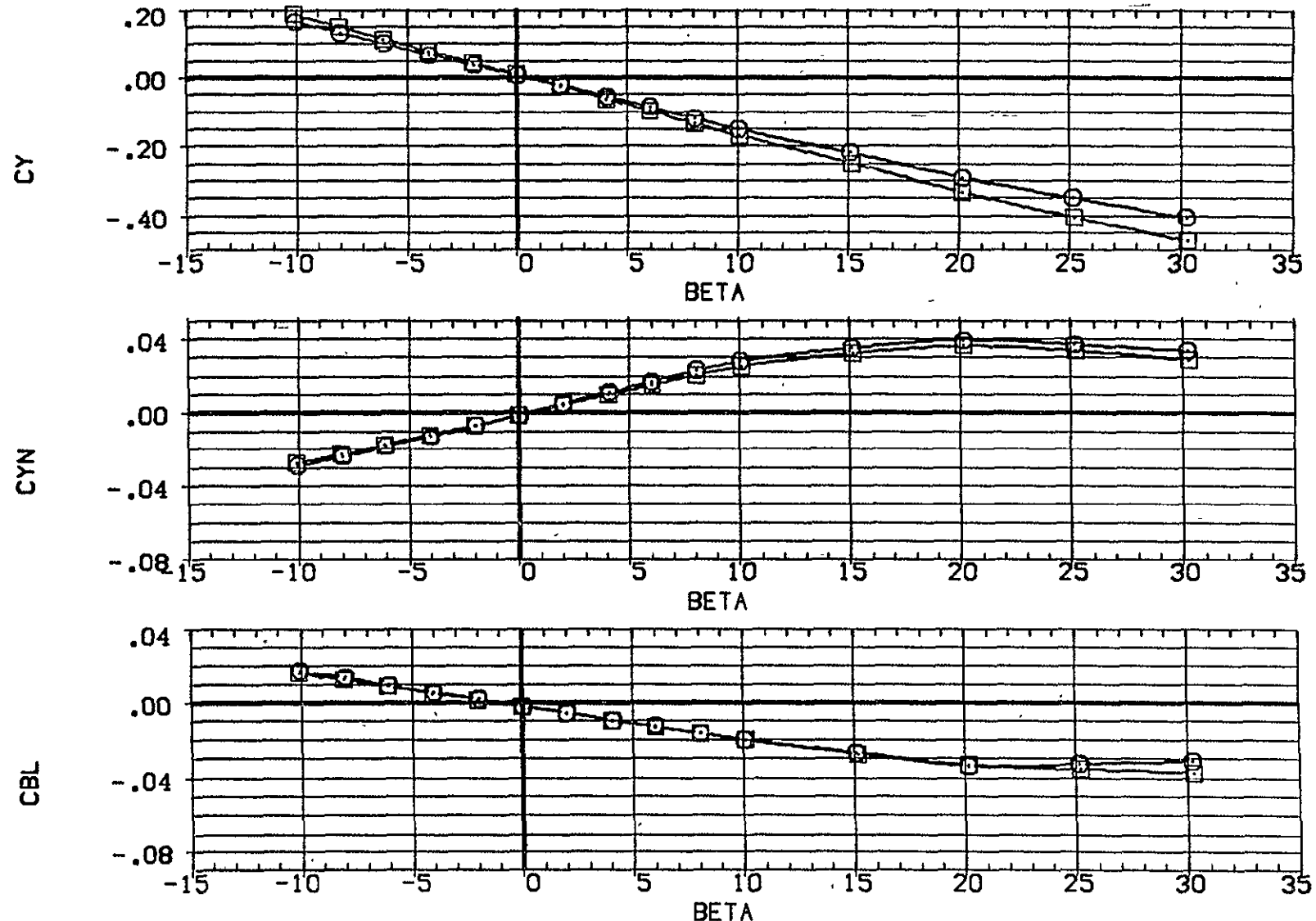


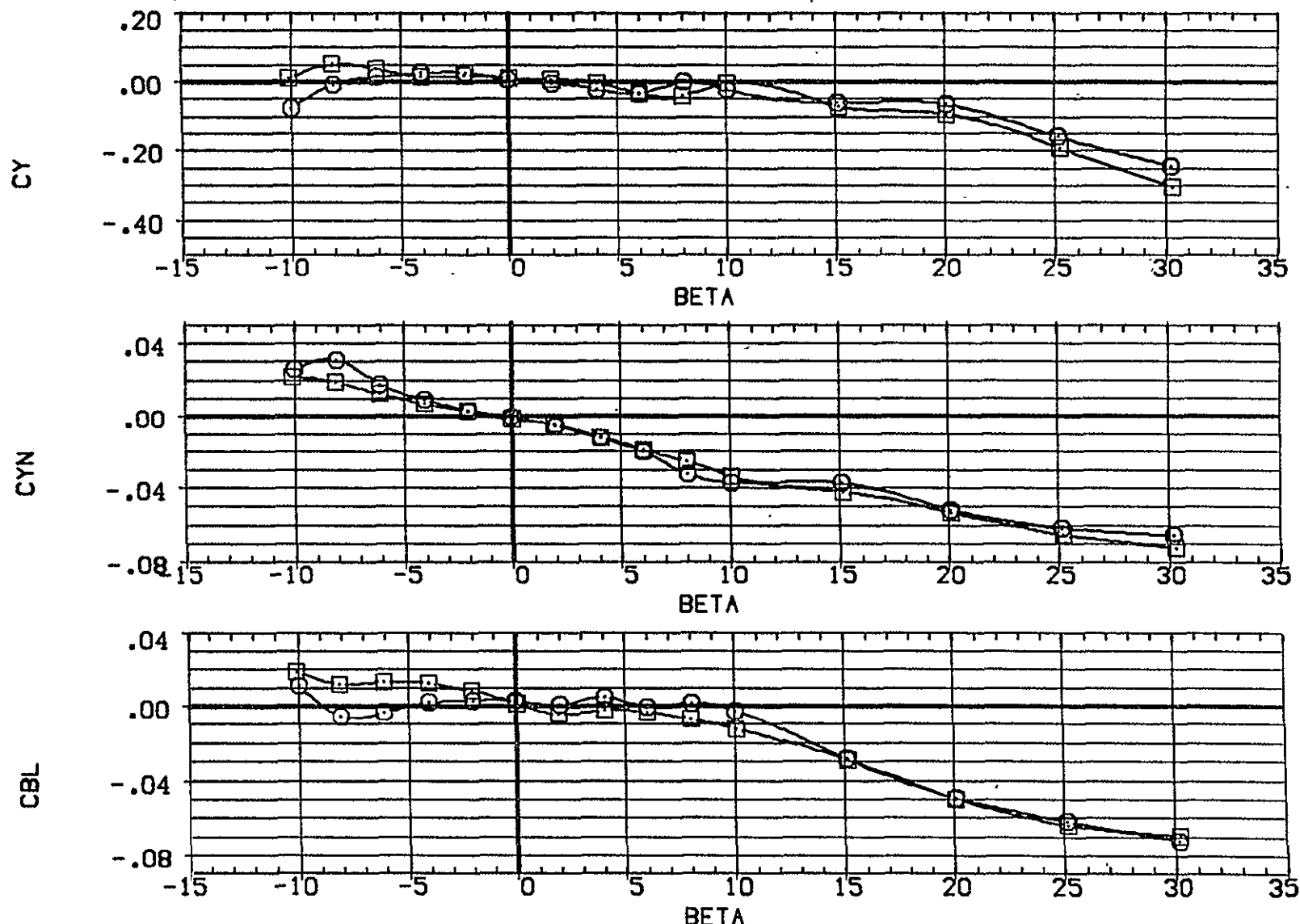
FIG. 8 EFFECT OF STORES ON AERODYNAMIC CHAR., REYNOLDS NO.= 13.12 MIL.

(A)ALPHA = -.24

DATA SET SYMBOL CONFIGURATION DESCRIPTION

(COW010)	O	BASIC, RHO=1.1 + GRIT
(COW012)	□	BASIC, RHO=1.1 + GRIT + A + B + C
(COW014)	○	DATA NOT AVAILABLE
(COW015)	×	DATA NOT AVAILABLE

	AIL-L	AIL-R	STB-L	STB-R
(COW010)	.000	.000	-25,000	-25,000
(COW012)	.000	.000	-25,000	-25,000
(COW014)	.000	.000	-25,000	-25,000
(COW015)	.000	.000	-25,000	-25,000



10<sup>3</sup>  
ORIGINAL PAGE IS  
OF POOR QUALITY

FIG. 8 EFFECT OF STORES ON AERODYNAMIC CHAR., REYNOLDS NO.= 13.12 MIL.

(B) ALPHA = 31.24

PAGE 72

DATA SET SYMBOL CONFIGURATION DESCRIPTION  
 (CDW010) O BASIC, RHO=11 + GRIT  
 (CDW012) □ BASIC, RHO=11 + GRIT + A + B + C  
 (CDW014) △ BASIC, RHO=11 + GRIT + D  
 (CDW015) ▲ BASIC, RHO=11 + GRIT + E

	AIL-L	AIL-R	STB-L	STB-R
(CDW010)	.000	.000	-25,000	-25,000
(CDW012)	.000	.000	-25,000	-25,000
(CDW014)	.000	.000	-25,000	-25,000
(CDW015)	.000	.000	-25,000	-25,000

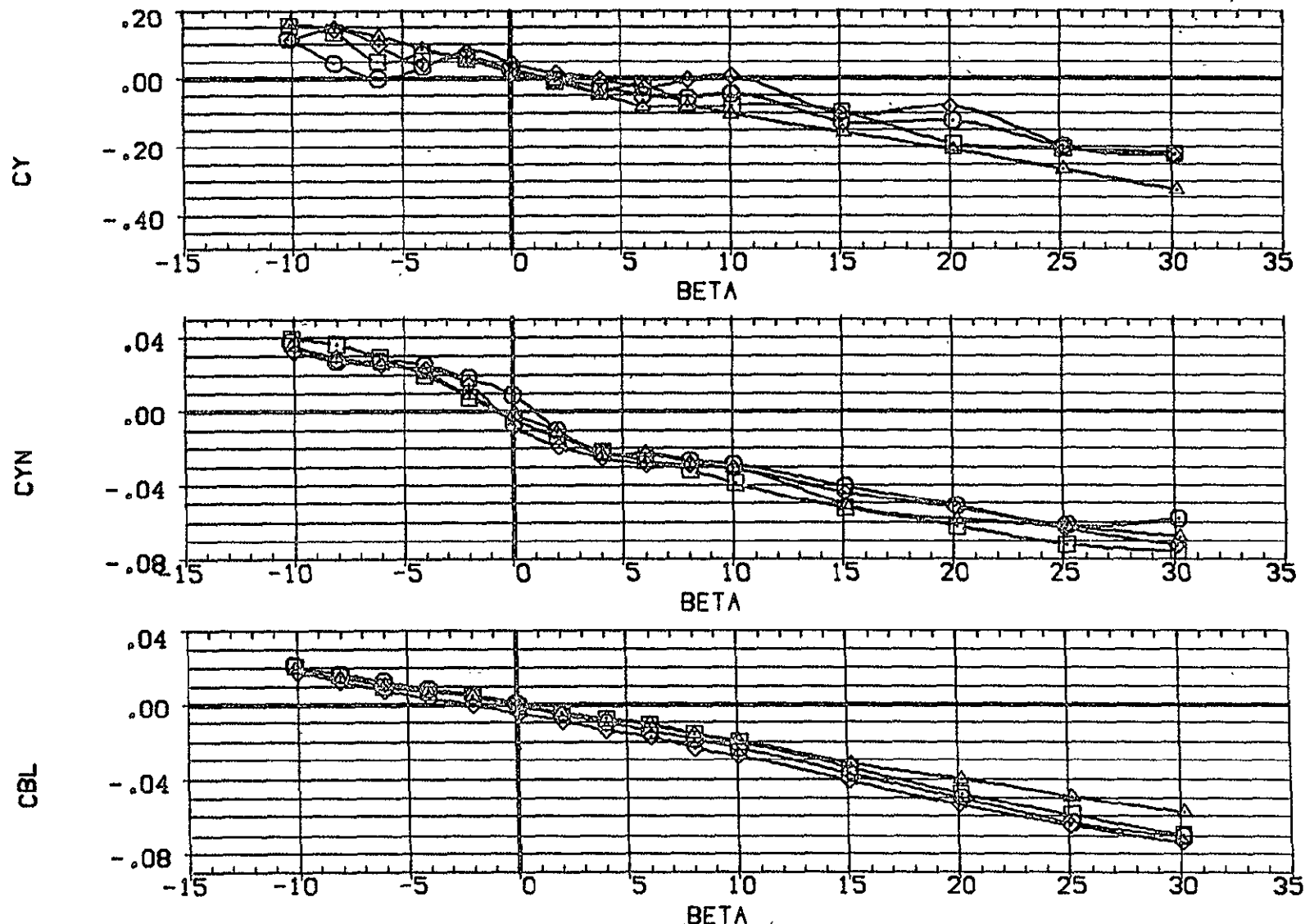


FIG. 8 EFFECT OF STORES ON AERODYNAMIC CHAR., REYNOLDS NO.= 13.12 MIL.

(C)ALPHA = 51.33

DATA SET SYMBOL CONFIGURATION DESCRIPTION

{CDW010}	○	BASIC: RHO=11 + GRIT
{CDW012}	□	BASIC: RHO=11 + GRIT + A + B + C
{CDW014}	◇	BASIC: RHO=11 + GRIT + D
{CDW015}	◇	BASIC: RHO=11 + GRIT + E

AIL-L	AIL-R	STB-L	STB-R
.000	.000	-25.000	-25.000
.000	.000	-25.000	-25.000
.000	.000	-25.000	-25.000
.000	.000	-25.000	-25.000

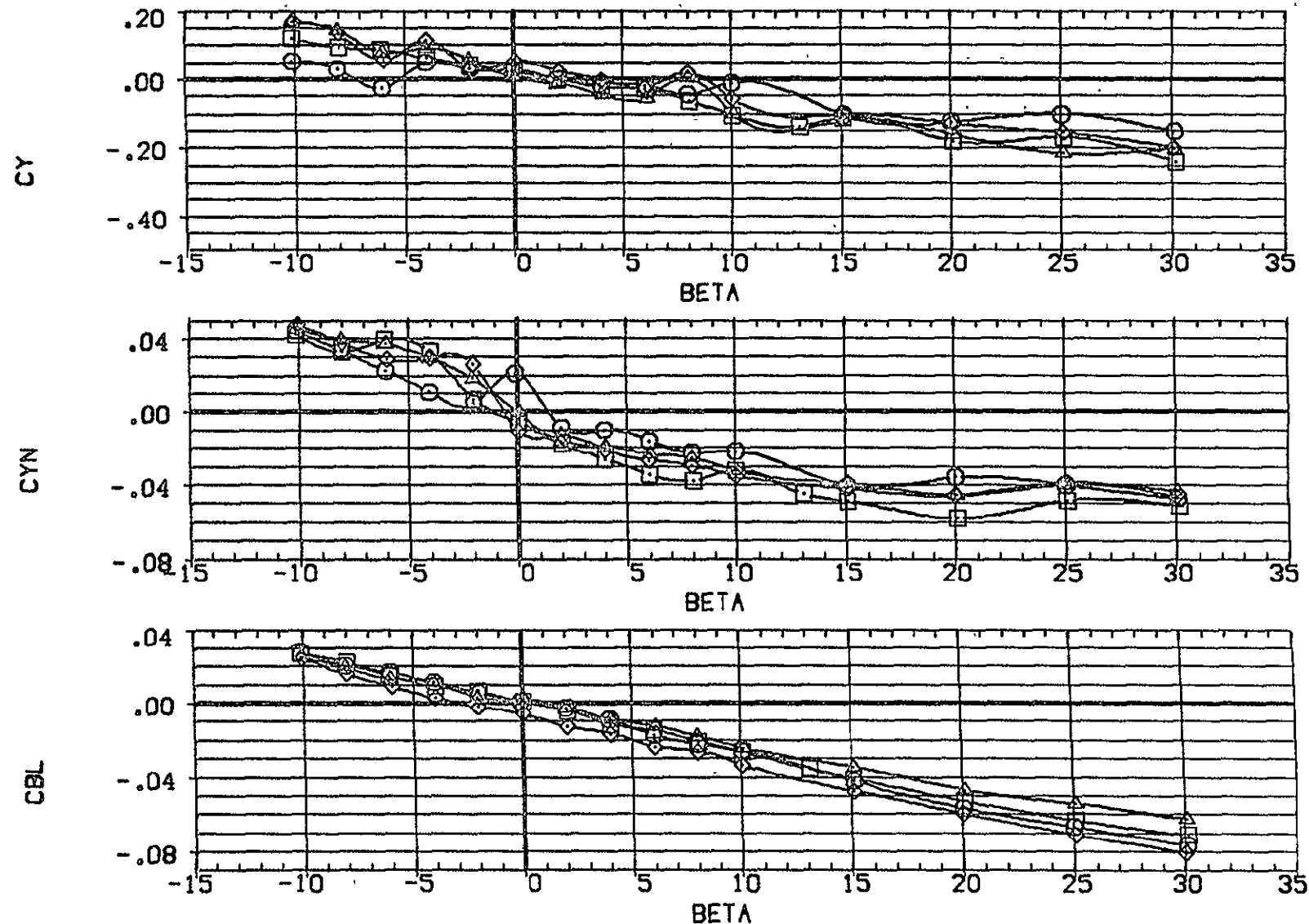


FIG. 8 EFFECT OF STORES ON AERODYNAMIC CHAR., REYNOLDS NO.= 13.12 MIL.

(D)ALPHA = 61.31

PAGE - 74

DATA SET SYMBOL CONFIGURATION DESCRIPTION  
 (CDW010) O BASIC, RHO=11 + GRIT  
 (CDW012) □ BASIC, RHO=11 + GRIT + A + B + C  
 (CDW014) Δ BASIC, RHO=11 + GRIT + D  
 (CDW015) X BASIC, RHO=11 + GRIT + E

	AIL-L	AIL-R	STB-L	STB-R
(CDW010)	.000	.000	-25.000	-25.000
(CDW012)	.000	.000	-25.000	-25.000
(CDW014)	.000	.000	-25.000	-25.000
(CDW015)	.000	.000	-25.000	-25.000

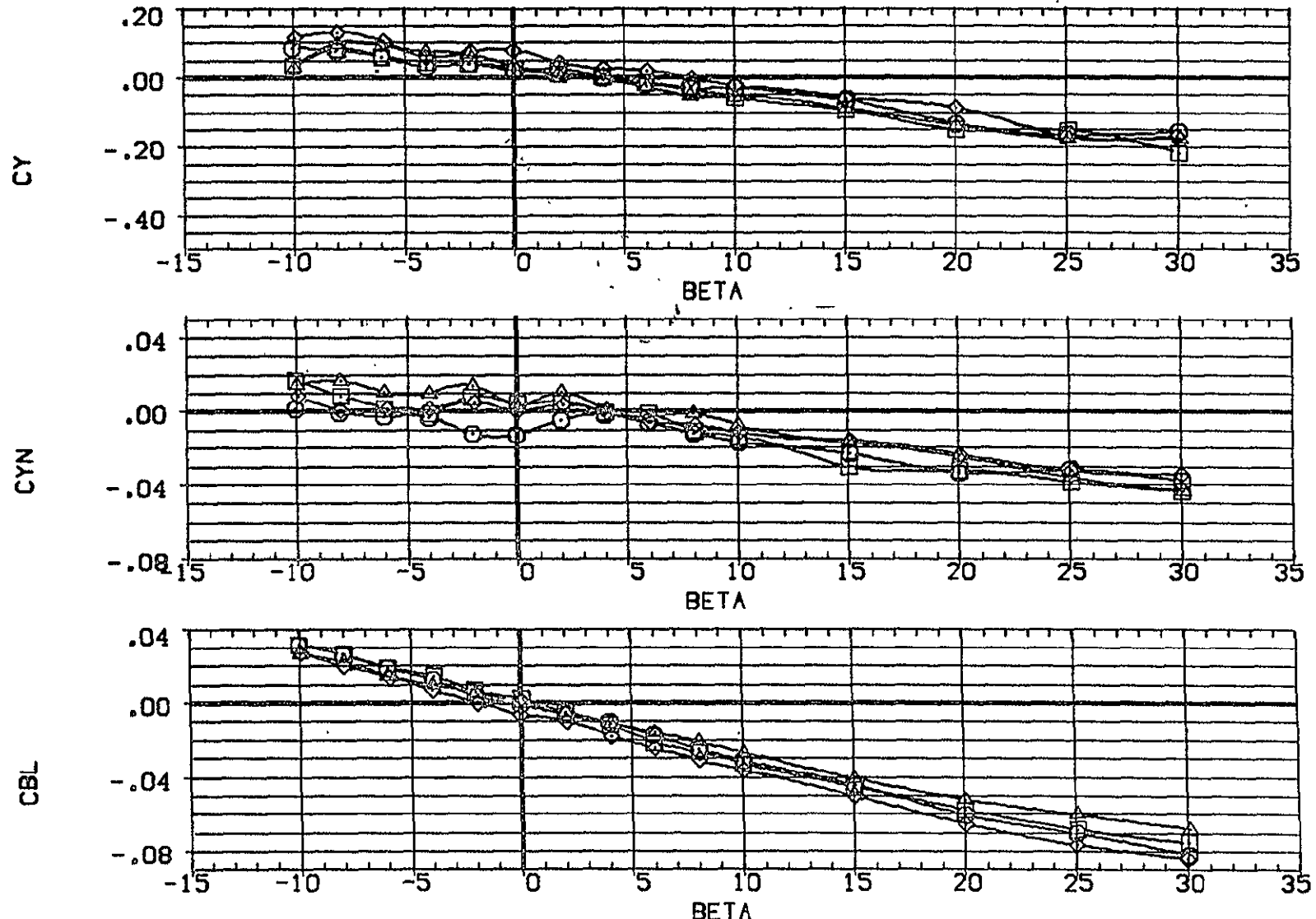


FIG. 8 EFFECT OF STORES ON AERODYNAMIC CHAR., REYNOLDS NO.= 13.12 MIL.

(E) ALPHA = 71.35

PAGE 75

DATA SET SYMBOL CONFIGURATION DESCRIPTION

{CDW010}	○	BASIC: RHO-II + GRIT
{CDW012}	□	BASIC: RHO-II + GRIT + A + B + C
{CDW014}	◇	BASIC: RHO-II + GRIT + D
{CDW015}	△	BASIC: RHO-II + GRIT + E

AIL-L	AIL-R	STB-L	STB-R
.000	.000	-25,000	-25,000
.000	.000	-25,000	-25,000
.000	.000	-25,000	-25,000
.000	.000	-25,000	-25,000

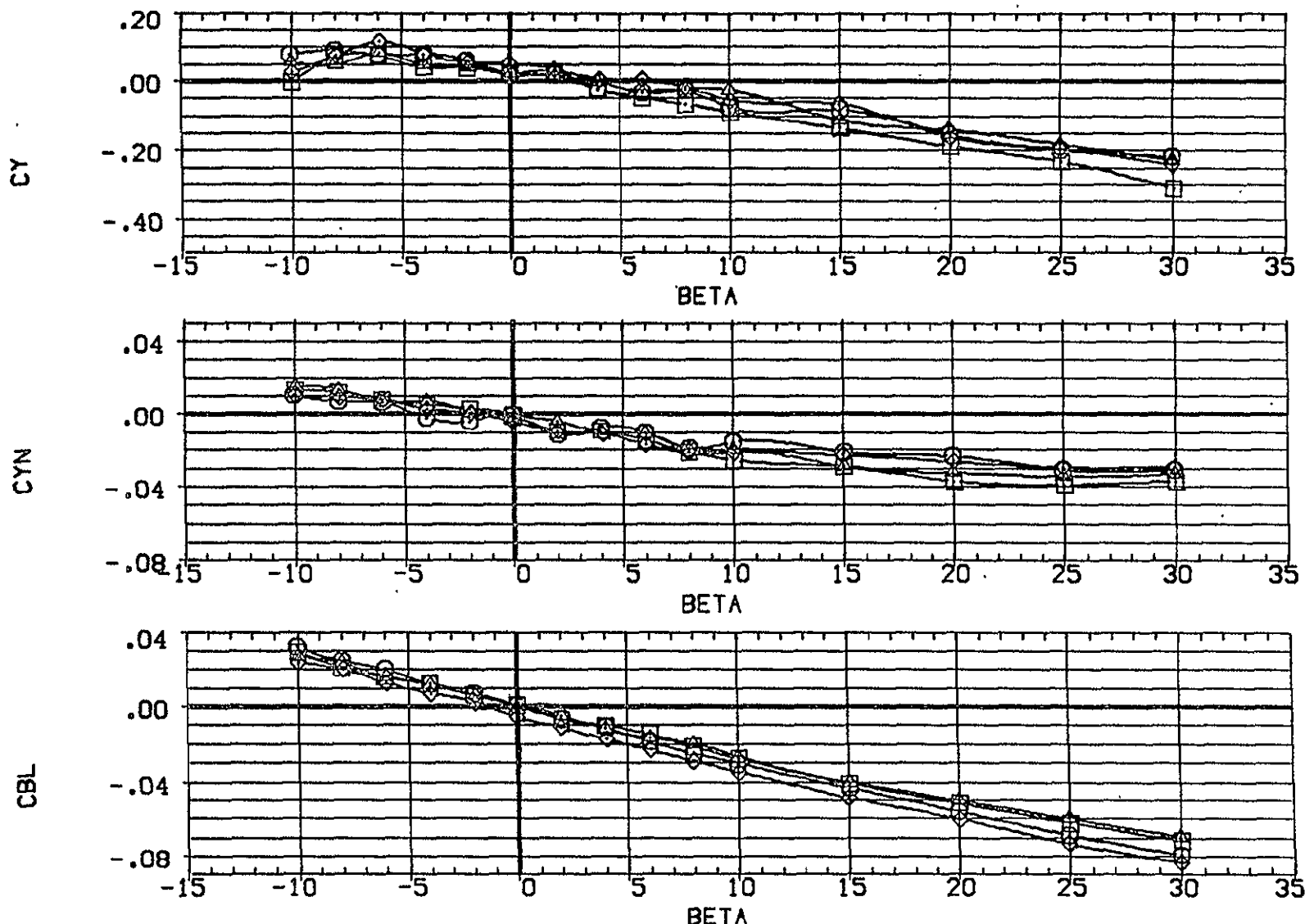


FIG. 8 EFFECT OF STORES ON AERODYNAMIC CHAR., REYNOLDS NO.= 13.12 MIL.

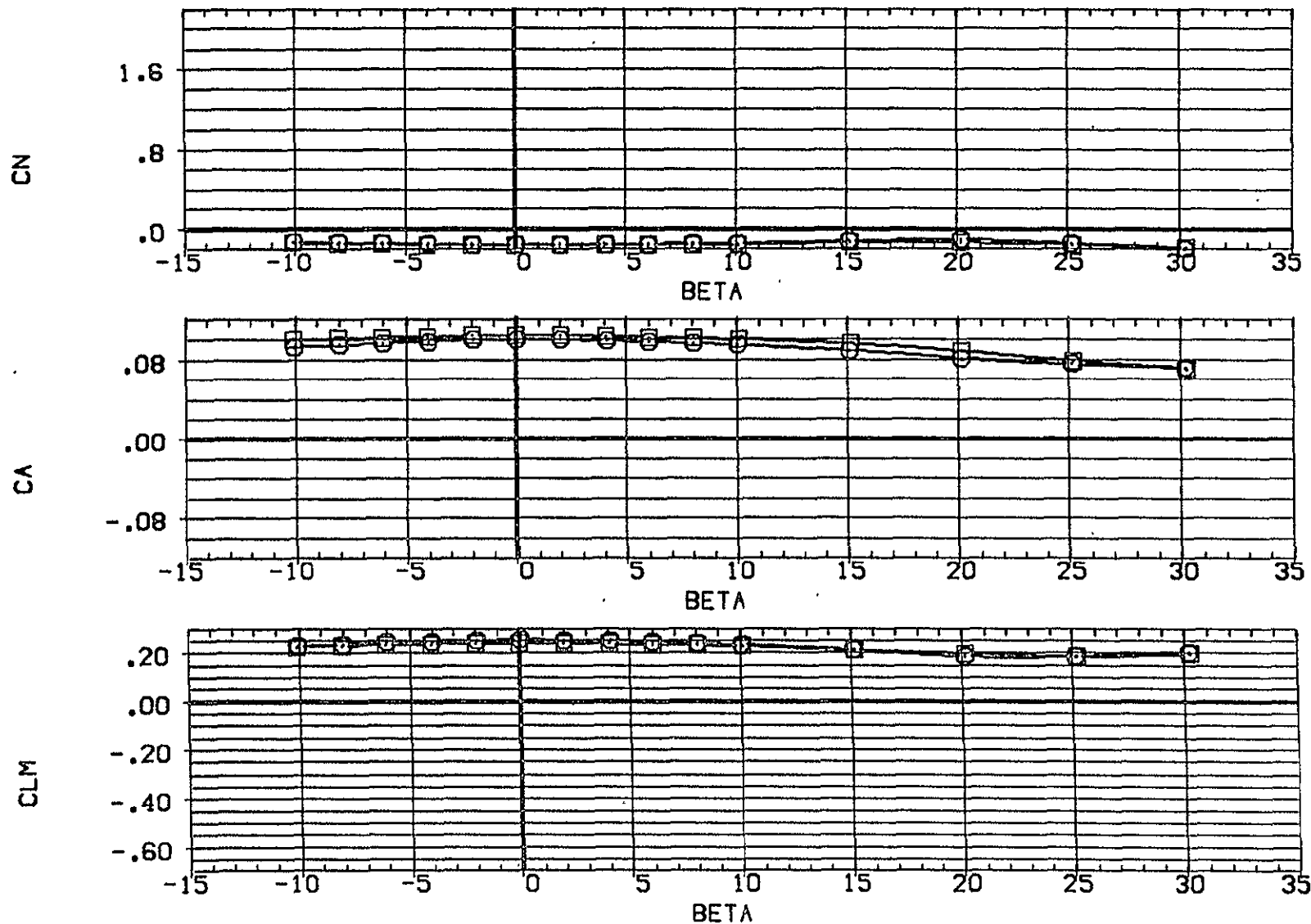
(F)ALPHA = 88.25

PAGE 76

DATA SET SYMBOL CONFIGURATION DESCRIPTION

(CDW010)	O	BASIC, RHO=11 + GRIT
(CDW012)	□	BASIC, RHO=11 + GRIT + A + B + C
(CDW014)	☒	DATA NOT AVAILABLE
(CDW015)	☒	DATA NOT AVAILABLE

	AIL-L	AIL-R	STB-L	STB-R
(CDW010)	.888	.000	-25.000	-25.000
(CDW012)	.888	.000	-25.000	-25.000
(CDW014)	.888	.000	-25.000	-25.000
(CDW015)	.888	.000	-25.000	-25.000



ORIGINAL PAGE IS  
OF POOR QUALITY

301

FIG. 8 EFFECT OF STORES ON AERODYNAMIC CHAR., REYNOLDS NO.= 13.12 MIL.

CALPHA = -.24

PAGE 77

DATA SET SYMBOL CONFIGURATION DESCRIPTION

{CDW010}	○	BASIC, RHO=1.1 + GRIT
{CDW012}	□	BASIC, RHO=1.1 + GRIT + A + B + C
{CDW014}	○	DATA NOT AVAILABLE
{CDW015}	△	DATA NOT AVAILABLE

AIL-L	AIL-R	STB-L	STB-R
.000	.000	-25.000	-25.000
.000	.000	-25.000	-25.000
.000	.000	-25.000	-25.000
.000	.000	-25.000	-25.000

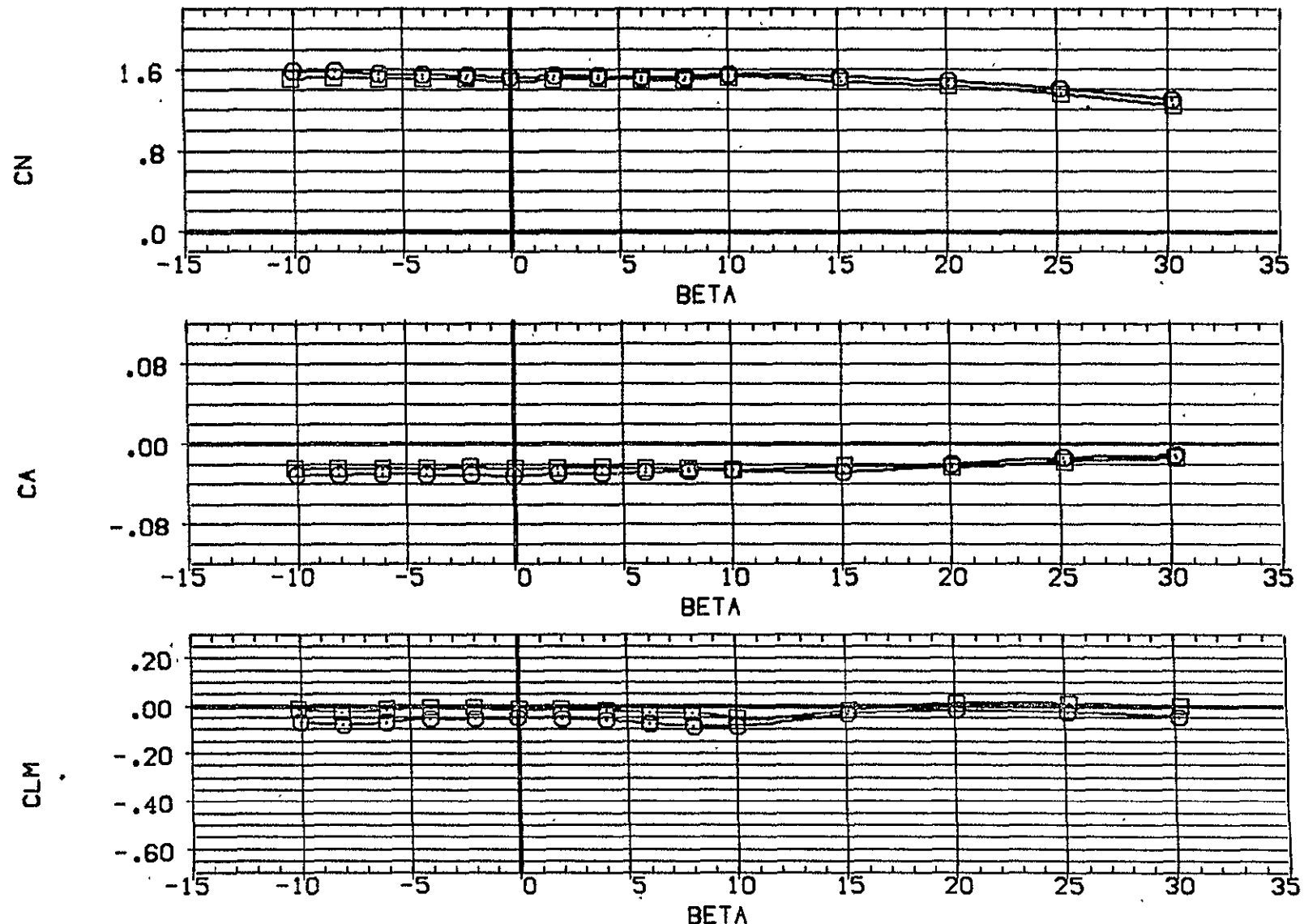


FIG. 8 EFFECT OF STORES ON AERODYNAMIC CHAR., REYNOLDS NO.= 13.12 MIL.

(B)ALPHA = 31.24

PAGE 78

DATA SET SYMBOL	CONFIGURATION DESCRIPTION	AIL-L	AIL-R	STB-L	STB-R
(CDW010)	BASIC, RHO-II + GRIT	.000	.000	-25.000	-25.000
(CDW012)	BASIC, RHO-II + GRIT + A + B + C	.000	.000	-25.000	-25.000
(CDW014)	BASIC, RHO-II + GRIT + D	.000	.000	-25.000	-25.000
(CDW015)	BASIC, RHO-II + GRIT + E	.000	.000	-25.000	-25.000

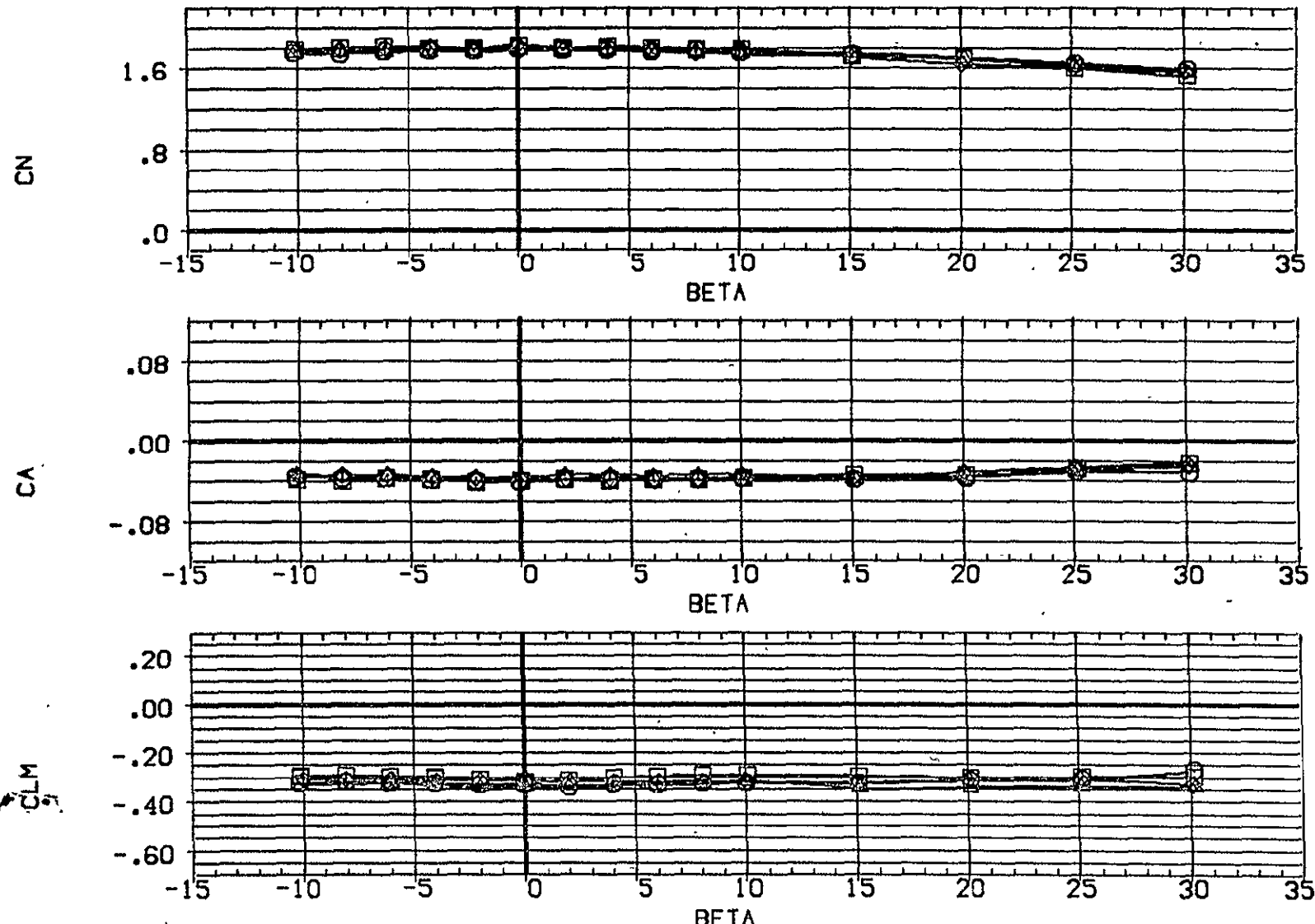


FIG. 8 EFFECT OF STORES ON AERODYNAMIC CHAR., REYNOLDS NO.= 13.12 MIL.

(C)ALPHA = 51.33

ORIGINAL PAGE IS  
OF POOR QUALITY

DATA SET SYMBOL CONFIGURATION DESCRIPTION

(CDW010)	$\square$	BASIC, RHO=11 + GRIT
(CDW012)	$\square$	BASIC, RHO=11 + GRIT + A + B + C
(CDW014)	$\diamond$	BASIC, RHO=11 + GRIT + D
(CDW015)	$\diamond$	BASIC, RHO=11 + GRIT + E

AIL-L	AIL-R	STB-L	STB-R
.000	.000	-25,000	-25,000
.000	.000	-25,000	-25,000
.000	.000	-25,000	-25,000
.000	.000	-25,000	-25,000

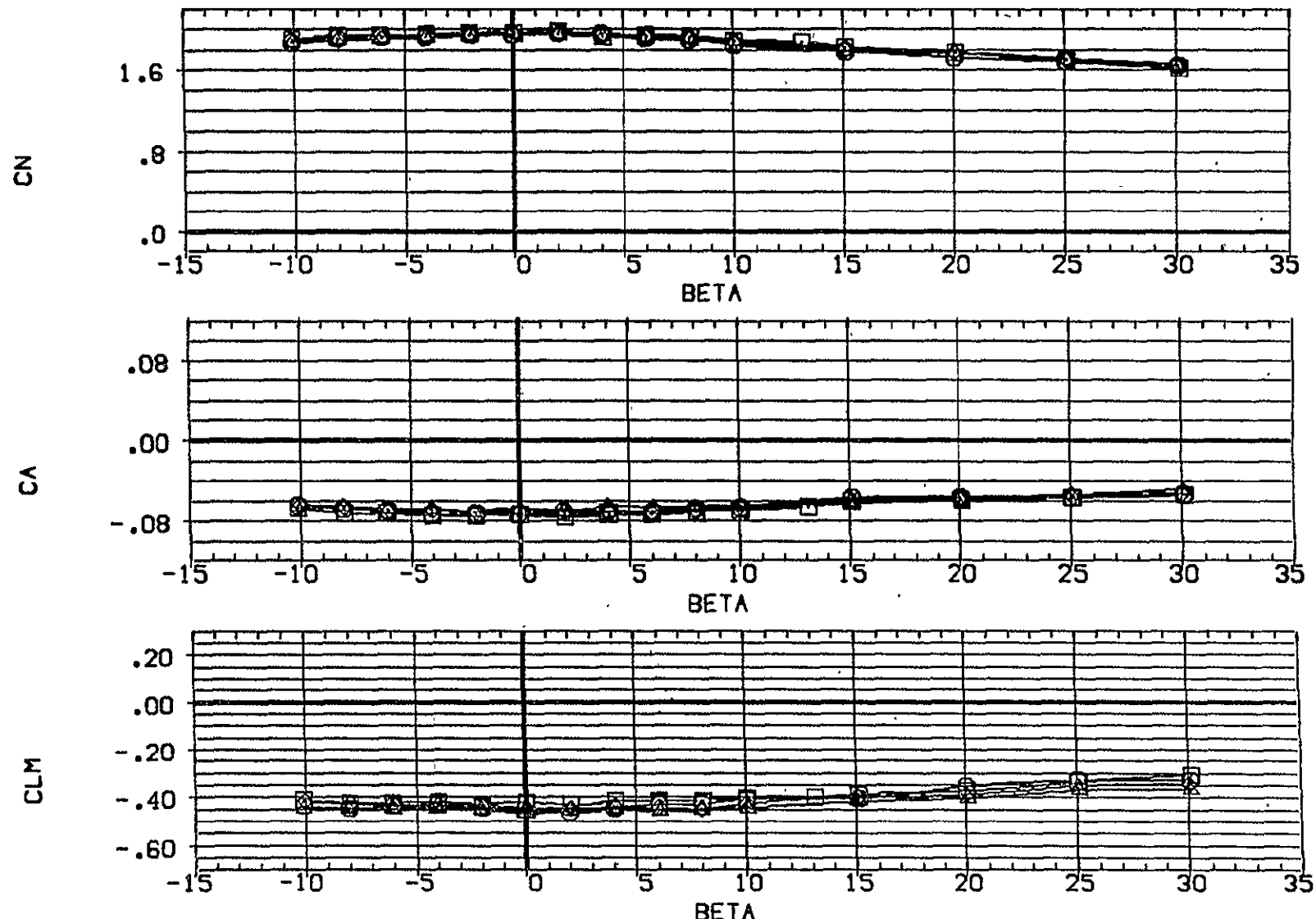


FIG. 8 EFFECT OF STORES ON AERODYNAMIC CHAR., REYNOLDS NO.= 13.12 MIL.

(D)ALPHA = 61.31

PAGE 80

ORIGINAL PAGE IS  
OF POOR QUALITY

DATA SET SYMBOL CONFIGURATION DESCRIPTION

(CDW010)	○	BASIC, RHO-11 + GRIT	AIL-L	.000	AIL-R	.000	STB-L	-25.000	STB-R	-25.000
(CDW012)	□	BASIC, RHO-11 + GRIT + A + B + C		.000	.000	-25.000	-25.000			
(CDW014)	⊗	BASIC, RHO-11 + GRIT + D		.000	.000	-25.000	-25.000			
(CDW015)	×	BASIC, RHO-11 + GRIT + E		.000	.000	-25.000	-25.000			

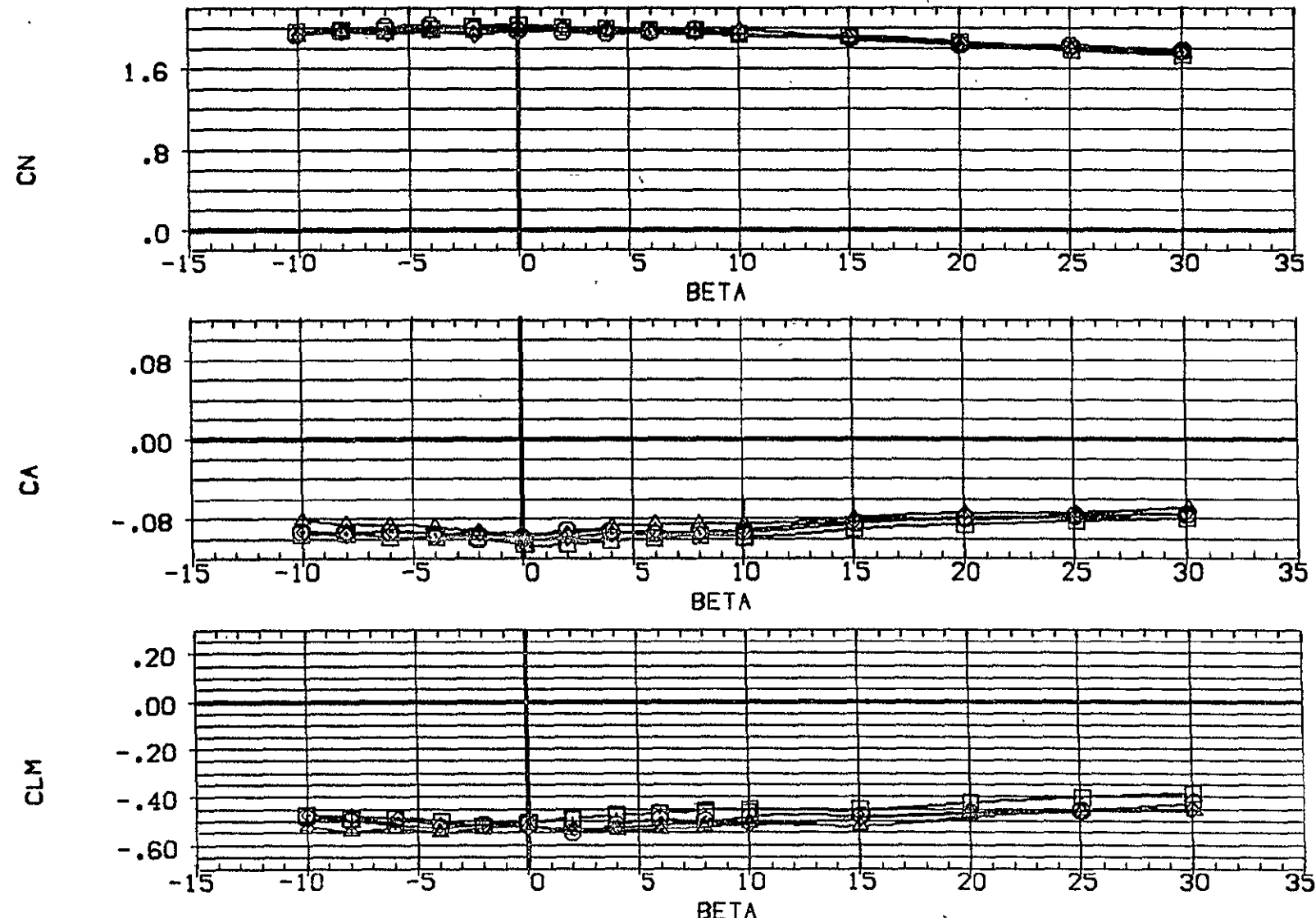


FIG. 8 EFFECT OF STORES ON AERODYNAMIC CHAR., REYNOLDS NO.= 13.12 MIL.

(E)ALPHA = 71.35

PAGE 81

DATA SET SYMBOL CONFIGURATION DESCRIPTION

(CDW010)	<input type="checkbox"/>	BASIC, RHO-III + GRIT
(CDW012)	<input checked="" type="checkbox"/>	BASIC, RHO-III + GRIT + A + B + C
(CDW014)	<input type="checkbox"/>	BASIC, RHO-III + GRIT + D
(CDW015)	<input type="checkbox"/>	BASIC, RHO-III + GRIT + E

AIL-L	AIL-R	STB-L	STB-R
.000	.000	-25,000	-25,000
.000	.000	-25,000	-25,000
.000	.000	-25,000	-25,000
.000	.000	-25,000	-25,000

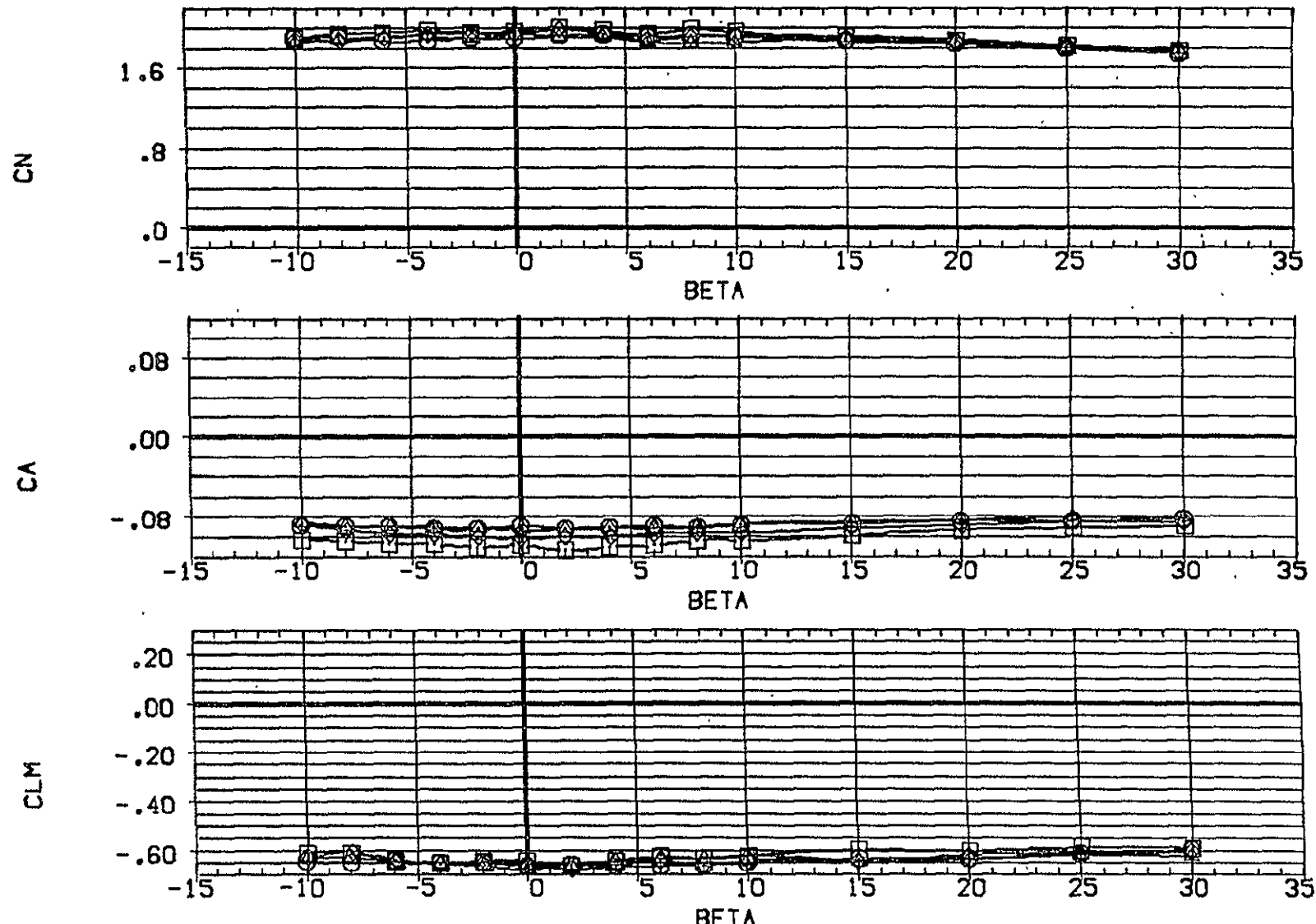


FIG. 8 EFFECT OF STORES ON AERODYNAMIC CHAR., REYNOLDS NO.= 13.12 MIL.

(F)ALPHA = 88.25

PAGE 82

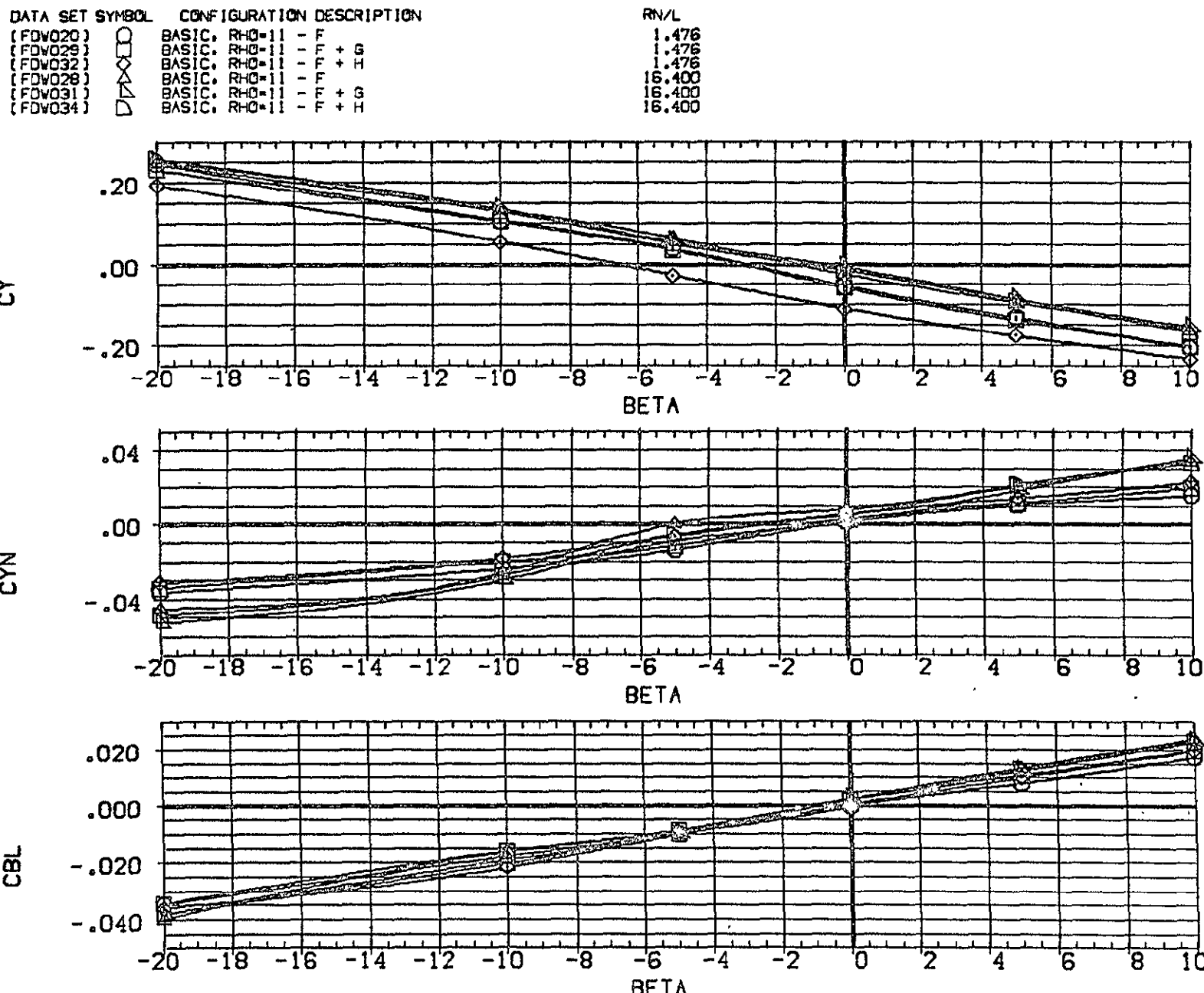


FIG. 9 EFFECT OF NOSE SHAPE FOR 2 REYN. NOS. AT VARIOUS ALPHAS, ZERO CON. SURF.  
(A) ALPHA = -80.00

DATA SET SYMBOL	CONFIGURATION DESCRIPTION	RN/L
FDV020	BASIC, RHO=11 - F	1.476
FDV029	BASIC, RHO=11 - F + G	1.476
FDV032	BASIC, RHO=11 - F + H	1.476
FDV028	BASIC, RHO=11 - F	16.400
FDV031	BASIC, RHO=11 - F + G	16.400
FDV034	BASIC, RHO=11 - F + H	16.400

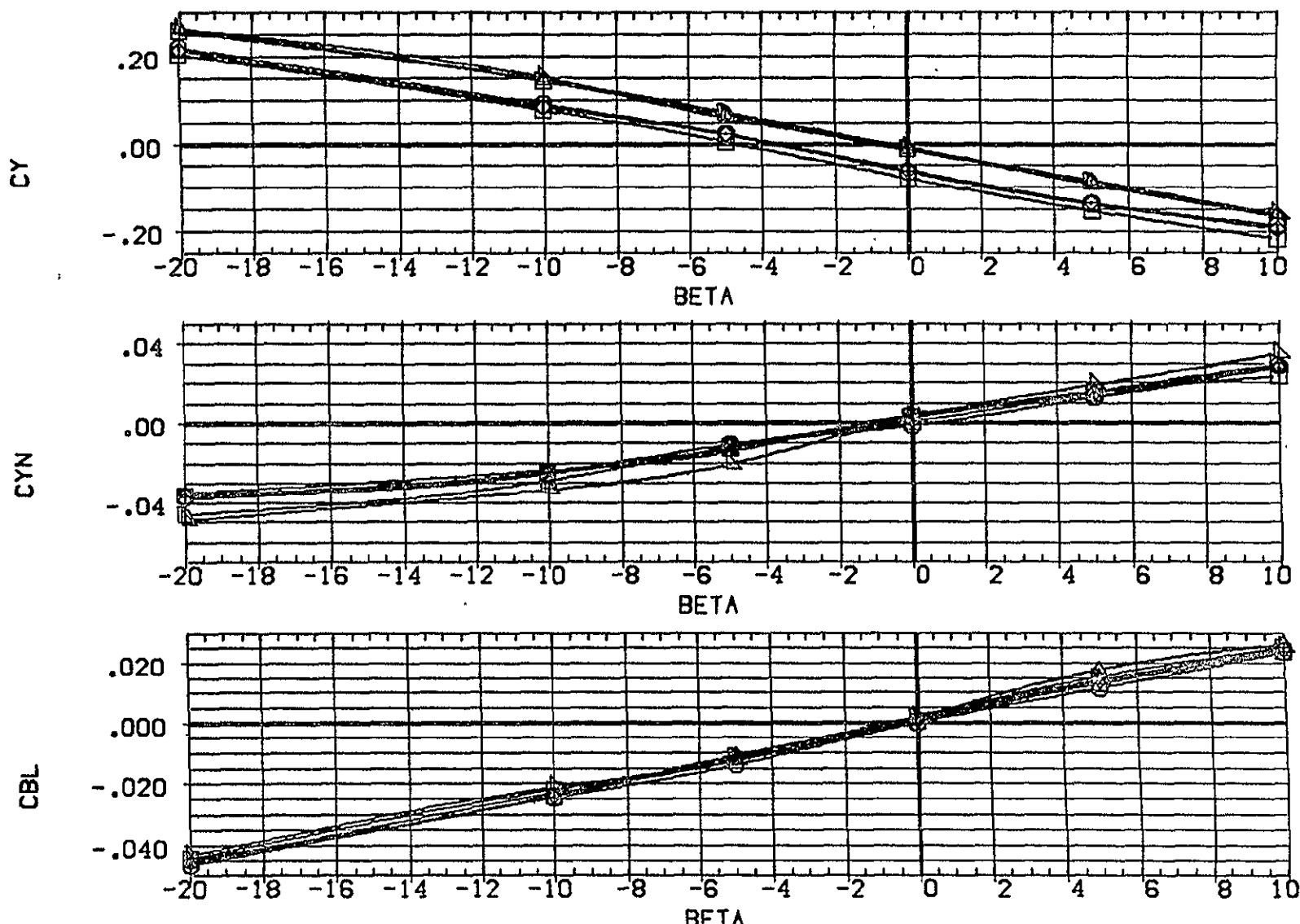


FIG. 9 EFFECT OF NOSE SHAPE FOR 2 REYN. NOS. AT VARIOUS ALPHAS. ZERO CON. SURF.  
(B) ALPHA = -70.00

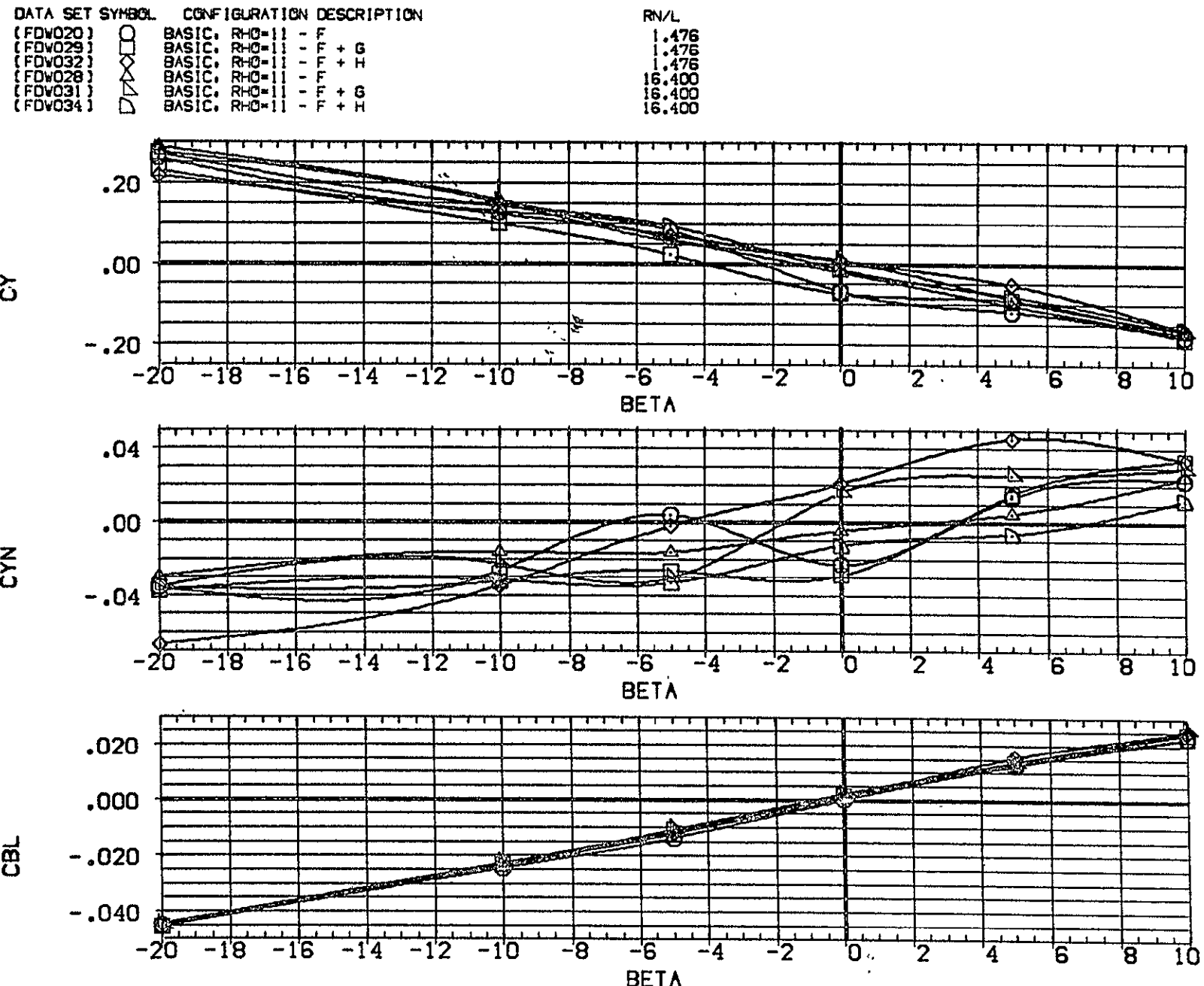


FIG. 9 EFFECT OF NOSE SHAPE FOR 2 REYN. NOS. AT VARIOUS ALPHAS. ZERO CON. SURF.  
(C)ALPHA = -60.00

DATA SET SYMBOL	CONFIGURATION DESCRIPTION	RN/L
{ GDW020 }	BASIC: RHO-111 - F	1.476
{ GDW029 }	BASIC: RHO-111 - F + G	1.476
{ GDW032 }	BASIC: RHO-111 - F + H	1.476
{ GDW028 }	BASIC: RHO-111 - F	16.400
{ GDW031 }	BASIC: RHO-111 - F + G	16.400
{ GDW034 }	BASIC: RHO-111 - F + H	16.400

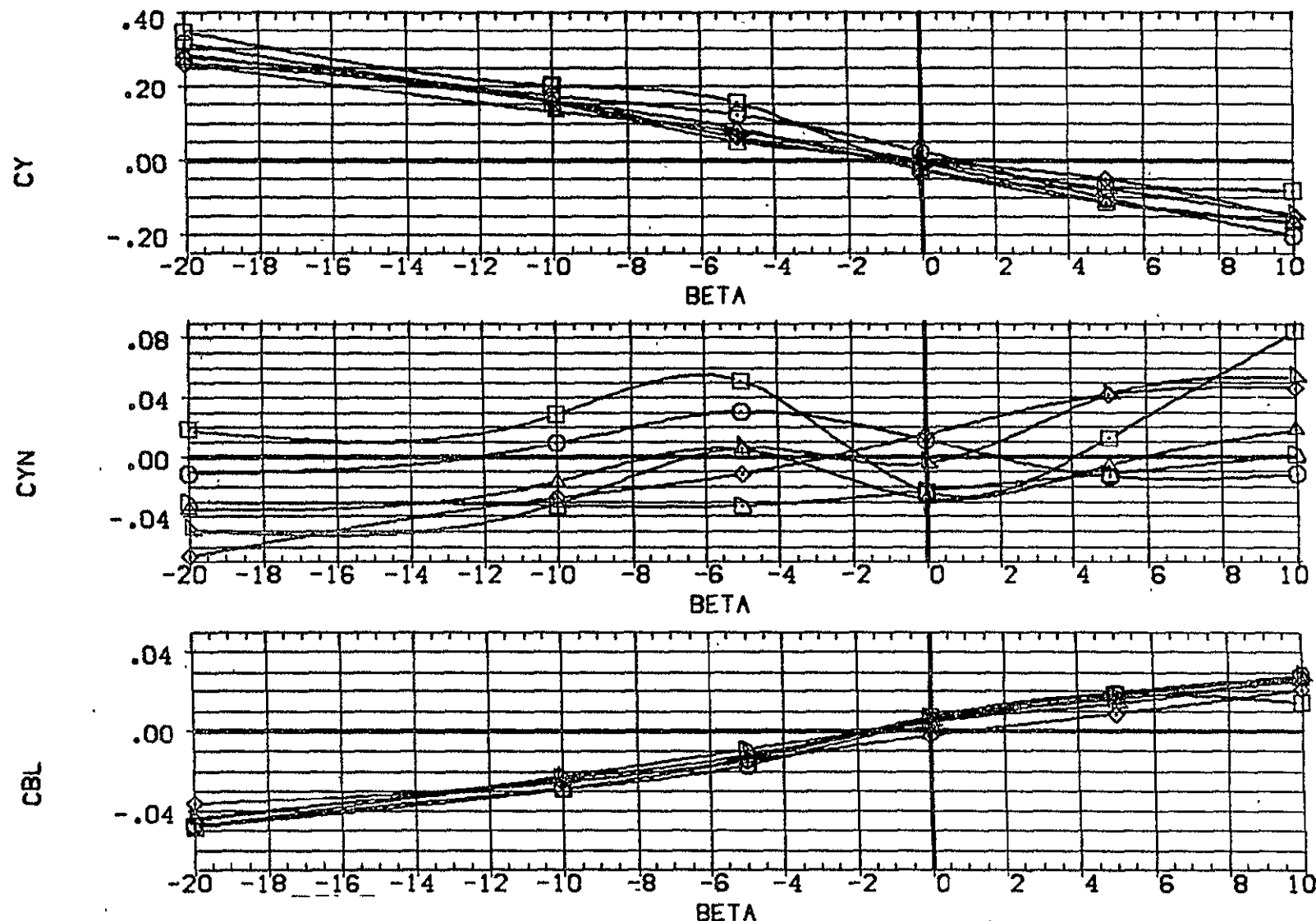
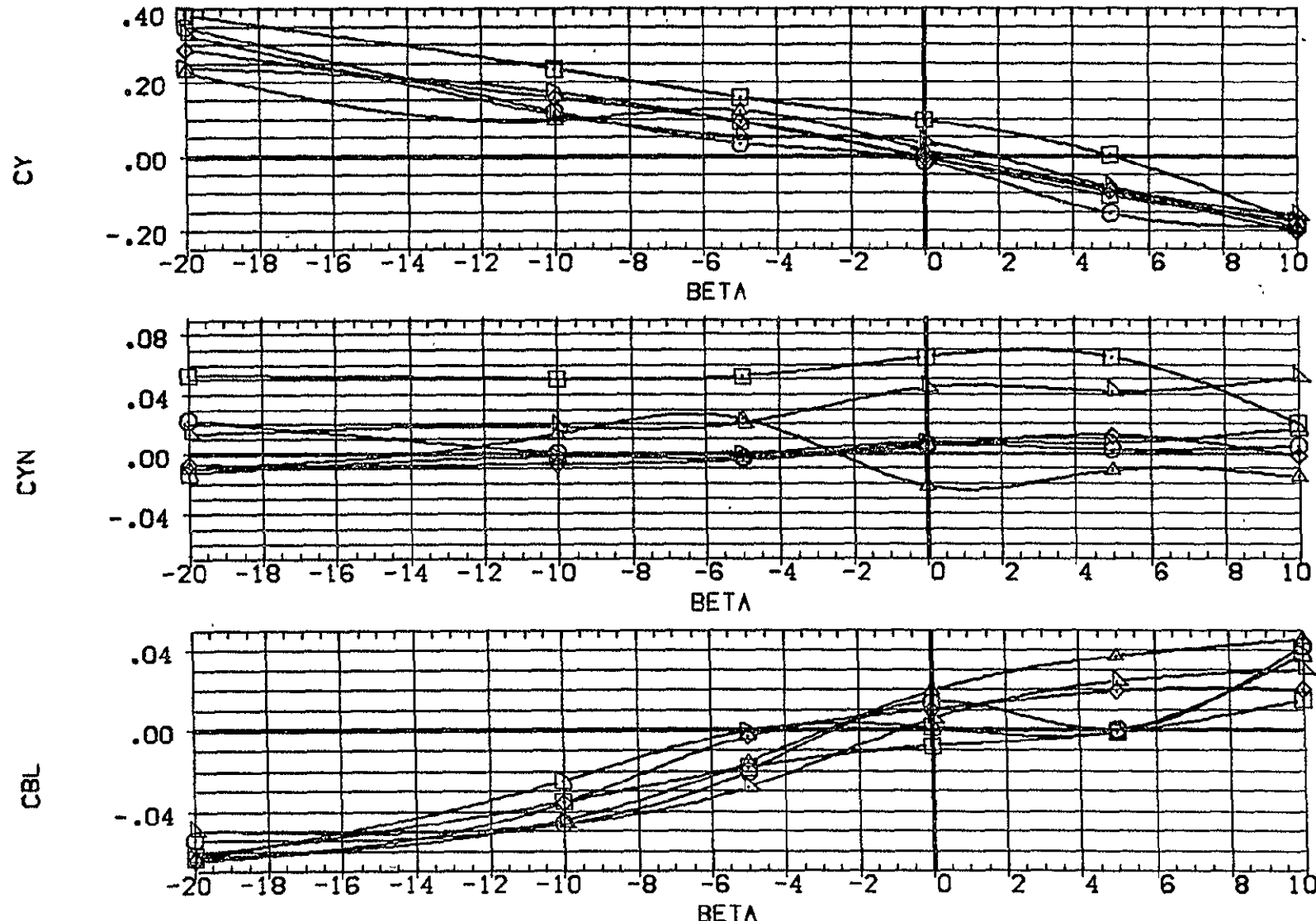


FIG. 9 EFFECT OF NOSE SHAPE FOR 2 REYN. NOS. AT VARIOUS ALPHAS. ZERO CON. SURF.  
(A) ALPHA = -50.00

DATA SET SYMBOL	CONFIGURATION DESCRIPTION	RN/L
(GDW020)	BASIC: RHO=11 - F	1.476
(GDW029)	BASIC: RHO=11 - F + G	1.476
(GDW032)	BASIC: RHO=11 - F + H	1.476
(GDW028)	BASIC: RHO=11 - F	16.400
(GDW031)	BASIC: RHO=11 - F + G	16.400
(GDW034)	BASIC: RHO=11 - F + H	16.400



ORIGINAL PAGE IS  
OF POOR  
QUALITY

FIG. 9 EFFECT OF NOSE SHAPE FOR 2 REYN. NOS. AT VARIOUS ALPHAS, ZERO CON. SURF.  
CRITICAL ALPHA = -10.00